TRANSPORTATION RESEARCH
RECORD

No. 1488

Materials and Construction

Unmodified and Modified Asphalt Binders

A peer-reviewed publication of the Transportation Research Board

TRANSPORTATION RESEARCH BOARD
NATIONAL RESEARCH COUNCIL

NATIONAL ACADEMY PRESS
WASHINGTON, D.C. 1995

Transportation Research Record 1488
ISSN 0361-1981
ISBN 0-309-06159-8
Price: $26.00

Subscriber Category
IIIB materials and construction

Printed in the United States of America

Sponsorship of Transportation Research Record 1488

GROUP 2—DESIGN AND CONSTRUCTION OF TRANSPORTATION FACILITIES
Chairman: Michael G. Katona, U.S. Air Force Armstrong Laboratory

Bituminous Section
Chairman: Harold R. Paul, Louisiana Transportation Research Center

Committee on Characteristics of Bituminous Materials
Chairman: Leonard E. Wood, Purdue University
David A. Anderson, Chris A. Bell, S. W. Bishara, Joe W. Button, Brian H. Chollar, Eileen Connolly, John J. Emery, Claude P. Fevre, Norman W. Garrick, Eric E. Harm, Paul W. Jennings, Prithvi S. Kandhal, Thomas W. Kennedy, Gayle N. King, Dean A. Maurer, Thomas B. Nelson, Tinh Nguyen, Larry F. Ostermeyer, Charles F. Potts, Raymond E. Robertson, Bernard A. Vallerga, John S. Youtcheff, Ludo Zanzotto, Michael Zupanick

Transportation Research Board Staff
Robert E. Spicher, Director, Technical Activities
Frederick D. Hejl, Engineer of Materials and Construction
Nancy A. Ackerman, Director, Reports and Editorial Services

The organizational units, officers, and members are as of December 31, 1994.

Transportation Research Record 1488

Contents

Foreword

The papers in this volume, dealing with various facets of unmodified and modified asphalt binders, should be of interest to state and local construction, design, materials, and research engineers as well as contractors and material producers.

In the first five papers Bishara and McReynolds, Phromsorn and Kennedy, Hanson and Duncan, Bahia and Anderson, and Hanson et al. describe their respective efforts related to the laboratory characterization of asphalt binders. In the next five papers Curtis et al., McGennis, Stroup-Gardiner and Newcomb, Bahia, and Shashidhar et al. discuss their work related to the characteristics of modified asphalts. In the last paper Oliver describes the results of field trials of two antioxidants in Australia.

Effect of Microwave Energy on the Properties of Asphalt and Its Use as an Aging Tool

S. W. BISHARA AND R. L. MCREYNOLDS

Microwave energy causes changes in asphalt properties. Unsymmetric organic molecules with dipoles, that is, with a permanent separation of positive and negative charges, undergo excitational rotation when they are subjected to microwave radiation. The excitational rotation depends on the material's dielectric constant. Because the radiation frequency is relatively high and the dielectric constant of asphalt is low, asphalt molecules cannot rotate as fast as the applied electromagnetic field, and an out-of-phase component of the dielectric constant, called dielectric loss, is dissipated as heat. Treatment of asphalt for a short time with low-power microwave radiation decreases the dispersitivity (*D*) and molecular size index (MSI) values obtained by high-performance size exclusion chromatography (HPSEC). Alternately, exposure for a longer time to a higher-power radiation increased both the *D* and MSI values for 12 asphalts studied. Microwave conditions (power level, treatment time, sample weight, and sample container material) were tailored to simulate the effects obtained after rolling thin film oven-pressure aging vessel (RTFO-PAV) aging of 18 asphalts. HPSEC gave comparable results for the two aging techniques: RTFO-PAV aging versus microwave aging. The difference in MSI amounted to ±7.3 and ±4.2 percent by using gravimetry and ultraviolet detection at 345 nm, respectively. The bending beam rheometer showed that microwave energy underestimates aging by a maximum of about 3°C in the limiting low temperature. Accelerated aging by microwave radiation is very simple and consumes less than 3 hr.

The electromagnetic radiation spectrum covers a wide wavelength range starting with cosmic rays and followed by γ-ray, X-ray, ultraviolet (UV), visible, infrared (IR), microwave, and then radio-frequency radiations. Cosmic rays have a very short wavelength (1.00×10^{-12} m), whereas radio waves have wavelengths greater than 1.00 m. The microwave region extends from 3.00×10^{-4} to 1.00 m. Electromagnetic radiation is described in terms of both particles and waves (*1*). The following equations relate the energy (*E*) of a particle along the electromagnetic spectrum to the velocity of light (*c*), frequency (*v*), and wavelength λ; *h* is Planck's constant (6.626×10^{-34} J·sec):

$$E = h\nu \quad (1)$$

$$\nu = c/\lambda \quad (2)$$

$$E = hc/\lambda \quad (3)$$

Equation 3 indicates that λ is inversely proportional to *E*. Thus, across the spectrum λ increases and *E* decreases. Cosmic rays and γ-radiation have high penetrating powers; γ-radiation causes excitation at the nuclear level. X-rays excite inner electrons. Spectrophotometric techniques of chemical analysis make use of the energy of UV, visible, and IR radiation. Usually, the analyte is subjected to a sweep of the wavelength region of interest (UV, visible, or IR), and the difference in radiation energy is measured. UV radiation excites the outermost (valency) electrons of an atom from one energy level to a higher one. IR radiation, with its lower particle energy, can only cause molecular vibrational-rotational excitations within the same electronic state. Microwaves lead to the rotational excitation of molecules. In the rotationally excited state molecules rotate faster than they do in the ground state.

Most organic molecules have structural unsymmetry and, accordingly, possess a dipole moment as a result of the permanent separation of the positive and negative charges within the molecule. A simplified model entails an electric dipole that is contained in a spherical molecule, that is free to rotate into alignment with an applied electromagnetic field, and that is subject to the viscous drag of the surrounding medium and to collisions with other molecules (*2*).

At very low frequencies dipoles (molecules) are able to rotate in phase with the applied field. At higher frequencies restraints on dipole rotation become more significant and molecules are no longer able to follow the rapid oscillations of the applied field. This gives rise to an out-of-phase component of the dielectric constant representing a dielectric loss (ε″) (that is, a dissipation of energy as heat). Thus, the dielectric constant (ε′) of material is related to the energy stored as electric energy (excites molecular rotations); the dielectric loss (ε″) is related to the energy dissipated as heat energy (heats the material). The dissipation factor or loss tangent, tan δ, is equal to ε″/ε′ (*3*). At 25°C and a microwave radiation frequency of 3000 MHz, an asphalt cement has an ε′ of 2.5 and a tan δ of 1.10×10^{-3}; under the same conditions water has an ε′ of 76.7 and a tan δ of 1.57×10^{-1} (*3,4*). Therefore, the ε″ for asphalt is 2.75×10^{-3}, whereas that for water is 1.20×10. Not surprisingly, water heats more quickly than asphalt when it is subjected to microwaves. Low values of ε′ and tan δ for asphalt may explain the lack of studies on the effect of microwave energy on asphalt (in the absence of aggregates).

MICROWAVE ENERGY AND SHRP MODEL OF ASPHALT

The Strategic Highway Research Program (SHRP) version of a chemical model of asphalt depicts a mixture of polar materials dispersed in nonpolar materials, with polar materials forming continu-

Materials and Research Center, Kansas Department of Transportation, 2300 Van Buren, Topeka, Kans. 66611-1152

ous, three-dimensional networks or a microstructure (*5*). The close proximity of polar materials allows the formation of hydrogen bonds, in which the hydrogen atom (positive end) of one molecule bonds with an oxygen or a nitrogen atom (negative end) of the same or another molecule. Other secondary bonds or intermolecular forces, for example, pi–pi bonding, dipole forces, and Van der Waals forces, are also present and, together with hydrogen bonding, determine many of the properties of asphalt. Intermolecular forces are weak and are easy to break by heat or stress; they have a low dissociation energy of 8 to 40 kJ/mol, depending on the polarizabilities and the dipole moments of the bonding molecules (*6*).

The SHRP chemical model of asphalt considers the breaking and reformation of weak, secondary bonds or forces between polar molecules to be responsible for many changes in the characteristics of asphalt. Because the in-phase component ϵ' can excite molecular rotations, whereas the out-of-phase component ϵ'' provides heat, microwave energy causes changes in asphalt. Once the microwave source is permanently removed, intermolecular forces again come into play, leading to different associations of molecules and, accordingly, a change in properties.

MICROWAVE CONDITIONS AND PROPERTY CHANGES

To study the effect of microwave energy on asphalt, the first stages of this work used semipreparative high-performance size exclusion chromatography (HPSEC) or high-performance gel permeation chromatography (HPGPC). Property changes were followed by measuring the molecular size index (MSI)) (*7–9*), where

$$\text{MSI} = \text{percent first fraction / percent second fraction} \quad (4)$$

As it is known, larger molecular associations elute first from the chromatographic column followed progressively by smaller entities.

Another variable used to measure property changes was the dispersitivity (D), weight average molecular weight/number average molecular weight ($\bar{M}_w/\bar{M}_n$), which is a measure of the breadth of molecular weight distribution curve (*6*).

MICROWAVE ENERGY AND AGING

The type and magnitude of changes in MSI due to long-term exposure to a high power level of radiation are similar to the changes observed after aging: an increase in the population of larger associations (first fraction) and a decrease in the population of smaller entities (second fraction). To test the feasibility of using microwave radiation as an aging tool, 18 tank asphalts used in Kansas were selected. Each asphalt was laboratory aged by two different techniques: (a) SHRP long-term aging [rolling thin film oven and pressure aging vessel (RTFO-PAV)] and (b) microwave oven.

Comparison between the two aging techniques was studied by (a) HPSEC with a gravimetric (*9*) and a UV spectrophotometric finish and with a (b) bending beam rheometer (BBR), the only SHRP binder testing equipment available at this time.

Microwave aging is simple and rapid compared with RTFO-PAV aging. It requires treatment for less than 3 hr in a household microwave oven; a quartz petri dish serves as the sample container. Aging by the RTFO-PAV technique requires more operator effort, a much longer time, more equipment with accessories that are susceptible to failure, larger volumes of cleaning solvents, and hazards associated with a 2.1-MPa pressure.

EXPERIMENTAL DETAILS

Aging

1. A household microwave oven (Tappan) with an output power of 1000 W, a turntable, and a 0.037-m^3 capacity was used. Power can be adjusted from high power (HP) to 10, 20, . . . , 90 percent of HP. A quartz petri dish (100 × 10 mm) served as a container for the 16-g sample. This yields a 1.5-mm-thick film of asphalt. Figure 1

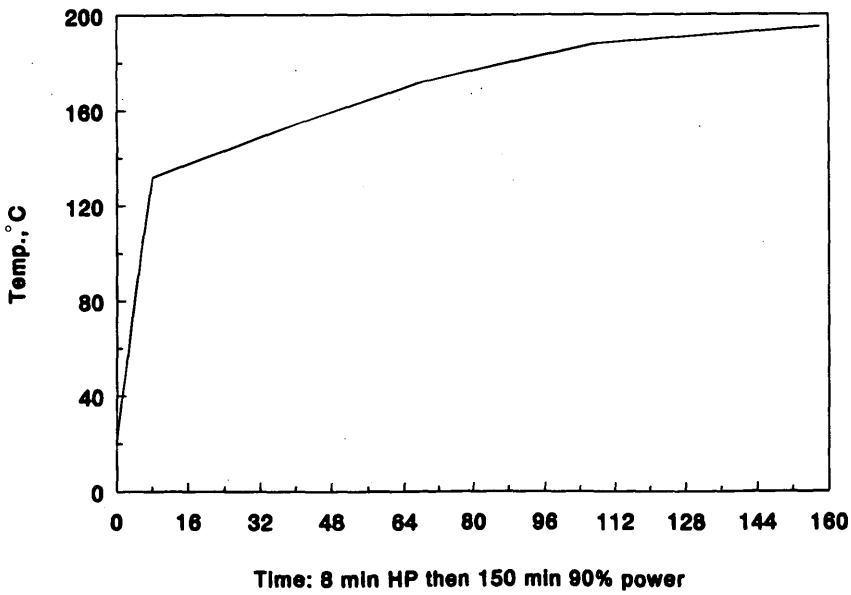

FIGURE 1 Variation of temperature with time.

shows the increase in the temperature inside the oven with treatment time and power level of radiation. A fluoroptic thermometer (Model 790 from Luxtron) was used to measure temperature.

Initial experiments used a 750-W oven with adjustable power, a turntable, and a 50-mL glass beaker as a sample container; 1.5 g of asphalt was spread over the sides and bottom of the beaker before treatment.

Sampling of 1.5- or 16-g samples was done after annealing tank asphalt for 1.5 hr at 160°C in a convection oven.

2. RTFO-PAV aging was conducted according to AASHTO T240-87; this was followed by Standard Practice for Accelerated Aging of Asphalt Binder Using a Pressurized Aging Vessel (PAV) (AASHTO PP1, Edition 1A).

Sampling was done after annealing the tank asphalt in a convection oven for 1 hr at 150°C.

Testing

1. A BBR applied test system was used. Methanol was used to fill the cooling chamber. Testing was carried out by following the Standard Test Method for Determining the Flexural Creep Stiffness of Asphalt Binder Using the BBR (AASHTO TP1, Edition 1A).

Aged material (material aged by the microwave or the RTFO-PAV technique) was allowed to cool overnight. Annealing for 1 hr at 150°C in a convection oven preceded molding. A similar annealing process, that is, 1 hr at 150°C, preceded sampling for HPSEC measurements.

2. In previous work (*9*) a procedure was developed to address the problems associated with the column source because HPSEC data change with every new column, even though the columns would have identical characteristics, that is, packing and dimensions. A similar procedure was used in the present work. The procedure relied on the retention time of polystyrene standards to designate fraction cut-off points, a modification that eliminated variation in HPSEC data upon replacement of a column by an identical one.

In the present work a Waters HPSEC system was used. A Shodex 6-μm, 500-Å, KF-2002.5 semipreparative column (300 × 20 mm) was used. A Waters R401 differential refractive index detector was used to analyze polystyrene standards. A liquid chromatography spectrophotometer (Lambda Max Model 481 from Waters) was used to analyze asphalts by UV detection at 345 nm.

a. Analysis of standards. A set of six polystyrene standards and acetone were analyzed by using a mobile phase of 97% toluene and 3% pyridine flowing at 3.5 mL/min. The column was maintained at 70°C.
b. Selection of cutoff points. For the analysis of asphalt cement collection of the first fraction starts at a retention time (t_R) of 7.70 min from injection. The midpoint between the t_R of standard A-2500 and that of standard A-1000 served as the cutoff point for collection of the first fraction. The cutoff point for collection of the second fraction was 21.00 min from injection.
c. Analysis of asphalt cement. An asphalt sample in a 50-mL beaker was weighed accurately (to within 0.1 mg) in the range of 1.5 ± 0.1 g. Asphalt was spread on the sides and bottom of the beaker. About 20 mL of toluene was added, and the mixture was heated on a hot plate set at the lowest possible setting (approximately 50 to 60°C).

Dissolution takes 10 to 15 min. The contents were transferred quantitatively to a 50-mL volumetric flask, and the volume was completed with toluene. An aliquot was filtered through a 0.45-μm-pore-size membrane.

An aliquot of 150 μL asphalt sample solution (about 4.5 mg of asphalt) was injected in the HPSEC system. The mobile phase, flow rate, and column temperature are the same as described for the analysis of standards. The asphalt material was eluted into two, accurately weighed (to within 2 μg) glass petri dishes (60 × 15 mm). The petri dishes containing the two fractions were set on a hot plate maintained at 50 to 60°C. After the mobile-phase solvents evaporated, the petri dishes were heated in a convection oven for 90 min at 160°C. The petri dishes were then cooled in a desiccator to a constant weight.

A Mettler AT 20 microbalance (sensitivity of 2 μg and capacity of 22 g) was used to weigh the glass petri dishes.

HPSEC analysis was also followed spectrophotometrically at 345 nm. The area under the chromatogram was divided at the same cutoff point used for the gravimetric finish to designate the first and second fractions.

RESULTS AND DISCUSSION OF RESULTS

HPSEC to Study Asphalt

The SHRP chemical model of asphalt emphasizes the significance of weak, secondary bonds between molecules, including dipole forces between polar sites of constituent molecules to form molecular associations. HPSEC separates constituent associations according to their effective size or, more precisely, hydrodynamic volume (V_h):

$$V_h \rightarrow M_n/N \qquad \text{dL/molecule} \tag{5}$$

where

M = molecular weight (g/mol),
n = intrinsic viscosity, (dL/g), and
N = Avogadro's number (molecule/mol).

Previous work (*8*), in which HPSEC was used, has reported a perfect correlation between MSI of Corbett's fractions and polarity for 20 asphalts. For any given asphalt MSI increased progressively from the nonpolar (saturates) on the one end to the highly polar (asphaltenes) at the other end. Thus, for asphalt, the V_h of molecular entities is perfectly related to polarity; highly polar materials have high MSI values because the constituent entities are mainly made up of polar molecules leading to a predominance of larger entities with high V_h. In view of the significance of polarity in the behavior of asphalt, the use of HPSEC to study asphalts is well justified.

Toluene has been used as a mobile phase (carrier) for asphalt analysis by HPSEC because it is believed to have a solubility parameter similar to that of asphalt solvent phases (*5,10,11*). Furthermore, compared with other asphalt solvents, toluene has the lowest dielectric constant (2.38) and therefore causes the least disturbance to molecular associations. To avoid dissociation asphalt solutions were chromatographed rapidly (within 0 to 20 min from the time of dissolution). Inclusion of 3 percent pyridine in the mobile phase prevents the loss of some of the asphalt polar

material through adsorption on the stationary phase (column packing).

Table 1 gives the MSIs for a set of 12 tank asphalts selected randomly from those used by the Kansas Department of Transportation. It is noteworthy that the MSIs for the asphalts studied ranged between 0.26 and 0.44. This range agrees quite favorably with that of 0.15 to 0.44 obtained by Branthaver et al. (*12*) for the eight SHRP core asphalts, on a preparative scale, using fluorescence to 350-nm radiation to designate the cutoff points of Fractions I and II. Although the two studies used different approaches for the fractionation of yet unrelated sets of asphalts, the two MSI ranges are remarkably close.

Effect of Microwave Energy on Asphalt

Exposure of 1.5 g of asphalt to different levels of power (p) of microwave radiation for different time intervals (t) caused changes in both MSI (obtained gravimetrically) and D (obtained by using UV detection at 345 nm). A short t and a low p decreased both MSI and D (Table 2, series a to d). Alternately, a rather long t and a higher p increased both MSI and D (Table 2, series e). The two extreme conditions of microwave exposure time and power level were then applied to the whole set (Table 3).

Short-Term, Low-Power Treatment

A previous investigation (*9*) of the HPSEC procedure similar to the present one reported a precision of 0.02 for the MSIs of 18 asphalts. Table 3 shows that short-term exposure to low-power radiation decreased the MSIs of five asphalts; D generally decreased for the whole set except for Sample 4729, which showed a slight increase in D. Few unsuccessful trials were performed to further decrease MSI and D.

The decrease in D is illustrated in Figure 2, in which streamlining of molecular species occurs; the very large associations as well as the rather small entities diminish (D decreased from 4.011 to 3.504; Table 3). Streamlining may be viewed as follows. The applied microwave radiation creates an in-phase component that causes the rotational excitation of molecules and an out-of-phase component that represents the portion dissipated as heat. Both components break up some intermolecular forces, leading to a relative decrease in the population with larger associations. However, there seems to be enough energy (electric and heat) for the opposite process, that is, the formation of associations through activation of rather small molecules, to also take place. The breakup of larger associations, however, predominates, as evidenced by a decrease in MSI from 0.35 to 0.32 (Table 3) and from the data in Figure 2.

Usually, the magnitude of change in D of an asphalt paralleled that for MSI. However, Samples 4190 and 4506 showed practically the same MSIs after microwave treatment, even though D suffered an obvious decrease in value. Apparently, the breakup of some large associations may have taken place at about the same rate as the formation of new associations, with no net effect on the ratio between the two HPSEC fractions.

Streamlining of molecular entities (decrease in D) occurred for all asphalts studied except for Sample 4729. The anomalous behav-

TABLE 1 MSI of Set of Tank Asphalts Using a Gravimetric Finish

Sample #	Molecular Size Index, MSI	Change in Wt, %*
2110	0.34	-3.7
3087	0.28	-2.6
3385	0.35	-6.1
3418	0.32	-7.5
3455	0.28	-7.6
3488	0.35	-6.5
3829	0.34	-9.8
4190	0.26	-7.9
4506	0.26	-7.4
4653	0.31	+1.8
4729	0.44	+0.2
4897	0.35	-2.1

Average change in Wt.,% = ±5.3

* $\frac{\text{(Wt of Fractions Collected, mg - Sample Wt Injected, mg) X 100}}{\text{Sample Wt Injected, mg}}$

TABLE 2 Effect of Exposure Time *t* to Microwave Radiation of Power *p* on Tank Asphalt 4897

Series	Microwave Conditions t and p	Temp., °C*	MSI	D
a	3 min HP**; 45 min 20% p	55	0.32	3.504
b	3 min HP; 90 min 20% p	60	0.32	3.515
c	10 min HP; 15 min 60% p	125	0.32	3.675
d	10 min HP; 45 min 60% p	145	0.34	3.686
e	10 min HP; 90 min 60% p	155	0.41	4.581

[MSI = 0.35, and D = 4.011 (at 345 nm)]

*** Air temperature at center of a 750-W microwave oven at the end of treatment.**
**** HP = High power or 100% power.**

ior may be attributed to this asphalt's exceptionally high MSI (0.44) compared with those of the other asphalts studied. An asphalt with a high ratio of large associations relative to the smaller entities should encompass an abundance of a polar, three-dimensional network (*5*) that, on exposure to microwave radiation, causes the dielectric relaxation time τ to decrease, thus bringing $1/\tau$ closer in value to the angular frequency $2\pi f$ (maximum ϵ'' is attained when $1/\tau = 2\pi f$) (*13*). A higher ϵ'' causes Sample 4729 to heat more quickly than the rest of the samples over the short exposure time used, leading to an effect similar to that observed with other asphalts only after high-power long-term treatment, that is, an increase in *D* (Table 3).

TABLE 3 Effect of *t* and *p* on Tank Asphalts

Sample	Tank		3 Min HP; 45 min 20% p*		10 min HP; 90 min 60% p**	
	MSI	D	MSI	D	MSI	D
2110	0.34	3.785	0.33	3.612	0.41	4.615
3087	0.28	3.953	0.24	3.733	0.33	4.695
3385	0.35	3.500	0.33	3.464	0.43	4.463
3418	0.32	4.727	0.32	4.680	0.39	6.209
3455	0.28	4.287	0.24	3.895	0.32	4.856
3488	0.35	3.525	0.32	3.439	0.43	4.299
3829	0.34	4.448	0.33	4.324	0.36	5.225
4190	0.26	4.401	0.25	4.066	0.30	5.752
4506	0.26	4.184	0.25	3.940	0.30	5.255
4653	0.31	3.743	0.28	3.468	0.34	4.444
4729	0.44	3.825	0.43	4.100	0.49	4.895
4897	0.35	4.011	0.32	3.504	0.41	4.581

*** Short-term, low-power radiation treatment; air temperature at center of a 750-W microwave oven at end of treatment was 55°C.**
**** Long-term, higher-power radiation treatment; air temperature at center of a 750-W microwave oven at end of treatment was 155°C.**

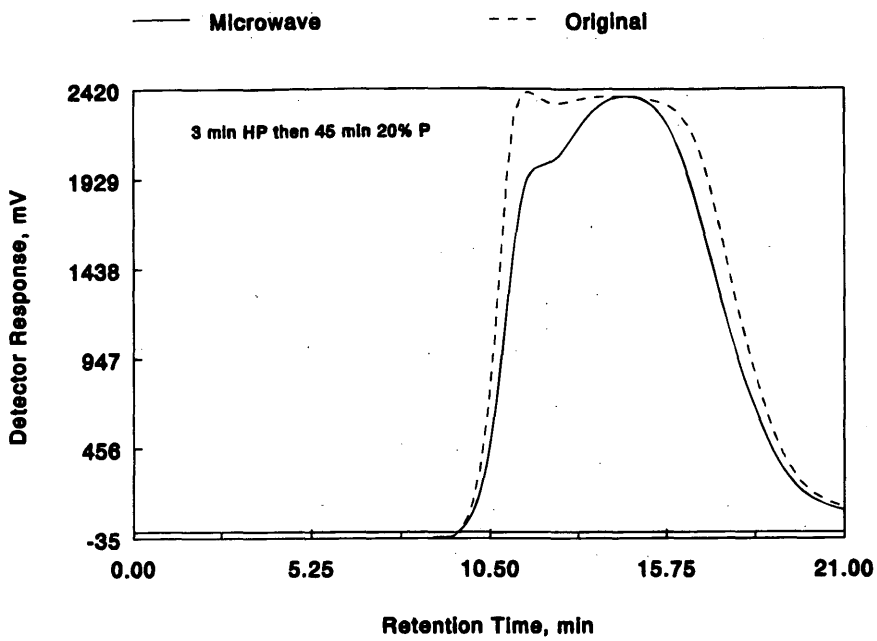

FIGURE 2 Comparison of Sample 4897 tank asphalt before and after microwave treatment.

Long-Term, High-Power Treatment

Table 3 shows that microwave energy increases the MSI and *D* values for asphalt cement. In contrast to short-term low-power treatment, all 12 asphalts showed increases in the values of both variables.

Microwave Energy for Laboratory Aging

Because microwave radiation increased the MSIs of a whole set of asphalts, its use is suggested for aging. To test its efficiency the effect of microwave radiation on asphalt was compared with that obtained by the SHRP long-term aging technique. A comparison of the two aging techniques, that is, the microwave versus the RTFO-PAV aging techniques, was carried out by two approaches: (a) HPSEC (gravimetry and UV absorption), and (b) BBR. In this way an asphalt's physicochemical and physical properties are independently tested.

The aforementioned experiments used 1.5 g of asphalt for HPSEC analysis. The BBR, however, requires >12 g of sample. The data in Table 4 reveal that the preselected microwave conditions of *t* and *p* are ineffective for larger samples; MSI and *D* values for microwave-aged asphalt were practically indifferent from those for tank asphalt.

Experimentation with pouring of the microwave-treated asphalt from a petri dish to fill an aluminum mold for BBR testing showed that 16 g of sample was required. To cause a change in asphalt properties the following was carried out. The microwave conditions (*t* and *p*) were intensified, and a quartz petri dish was used as a sample container. Quartz is highly transparent to microwave radiation ($\tan \delta = 6 \times 10^{-5}$) (*13*) and allows most microwave energy to affect

TABLE 4 Effect of Asphalt Sample Weight on Effectiveness of Microwave Energy

Sample	Microwave-Aged Asphalt*				Tank Asphalt	
	Sample Wt=1.5 g		Sample Wt=12 g		Sample Wt=1.5 g	
	MSI	D	MSI	D	MSI	D
2110	0.41	4.615	0.33	3.635	0.34	3.785
3418	0.39	6.209	0.31	5.057	0.32	4.727
3488	0.43	4.299	0.35	3.454	0.35	3.525

*** Treated in a 750-W microwave oven for 10 min at HP then 90 min 60% p (as in Table 3).**

the asphalt instead of being partially absorbed by Pyrex glass containers.

Modification of Microwave Conditions

To select the optimum microwave treatment conditions, a reference point was established. An asphalt sample was aged by the RTFO-PAV procedure and was then tested on a BBR to determine the lowest test temperature that satisfies SHRP requirements of a maximum stiffness (S) of 300 MPa and a minimum slope (m) of 0.300. Table 5 shows that a proper selection of t and p leads to an aging effect similar to that of the RTFO-PAV aging technique. Target values were practically achieved after exposure for 8 min at HP and then for 150 min at 90 percent p. These same settings were used to age a set of tank asphalts.

Comparing the Two Aging Techniques Using BBR

A set of 18 asphalts was randomly selected. Because these were viscosity-graded (AC-10 and AC-20) experimentation was necessary to determine the lowest test temperature for each asphalt that satisfied the requirements for S and m. Therefore, tank asphalt was aged by the RTFO-PAV technique. Aged material was tested on the BBR at different temperatures to determine S and m values at the limiting temperature. A 16-g sample of tank asphalt was then treated in a microwave oven for 8 min at HP and then for 150 min at 90 percent p and was tested on the BBR at the same limiting temperature. A comparison of the S and m values obtained by the two aging techniques is given in Table 6. For the set of asphalts the average difference was -16.0 percent for S and $+13.6$ percent for m; the calculation was based on values obtained by the RTFO-PAV aging technique as a reference.

Microwave aging marginally underestimated the aging effect. The difference in S and m values for individual samples obtained by the two aging techniques was approximately equivalent to 1°C to 3°C, depending on the asphalt material; that is, a given asphalt passing the BBR test at -12°C after RTFO-PAV aging would pass at a temperature of 1°C to 3°C lower (-13°C to -15°C) if it was aged with microwave energy.

Trials to minimize the difference between the two aging techniques were unsuccessful. Increasing t for Samples 3418 and 4190 caused "skimming"; after cooling and annealing for 1 hr, it was practically impossible to pour the samples into a mold. On the other hand small changes in t and p did not prove to be detrimental to S and m. Table 7 shows the minor variations in S and m after microwave aging at alternative settings. The results have standard deviations of 3.0 and 0.009 and coefficients of variation of 2.6 and 2.5 percent for S and m, respectively.

As mentioned earlier, microwave action depends on the material's electrical properties. Ferry (*14*) reported, "The complex dielectric constant bears certain formal analogies to the complex compliance, and the frequency dependence of its real and imaginary components is determined for some polymers by molecular motions similar to those which determine the rate of response to mechanical stresses."

Comparison of the Two Aging Techniques Using HPSEC

Asphalt material aged by each technique was analyzed by HPSEC, and the MSI was determined gravimetrically and spectrophotometrically at 345 nm (Table 8). Although UV detection has its own shortcomings (*15–17*), it was used in the present study only to compare the effects of the two aging techniques run on the same asphalt samples rather than to compare asphalts with each other.

TABLE 5 Effect of t and p of Microwave Radiation on S and m of Sample 3829 at test temperature of -14°C (target values, S = 139 MPa and m = 0.305, obtained after RTFO-PAV aging)

Microwave Conditions*	S (MPa)	m
8 min HP; 90 min 90% p	87	0.356
8 min HP; 145 min 90% p	124	0.314
8 min HP; 150 min 90% p	132	0.309
8 min HP; 160 min 90% p	144	0.310
8 min HP; 170 min 90% p	161	0.299
8 min HP; 180 min 70% p	156	0.293
9 min HP; 150 min 90% p	125	0.311
10 min HP; 150 min 90% p	135	0.327
160 min HP	133	0.313
170 min HP	134	0.321

*** A 1000-W microwave oven was used.**

TABLE 6 Comparison of the Two Aging Techniques by BBR Testing at Limiting Temperature

Sample	Test Temp., °C	'RTFO + PAV'		Microwave Energy*		Difference, %**	
		S, MPa	m	S, MPa	m	S	m
3829	-14	139	0.305	132	0.309	-5.0	+1.3
3087	-12	158	0.308	136	0.316	-13.9	+2.6
3385	-13	199	0.308	177	0.371	-11.1	+20.4
3488	-12	105	0.308	90	0.350	-14.3	+13.6
4190	-12	144	0.305	118	0.333	-18.1	+9.2
4506	-12	173	0.300	149	0.324	-13.9	+8.4
4653	-16	183	0.300	145	0.353	-20.8	+18.1
4162	-12	150	0.309	116	0.358	-22.7	+15.9
4163	-12	135	0.309	107	0.361	-20.7	+16.8
3590t	-12	156	0.311	121	0.362	-22.4	+16.4
4376t	-12	147	0.300	130	0.315	-11.6	+5.4
4897t	-10	125	0.309	98	0.365	-21.6	+18.1
4377t	-10	112	0.301	101	0.361	-9.8	+19.9
3418t	-11	170	0.300	130	0.349	-23.5	+16.7
4729t	-11	136	0.309	112	0.349	-17.6	+12.9
3587	-13	155	0.303	125	0.350	-19.4	+15.5
3455	-17	221	0.302	200	0.359	-9.5	+18.9
2110t	-12	223	0.305	197	0.350	-11.7	+14.8

* Treatment for 8 min HP then 150 min 90% p.
** The 'RTFO + PAV' is considered the reference value.
t AC-20; the rest are AC-10.

TABLE 7 Effect of Small Changes in Microwave Conditions on BBR Results for Asphalt 4162 at −12°C

Microwave Conditions*	S, MPa	m
8 min HP; 150 min 90% p**	116	0.358
8 min HP; 170 min 70% p	116	0.356
8 min HP; 160 min 80% p	109	0.371
8 min HP; 160 min 70% p	111	0.360
8 min HP; 200 min 70% p	113	0.344
8 min HP; 200 min 60% p	116	0.362

* A 1000-W microwave oven was used.
** Conditions already applied to age the whole set of asphalts, and to generate data in Table 6.

The data in Table 8 indicate that the two aging techniques give comparable MSIs, in which the microwave energy overestimated aging for approximately half of the set and underestimated aging for the other half. This observation applies to the two finishes used. For the 18 asphalts, the average differences in MSIs between the two aging procedures amounted to ±7.3 and ±4.2 percent for the gravimetric and UV detection methods, respectively. The chromatogram obtained after microwave aging was identical to that obtained after RTFO-PAV aging, and as expected, both chromatograms were distinct from that of the tank asphalt (Figures 3 and 4). The HPSEC data and Figures 3 and 4 indicate that microwave energy induces molecular interactions that resemble, in type and magnitude, those taking place by the RTFO-PAV aging technique.

Because microwave radiation creates a molecular rotational-excitation component in addition to a heat component, the two components might account for the short period of time required for microwave energy to induce such molecular changes that otherwise take longer if aging is done by conductive heating (RTFO-PAV technique).

Applications of Microwave Energy

Besides its potential as an alternate tool for laboratory aging, microwave radiation can be used to cause changes in the physicochemical and physical properties of asphalt. Table 9 shows that controlling t and p can decrease or increase the MSI and D values of tank asphalt; the most microwave-resistant asphalt exhibited a 40 percent difference between extreme values of MSI.

CONCLUSION

Treatment with microwave energy causes changes in the physical and physicochemical properties of asphalt. Time of treatment, power level of radiation, amount of asphalt used, and sample container material affect the type and the magnitude of change.

With a small amount (1.5 g) of asphalt, exposure for a short period of time to a low power level of radiation decreased the MSI and D values for about half of the 12 asphalts studied. Alternately,

TABLE 8 Comparison of the Two Aging Techniques by HPSEC with Gravimetric and UV Absorption Finishes To Determine MSI

Sample	'RTFO + PAV'		Microwave Energy*		Difference, %**	
	Grav.	UV	Grav.	UV	Grav.	UV
3829	0.42	1.84	0.47	2.01	+11.9	+9.2
3087	0.46	1.86	0.53	2.12	+15.2	+14.0
3385	0.49	1.72	0.48	1.65	-2.0	-4.1
3488	0.52	2.22	0.54	2.27	+3.8	+2.3
4190	0.42	1.71	0.38	1.78	-9.5	+4.1
4506	0.37	1.49	0.38	1.49	+2.7	0.0
4653	0.40	1.88	0.43	1.81	+7.5	-3.7
4162	0.39	1.75	0.35	1.70	-10.3	-2.9
4163	0.44	2.07	0.48	2.04	+9.1	-1.4
3590	0.63	2.38	0.57	2.25	-9.5	-5.5
4376	0.49	1.86	0.51	1.98	+4.4	+6.5
4897	0.51	1.93	0.47	1.90	-7.8	-1.6
4377	0.54	2.17	0.55	2.11	+1.9	-2.8
3418	0.52	1.97	0.46	1.87	-11.5	-5.1
4729	0.60	2.42	0.59	2.41	-1.7	-0.4
3587	0.50	2.14	0.48	2.10	-4.0	-1.9
3455	0.42	1.64	0.37	1.49	-11.9	-9.1
2110	0.50	1.88	0.53	1.87	+6.0	-0.5

* Treatment as in Table 6 (8 min HP then 150 min 90% p).
** The 'RTFO + PAV' aging is considered the reference value.

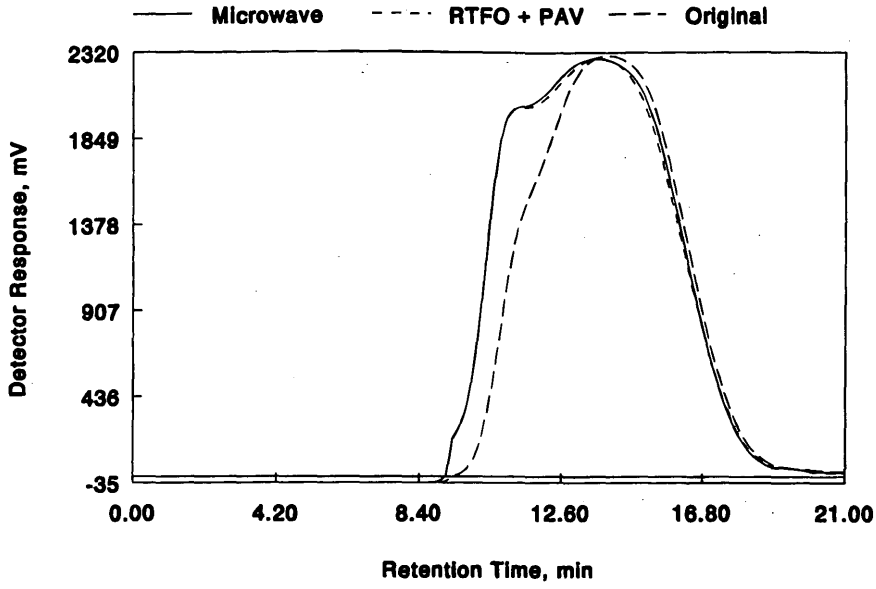

FIGURE 3 Chromatograms for microwave energy-aged asphalt, RTFO-PAV-aged asphalt, and tank asphalt (Sample 2110).

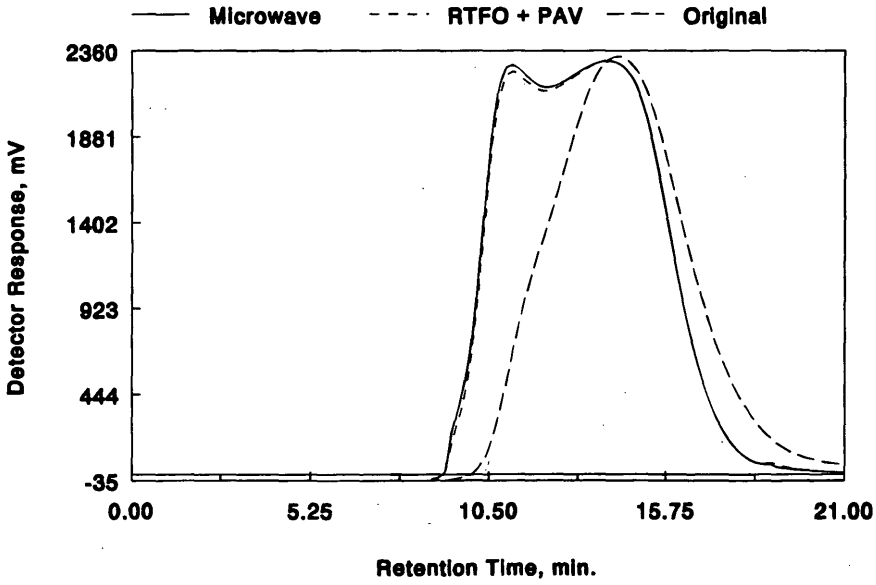

FIGURE 4: Chromatograms for microwave energy-aged asphalt, RTFO-PAV-aged asphalt, and tank asphalt (Sample 3488).

long-time exposure to a higher power level increased the MSI and D values for the set of asphalt samples.

Because of the ability of microwave radiation to increase the MSI (a behavior synonymous to aging) its use as an alternative tool for laboratory aging is promising. Microwave energy causes an extent of aging comparable to that caused by RTFO-PAV aging. Similarity between microwave aging and RTFO-PAV aging is evident from HPSEC and BBR measurements on 18 asphalts. The HPSEC procedure (which uses gravimetry and UV absorption at 345 nm) more or less gives the same MSI, regardless of the aging technique. The chromatograms obtained after microwave aging are identical to those obtained after RTFO-PAV aging. BBR shows that microwave aging underestimates aging. The difference between the two techniques corresponds to about 1°C to 3°C in limiting low temperature; that is, a given asphalt with a limiting temperature of −12°C may pass the BBR test at −13°C, −14°C, or −15°C, depending on the asphalt material, if it is aged with microwave radiation.

A maximum difference of 3°C in limiting low temperature between microwave aging and RTFO-PAV aging may be considered in view of the following: (a) RTFO-PAV aging is nothing but

TABLE 9 Variation in MSI and *D* Under Two Extreme Conditions of Microwave Energy

Sample	3 Min HP; 45 min 20% P*		8 min HP; 150 min 90% P**		Difference, %	
	MSI	D	MSI	D	MSI	D
2110	0.33	3.612	0.53	4.163	60.6	15.3
3087	0.24	3.733	0.53	4.517	120.8	21.0
3385	0.33	3.464	0.48	3.798	45.5	9.6
3418	0.32	4.680	0.46	5.170	43.8	10.5
3455	0.24	3.895	0.37	4.733	54.2	21.5
3488	0.32	3.439	0.54	4.022	68.8	17.0
3829	0.33	4.324	0.47	5.211	42.4	20.5
4190	0.25	4.066	0.38	5.098	52.0	25.4
4506	0.25	3.940	0.38	4.612	52.0	17.1
4653	0.28	3.468	0.43	4.247	53.6	22.5
4729	0.43	4.100	0.59	3.878	37.2	5.4
4897	0.32	3.504	0.47	4.431	46.9	26.5

*** Air temperature at center of a 750-W microwave oven at end of treatment was 55°C.**
**** Air temperature at center of a 1000-W microwave oven at end of treatment was 195°C.**

the best estimate of the long-term aging effects, and (b) aging with microwave energy is extremely simple and rapid (less than 3 hr).

ACKNOWLEDGMENTS

This work was accomplished in cooperation with FHWA and its Kansas division. Thanks are due to Cheh Lim and Donna Mahoney for carrying out some experiments and entering the text on word processors.

REFERENCES

1. Harris, D. C. *Quantitative Chemical Analysis.* W. H. Freeman and Co., San Francisco, 1982, pp. 467–512.
2. Clark, G. L. *Encyclopedia of Chemistry,* 2nd ed. Van Nostrand Reinhold Company, New York, 1966.
3. Al-Ohaly, A. A., and R. L. Terrel. Effect of Microwave Heating on Adhesion and Moisture Damage of Asphalt Mixtures. In *Transportation Research Record 1171,* TRB, National Research Council, Washington, D.C., 1988, pp. 27–36.
4. Von Hippel, A. R. *Dielectric Materials and Applications.* John Wiley, and Sons, Inc., New York, 1954.
5. Robertson, R. E., J. F. Branthaver, and J. C. Petersen. Development of a Performance Related Chemical Model of Petroleum Asphalt for SHRP. 204th American Chemical Society National Meeting, Washington, D.C., Aug. 23 to 28, 1992, Division of Fuel Chemistry, Vol. 37, No. 3, pp. 1272–1278.
6. Billmeyer, F. W. *Polymer Science,* 3rd ed. Wiley-Interscience, New York, 1984, pp. 12–18.
7. Bishara, S. W., R. L. McReynolds, and E. R. Lewis. Interrelationship Between Performance-Related Properties of Asphalt Cement and Their Correlation with Molecular Size Distribution. In *Transportation Research Record 1323,* TRB, National Research Council, Washington, D.C., 1991, pp. 1–9.
8. Bishara, S. W., and R. L. McReynolds. Correlation Between Performance Related Characteristics of Asphalt Cement and Its Physicochemical Parameters Using Corbett's Fractions and HPGPC. In *Transportation Research Record 1342,* TRB, National Research Council, Washington, D.C., 1992, pp. 35–49.
9. Bishara, S. W., and R. L. McReynolds. Gravimetric Determination of Molecular Size Distribution of Asphalt Using HPGPC. Overcoming Problems Associated with Column Source. Presented at 30th Annual Petersen Asphalt Research Conference, Laramie, Wyo., July 12 to 14, 1993.
10. Donaldsen, G. R., M. W. Hlavinka, J. A. Bullin, C. J. Glover, and R. R. Davison. The Use of Toluene as a Carrier Solvent for Gel Permeation Chromatography Analysis of Asphalt. *Journal of Liquid Chromatography,* Vol. 11, 1988, pp. 749–765.
11. Branthaver, J. F., J. J. Duvall, and J. C. Petersen. Separation of SHRP Asphalts by Preparative Size Exclusion Chromatography. 200th American Chemical Society National Meeting, Washington, D.C., Aug. 26 to 31, 1990, Division of Petroleum Chemistry, Vol. 35, No. 3, pp. 407–414.
12. Branthaver, J. F., J. J. Duvall, J. C. Petersen, H. Plancher, and R. E. Robertson. Preparative Size Exclusion Chromatography Separation of SHRP Asphalts: Correlation with Viscoelastic Properties. *Fuel*

Science and Technology International, Vol. 10, Nos. 4–6, 1992, pp. 1003–1032.

13. Neas, E. D., and M. J. Collins. *Introduction to Microwave Sample Preparation* (H. M. Kingston and L. B. Jassie, eds.), American Chemical Society, Washington, D.C., 1988.
14. Ferry, J. D. *Viscoelastic Properties of Polymers.* John Wiley and Sons, Inc., New York, 1980.
15. Bishara, S. W., and R. L. McReynolds. The Use of HPGPC for Determination of MWD of Asphalt Cement—A Spectrophotometric vs. Gravimetric Finish. 200th American Chemical Society National Meeting, Washington, D.C., Aug. 26 to 31, 1990, Division of Petroleum Chemistry, Vol. 35, No. 3, pp. 396–406.
16. Brule, B. *Contribution of Gel Permeation Chromatography (GPC) to the Characterization of Polymers and Related Materials II* (J. Cazes and X. Delamare, eds.), Marcel Dekker, Inc., New York, 1980, pp. 215–248.
17. Bartle, K. D., M. Burke, D. G. Mills, S. Pape, and S. L. Lu. New Chromatographic Methods for Asphalt Analysis. 200th American Chemical Society National Meeting, Washington, D.C., Aug. 26 to 31, 1990, Division of Petroleum Chemistry, Vol. 35, No. 3, pp. 415–420.

Evaluation of Laboratory Methods Simulating Aging Effects of Asphalt Binder

CHAYATAN J. PHROMSORN AND THOMAS W. KENNEDY

The effects of short-term and long-term aging are important when evaluating the properties of asphalt binder. Thus, the properties of asphalts aged for the short term and the long term are considered in the Superpave binder specification. The most practical way of predicting the effects of aging within an asphalt binder is through laboratory simulation methods. For many years the thin film oven test (TFOT) method and the rolling thin film oven test (RTFOT) method have been used to simulate short-term aging. To simulate long-term aging the pressure aging vessel (PAV) method was developed within the Strategic Highway Research Program. However, the Superpave binder specification uses only the RTFOT method for short-term aging and uses RTFOT along with the PAV method for long-term aging. For a short period of time AASHTO considered the use of either the TFOT method or the RTFOT method and then the PAV long-term aging procedure for short-term aging. Unfortunately, few published data address this issue. The test data from a testing program conducted to evaluate these laboratory procedures for short-term and long-term aging with different asphalt binders are presented. The effects of aging are evaluated by dynamic shear stiffness ($G^*\sin\delta$), measured by using the dynamic shear rheometer at three intermediate temperatures. The data indicate that there are no significant differences at the 95 percent confidence interval between the properties of RTFOT-aged residues and those of TFOT-aged residues after exposure to the PAV procedure. The differences before aging by the PAV procedure, however, still exist. It is recommended that only one short-term aging procedure be used for the Superpave binder specification and that work be conducted to develop or improve the short-term aging procedure.

Aging of asphalt binder causes increased stiffness of the asphalt because of volatilization and oxidation when the thin film of the asphalt binder is subjected to high temperatures during construction. Additional aging will occur after construction, primarily because of oxidation. The extent of this long-term aging depends on the crude source, degree of compaction, and temperature. Although the increase in stiffness will increase the resistance to rutting, the increased stiffness and the increased brittleness reduce the resistance to cracking and raveling (*1*).

Because asphalt binders produced from different petroleum crudes and by different refinery techniques have different aging characteristics, it is necessary to specify or control the aging characteristics of the asphalt binders used for paving. The most practical way to estimate the aging characteristics of an asphalt binder is to simulate aging by laboratory methods. Since aging can take place during two stages in pavement life, these methods must consider both short-term and long-term aging. Short-term aging occurs during the manufacturing of asphalt paving mixtures and the subsequent laying down and compaction; long-term aging continues as a result of exposure to oxygen at moderate temperatures.

Department of Civil Engineering, University of Texas at Austin, Austin, Tex. 78712-1076.

For many years the thin film oven test (TFOT) method (ASTM D-1754, AASHTO-T179), the rolling thin film oven test (RTFOT) method (ASTM D-2872, AASHTO-T240), and variations of these procedures have been used to simulate short-term aging. In addition, a long-term aging procedure was developed in the late 1960s (*2,3*). By this long-term aging method the asphalt was subjected to an elevated temperature and pressure in the presence of oxygen. During development of the Superpave binder specification by the Strategic Highway Research Program (SHRP) it was decided to adopt one of the standard short-term aging procedures. Early in the program a decision was made to adopt and further develop and validate the long-term pressure aging procedure. Thus, the final specifications required the use of the RTFOT method for short-term aging and the pressure aging vessel (PAV) procedure for long-term aging.

With regard to the two short-term aging procedures, it is often assumed by many users that the two methods are interchangeable and, thus, that either could be used in the Superpave specification. For a short period of time, AASHTO considered the use of either the TFOT method or the RTFOT method for short-term aging, this was followed by the use of the PAV long-term aging procedure (*4, 5*). To date, unfortunately, little work has been conducted to evaluate whether Superpave binder properties are significantly different for short-term-aged asphalts by the RTFOT method or the TFOT method and the effect of each short-term aging procedure on the properties of the asphalt binder after long-term aging.

A rather extensive evaluation, however, was reported by Zupanick (*6*), who made conclusions based on each of four commonly used aging ratios: viscosity ratio at 60°C (140°F), viscosity ratio at 135°C (275°F), percent retained penetration at 25°C (77°F), and percent weight change. He found that the RTFOT test is somewhat more precise and severe than the TFOT test. He also confirmed that these two tests are not identical. In addition, because of skin formation in the TFOT test, he believed that the RTFOT test is the better of the two tests for simulating hot-mix plant aging.

The purpose of this paper is to report on a testing program conducted to evaluate these laboratory aging procedures for short-term and long-term aging by using different asphalt binders.

EXPERIMENT DESIGN

The experiment involved 10 asphalt binder types, two short-term aging methods, one long-term aging method, and three testing temperatures. Six of 10 asphalt binder types were unmodified asphalts, and 4 were modified asphalts.

The six asphalts used in the study were from the SHRP Material Reference Library and are described in Table 1. The aging index, which is the ratio of the viscosity at 60°C (140°F) after TFOT to that before TFOT, was used as the criterion of selection. Two asphalts

TABLE 1 Selective Asphalt Binders from SHRP Material Reference Library Used

Unmodified Asphalt	PG-grade	Source	Aging Sensitivity	Aging Index
AAD-1 (AR-4000)	58-28	California	HIGH	3.24
AAK-1 (AC-30)	64-22	Boscan	HIGH	2.98
AAB-1 (AC-10)	58-22	Wyoming	INTERMEDIATE	2.31
AAS-2 (AC-10)	58-28	Middle East (Arab)	INTERMEDIATE	2.25
AAG-1 (AR-4000)	58-10	California Valley	LOW	1.75
AAZ (AC-20)	58-16	West Texas	LOW	1.65

Modified Asphalt	Modifier type
AAG-1 + SBS	Styrene-Butadiene Styrene Block Copolymer
AAK-1 + SBS	Styrene-Butadiene Styrene Block Copolymer
AAG-1 + PE	Polyethylene
AAK-1 + PE	Polyethylene

had high aging indexes, two had low values, and two had intermediate values. In addition, two stiff (high-viscosity) asphalt cements from those selected were added to modifiers such as styrene-butadiene styrene block copolymer and polyethylene.

The short-term aging procedures used were the TFOT method and the RTFOT method. The long-term aging procedure used was the PAV method. All long-term-aged specimens were first short-term aged by the RTFOT method or the TFOT method. The effects of aging were evaluated in terms of dynamic shear stiffness, ($G^*\sin\delta$) where G^* is the complex shear modulus and δ is the phase angle), measured with a dynamic shear rheometer (DSR) at three intermediate temperatures (20°C, 25°C, and 30°C). $G^*\sin\delta$ is the parameter used in the new SHRP performance-based binder specification for controlling the properties of long-term-aged asphalt binder. Four replicates of each cell of testing (Table 2) were performed, and the averages and standard deviations were calculated. Residues aged over the short term by the RTFOT method and the TFOT method were tested and compared (Table 3). Residues aged over the long term by the RTFOT method and the TFOT method and then the PAV aging procedure were also tested (Table 4).

SHORT-TERM AGING

Both the TFOT method and the RTFOT method were used for short-term aging.

TFOT Method

The TFOT aging technique is conducted by placing a 50-g sample of asphalt binder in a cylindrical flat-bottom pan producing an approximate 3.2-mm (1/8-in.) asphalt binder layer. The pan containing the asphalt binder sample is transferred to a shelf in a ventilated oven maintained at 163°C (325°F). The shelf can carry four pans at a time and rotates at a rate of 5 to 6 rpm. The sample is kept in the oven for 5 hr. In the present study the samples either were tested with the DSR or were transferred to PAV pans for long-term aging.

RTFOT Method

The RTFOT aging technique involves placing 35 g of asphalt into a bottle, which is placed in a rack within an electrically heated convection oven. The oven contains a vertical circular carriage that contains holes to accommodate sample bottles. The carriage is mechanically driven and rotates about its center. The oven also contains an air jet that is positioned to blow air into each sample bottle at its lowest travel position. During the test the sample is required to remain in the oven at a temperature of 163°C (325°F) for 85 min. In the present study the aged samples either were tested with the DSR or were transferred to PAV pans for long-term aging.

LONG-TERM AGING

The pressure aging procedure, developed by SHRP from previous work (2), simulates the long-term aging that asphalt experiences in service. The apparatus consists of the PAV and a temperature chamber. Air pressure is provided by a cylinder of dry, clean compressed air with a pressure regulator, release valve, and a slow-release bleed valve.

The pressure vessel is fabricated from stainless steel and is designed to operate under the pressure (2070 kPa) and temperature (90°C, 100°C, or 110°C) of the test. The vessel can accommodate 10 stainless steel TFOT sample pans at one time. A forced draft oven is used as a temperature chamber. The oven must control temperature to within a 0.2°C range for 20 hr. A digital readout connected to a platinum-resistant thermometer is used to control the internal vessel temperature. During the test the pans loaded

TABLE 2 Experiment Design

TEST EQUIPMENT		DYNAMIC SHEAR RHEOMETER											
TEST TEMPERATURE		20 °C				25 °C				30 °C			
AGING METHOD		TFOT	RTFOT	TFOT+ PAV	RTFOT+ PAV	TFOT	RTFOT	TFOT+ PAV	RTFOT+ PAV	TFOT	RTFOT	TFOT+ PAV	RTFOT+ PAV
SAMPLE													
UNMODIFIED	AAD-1	4	4	4	4	4	4	4	4	4	4	4	4
	AAK-1	4	4	4	4	4	4	4	4	4	4	4	4
	AAB-1	4	4	4	4	4	4	4	4	4	4	4	4
	AAS-2	4	4	4	4	4	4	4	4	4	4	4	4
	AAG-1	4	4	4	4	4	4	4	4	4	4	4	4
	AAZ	4	4	4	4	4	4	4	4	4	4	4	4
MODIFIED	AAG-1+SBS	4	4	4	4	4	4	4	4	4	4	4	4
	AAK-1+SBS	4	4	4	4	4	4	4	4	4	4	4	4
	AAG-1+PE	4	4	4	4	4	4	4	4	4	4	4	4
	AAK-1+PE	4	4	4	4	4	4	4	4	4	4	4	4
											TOTAL	=	480

with short-term-aged residue are placed in the vessel, and the vessel is then loaded into the temperature chamber to which the pressure hose and temperature transducer are attached. When the temperature is within 2°C of the test temperature, air pressure is slowly applied. When the air pressure and temperature reach 2070 kPa (300 lb/in.^{2}) and the designated temperature the test time begins.

After 20 hr the pressure is slowly released (8 to 10 min) by using the bleed valve to avoid excessive air bubbles in the sample. The pans are removed from the sample holder and are placed in an oven at 150°C for 30 min or less to remove entrapped air from the samples. The samples are then transferred to a single container that can be covered to avoid any contamination if tests to determine dynamic shear modulus are not performed immediately (*4*).

In the present study a temperature of 100°C was used, which is recommended for most of the United States.

DYNAMIC SHEAR STIFFNESS EVALUATION METHOD

The dynamic shear stiffness (G^* sin δ), which is used to control the properties of short-term- and long-term-aged asphalt binder in the Superpave binder specification, was used as an evaluation property in the present study. This value was determined at temperatures of 20°C, 25°C, and 30°C with the DSR (model CS of Bohlin) at a constant frequency of 10 rad/sec. A constant stress mode was used.

The testing system applies a selected constant oscillating stress (linear viscoelastic range) to a 2-mm asphalt disk sandwiched between the oscillating spindle 8 mm in diameter and the fixed base. The resulting strain is measured. From the shear stress and strain data obtained by the testing system, the complex shear modulus (G^*) and the phase angle (δ) can be estimated and the dynamic shear stiffness (G^*sin δ) can be calculated.

ANALYSIS OF RESULTS

The results of the dynamic shear stiffness evaluation, measured from both short-term-aged and long-term-aged specimens, are summarized in Tables 3 and 4, respectively.

Two statistical analyses were conducted to compare the test data for residues measured by the TFOT method before and after the PAV procedure and those measured by the RTFOT method before and after the PAV procedure. A paired *t*-test (*7*) was conducted to examine the differences between the two short-term aging methods both before and after long-term aging by the PAV procedure. The results of the analysis are given in Tables 5, 6, and 7. In addition, a *t*-test (*7,8*) was used to test hypotheses concerning whether there were significant differences between the properties for individual asphalt binders that were aged by the RTFOT method or the TFOT method and whether the two short-term aging procedures produced significant effects on the properties of the long-term-aged asphalt

TABLE 3 Comparison of Dynamic Shear Stiffness Data Between Two Short-Term Aging Methods

TEST TEMPERATURE		20 °C						25 °C						30 °C					
		TFOT		RTFOT		%		TFOT		RTFOT		%		TFOT		RTFOT		%	
	SAMPLE	G*sin delta (MPa)	RSD	G*sin delta (MPa)	RSD	Difference		G*sin delta (MPa)	RSD	G*sin delta (MPa)	RSD	Difference		G*sin delta (MPa)	RSD	G*sin delta (MPa)	RSD	Difference	
UNMODIFIED	AAD-1	1.04	3%	1.28	9%	23.60%	S	0.46	4%	0.58	9%	25.00%	S	0.21	2%	0.26	9%	22.90%	S
	AAK-1	2.39	4%	2.96	6%	24.10%	S	1.14	4%	1.45	7%	26.90%	S	0.54	4%	0.69	7%	27.30%	S
	AAB-1	1.72	4%	1.84	7%	7.00%	NS	0.86	5%	0.94	5%	8.40%	S	0.40	6%	0.44	5%	10.00%	NS
	AAS-2	0.90	8%	1.15	7%	28.50%	S	0.44	8%	0.57	9%	31.60%	S	0.20	6%	0.27	8%	33.30%	S
	AAG-1	7.18	7%	9.05	5%	26.00%	S	2.54	6%	3.48	6%	37.00%	S	0.85	6%	1.23	6%	44.00%	S
	AAZ	4.19	2%	5.32	5%	26.90%	S	1.76	3%	2.27	5%	29.00%	S	0.69	2%	0.90	5%	30.00%	S
MODIFIED	AAG-1+SBS	4.68	7%	5.18	7%	10.60%	NS	1.69	7%	1.94	7%	14.84%	S	0.61	6%	0.70	6%	15.20%	S
	AAK-1+SBS	1.72	6%	2.23	10%	29.70%	S	0.93	5%	1.28	11%	38.00%	S	0.50	6%	0.66	8%	33.80%	S
	AAG-1+PE	10.73	9%	12.85	4%	19.70%	S	4.71	6%	5.81	4%	23.40%	S	1.91	5%	2.39	5%	25.50%	S
	AAK-1+PE	3.55	7%	5.14	5%	44.55%	S	1.77	6%	2.70	5%	52.62%	S	0.85	5%	1.33	5%	57.69%	S

S means "There are significant differences between TFO method and RTFO method at 95% confidence interval"

NS means " There is no significant difference between TFO method and RTFO method at 95% confidence interval"

RSD means "The coefficient of variation (the ratio of standard deviation and mean)"

TABLE 4 Comparison of Dynamic Shear Stiffness Data Between Two Long-Term Aging Methods

TEST TEMPERATURE		20 °C						25 °C						30 °C					
		TFOT+PAV		RTFOT+PAV		%		TFOT+PAV		RTFOT+PAV		%		TFOT+PAV		RTFOT+PAV		%	
	SAMPLE	G*sin delta (MPa)	RSD	G*sin delta (MPa)	RSD	Difference		G*sin delta (MPa)	RSD	G*sin delta (MPa)	RSD	Difference		G*sin delta (MPa)	RSD	G*sin delta (MPa)	RSD	Difference	
UNMODIFIED	AAD-1	3.00	4%	2.85	3%	5.17%	NS	1.49	3%	1.53	5%	2.20%	NS	0.78	4%	0.84	9%	8.40%	NS
	AAK-1	4.72	1%	4.90	6%	3.80%	NS	2.44	3%	2.67	6%	9.60%	S	1.19	3%	1.36	6%	14.60%	S
	AAB-1	3.67	2%	3.62	7%	1.40%	NS	2.02	9%	1.91	10%	5.10%	NS	1.14	4%	1.12	9%	1.80%	NS
	AAS-2	2.64	1%	2.72	4%	3.30%	NS	1.43	1%	1.47	4%	2.80%	NS	0.74	1%	0.76	3%	2.70%	NS
	AAG-1	14.60	4%	14.56	13%	0.30%	NS	6.51	5%	6.74	15%	3.50%	NS	2.56	5%	2.64	17%	3.30%	NS
	AAZ	8.44	3%	8.45	3%	0.20%	NS	4.29	4%	4.40	3%	2.50%	NS	1.98	5%	2.02	3%	2.00%	NS
MODIFIED	AAG-1+SBS	9.23	6%	9.51	9%	3.00%	NS	4.01	6%	4.19	9%	4.60%	NS	1.58	6%	1.67	10%	5.70%	NS
	AAK-1+SBS	3.94	7%	3.86	6%	2.10%	NS	2.19	7%	2.16	7%	1.50%	NS	1.19	8%	1.15	6%	3.60%	NS
	AAG-1+PE	15.70	4%	18.89	8%	20.30%	S	8.31	5%	10.21	9%	22.90%	S	3.95	10%	4.79	9%	21.20%	S
	AAK-1+PE	6.30	7%	8.22	5%	30.58%	S	3.60	7%	4.92	4%	36.62%	S	1.93	6%	2.74	4%	42.15%	S

S means "There are significant differences between TFO method and RTFO method at 95% confidence interval"

NS means " There is no significant difference between TFO method and RTFO method at 95% confidence interval"

RSD means "The coefficient of variation (the ratio of standard deviation and mean)"

TABLE 5 Paired *t*-Test for Short- and Long-Term Aging Methods at 20°C

Value: G*sin delta (MPa) at 20°C				
Short-term aging methods between TFOT and RTFOT				
Sample	TFOT	RTFOT	Differences	
AAD-1	1.04	1.28	0.24	
AAK-1	2.39	2.96	0.57	
AAB-1	1.72	1.84	0.12	
AAS-2	0.90	1.15	0.25	
AAG-1	7.18	9.05	1.87	
AAZ	4.19	5.32	1.13	
AAG-1+SBS	4.68	5.18	0.50	
AAK-1+SBS	1.72	2.23	0.51	
AAG-1+PE	10.73	12.85	2.12	
AAK-1+PE	3.55	5.14	1.59	
		Mean =	**0.89**	
		Std. =	0.73	
		SQ(Std.) =	0.54	
		t-value =	**3.84**	significant at 95%
		t*(n-1=9) =	2.262	confidence interval
Long-term aging methods between TFOT+PAV and RTFOT+PAV				
Sample	TFOT+PAV	RTFOT+PAV	Differences	
AAD-1	3.00	2.85	-0.15	
AAK-1	4.72	4.90	0.18	
AAB-1	3.67	3.62	-0.05	
AAS-2	2.64	2.72	0.08	
AAG-1	14.60	14.56	-0.04	
AAZ	8.44	8.45	0.01	
AAG-1+SBS	9.23	9.51	0.28	
AAK-1+SBS	3.94	3.86	-0.08	
AAG-1+PE	15.70	18.89	3.19	
AAK-1+PE	6.30	8.22	1.92	
		Mean =	**0.53**	
		Std. =	1.11	
		SQ(Std.) =	1.24	
		t-value =	**1.52**	Not significant at 95%
		t*(n-1=9) =	2.262	confidence interval

TABLE 6 Paired *t*-Test for Short- and Long-Term Aging Methods at 25°C

Value : G* sin delta (MPa) at 25 °C				
Short-term aging methods between TFOT and RTFOT				
Sample	TFOT	RTFOT	Differences	
AAD-1	0.46	0.58	0.12	
AAK-1	1.14	1.45	0.31	
AAB-1	0.86	0.94	0.08	
AAS-2	0.44	0.57	0.13	
AAG-1	2.54	3.48	0.94	
AAZ	1.76	2.27	0.51	
AAG-1+SBS	1.69	1.94	0.25	
AAK-1+SBS	0.93	1.28	0.35	
AAG-1+PE	4.71	5.81	1.10	
AAK-1+PE	1.77	2.70	0.93	
		Mean =	**0.47**	
		Std. =	0.38	
		SQ(Std.) =	0.15	
		t-value =	**3.91**	significant at 95%
		t*(n-1=9) =	2.262	confidence interval
Long-term aging methods between TFOT+PAV and RTFOT+PAV				
Sample	TFOT+PAV	RTFOT+PAV	Differences	
AAD-1	1.49	1.53	0.04	
AAK-1	2.44	2.67	0.23	
AAB-1	2.02	1.91	-0.11	
AAS-2	1.43	1.47	0.04	
AAG-1	6.51	6.74	0.23	
AAZ	4.29	4.40	0.11	
AAG-1+SBS	4.01	4.19	0.18	
AAK-1+SBS	2.19	2.16	-0.03	
AAG-1+PE	8.31	10.21	1.90	
AAK-1+PE	3.60	4.92	1.32	
		Mean =	**0.39**	
		Std. =	0.67	
		SQ(Std.) =	0.44	
		t-value =	**1.86**	Not significant at 95%
		t*(n-1=9) =	2.262	confidence interval

binders. The results of this analysis are summarized in Tables 3 and 4. A significance level of 5 percent, or a 95 percent confidence interval, was used for all statistical analyses in the study.

Short-Term Aging

The data presented in Table 3 show that the RTFOT method is more severe in terms of aging than the TFOT method for all test specimens. Although the TFOT method might be expected to produce more variability in the test results because of skin formation of the asphalt binder (*6*), the data from the present study indicate that the coefficients of variation or the relative standard deviations (RSDs) for the TFOT method are equal to or less than those for the RTFOT method for most asphalt binders. The results of the paired *t*-test, presented in Tables 5, 6, and 7, confirmed that there were significant differences between the two short-term aging methods. In addition, a comparison of the individual asphalt binders indicated that significant differences between the properties of the TFOT-aged residues and the RTFOT-aged residues were found in 8 of 10 test binders at 20°C, 10 of 10 test binders at 25°C, and 9 of 10 test binders at 30°C (Table 3).

Long-Term Aging

The data presented in Table 4 and the graphs in Figures 1 through 3 indicate that the PAV long-term aging process reduced the differences in the properties produced by the TFOT and the RTFOT methods of short-term aging. The stiffness of long-term-aged residues obtained from two different short-term aging processes become very similar. Results of the paired *t*-test analyses presented in Tables 5, 6, and 7 indicated that there was no significant difference between the properties of RTFOT-aged residues and those of TFOT-aged residues after exposure to the PAV aging procedure. Nevertheless, the *t*-test analyses of the properties of the individual asphalt binders indicated that there were significant differences for 3 of the 10 test binders at 25°C and 30°C and 2 of the 10 test binders at 20°C (Table 4). It was also found that there was a significant effect for the polyethylene-modified asphalt binder. After exposure to the PAV aging procedure, this binder tended to separate and a skin was observed on the surface of the binder in the pan.

CONCLUSIONS

The following conclusions can be drawn from the results of the present study:

1. For short-term aging, the RTFOT method produced more severe aging than the TFOT method for both unmodified and modified asphalt binders. These differences in properties were significant at the 95 percent confidence interval.

TABLE 7 Paired *t*-Test for Short- and Long-Term Aging Methods at 30°C

Value : G* sin delta (MPa) at 30°C				
Short-term aging methods between TFOT and RTFOT				
Sample	TFOT	RTFOT	Differences	
AAD-1	0.21	0.26	0.05	
AAK-1	0.54	0.69	0.15	
AAB-1	0.40	0.44	0.04	
AAS-2	0.20	0.27	0.07	
AAG-1	0.85	1.23	0.38	
AAZ	0.69	0.90	0.21	
AAG-1+SBS	0.61	0.70	0.09	
AAK-1+SBS	0.50	0.66	0.16	
AAG-1+PE	1.91	2.39	0.48	
AAK-1+PE	0.85	1.33	0.48	
		Mean =	**0.21**	
		Std. =	0.17	
		SQ(Std.) =	0.03	
		t-value =	**3.86**	significant at 95%
		t*(n-1=9) =	2.262	confidence interval
Long-term aging methods between TFOT+PAV and RTFOT+PAV				
Sample	TFOT+PAV	RTFOT+PAV	Differences	
AAD-1	0.78	0.84	0.06	
AAK-1	1.19	1.36	0.17	
AAB-1	1.14	1.12	-0.02	
AAS-2	0.74	0.76	0.02	
AAG-1	2.56	2.64	0.08	
AAZ	1.98	2.02	0.04	
AAG-1+SBS	1.58	1.67	0.09	
AAK-1+SBS	1.19	1.15	-0.04	
AAG-1+PE	3.95	4.79	0.84	
AAK-1+PE	1.93	2.74	0.81	
		Mean =	**0.21**	
		Std. =	0.33	
		SQ(Std.) =	0.11	
		t-value =	**1.95**	Not significant at 95%
		t*(n-1=9) =	2.262	confidence interval

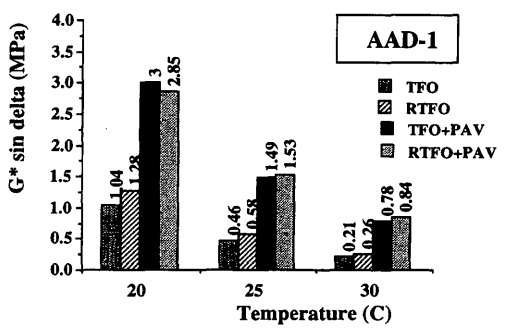

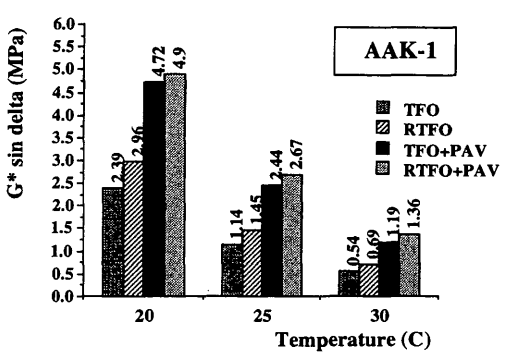

FIGURE 1 Dynamic shear stiffnesses of two high-aging-index asphalts after short- and long-term aging.

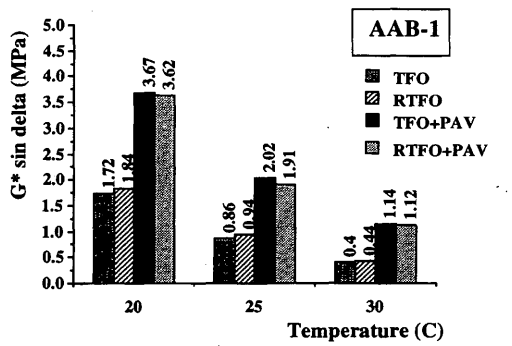

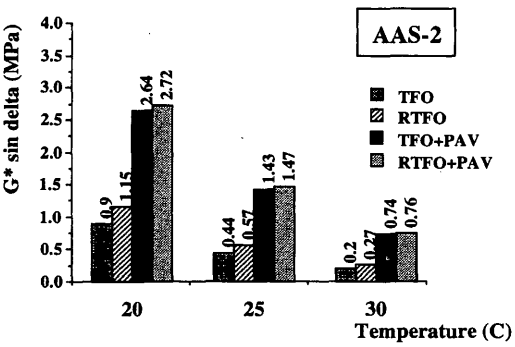

FIGURE 2 Dynamic shear stiffnesses of two intermediate-aging-index asphalts after short- and long-term aging.

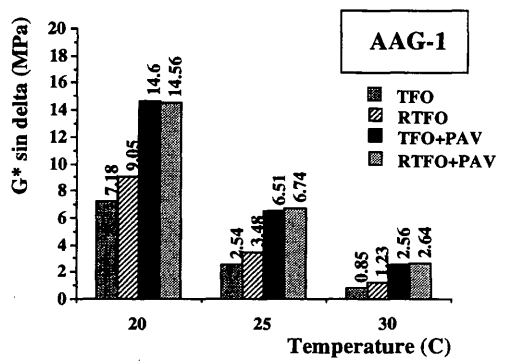

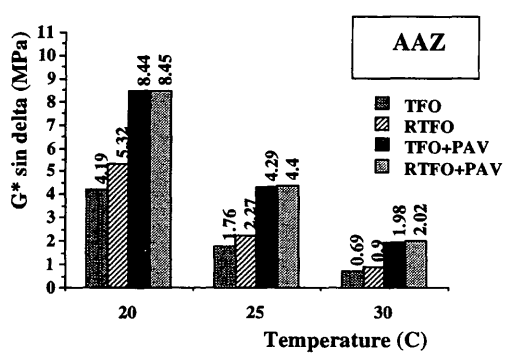

FIGURE 3 Dynamic shear stiffness of two low-aging-index asphalts after short- and long-term aging.

2. Based on the results of the study the TFOT and RTFOT methods should not be used interchangeably for short-term aging.

3. Long-term (PAV) aging reduced the differences in the properties of asphalts over the long term produced by the TFOT and the RTFOT methods of short-term aging. The differences were not significant at the 95 percent confidence interval.

4. There was a significant difference for the PAV-aged polyethylene-modified asphalt binders and for some of the asphalt binders.

5. The study showed that the TFOT method of short-term aging produces less variability than the RTFOT method in most asphalt binders both before and after long-term aging by the PAV procedure.

6. Because of differences or potential differences only one method of short-term aging should be used for the Superpave binder specification.

7. It is recommended that a new or modified short-term aging procedure be developed.

REFERENCES

1. Vallerga, B. A. Pavement Deficiencies Related to Asphalt Durability. *Proc., Association of Asphalt Pavement Technologists,* Vol. 50, 1981, pp. 481–491.
2. Lee, D. Y. Development of a Laboratory Durability Test for Asphalts. In *Highway Research Record 231,* HRB, National Research Council, Washington, D.C., 1968.
3. Bell, C. A. *Aging of Asphalt-Aggregate Systems.* Summary Report SHRP-A/IR-89–004. SHRP, National Research Council, Washington, D.C., 1989.
4. *The Superpave Mix Design System, Manual of Specifications, Test Methods and Practices.* Report SHRP-A-379. SHRP, National Research Council, Washington, D.C., 1994.
5. *Standard Practice for Grading or Verifying the Performance Grade of an Asphalt Binder.* AASHTO-PP-6. AASHTO, 1993.
6. Zupanick, M. Comparison of the Thin Film Oven Test and the Rolling Thin Film Oven Test. *Proc., Association of Asphalt Pavement Technologists,* Vol. 63, 1994.
7. John, P. W. M. *Statistical Methods in Engineering and Quality Assurance.* John Wiley and Sons, Inc., New York, 1990.
8. Hays, W. L. *Statistics,* 4th ed. Holt, Rinehart and Winston, Inc., Orlando, Fla., 1988.

Characterization of Crumb Rubber-Modified Binder Using Strategic Highway Research Program Technology

DOUGLAS I. HANSON AND GREGORY M. DUNCAN

The objective of the study was to characterize several different types of crumb rubber-modified binders and to develop information relating their properties. Different concentrations, gradations, and asphalt cement sources were evaluated to determine what effect these had on the properties of the modified binders. The asphalt cement and rubber were reacted at 177°C (350°F) until the stiffness had reached a maximum level. Tests were performed to evaluate both the reaction properties and the final properties of the binders. The concentration was found to have the largest effect on the final properties of the binders. The asphalt cements used in the study had little effect on the rubber-asphalt cement reaction. Strategic Highway Research Program (SHRP) binder properties indicated that the asphalt rubber binder performed better than an AC-20 asphalt cement used for comparison. Conventional asphalt tests were also performed on the mature binders. The softening point was found to produce results similar to those of the SHRP tests and may offer a method for field verification for asphalt rubber binders.

Since the enactment of 1038B of the Intermodal Surface Transportation Efficiency Act the use of crumb rubber-modified asphalt cements has become a topic of increased interest to the transportation industry. Insufficient information is available to make well-founded decisions regarding the use and properties of crumb rubber-modified asphalt cements. Mix properties as well as binder properties are needed to evaluate different sizes of rubber, asphalt type, and the concentration of rubber that could optimize the properties of hot-mix asphalt (HMA).

OBJECTIVE

The objective of the National Center for Asphalt Technology (NCAT) crumb rubber study was to evaluate the use of crumb rubber-modified binders for use in HMA pavements.

SCOPE

The study used conventional asphalt cement binder tests and the Strategic Highway Research Program (SHRP) asphalt cement binder tests to evaluate changes in the properties of the modified binder created by the addition of crumb rubber modifier. The factors evaluated were asphalt cement supplier, size and gradation of the rubber particles, and concentration of rubber added. Two sources of AC-10 asphalt cement were evaluated with four different gradations of rubber. Five different concentrations of each gradation, including the zero concentration, were evaluated with each asphalt cement source. An AC-20 asphalt cement was also included in the study for comparison. The actual tests used to evaluate the binders are discussed further in the section Plan of Study.

The mix portion of the study addressed fatigue and rut resistance of crumb rubber-modified asphalt in a densely graded aggregate HMA. This paper presents the results of only the binder phase of the overall study.

D. I. Hanson, National Center for Asphalt Technology, 211 Ramsay Hall, Auburn University, Auburn, Ala. 36849-5354. G. M. Duncan, Tennessee Department of Transportation, Nashville, Tenn. 37209.

PLAN OF STUDY

The study was broken into a matrix of four gradations of rubber, five concentrations of rubber, two sources of AC-10, and one source of AC-20. Table 1 provides a schedule of the binders that were tested during the study. A binder consisted of one concentration of a particular gradation of rubber being mixed with a specific AC-10. The rubber concentrations chosen were 0, 5, 10, 15, and 20 percent by weight of asphalt cement. Zero percent was considered to be a control binder for each asphalt cement type. The gradations of rubber chosen were GF16, GF40, GF80, and GF120, as provided by Rouse Rubber Company of Vicksburg, Mississippi. The GF number represents the nominal maximum sieve size of the rubber. Results of particle size analysis for the rubber are given in Table 2. An AC-20 was chosen as a control to represent a binder currently used in many parts of the country and for which these rubber-modified binders may be a replacement.

The tests chosen to characterize the asphalt rubber binders are given in Figure 1 and are discussed in the following sections.

Brookfield Viscometer

Since the conventional capillary viscometers have been shown to be inappropriate for use in evaluating crumb rubber particles suspended in asphalt, the Brookfield rotational viscometer was chosen (*1*). The rotational viscometer was applicable for the binder with suspended particles and was also viewed as a possible method of field verification for the binders (*2*). The viscometer was used to monitor the reaction of the asphalt cement with the rubber particles at 177°C (350°F). As the reaction continued the viscosity rose to a peak and leveled at that point or slightly below that peak.

Dynamic Shear Rheometer

The dynamic shear rheometer (DSR), like the Brookfield viscometer, was used to characterize the binders as the reaction between the rubber and the asphalt took place. The DSR was also used to char-

TABLE 1 Crumb Rubber Binder Schedule

Base Asphalt	Concentration	GF16	GF40	GF80	GF120
AC-10-A	0%	X			
	5%	X	X	X	X
	10%	X	X	X	X
	15%	X	X	X	X
	20%	X	X	X	X
AC-10-B	0%	X			
	5%	X	X	X	X
	10%	X	X	X	X
	15%	X	X	X	X
	20%	X	X	X	X
AC-20-C	0%	X			

acterize the binders in their final original stage, after the thin film oven (TFO) aging and after aging in the pressure aging vessel (PAV). The "original" stage refers to a completely reacted asphalt rubber binder before any of the aging techniques. The DSR tests were conducted according to AASHTO Provisional Standard TP5 (*3*) with one deviation. The gap used with the 25-mm plate was set at 2 mm so that any large rubber particles would not interfere with the test. The gap normally used with asphalt cement is 1 mm (*3*). The original and TFO test (TFOT) binders were tested at 52°C, 58°C, 64°C, 70°C, and 76°C. A complex modulus reaction curve was gathered at 55°C to be consistent with data that were collected previously under SHRP specification 7G. The material tested after treatment by PAV and TFOT was characterized at lower temperatures by using the 8-mm spindle and a 2-mm gap. The temperatures selected for this stage of testing were 7°C, 13°C, 19°C, 25°C, and 31°C. These temperatures were chosen because most of the United States is characterized by climates with these temperatures.

Bending Beam Rheometer

The bending beam rheometer (BBR) was chosen to evaluate the cold temperature properties of the binders. BBR test were performed in accordance with AASHTO TP1 (*3*). The temperatures selected for the BBR tests were −12°C and −24°C. This range of temperatures is typical of areas that now use AC-10 and AC-20 asphalt cements.

Direct Tension

The direct-tension (DT) tester was also used to evaluate the cold temperature properties of the binders. The DT tests were performed according to AASHTO TP3 (*3*). The same temperatures used in the BBR tests (−12°C and −24°C) were used in the DT tests to remain consistent.

Penetration and Softening Point

Penetration and softening point tests are being used in many states to specify a crumb rubber-modified binder. Therefore, penetration and softening point testing was included to tie the characteristics of these binders to the current data base. These tests were performed according to ASTM D5 and AASHTO T53–91, respectively.

TABLE 2 Particle Size Analysis of Crumb Rubber Modifier

Sieve No.	Percent Passing			
	GF16	GF40	GF80	GF120
10	100	100	100	100
16	95.5	100	100	100
20	75.0	100	100	100
30	56.5	95.0	90.9	100
40	39.5	90.9	83.1	100
80	6.4	20.7	28.0	95.0
100	3.0	13.2	21.0	94.6
120	–	9.0	16.1	87.0
140	–	7.0	12.1	80.2

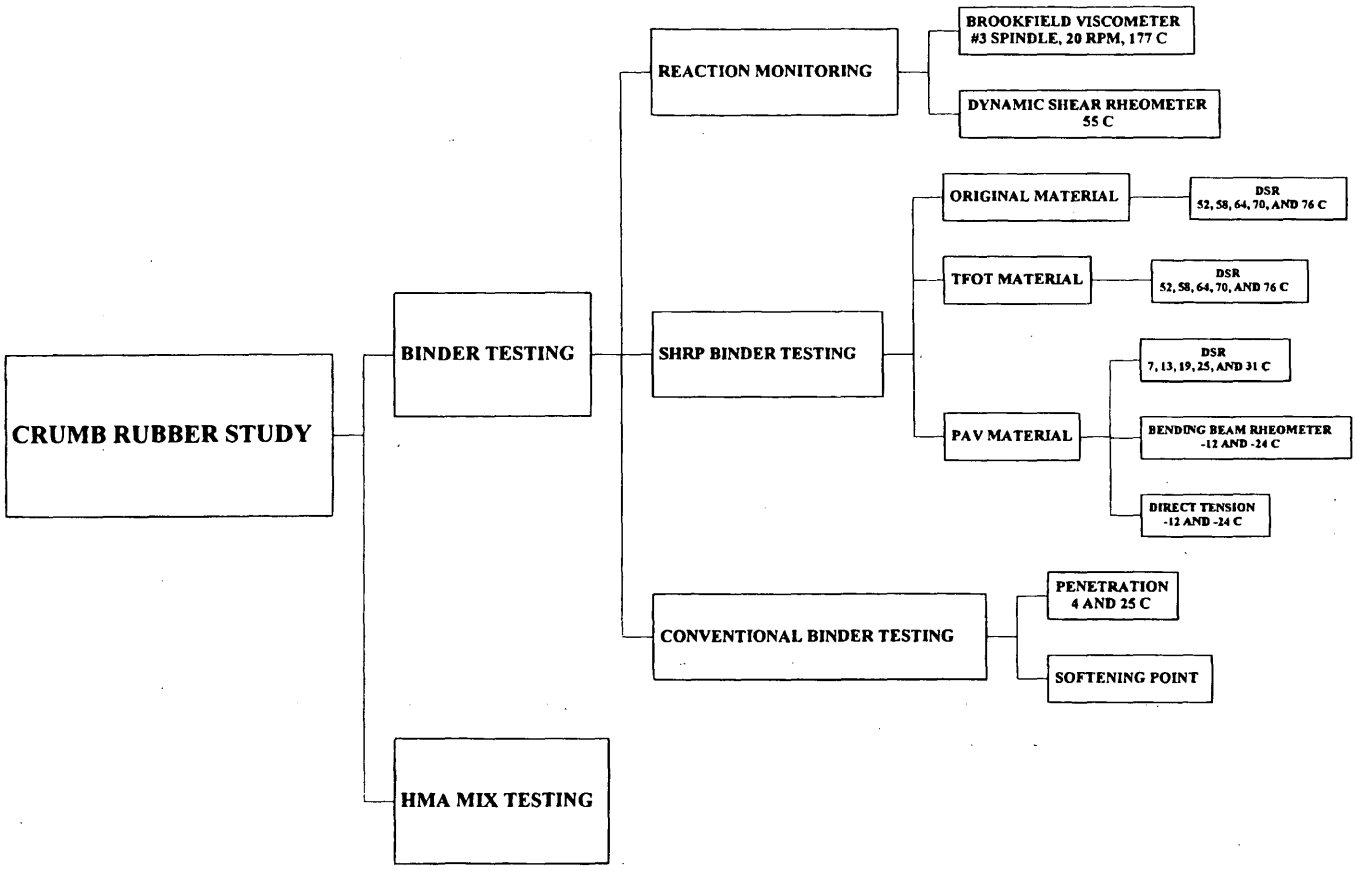

FIGURE 1 Test schedule for binder portion of crumb rubber study.

RESULTS AND DISCUSSION OF RESULTS

Binder Testing

The asphalt rubber binder was prepared by heating the base AC-10 to 177°C (350°F) in an asphalt dispensing pot. The corresponding percentage of dry crumb rubber was added by weight of asphalt cement. After the rubber was added to the asphalt cement the stiffness of the mixture will rise. There was an initial increase in the stiffness of the mixture that dealt with suspending solid particles in a fluid. However, the stiffness continues to rise, indicating that some sort of reaction is taking place.

Reaction Monitoring

The stiffness with time was measured by using the Brookfield viscometer and DSR. The stiffness increased for 2 to 5 hr and then began to decrease slightly. The reaction was monitored until a stiffness peak was noted and confirmed with another test.

Brookfield Viscosity

Viscosity curves for different concentrations of GF80 with AC-10-A are presented in Figure 2 as a typical plot for any given size. The increase in viscosity for increased percentages of rubber is typical for all of the different gradations and asphalt cement types used in the present study.

The procedure for the measurement of viscosity was to use the Brookfield RV series no. 3 spindle at 20 rotations per minute with the Brookfield DV-III viscometer. At several points in the reaction the spindle was lowered into the well-blended binder for 1 min with no rotation to allow the temperature to calibrate. The rotations were begun (time zero), and the first viscosity reading was taken at 1 min, the next one was taken at 2 min, and the third one was taken at 3 min. The three readings were averaged to obtain a viscosity at that average time in the reaction. Four to 10 viscosity tests were performed on each binder during the reaction process. It was noticed early in the testing that after the spindle began rotating the viscosity would continually drop. It is believed by the researchers that the rubber particles were being centrifugally forced away from the spindle so that the rubber concentration in the fluid being measured was lower than that in the entire mixture. Therefore, the viscometer procedure presented earlier was followed rigorously to avoid inconsistencies.

No clear trend in the data was found regarding the effect of gradation on the reaction rate of the binders. The datum points showed extensive scatter. Several conditions contributed to the high scatter of the points, including different operators, difficulty in maintaining temperature, and the method and amount of mixing done to the binder before the measurement of viscosity.

DSR

Slightly before or slightly after the viscosity of the binder was determined, a sample was taken for testing with the DSR. The Bohlin rheometer was used in the constant strain mode to measure the

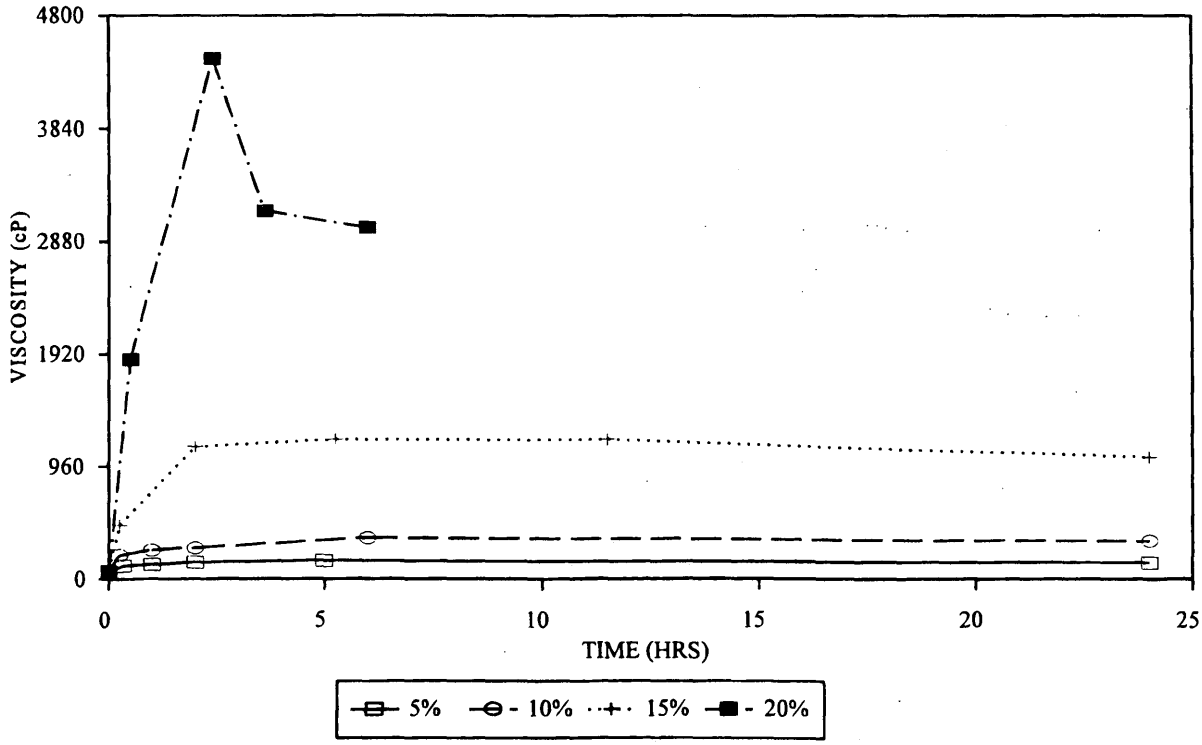

FIGURE 2 Viscosity versus reaction time for AC-10-A with four concentrations of GF80.

complex modulus of the material. The dynamic shear test for reaction observation was performed at 55°C for all binders. This temperature was chosen because when the study began SHRP specification 7G was applicable and 55°C was one of the performance graded specification temperatures.

As with viscosity, the complex modulus rises for 3 to 5 hr, but it then stabilizes or drops slightly. The higher the concentration of rubber, the higher the complex modulus. Again, these test data showed no clear trends regarding differences in reaction rates for different gradations of rubber. The dynamic shear provides a more consistent means of characterizing the reaction of asphalt and crumb rubber, but it is not suited to be a field verification device like the Brookfield viscometer may be.

SHRP Binder Tests

SHRP binder tests were performed on the two base AC-10 asphalt cements, the AC-20 asphalt cement, and the rubber-modified binders to evaluate the rubber-modified binders in comparison with an asphalt cement. The tests performed are indicated in Figure 1. The characterization process began as soon as the binder had reached the mature stage in the reaction, that is, maximum stiffness as measured by the viscometer and the dynamic shear tester. The first step was to evaluate the original binder and to age the material in the TFO. The TFO was used instead of the rolling thin film oven because the asphalt rubber was found to migrate out of the bottles in the rolling thin film oven, resulting in a smoke problem. On completion of the TFOT the dynamic shear test was performed on a sample of the material. The remaining material was placed in the PAV for 20 hr of aging at a pressure of 2.1 MP (300 lb/in.^{2}) and a temperature of 100°C (*3*). After the aging in the PAV was completed the material was removed and the air bubbles were eliminated in accordance with AASHTO procedures. The material was again sampled for testing with the DSR, and specimens for the BBR and DT tester were prepared.

DSR

Characterization of the original material by the DSR showed an increase in the $G^*/\sin\delta$ parameter (where G^* is the complex shear modulus and δ is the phase angle) when rubber was added. Figure 3 shows the original data, with those for AC-20-C also included. The trend for the original data is that stiffness increases with concentration and that there is little variation in $G^*/\sin\delta$ between different gradations of rubber. Figure 3 indicates that there is very little difference between the two asphalt cement types. From Figure 3 most of the asphalt rubber binders met the criteria of $G^*/\sin\delta$ exceeding 1 kPa at 64°C. From Figure 4 there appears to be little difference between the two types of AC-10 for original and TFO- and PAV-aged asphalts. Both of these binders meet the AASHTO criteria in MP1, Standard Specification for Performance Graded Asphalt, and received a grading of PG 58–22. (The -22 portion of the grading will be demonstrated later.) Figure 5 shows the relationship of dynamic shear parameters versus temperature at the different stages of testing. The effect of increasing rubber content can

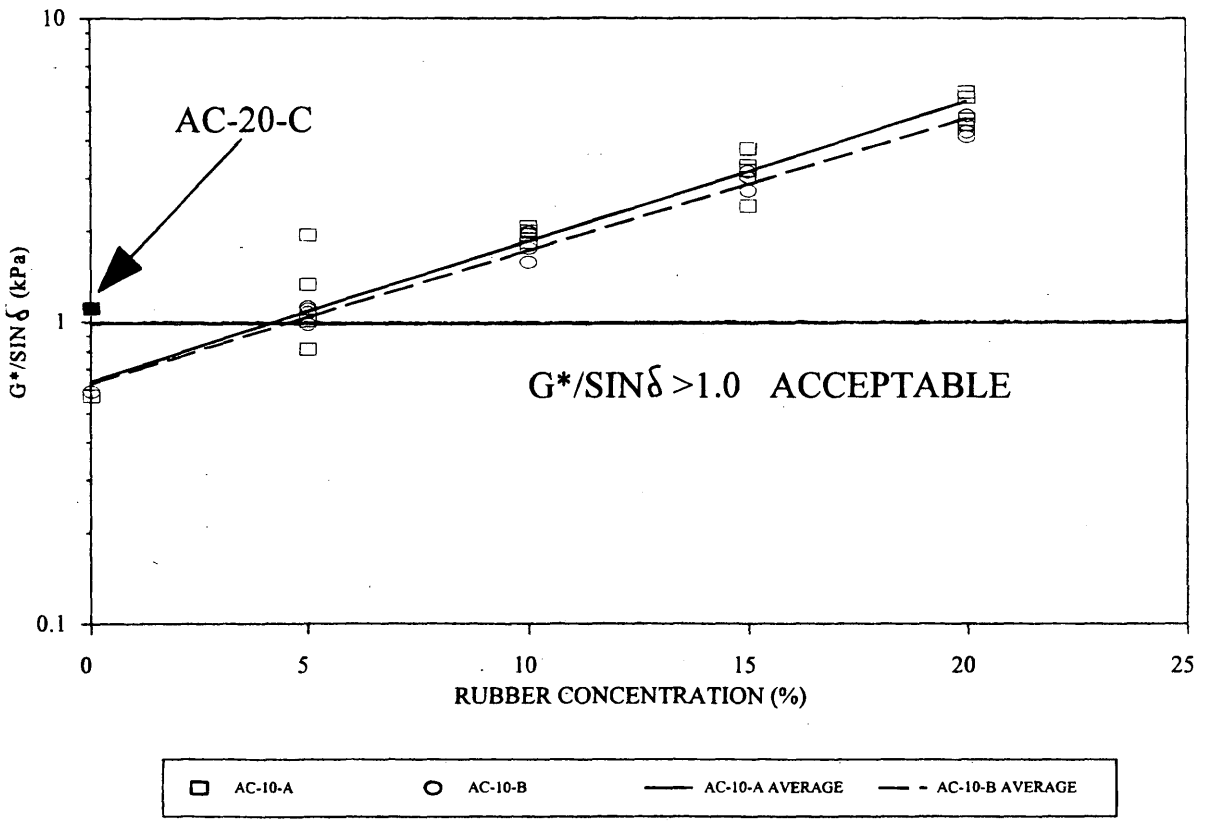

FIGURE 3 DSR binder parameters for original AC-10-A and AC-10-B and all rubber combinations at 64°C.

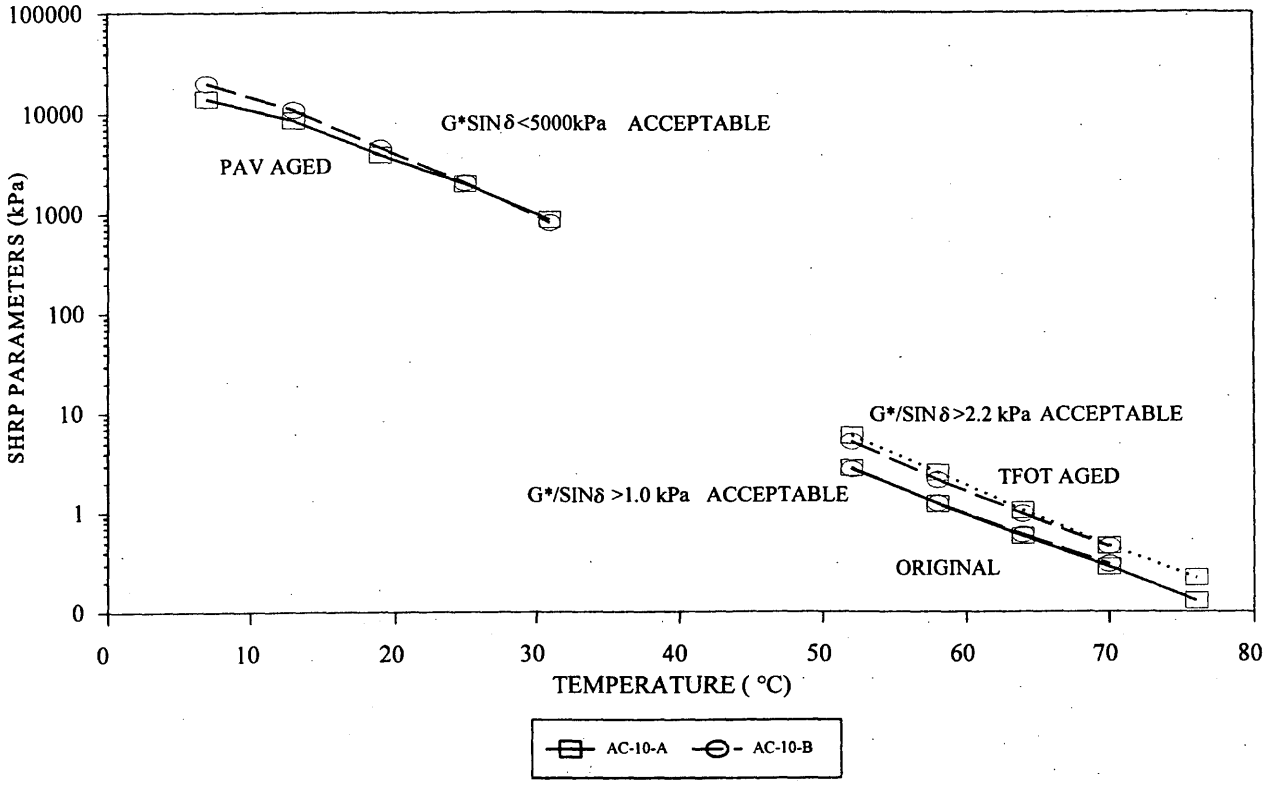

FIGURE 4 DSR SHRP parameters for base AC-10 asphalt cements used in crumb rubber study.

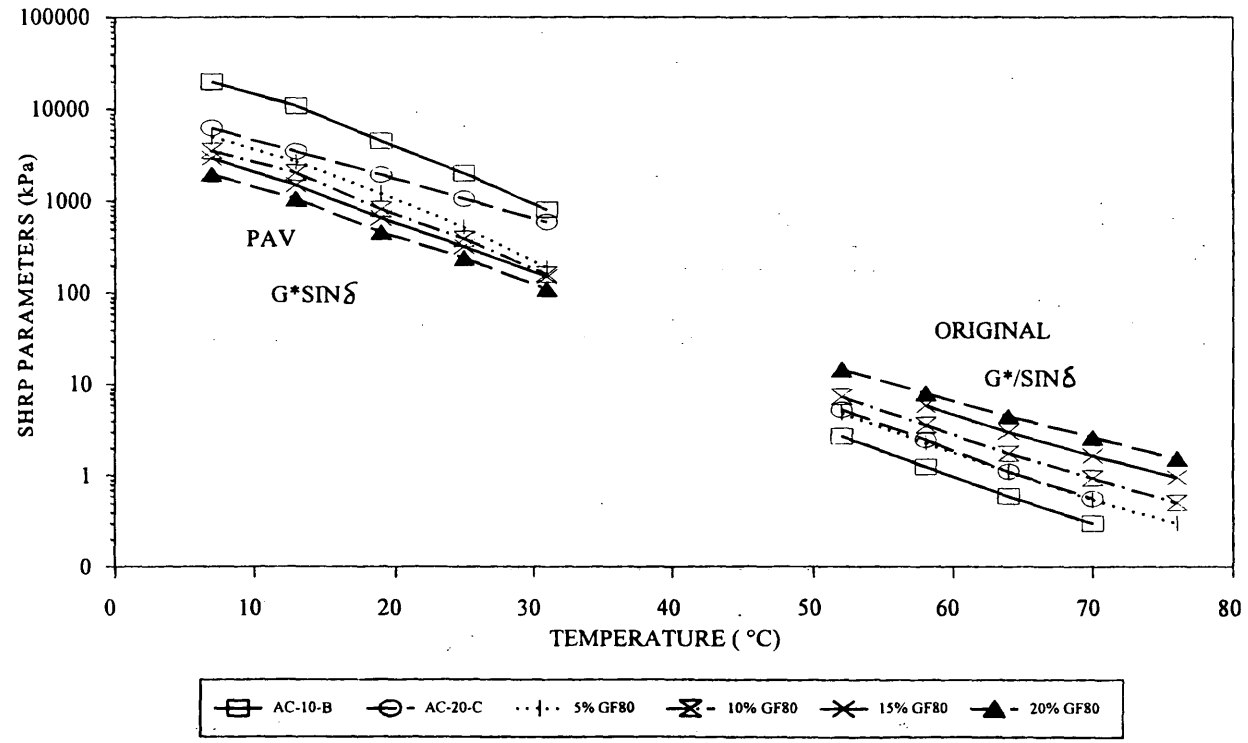

FIGURE 5 DSR SHRP parameters for AC-10-B, AC-20-C, and all concentrations of GF80 and AC-10-B in original and PAV stages. (DSR binder stiffness, AC-10-B, AC-20-C, and CRM binders.)

be seen at the higher temperatures in original materials because $G^*/\sin\delta$ increases as the concentration increases.

Characterization of the TFOT material indicates dynamic shear results similar to those for the original stage. Figure 6 shows that $G^*/\sin\delta$ increases as the percentage of crumb rubber is increased. From these graphs there is no clear trend that the properties of aged material differ for different gradations of rubber, but $G^*/\sin\delta$ is affected by concentration. At 64°C a minimum of 10 percent rubber material must be added to AC-10 to achieve a stiffness of greater than 2.2 after TFO aging. It is apparent that the $G^*/\sin\delta$ for the AC-10-A binders is slightly higher than that for the AC-10-B binders.

Figure 7 shows the relationship of the binder stiffness after the PAV procedure for both AC-10 and the AC-20. Most of the rubberized binders meet the criteria of $G^*\sin\delta < 5{,}000$ at 7°C. The rubber seems to make the rubber-modified binder more elastic at the intermediate temperatures, whereas it makes the modified binder stiffer at higher temperatures.

In summary for SHRP DSR testing, there appears to be little difference in how the different asphalt sources react with the rubber particles. As shown earlier the gradation or size of the rubber has little effect on the stiffness of the binder in all three stages of DSR testing. According to DSR, when trying to produce a rut- and fatigue-resistant rubber-modified binder, the concentration of rubber is the only factor that matters. Considering only the final properties the cheapest gradation of rubber could be chosen without any detrimental effects to the modified binder. The base asphalt cements used in the study appear to have little effect on the reaction between the rubber and the asphalt cement.

BBR

BBR applies a 100-g static load to an asphalt beam for 4 min while measuring the deflection of the beam throughout the duration of the test. The beam is simply supported, and the BBR creep stiffness can be found through the basic deflection equation involving the modulus of elasticity of the beam. Since the deflection of the beam changes with time, the stiffness is also a function of time. An asphalt cement's ability to endure low temperatures over the long term has been shown to be proportional to the slope of the log stiffness-versus-time curve, or m. If this value is greater than 0.30 at the lowest sustained pavement temperature, the asphalt will perform adequately according to AASHTO MP1 (*3*). A higher m-value indicates better stress relaxation characteristics and, therefore, less susceptibility to thermal cracking. AASHTO TP1 states that the m-value determined at 1 min into the test should be used to grade the binder (*3*). The BBR m-value (at 1 min) must exceed 0.30 at the given temperature to pass; also, the BBR creep stiffness at 1 min must be below 300 MPa to pass the test.

The characterization of asphalt rubber binder in the BBR has shown a decrease in BBR creep stiffness as rubber is added to asphalt cement (*4*). The effect of concentration is seen in Figure 8, which shows the BBR creep stiffness versus the gradation of rubber at different concentrations. The stiffness continually drops as the rubber concentration increases for both temperatures, but the drop in stiffness is more significant at the lower temperature. The BBR m-value for AC-10-B increases with rubber concentration (Figure 9).

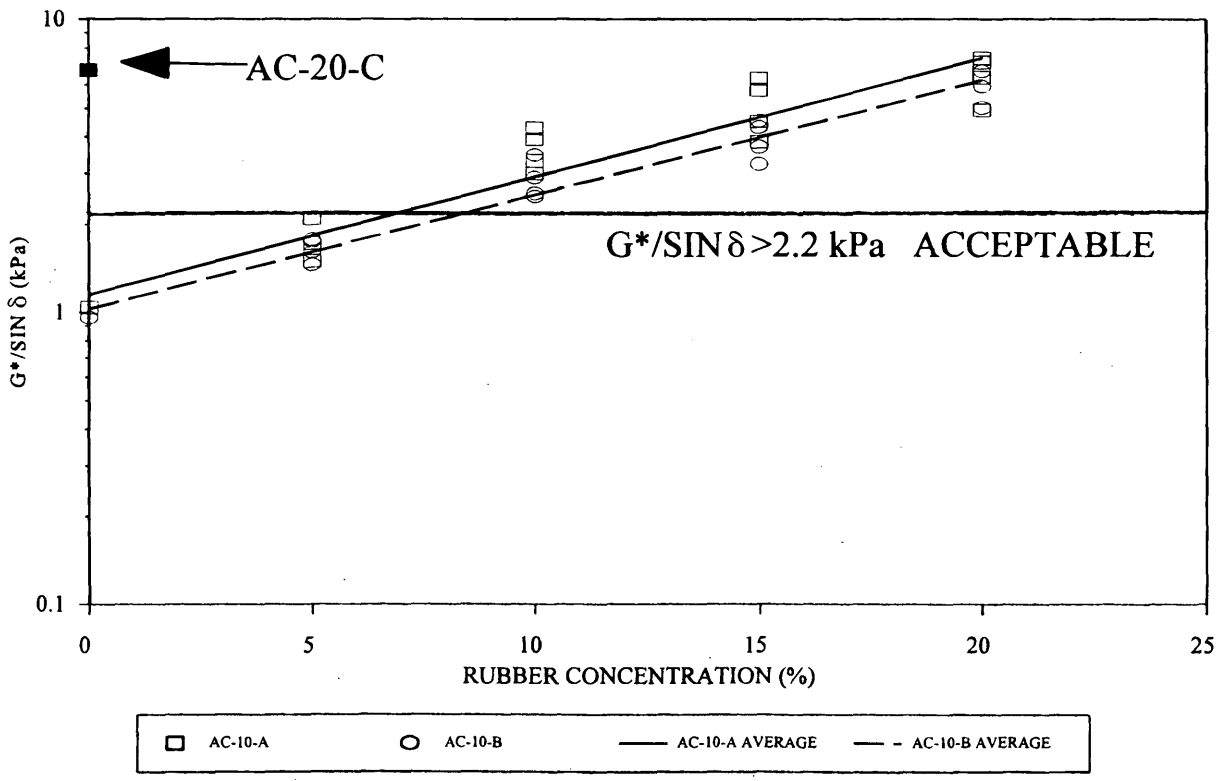

FIGURE 6 DSR SHRP parameters for AC-10-A and AC-10-B with all combinations of rubber after TFO aging at 64°C.

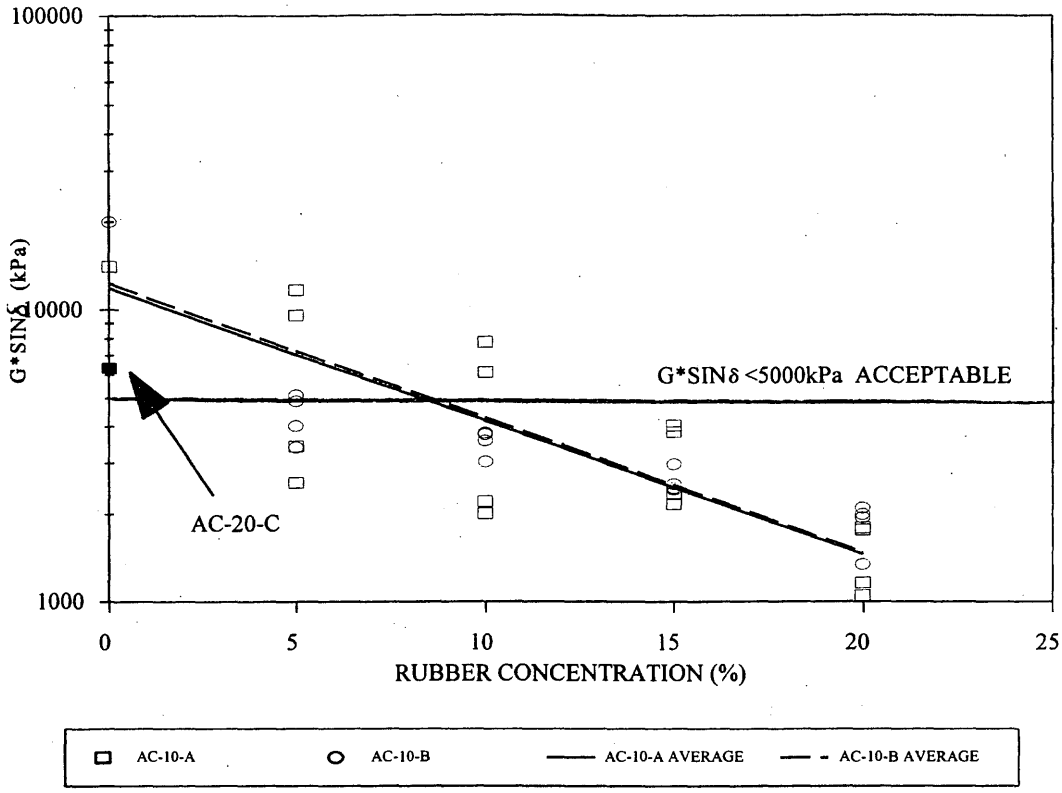

FIGURE 7 DSR $G^*/\sin\delta$ values for AC-10-A and AC-10-B with all combinations of rubber after PAV aging at 7°C.

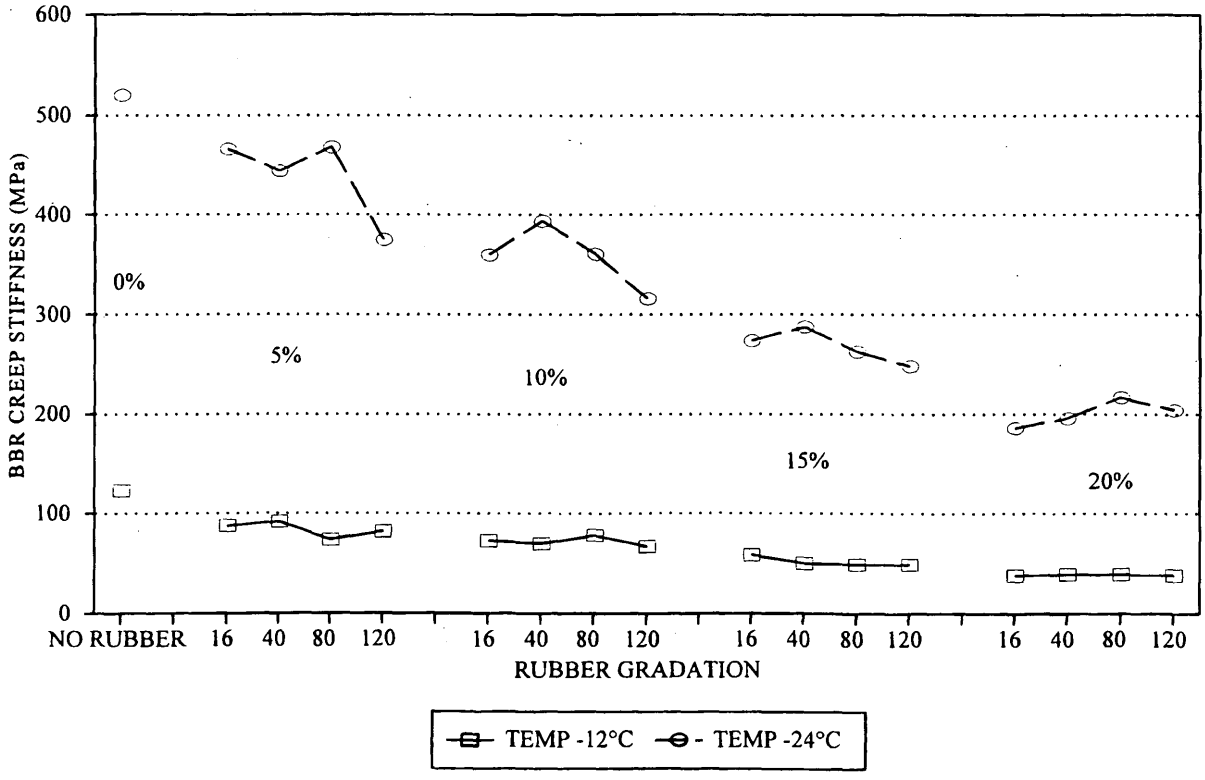

FIGURE 8 BBR creep stiffness for AC-10-B with all combinations of rubber at −12°C and −24°C.

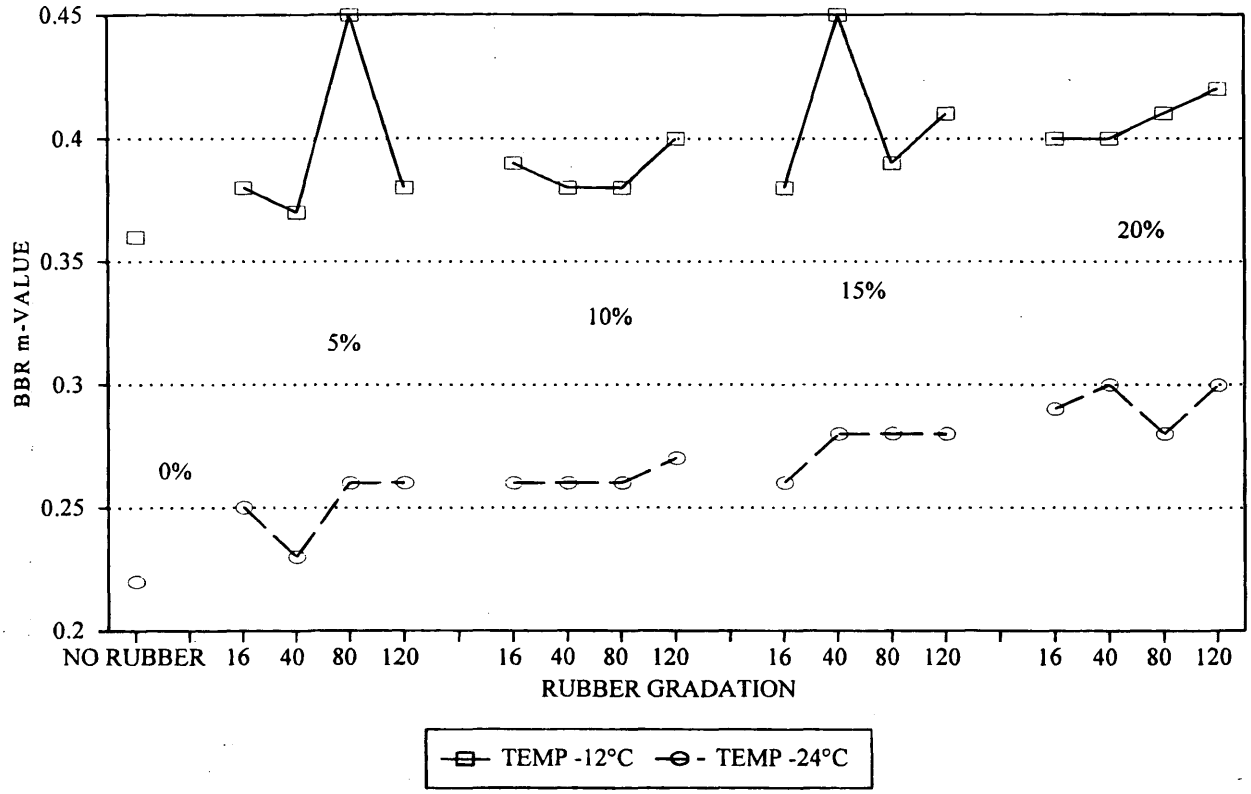

FIGURE 9 BBR *m*-value for AC-10-B with all combinations of rubber at −12°C and −24°C.

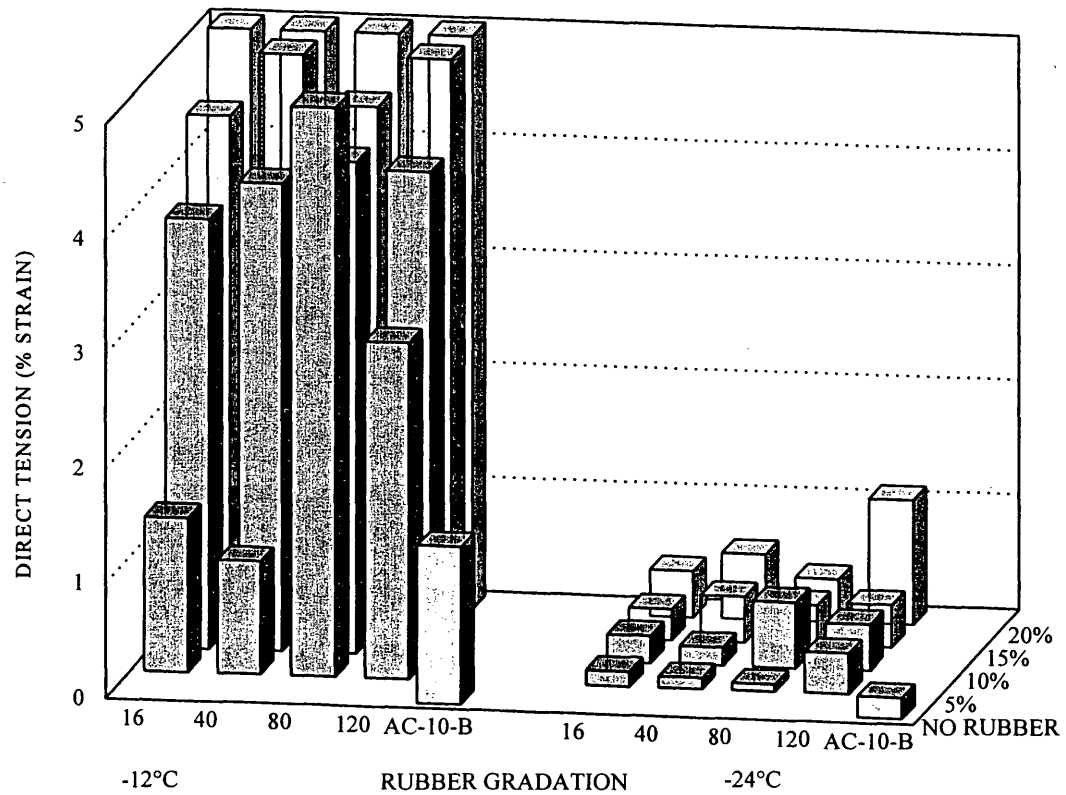

FIGURE 10 Direct tension strain at failure for AC-10-B and all combinations of rubber at −12°C and −24°C.

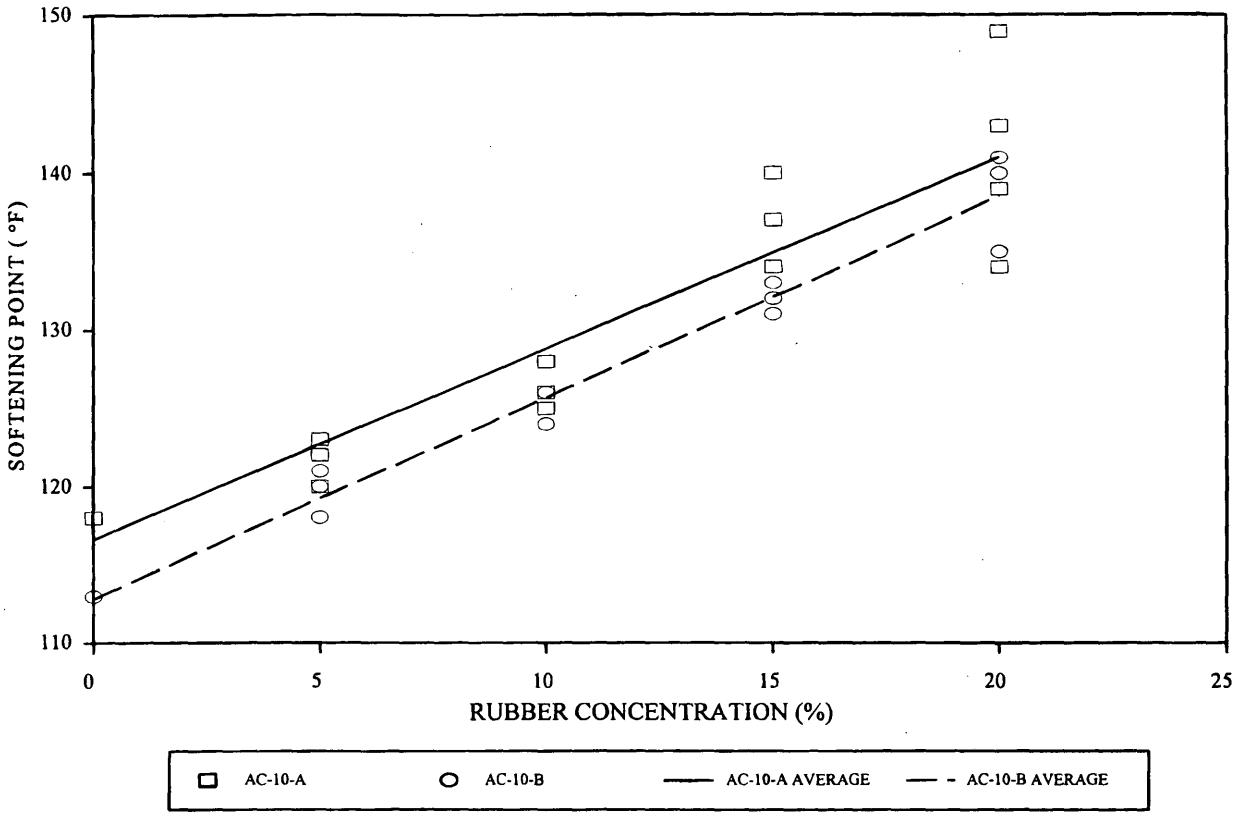

FIGURE 11 Softening point for AC-10-A and AC-10-B with all combinations of rubber.

DT Test

The DT test was the final SHRP test used to evaluate the crumb rubber binders. This test was performed at −12°C and −24°C by using the standard rate of strain of 1 mm/min (*3*). The data from the direct tension test are presented in Figure 10. As Bahia and Davies (*4*) reported, the strain at failure seems to increase as the rubber concentration increases. Also, the strain at failure decreases as the temperature decreases. The data showed considerable scatter.

Conventional Binder Tests

Conventional binder tests were included in the study to tie the data to the existing data base of binder properties. The conventional tests presented are easily performed and are being used for field verification for the modified binder.

Penetration

The penetration test was performed in this series of tests to establish a data base with which to compare the data for the modified binders. The penetration tests were performed at 4°C and 25°C according to ASTM D5. Compared with the original base asphalt cement, the data indicated a decrease in the penetration of the binder at 25°C as the rubber concentration increased. The penetration at 4°C presents no clear trend in the data. Because of the variability observed in the study, it is concluded that this conventional test may not be appropriate for evaluating crumb rubber-modified asphalt.

Softening Point

The softening point test was also performed to provide a data base for conventional binder tests. Figure 11 presents the data accumulated through softening point testing. The data indicate that the softening point increases with increasing rubber concentration and that the size of the particles has no effect. This confirms work done by Chehovitz (*1*).

CONCLUSION

Based on the research performed for this phase of the crumb rubber study, the following conclusions are made.

1. As shown from the DSR, BBR, DT, and softening point tests, the concentration of rubber seems to be the major contributor for the increased stiffness of the asphalt rubber binder at high temperatures and the lower stiffness at the low temperatures.
2. Those same tests indicated that the gradation of the rubber was not a factor in the change in stiffness.
3. The softening point test provides a quick, easy check of the modified binder and may complement the Brookfield viscosity test in the field.
4. The crumb rubber provides a lower temperature susceptibility, as shown in the BBR test.
5. As seen in the DSR test the crumb rubber provides a more rut-resistant binder in the original and TFOT stages and a softer, less brittle binder in the PAV test stage.

6. DSR data typically indicate that rubber binders made with the two AC-10 sources used in the study have similar properties.

REFERENCES

1. Chehovitz, J. *Binder Design Procedures.* Crumb Rubber Modifier Workshop Notes. FHWA, U.S. Department of Transportation, Feb. 1993.
2. Heitzman, M. *Specification Guidelines.* Crumb Rubber Modifier Workshop Notes. FHWA, U.S. Department of Transportation, Feb. 1993.
3. AASHTO Provisional Standards, January 1994 Edition. AASHTO, Washington, D.C., 1994.
4. Bahia, H. U., and R. Davies. Effect of Crumb Rubber Modifiers (CRM) on Performance-Related Properties of Asphalt Binders. Association of Asphalt Pavement Technologists Journal, Vol. 62, 1994.

Strategic Highway Research Program Binder Rheological Parameters: Background and Comparison with Conventional Properties

HUSSAIN U. BAHIA AND DAVID A. ANDERSON

As a result of the research conducted for the Strategic Highway Research program (SHRP), a set of new testing methods to characterize the rheological, failure, and durability properties of asphalt binders has been developed. These methods use testing devices that either are completely new or that have been used before only for research purposes. The methods also call for measuring mechanical response parameters that are not very common for asphalt pavement engineers or for many asphalt producers. The purpose is to discuss the following points: (a) the viscoelastic nature of asphalts and its relation to pavement performance, (b) the concepts behind selecting the new test methods and the new characteristic properties, and (c) how the new measured properties compare with the conventional properties. These points are addressed by providing a theoretical-conceptual background about the conventional and new tests and by comparing new and conventional data measured for a large number of asphalts that vary in their sources and their grades. The comparison identifies the advantages of the new testing methods and the need to implement the proposed testing and specification system.

One of the main objectives of the Strategic Highway Research Program (SHRP) A002A project was to identify the physical properties of asphalt cement binders that are related to pavement performance and the methods of reliably measuring these properties (*1*).

The first step to achieving this objective involved an extensive review of the literature related to asphalt materials and pavements. The review resulted in more than 500 abstracts and included information published since the beginning of the century (*2*). The review indicated that there is no lack of realization of the types of pavement failures; rutting, fatigue cracking, and thermal cracking are the main failure modes that asphalt researchers have commonly related to the physical properties of binders. Also, it was clear that age hardening is a main factor in changing the properties of asphalts during pavement service life and that thus affects performance. Moisture damage, although a major distress mode, was known to be the result of the interaction between asphalt binders and aggregate, and hence cannot be appropriately addressed by binder properties alone. The review, however, indicated that there is a significant confusion about important binder properties and which of these properties can more reliably be related to pavement performance. The confusion mainly comes from underestimation of the complexity of the binder properties and the empirical nature of the methods used to measure these properties. Although many asphalt researchers and practitioners realized the viscoelastic nature of the material and the need for fundamental rheological methods for proper characterization, few had the resources or the background to study asphalt binders by rigorous rheological methods.

The findings of the SHRP asphalt binder research indicated that to better select asphalts there is no substitute for fundamental rheological and failure characterization. The findings indicated that the existing methods are handicapped by empiricism and simplifications to levels that are not acceptable to meet the present needs of the industry. As part of the research new methods and parameters were introduced to measure more fundamental properties that can be easily related to pavement performance on the basis of sound engineering concepts. The new testing and aging methods include the dynamic shear rheometer (*3*), the bending beam rheometer (*4*), the direct tension test (*5*), and the pressure aging vessel (*6*). The new parameters include complex shear modulus (G^*), phase angle (δ), creep stiffness [$S(t)$], logarithmic creep rate [$m(t)$], and failure strain (ϵ_f).

The purpose of this paper is to provide a theoretical-conceptual background about the conventional and new tests and a comparison of properties measured by conventional and new methods for a large number of asphalts. The background and the data comparison identify the advantages of the new parameters and the importance of the properties measured with the new testing systems.

VISCOELASTIC NATURE OF ASPHALT BINDERS

The most unique behavior of viscoelastic materials is the dependency of their mechanical response on time of loading and temperature. At any combination of time and temperature, viscoelastic behavior, within the linear range, must be characterized by at least two properties: the total resistance to deformation and the relative distribution of that resistance between an elastic part and a viscous part. Although there are many methods of characterizing viscoelastic properties, dynamic (oscillatory) testing is the best technique to explain the uniqueness of the behavior of this class of materials. In the shear mode G^* and angle δ are measured. G^* represents the total resistance to deformation under load, whereas δ represents the relative distribution of this total response between an in-phase component and an out-of-phase component. The in-phase component is an elastic component and can be related directly to the energy stored in a sample for every loading cycle, whereas the out-of-phase com-

H. U. Bahia, Department of Civil and Environmental Engineering, The University of Wisconsin-Madison, Madison, Wis. 53706. D. A. Anderson, The Pennsylvania Transportation Institute, The Pennsylvania State University, University Park, Pa. 16802.

ponent represents the viscous component and can be related directly to the amount of energy lost per cycle in permanent flow. The relative distribution of these components is a function of the composition of the material, loading time, and temperature.

Rheological properties can be represented either by the variation of G^* and δ as a function of frequency at a constant temperature (commonly referred to as a *master curve*) or by the variation of G^* and δ with temperature at a selected frequency or loading time, commonly called an *isochronal curve.* Although time and temperature dependency can be related by a temperature-frequency shift function (*7*), for practical purposes it is much easier to present data with respect to one of the variables. Figure 1 depicts typical rheological properties of an AC-40 and an AC-5 asphalt binder at a wide range of temperatures and frequencies. Figure 1(*a*) shows master curves at 25°C, and Figure 1 (*b*) shows isochronal curves at 10 rad/sec.

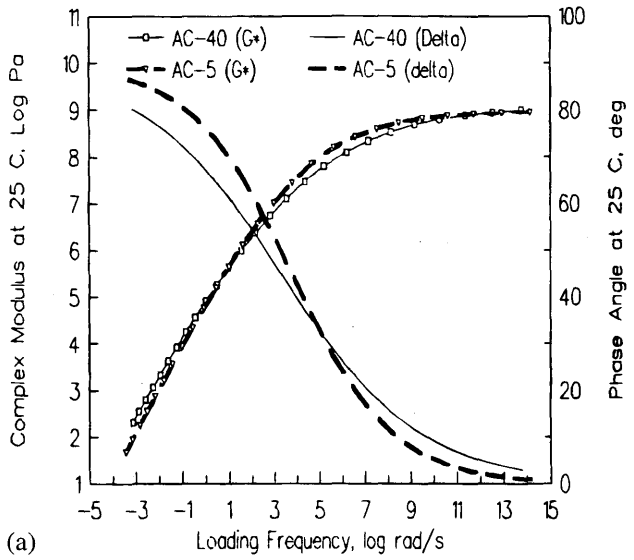

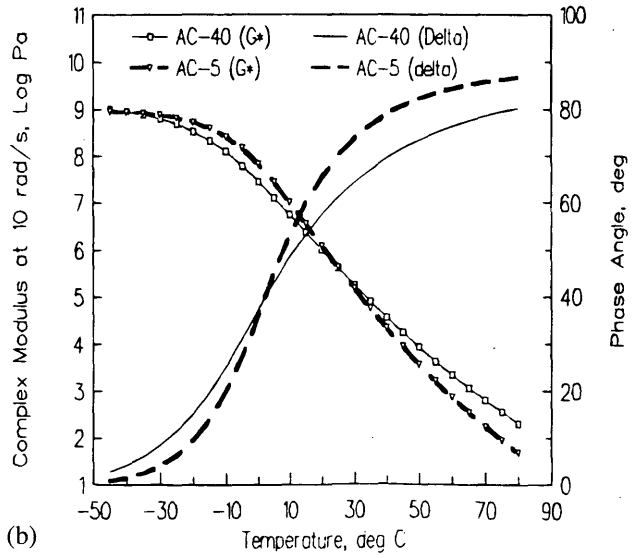

FIGURE 1 Typical rheological spectra for AC-5 and AC-40 asphalt binders: (*a*) frequency master curves; (*b*) isochronal curves.

Some common unique characteristics of the rheological behaviors of asphalts can be seen in the typical plots of Figure 1:

- At low temperatures or high frequencies both asphalts tend to approach a limiting value of G^* of approximately 1.0 GPa and a limiting value of δ of 0.0 degrees. The 1.0 GPa reflects the rigidity of the carbon hydrogen bonds as the asphalts reach their minimum thermodynamic equilibrium volume. The 0.0 value of δ represents the completely elastic nature of the asphalts at these temperatures.
- As the temperature increases or as the frequency decreases, G^* decreases continuously, whereas δ increases continuously. The first reflects a decrease in resistance to deformation (softening), whereas the second reflects a decrease in elasticity or ability to store energy. The rate of change is, however, dependent on the composition of the asphalt. Some will show a rapid decline with temperature or frequency; others will show a gradual change. Asphalts within this range may show significantly different combinations of G^* and δ.
- At high temperatures the δ values approach 90 degrees for all asphalts, which reflects the approach to complete viscous behavior or the complete dissipation of energy in viscous flow. The G^* values, however, vary significantly, reflecting the different consistency properties (viscosity) of the asphalts.

From this simplified description of asphalt properties it is clear that without the distinction between types of asphalt response in terms of total resistance to deformation (G^*) and relative elasticity (δ) and without measuring properties at the temperature or loading frequency ranges that correspond to pavement climatic and loading conditions, selection of asphalt binders for better-performing pavements is not possible. One of the main problems with the methods used currently is their failure to measure properties at application temperatures and to distinguish between elastic and nonelastic binder behavior.

ASPHALT PROPERTIES AND PAVEMENT PERFORMANCE

Figure 2 is an isochronal plot that depicts the rheological properties of an asphalt in its unaged condition and after aging in the field under a moderate climate for approximately 16 years. To relate asphalt properties to pavement performance reference can be made to four temperature zones. At temperatures above 100°C mixing and construction take place, and thus, the binder consistency needs to be controlled. At temperatures above 100°C most asphalt binders behave like Newtonian fluids, whose response is totally viscous. Therefore, a measure of viscosity is sufficient to represent the workability of the asphalt during mixing and construction of hot-mix asphalt.

At temperatures in the range of 45°C to 85°C, which are typical of the highest pavement in-service temperatures, the main distress mechanism is rutting, and therefore, G^* and δ need to be measured. A measure of viscosity alone cannot be sufficient, since viscosity measurements are done on the assumption that asphalt response has only a viscous component. For rutting resistance a high G^* value is favorable because it represents a higher total resistance to deformation. A lower δ is favorable because it reflects a more elastic component of the total deformation.

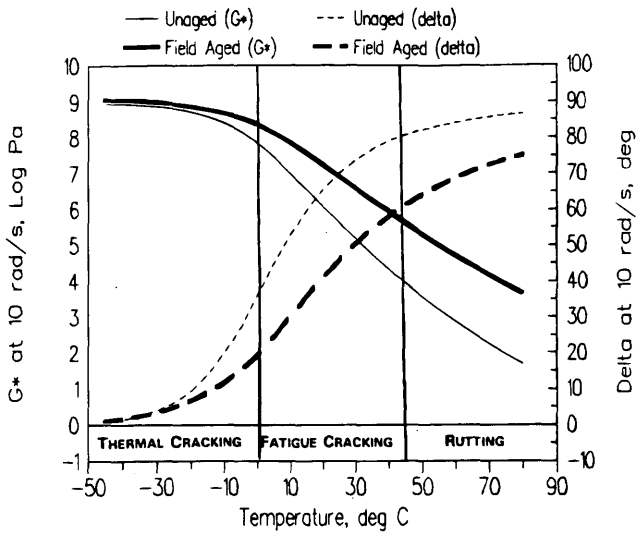

FIGURE 2 Typical rheological behavior of asphalt binders before and after aging in the field in relation to pavement main distress modes.

Within the intermediate temperature zone asphalts are generally harder and more elastic than at higher temperatures. The prevailing failure mode at these temperatures is fatigue damage, which is caused by repeated cycles of loading at levels lower than the static strength of a material. For viscoelastic materials like asphalt binders, both G^* and δ play a role in damage caused by fatigue. They are both important because during every cycle of loading the damage is dependent on how much strain or stress is developed by the cyclic load and how much of that deformation can be recovered or dissipated. A softer material and a more elastic material will be more favorable for resisting fatigue damage because the stress developed for a given deformation is lower and the asphalt will be more capable of recovering to its preloading condition. Similar to the case for rutting, a single measure of hardness or viscosity cannot be sufficient to select better-performing asphalts with respect to fatigue resistance. Rutting and fatigue damage are both functions of frequency of loading, and therefore, the rate of loading of the pavement under traffic needs to be simulated in measurement to obtain a reliable estimate of the binder's contribution to pavement performance.

The fourth and last temperature zone is the low-temperature zone, at which thermal cracking is the prevailing failure mode. Thermal cracking results from the thermal stresses generated by pavement shrinkage as a result of thermal cooling. During thermal cooling asphalt stiffness increases continuously and thus results in higher stresses for a given shrinkage strain. Simultaneously, thermal stresses relax because of the viscoelastic flow of the binder. To reliably predict the binder's contribution to cracking both the stiffness of a binder and its rate of relaxation need to be evaluated. The stiffness of the binder is directly proportional to G^*, and the rate of relaxation is directly related to δ. A lower stiffness and higher rate of relaxation are favorable for resistance to thermal cracking. As with other temperature zones, a single measure of the stiffness or viscosity of the binder is not sufficient to select better binders that will resist cracking at the lowest pavement temperatures.

This discussion of the relation between asphalt binder properties and pavement performance is further complicated by the aging phenomenon. Asphalts are hydrocarbon materials that oxidize when they come into contact with oxygen from the environment. This oxidation process changes the rheological and failure properties of the asphalt. As shown in Figure 2 the rheological master curve becomes flatter with aging, which indicates higher G^* values and lower δ values at all temperatures. These changes translate into less sensitivity of G^* and δ to temperatures or loading frequency and into a more elastic component (lower δ values). Significant oxidation effects usually appear after considerable service life. Increased G^* values and lower δ values are favorable changes with respect to rutting performance, but they are unfavorable for thermal cracking performance. For fatigue cracking the increase in the G^* value is not favorable, whereas the decreased δ value is generally favorable, depending on the type of pavement and the mode of fatigue damage.

NEW PROPOSED MEASUREMENTS AND PROPERTIES

The properties that are proposed for the new SHRP binder specification were derived and selected by addressing each type of pavement failure, understanding the failure mechanism, understanding the contribution of the binder to resistance to that failure, and selecting the required measure that will best reflect that contribution of the binder (*1*). The new binder specification is based on climatic conditions; the criteria that a binder must meet do not change, but the temperature at which the property is measured depends on the specific field climate and on the failure mode being considered.

Three failure modes were identified as critical pavement distress modes in which binder plays an important role: rutting, fatigue cracking, and thermal cracking. Oxidative aging and physical hardening were considered durability factors that cause changes in properties of binders and that thus affect performance. Four types of tests were selected (*8*):

- The rotational viscometer, to measure flow properties at temperatures that mimic temperatures at which the pumping and mixing of binders occur.
- The dynamic shear rheometer, to measure properties at temperatures that mimic high and intermediate pavement temperatures and to mimic loading rates typical of traffic loadings.
- The bending beam rheometer, to measure properties at the lowest pavement temperatures and to mimic loading conditions that result from thermal cooling.
- The direct tension test, to measure failure properties at the lowest pavement temperatures and to mimic loading that results from thermal cooling.

High-Temperature Consistency

Although workability is not directly related to pavement distress modes, asphalt binders must be workable enough at high temperatures such that pumping, mixing with aggregates, and compaction can be done efficiently to produce the required mixture properties. To ensure binder workability the Brookfield viscometer has been selected to measure steady-state viscosity at one or more temperatures. In the binder specification the binder is required to have a maximum viscosity of 3.0 Pa · sec to ensure workability. Although the rotational viscometer is already a standard test (ASTM D4402),

its use will result in two changes with respect to the existing specification practices (ASTM 3381). First, it will replace the kinematic viscosity measurement; second, a maximum limit, instead of the minimum limit required in the current specification, is specified. The rotational viscometer is more suitable for modified asphalts, which are difficult to test with the capillary tubes used for kinematic viscosity. Also, a maximum limit is more appropriate to ensure the workability of asphalts.

Contribution of Binder to Rutting Resistance

Opinions about the contribution of binder to rutting resistance differ. It is a fact, however, that soft asphalts are not used to construct pavements in hot desert climates. It is also a fact that during the past decade more and more engineers are specifying polymer-modified binders, at much higher costs, to mitigate rutting problems. Aggregate properties are without doubt very important. Many engineers, however, agree that it is not good engineering practice to ignore binder properties.

Rutting is caused by the accumulation of permanent deformations caused by the repeated applications of traffic loading. Assuming that pavement rutting is mainly caused by deformations of the surface layer, rutting can be considered a stress-controlled, cyclic loading phenomenon. During each cycle of traffic loading a certain amount of work is being done in deforming the surface layer. Part of this work is recovered in elastic rebound of the surface layer, whereas the remaining work is dissipated in permanent deformation and heat. To minimize rutting the work dissipated during each loading cycle should be minimized. For a viscoelastic material the work dissipated per cycle (W_c) is calculated in terms of stress (σ) and strain (ϵ) as follows:

$$W_c = \pi \cdot \sigma \cdot \epsilon \cdot \sin \delta$$

Rutting within the asphalt concrete layer can be assumed to be a *stress*-controlled (σ_0) repetitive phenomenon. Therefore, the following substitution can be made:

$$\therefore W_c = \pi \cdot \sigma_0 \cdot \varepsilon \cdot \sin \delta$$

since

$$\epsilon = \frac{\sigma_0}{G^*}$$

$$\therefore W_c = \pi \cdot \sigma_0^2 \cdot \left(\frac{1}{G^*/\sin \delta} \right)$$

This relationship indicates that the work dissipated per loading cycle is inversely proportional to the parameter $G^*/\sin \delta$, which is the parameter selected for the SHRP specification. The parameter combines the total resistance to deformation, as reflected by G^*, and the relative nonelasticity of the binder, as reflected by $\sin \delta$. $\sin \delta$ is the ratio of the loss modulus (G'') to the complex modulus G^*. G'' is directly related to the work dissipated during a loading cycle, and thus, its ratio to G^* gives a relative measure of the nonelastic (permanent) component of the total resistance to deformation. The logic associated with the parameter is that the contribution of the binder to rutting resistance can be increased by increasing its total resistance to deformation (G^*) or decreasing its nonelasticity ($\sin \delta$).

G^* and δ are functions of temperature and frequency of loading. Therefore, to relate the measurements to pavement conditions, the specification requires testing at the average 7-day maximum pavement design temperature and at a frequency of 10 rad/sec. The proposed measurements take into account the viscoelastic nature of the material, the climatic conditions of the specific application, and the loading condition (traffic) that is causing the pavement distress.

Figure 3 depicts the values of G^* and δ for a large number of asphalts that were tested for SHRP. All measurements were done at a frequency of 10 rad/sec, which is assumed to simulate the average frequency of a stress wave in the surface layer of a typical pavement as caused by a vehicle moving at 50 to 60 mph. Figure 3 shows no specific trend between G^* and δ values. This indicates that at a certain frequency and temperature asphalts vary significantly in their G^* and δ properties. It is therefore necessary to measure both and to consider both in estimating the contributions of binders to rutting resistance. The group of datum points to the left of the plot are data measured for polymer-modified asphalts that were formulated to increase the elasticities of specific binders. The testing was done at temperatures in the range of 72°C to 82°C. This set of data points out the importance of measuring δ to characterize the elasticity at high temperatures that may significantly contribute to resistance to rutting.

Figure 3 represents the properties of unaged binders and binders aged by the thin film oven test (ASTM D1754). For all unmodified asphalts and most modified asphalts, oxidative aging results in increased G^* values and decreased δ values. These changes result in more resistance to deformation and more elasticity, which means more contribution to rutting resistance. The initial properties of the binders (early pavement life) are therefore more critical than the aged properties, and that is why the SHRP specification minimum limits are required for $G^*/\sin \delta$ measured on the unaged and the oven-aged binders.

Figure 4 compares the new measure with the absolute viscosity. Although the figure shows that there is a fair correlation between the two measures, it indicates that there is a wide range of values of $G^*/\sin \delta$ for each value of viscosity and vice versa. For example, at a value of 2000 P, typical of an AC-20 asphalt, the value of $G^*/\sin \delta$ may vary between 1700 and 3200 Pa, which is a range of -15 to $+60$ percent. In fact the standard error for the estimate by using a

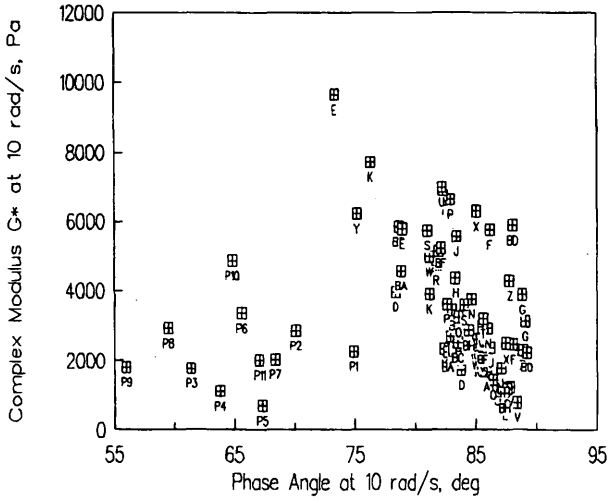

FIGURE 3 Typical values of G^* and δ at high pavement temperature.

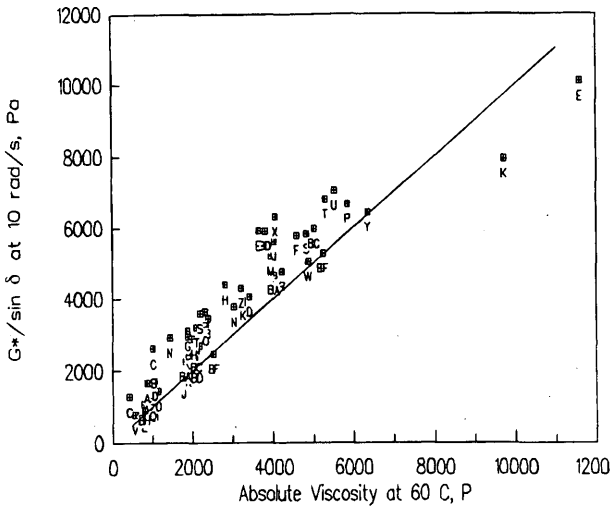

FIGURE 4 Comparison between capillary viscosity and $G^*/\sin\delta$ at 60°C.

linear relation is estimated at approximately 750 Pa, a range that cannot be considered acceptable for many engineering purposes. The discrepancy between the $G^*/\sin\delta$ and absolute viscosity is a reflection of the difference in the two measures; absolute viscosity is measured at a different shear rate, a different mode of loading, and a different strain and stress level. Absolute viscosity also does not consider the elastic response of a binder. All of these factors point out the advantages of the new parameter and indicate that absolute viscosity cannot be substituted for $G^*/\sin\delta$.

Contribution of Binder to Fatigue Cracking Resistance

As shown in Figure 2, at intermediate pavement temperatures the main distress mode is fatigue cracking. Fatigue of pavement can be a controlled-stress phenomenon (typical for thick pavement layers) or a controlled-strain phenomenon (typical of thin pavement layers). Fatigue cracking, however, is known to be more prominent in pavements with thin layers. Based on the assumption that the fatigue cracking mechanism is mainly driven by relatively large deformations of thin surface layers under traffic loading, it can be considered predominantly a strain-controlled phenomenon. The large deformations usually result from the low level of support of subsurface layers that may result from poor design and construction or because of the saturation of base layers during the spring season. Based on these assumptions the dissipated work concept can be used to derive the parameter used in the SHRP specification, $G^* \sin\delta$. For a strain-controlled cyclic loading the work per cycle equation can be rewritten as follows:

$$\therefore W_c = \pi \cdot \sigma \cdot \epsilon_0 \cdot \sin\delta$$

where ϵ_0 is the strain amplitude being applied. Since stress (σ) is related to strain by G^*:

$$\sigma = \epsilon_0 \times G^*$$

Substitution leads to the following equation, which shows that W_c under strain-controlled conditions is directly related to $G^* \sin\delta$:

$$\therefore W_c = \pi \cdot \epsilon_0^2 \cdot (G^* \times \sin\delta)$$

The work done during a loading cycle can be dissipated in one or more damage mechanisms: cracking, crack propagation, dissipated heat, or plastic flow. Although the dissipation in heat or plastic flow may be better than dissipation in cracking, heat and plastic flow are only other types of damage that may cause permanent deformation, allow faster crack propagation, or permit detrimental distortion of the asphalt mixture structure. To prevent all types of damage it is therefore best to limit the energy dissipation by limiting the value of the parameter $G^* \sin\delta$. This is the concept on which the SHRP specification is based. The logic associated with the parameter is that the amount of work dissipated is directly proportional to $G^* \sin\delta$; asphalts with lower G^* values will be softer and thus can deform without developing large stresses. Also, asphalts with lower δ values will be more elastic and thus will recover to their original condition without dissipating energy in any fashion.

Figure 5 depicts the typical range of values for G^* and δ for a large number of asphalts tested for SHRP. Similar to the rutting parameter, the values are measured at 10 rad/sec to simulate traffic loading. They are, however, measured on binders after aging in the pressure aging vessel (PAV), which has been shown to simulate long-term oxidative aging in the field. The PAV-aged condition is assumed to be more critical because for most binders it results in a significant increase in G^*, which offsets the effect of the decrease in δ. The tests are done at intermediate pavement temperatures as determined from the average of the 7-day maximum and the lowest pavement design temperatures.

The only conventional measure that is in the same temperature range of average pavement temperatures is the penetration at 25°C. Figure 6(*a*) and 6(*b*) show plots of $G^* \sin\delta$ values before and after PAV aging versus the penetration values of the unaged asphalts. The plots show that asphalts with $G^* \sin\delta$ values ranging between 0.45 and 1.8 MPa, a range of more than fourfold, can have penetration values that vary only between 50 and 60 dmm. Similarly, after PAV aging asphalts with approximately the same penetration values may have a range of $G^* \sin\delta$ values of between 1.6 and 7.0

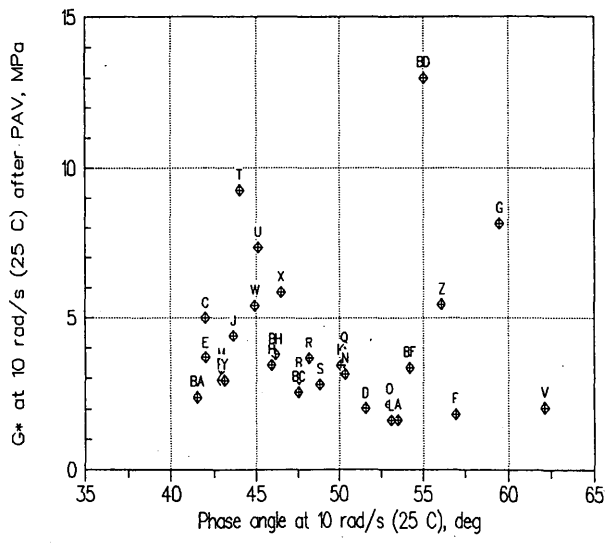

FIGURE 5 Relationship between G^* and phase angle at 25°C for PAV-aged binders.

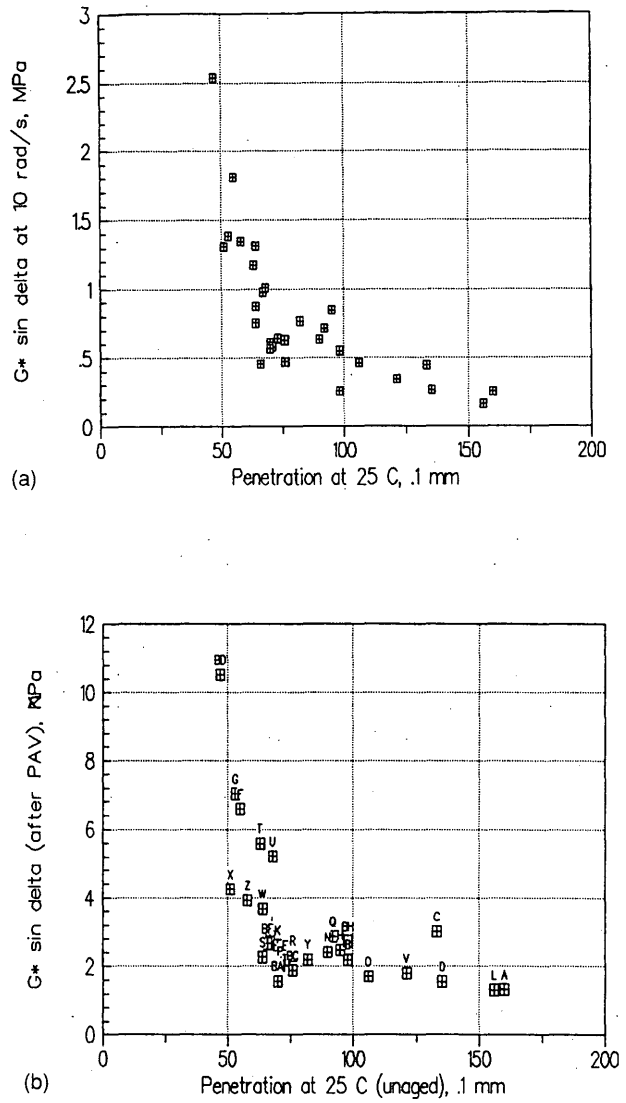

FIGURE 6 Relationship between penetration of unaged asphalts and G^* sin δ (*a*) before and (*b*) after PAV aging at 25°C.

MPa. The plots demonstrate the failure of the penetration measure to give a reasonable indication about the critical properties of asphalts. The selection of the fatigue parameter, similar to the rutting parameter, is derived on the basis of sound engineering principles; it considers the climatic conditions by testing at average pavement temperatures; it is measured by using a loading mode that simulates traffic loading; and it considers the viscoelastic nature of the asphalt material.

Contribution of Binder to Resistance to Thermal Cracking

Thermal cracking is the result of stresses developed in pavement layers because of thermal shrinkage caused by environmental cooling. Although cracking may be caused by rapid thermal cycling in relatively moderate climates, low-temperature cracking in cold regions is the predominant failure distress. During a thermal cooling cycle shrinkage of the asphalt layer in a pavement is restrained by friction with the underlying layers that either are warmer or undergo less shrinkage because of a smaller coefficient of thermal contraction. This restraint will result in the development of tensile stresses that, if not relaxed by the flow of the asphalt layer, will eventually exceed the tensile strength of the material and cause cracking. The total amount of stresses developed depends on the stiffness (resistance to deformation) of the asphalt binder and on its ability to relax stresses by dissipating energy in permanent flow. Traditionally, thermal cracking has been correlated with the stiffness of asphalts measured or estimated at certain loading times (*8,9*). Stiffness, however, does not reflect the stress relaxation ability of a binder. To be able to relax stresses an asphalt should be able to flow readily under stress and to have a less elastic component in its response. By measuring the creep response of asphalts with the bending beam rheometer the stiffness of asphalts, $S(t)$, can be measured at the lowest pavement temperatures. Also, by measuring the logarithmic creep rate, $m(t)$, the ability of an asphalt to relax stresses can be evaluated. A higher $S(t)$ reflects more stresses resulting from a given thermal strain (shrinkage), and a higher $m(t)$ reflects a higher creep rate and thus a faster relaxation rate. $S(t)$ and $m(t)$ are, however, both functions of loading time; therefore, a certain loading time must be selected to reflect pavement thermal cracking. In the asphalt literature loading times ranging between 3,600 and 20,000 sec have been correlated with thermal cracking (*2*). Such loading times are not practical for laboratory testing. To shorten the testing time the time-temperature superposition principle was used to perform tests at a higher temperature, but for a shorter loading time. During SHRP the studies of low-temperature properties have indicated that time-temperature equivalency factors are approximately the same for most asphalts (*4*). This finding was used to calculate the temperature shift required to reduce the 7,200-sec loading time, most commonly recommended in the asphalt literature, to a loading time within a 240-sec loading time range. A 10°C increase in temperature was found to be equivalent to a time shift from 7,200 sec to approximately 60 sec (*4*). In the current specification a maximum limit of 300 MPa is placed on $S(60)$, and a minimum $m(60)$ of 0.3 is required.

The logic associated with the low-temperature measures is that by placing a maximum limit on $S(t)$ the level of stresses developed in the pavement is limited, and by placing a minimum limit on $m(t)$ the rate of relaxation is kept above a certain limit. Figure 7 is a plot of $S(60)$ versus $m(60)$ for a large number of asphalts varying in source and physical properties. The measurements were done on binders aged in the PAV with the bending beam rheometer. Oxidative aging always results in increased $S(t)$ and decreased $m(t)$. Therefore, testing in the specification is required on PAV-aged binders to represent the critical aging condition. The testing is done at the minimum pavement temperature plus 10°C to reflect pavement climatic conditions. The loading condition in the pavement is also simulated by using a transient loading mode to measure the extensional stiffness. Figure 7 reflects the wide variation in $m(60)$ values for a given $S(60)$ and vice versa.

One other factor related to the low-temperature behavior of asphalts is the newly discovered physical hardening at low temperatures (*10*). Physical hardening is the increase in $S(t)$ and the decrease in $m(t)$ that occurs as a result of time-dependent volume shrinkage of asphalts. The phenomenon is caused by the deviation from thermodynamic equilibrium because of the lag of molecular adjustment behind the thermal change during cooling of the material through its glass transition temperature range. The phenomenon

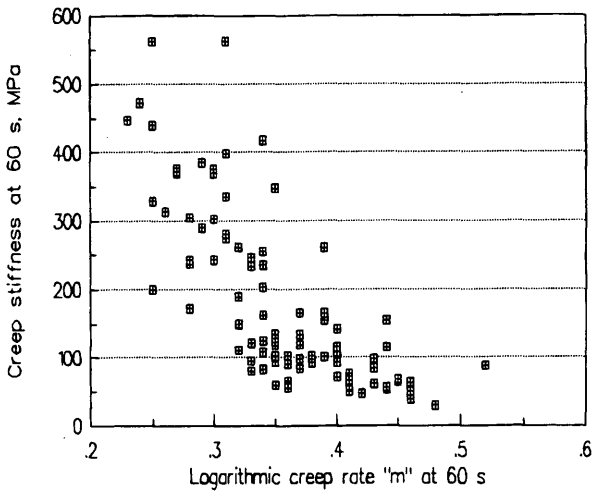

FIGURE 7 Relationship between creep stiffness and logarithmic creep rate at 60 sec for a large set of asphalts after PAV aging.

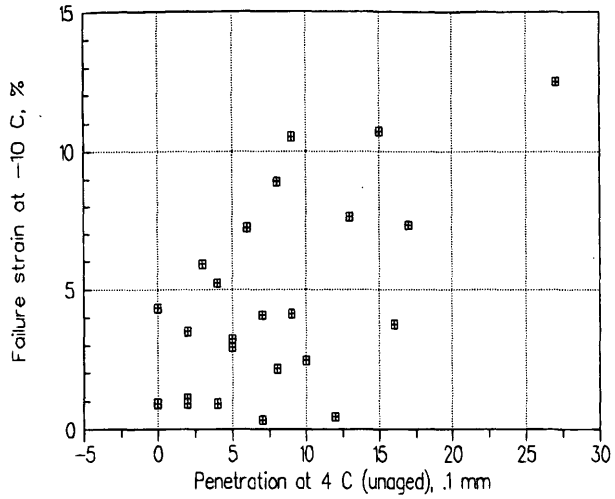

FIGURE 8 Relationship between strain at failure measured at −10°C and 1-mm/min test rate and penetration at 4°C.

resembles what is known as physical aging, which is a cause of time-dependent hardening for many plastics and polymers (*8,9*). For many asphalts physical hardening was found to increase $S(t)$ by 50 to 100 percent within 24 hr. Its consequences on asphalt concrete mixture properties and pavement performance are not yet known. Therefore, the SHRP specification requires the measurement and reporting of the values of $S(60)$ and $m(60)$ at 1 and 24 hr to provide an indication of the potential of the binder for hardening. The reported value is intended to make engineers aware of the existence of this phenomenon and to encourage the research and engineering community to evaluate the effect of this phenomenon on pavement thermal cracking. As for the measurements used in controlling $S(60)$ and $m(60)$, a constant conditioning time of 60 ± 5 min is required to test all asphalts at an equal isothermal conditioning time. Physical hardening has been found to be a strong function of asphalt chemical composition and molecular structure. Its consequences, if proved to be carried at the same level as the mixture's properties, can be very important in estimating binder contribution to thermal cracking resistance.

In addition to the creep measurements the new specifications include the direct tension test, which is a true strength test. For a wide variety of materials prefailure properties do not necessarily correlate very well with the failure properties. Unmodified asphalts, however, have been shown to have failure properties that correlate well with the stiffness values at low temperatures (*1*). Based on this finding the specification does not require testing for strain at failure if the $S(t)$ and $m(t)$ criteria are met. For some modified asphalts the relation between the stiffness and failure properties can be different. Therefore, to accommodate those modified asphalts that may have high $S(t)$ values but that can still show high strain tolerance, the direct tension test can be used to measure the strain and failure and override the $S(t)$ criterion if $S(60)$ is between 300 and 600 MPa. The direct tension test is another new test that gives the opportunity to directly evaluate the strain tolerance properties of specially modified binders. Figure 8 gives typical values of strain at failure for a wide variety of asphalts tested at temperatures resembling low pavement temperatures.

To compare creep measurements with conventional measures, Figure 9 shows penetration at 4°C with $S(60)$ and $m(60)$ measured at −10°C. At a value of $S(60)$ of 100 MPa asphalts can have penetration values ranging between 1 and 10 dmm. Similarly, at a value of $m(60)$ of approximately 0.35 asphalts can have penetration values ranging between 0.0 and 13 dmm. The data in Figure 9 are a clear indication of the insensitivity of penetration to the true rheological properties of asphalts at low temperatures.

SUMMARY AND CONCLUSIONS

A conceptual analysis of the viscoelastic nature of asphalt binders and the relation between their rheological properties and pavement performance has been presented. The types of conventional measures that are used at present and their failure in reflecting the crit-

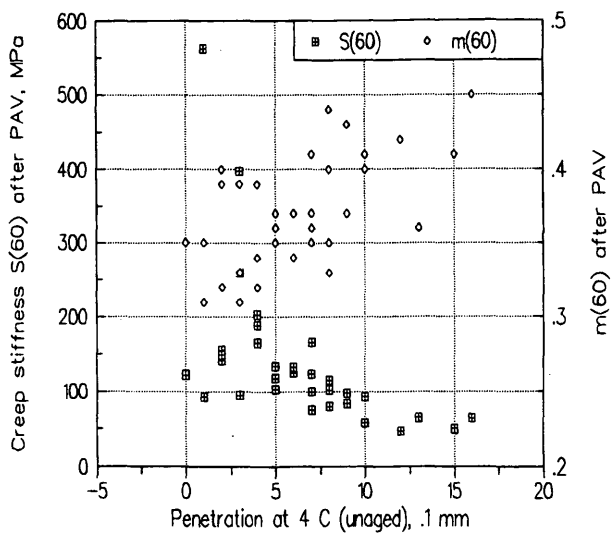

FIGURE 9 Relationship between $S(60)$ and $m(60)$ measured at −10°C and penetration at 4°C.

ical properties of binders were discussed. The concept on which the new testing and characterization methods introduced by SHRP are based has been presented with emphasis on how these new measures relate to pavement behavior and failure mechanisms. The conceptual analyses and the typical data comparing the conventional and the new SHRP measurements lead to the following conclusions:

1. Asphalt binders vary in their rigidities (total resistance to deformation) and their relative elasticities (distribution of that resistance between an elastic and a viscous part). For pavement applications both of these characteristics need to be measured at temperatures and loading rates that resemble climatic and traffic conditions.
2. Conventional measurements of the physical properties of asphalt include empirical measurements, viscosity measurements, and susceptibility parameters. These measurements cannot be considered reliable for characterizing the asphalt properties that are critical for pavement performance because of the empiricism involved and because of the engineering complications related to the method by which they are interpreted.
3. The new measurements proposed by SHRP are based on sound engineering principles derived from an understanding of the mechanisms of failure or damage in the pavement. They reflect the best estimate of the contribution of binders to pavement performance. They cover the main distress mechanism of flexible pavements, and they are measured under conditions that mimic climatic and loading conditions in the field.
4. No strong relationships between the new SHRP measurements and the conventional measurements exist. These two sets of measurements differ in the material characteristics that they represent and the test conditions at which they are obtained.

ACKNOWLEDGMENTS

The work reported herein is a part of Project A002A of SHRP. Project A002A was conducted by the Western Research Institute, Laramie, Wyoming, in cooperation with the Pennsylvania Transportation Institute (PTI). Acknowledgments go in particular to D. Christensen, R. Dongre, and M. G. Sharma, who were principal members of the research team at PTI. Acknowledgments also go to T. Kennedy, E. Harrigan, J. Moulthrop, and D. Jones for their contributions in discussions and their feedback during the development of the specification concepts and parameters. Acknowledgments also go to all members of the FHWA Expert Task Group for their valuable discussions and comments on the work conducted in the project.

REFERENCES

1. Anderson, D. A., H. U. Bahia, D. W. Christensen, R. Dongre, M. G. Sharma, C. Antle, and J. Button. *Binder Characterization and Evaluation,* Vol. 3. *Physical Characterization* Report SHRP-A-369. Strategic Highway Research Program, National Research Council, Washington, D.C., 1994.
2. Bahia, H. U. *Bibliographies for Physical Properties of Asphalt Cement.* Report SHRP-A-626. Strategic Highway Research Program, National Research Council, Washington, D.C., 1993.
3. Anderson, D. A., and H. U. Bahia. Evaluation of Operating Conditions for Dynamic Shear Rheometers Used for Asphalt Binder Specification Testing. Presented at ASTM Symposium on Physical Properties of Asphalt Cements, Dallas/Ft. Worth, Tex., Dec. 7, 1993.
4. Bahia, H. U., and D. A. Anderson. The Development of the Bending Beam In Rheometer: Basics and Critical Evaluation. In *Physical Properties of Asphalt Cement Binders: ASTM STP 1241* (J. C. Harden, ed.) ASTM, 1994.
5. Anderson, D. A., and R. Dongre. The SHRP Direct Tension Specification Test—Its Development and Use. Presented at the ASTM Symposium on Physical Properties of Asphalt Cements, Dallas/Ft. Worth, Tex., Dec. 7, 1993.
6. Bahia, H. U., and D. A. Anderson. The Pressure Aging Vessel (PAV): A Test to Simulate Rheological Changes Due to Field Aging. In *Physical Properties of Asphalt Cement Binders: ASTM STP 1241* (J. C. Harden, ed.) ASTM, 1994.
7. Ferry, J. D. *Viscoelastic Properties of Polymers.* John Wiley and Sons, Inc. New York, 1980.
8. Bahia, H. U., and D. A. Anderson. "Physical Hardening of Asphalt Binders and Relation to Compositional Parameters," Preprints of the 204th American Chemical Society National Meeting, Division of Fuel Chemistry, Vol. 37, Nos. 3 and 4, 1992.
9. Bahia, H. U., D. A. Anderson, and D. W. Christensen. The Bending Beam Rheometer; A Simple Device for Measuring Low Temperature Rheology of Asphalt Binders. *Journal of the Association of Asphalt Paving Technologists,* Vol. 61, 1992, pp. 117–153.
10. Bahia, H. U., and D. A. Anderson. Glass Transition Behavior and Physical Hardening of Asphalt Binders. *Journal of the Association of Asphalt Paving Technologists,* Vol. 62, 1993, pp. 93–130.

Strategic Highway Research Program Properties of Asphalt Cement

DOUGLAS I. HANSON, RAJIB BASU MALLICK, AND KEE FOO

In the spring of 1993 the Strategic Highway Research Program (SHRP) asphalt research program was completed. As the result of that effort a new specification for asphalt cements was developed along with new testing procedures. The results of a study of asphalts being used in the southeastern United States in which the asphalts were tested by using the current capillary tube testing technology and the new SHRP technology are presented. Fifty-eight asphalt cements from throughout the United States were tested. Viscosity of neat asphalt cements (60°C) showed strong correlations with dynamic shear rheometer stiffness at 60°C and 70°C. For the asphalt cements tested, the value of the slope of the log stiffness-versus-time curve obtained from regressed stiffness *S*-versus-*m* data from bending beam rheometer tests corresponding to an *S* value of 300 MPa was found to be 0.27.

In the spring of 1993 one of the largest research efforts ever conducted on asphalt cement and hot-mix asphalt mixtures ended. This effort, which involved 5 years of intensive study by many researchers, was the $50 million Strategic Highway Research Program (SHRP) on asphalts. In August 1993 the AASHTO Subcommittee on Materials approved a new provisional specification for asphalt cement and test procedures to support that specification. There was a desire to develop an understanding of how asphalt cements being used throughout the United States related to the SHRP specification. Thus, the National Center for Asphalt Technology (NCAT) tested and analyzed a number of the asphalt cements from throughout the United States.

OBJECTIVES

The objective of the present work was to develop a data base of asphalts being used throughout much of the United States graded by using the new SHRP procedures and to determine how asphalts graded by SHRP procedures relate to those being graded by the current viscosity grading system.

SCOPE

This report provides data and an analysis of the results for the 58 asphalts currently being supplied. These asphalts come from 20 states throughout the United States. The asphalts were tested by both the conventional penetration and capillary tube viscosity tests and the new SHRP test procedures.

D. I. Hanson, National Center for Asphalt Technology, 211 Ramsay Hall, Auburn University, Auburn, Ala. 36849-5354. R. B. Mallick and K. Foo, Auburn University, Auburn, Ala. 36849.

DESCRIPTION OF MATERIALS AND EXPERIMENTAL PROCEDURES

In January 1994 a request was made of a number of state highway agencies and refineries for test data and 4-L (1-gal) samples of the asphalt cements currently being used or supplied. No modified asphalts were included in the study. Work conducted on modified asphalts will be included in the data bank at a later date. In response to that request a total of 58 asphalt cements were sent to NCAT for testing.

The state highway agencies were requested to provide specific data on each of the asphalt cements supplied. The data requested included

1. Grade and source of the asphalt (refinery and supplier);
2. The following properties on the unaged or neat asphalt cement:
   a. Viscosity at 60°C,
   b. Viscosity at 135°C,
   c. Penetration at 4°C,
   d. Penetration at 25°C,
   e. Ductility at 25°C, and
   f. Softening point; and
3. The following properties on the asphalt cement after aging in the thin film oven:
   a. Viscosity at 60°C,
   b. Viscosity at 135°C,
   c. Penetration at 4°C,
   d. Penetration at 25°C,
   e. Ductility at 25°C,
   f. Softening point, and
   g. Percent loss

After receipt of the samples at NCAT they were broken down into 1-L (1-qt)-size samples for testing. Each sample was heated and stirred before it was poured into the containers. The samples were not heated more than once before testing. Some of the samples were obtained directly from the refiners and on those samples the testing described earlier was accomplished by NCAT.

All of the samples received were tested by using the procedures described in the AASHTO Provisional Standards described elsewhere (1–4). The following tests were performed on each sample:

1. Stiffness on the original or neat asphalt, as determined by the dynamic shear rheometer (DSR) at 64°C and 70°C.
2. Stiffness of the asphalt after aging in the rolling thin film oven (RTFO), as determined by the DSR at 64°C and 70°C.
3. Stiffness on the asphalt after aging in the RTFO and the pressure aging vessel (PAV), as determined by the DSR at 7°C, 10°C, and 13°C.

4. Stiffness on the asphalt after aging in the RTFO and the PAV as determined by the bending beam rheometer at −6°C, −12°C, and 18°C.

A specification-grade Bohlin rheometer for dynamic shear testing and a Cannon bending beam rheometer were used for these tests.

DISCUSSION OF TEST RESULTS

Table 1 presents the detailed test data showing the properties of the asphalt cement as determined by both the current testing technology and the SHRP testing procedures.

All seven AC-10 asphalt cements tested graded to be performance grade PG 58–22. On the upper-temperature regime 20 of the AC-20 asphalt cements graded to be PG 64 and 4 graded to be PG 58. On the cold-temperature regime 16 of the AC-20 asphalt cements graded to be PG -22, 4 graded to be PG -16, and 3 graded to be PG -28. On the upper-temperature regime 23 of the AC-30 asphalt cements graded to be PG 64 and 1 graded to be PG 70. On the cold-temperature regime 16 of the AC-30 asphalt cements graded to be PG -22, 6 graded to be PG -16, 1 graded to be PG -28, and 1 graded to be PG -34. In summary, of the 48 AC-20 and AC-30 asphalt cements tested, 29 of them graded to be PG 64–22, 8 graded to be PG 64–16, 2 graded to be PG 58–16, 2 graded to be PG 58–16, 5 graded to be PG 64–28, 1 graded to be PG 64–34, and 1 graded to be PG 70–22.

Table 2 presents the averages for the various properties determined from testing the AC-10, AC-20, and AC-30 asphalt cements. For the AC-10 asphalt cements the average viscosity was 1130 P, which correlated to a DSR complex modulus of 0.593 kPa at 64°C and a bending beam stiffness of 231 MPa and slope of the log stiffness-versus-time curve value, (m-value) of 0.28 at −18°C. For the AC-20 asphalt cements the average viscosity was 2051 P, which correlated to a DSR complex modulus of 1136 MPa at 64°C, a bending beam stiffness of 335.5 MPa, and an m-value of 0.276 at −18°C. For the AC-30 asphalt cements the average viscosity was 3107 P, which correlated to a DSR complex modulus of 1.715 at 64°C, a bending beam stiffness of 345 MPa, and an m-value of 0.263 at −18°C.

Properties of Asphalt Cement by SHRP Techniques

Viscosity versus $G^*/\sin\delta$

Figure 1 shows the absolute viscosity at 60°C of the neat asphalt cement plotted against the $G^*/\sin\delta$ (stiffness) at 64°C and 70°C for all of the asphalts tested. $G^*\sin\delta$ where G^* is the complex shear modulus and δ is the phase angle) increases as the viscosity increases. The relationship at 64°C is very strong, with an R^2 value of 0.85. It can be seen from the best-fit lines through the plotted data that for the asphalts tested in the present study an AC-16 asphalt cement would typically meet the requirements of a PG 64 and that an AC-40 asphalt cement would meet the requirements of a PG 70.

Comparison of Aging Properties

Figure 2 shows the absolute viscosities at 60°C and 70°C of the asphalt cement after TFOT aging versus $G^*/\sin\delta$ at 64°C after

TABLE 1 SHRP Asphalt Data Base

STATE	AL	AL	AL	AL
GRADE OF AC	AC-20	AC-20	AC-20	AC-20
CODE	1	2	3	4
Vis @ 60°C, P	2302	2347	2082	2154
Vis @ 135°C, cST	367	396	476	406
Pen @ 4°C	3	2	2	28
Pen @ 25°C	71	70	75	96
Ductility @ 25°C, mm	100	100	100	-
Softening Pt., C	47	48	48	47
TFO RESIDUE				
Vis @ 60°C, P	4434	5043	6851	4659
Vis @ 135°C, cST	539	585	759	570
Pen @ 4°C	2	1	1	21
Pen @ 25°C	50	44	42	63
Softening Pt., C	52	53	54	51
% Loss	0.26	0.34	0.23	0.22
SHRP				
Grade	PG 64-22	PG 64-22	PG 64-22	PG 64-28
DSR-Original 64°C, KPa	1.07	1.25	1.11	1.125
DSR-Original 70°C, KPa	0.49	0.59	0.56	0.52
DSR-RTFO-64°C, KPa	2.64	3.22	6.72	2.341
DSR-RTFO-70°C, KPa	1.25	1.49	3.16	1.07
DSR-PAV-13°C, MPa	5.02	4.37	3.51	-
Flexural Creep-18°C	471	383	296	219
MPa				
m	0.27	0.29	0.27	0.3

- NOT AVAILABLE

(continued on next page)

TABLE 1 (*continued*)

STATE	AR	AR	AR	AR	CO
GRADE OF AC	AC-30	AC-30	AC-30	AC-20	AC-10
CODE	1	2	3	4	1
Vis @ 60°C, P	2690	3087	2795	2128	1190
Vis @ 135°C, cST	392	552	520	652	284
Pen @ 4°C	18	13	18	21	30
Pen @ 25°C	60	56	56	76	97
Ductility @ 25°C, mm	150+	150+	-	-	-
Softening Pt., C	54	55	50	48	47
TFO RESIDUE					
Vis @ 60°C, P	5593	7249	4298	4853	3180
Vis @ 135°C, cST	576	860	558	523	413
Pen @ 4°C	16	18	15	16	21
Pen @ 25°C	44	39	42	52	57
Softening Pt., C	56	57	57	56	52
% Loss	0.125	0.06	0	0.1	-
SHRP					
Grade	PG 64-22	PG 64-22	PG64-22	PG64-22	PG 58-22
DSR-Original 64°C, KPa	1.57	1.69	1.63	1.28	0.630
DSR-Original 70°C, KPa	0.73	0.81	0.78	0.63	1.433
DSR-RTFO-64°C, KPa	3.25	4.03	3.08	2.63	1.578
DSR-RTFO-70°C, KPa	1.45	1.89	1.38	1.22	3.794
DSR-PAV-10°C, MPa	8.45	7.27	7.41	6.50	-
Flexural Creep-18°C	532.0	355.0	427.5	444.5	224
MPa					
m	0.24	0.24	0.25	0.27	0.285

STATE	FL	FL	FL
GRADE OF AC	AC-30	AC-30	AC-30
CODE	1	2	3
Vis @ 60°C, P	3272	-	-
Vis @ 135°C, cST	638	-	-
Pen @ 4°C	24	-	-
Pen @ 25°C	64	-	-
Ductility @ 25°C, mm	1004	-	-
Softening Pt., C	51	-	-
TFO RESIDUE			
Vis @ 60°C, P	11512	-	-
Vis @ 135°C, cST	998	-	-
Pen @ 4°C	18	-	-
Pen @ 25°C	39	-	-
Softening Pt., C	58	-	-
% Loss	0.31	-	-
SHRP Grade	PG 64-22	PG 70-22	PG 64-16
DSR-Original 64°C, KPa	1.93	1.98	1.86
DSR-Original 70°C, KPa	0.96	1.01	0.97
DSR-RTFO-64°C, KPa	4.67	6.41	4.51
DSR-RTFO-70°C, KPa	2.16	3.16	10.08
DSR-PAV-10°C, MPa	6.06	5.10	7.63
Flexural Creep-18°C	307.0	257.5	419.5
MPa			
m	0.24	0.25	0.24

- NOT AVAILABLE

(continued on next page)

TABLE 1 *(continued)*

STATE	GA	GA	GA	GA	GA
GRADE OF AC	AC-20	AC-30	AC-30	AC-20	AC-30
CODE	1	2	3	4	5
Vis @ 60°C, P	1943	3343	3317	2333	2733
Vis @ 135°C, cST	408	543	557	392	443
Pen @ 4°C	21	25	26	20	17
Pen @ 25°C	66	60	67	67	56
Ductility @ 25°C, mm	150+	150+	150+	150+	150+
Softening Pt., C	50	50	50	50	50
TFO RESIDUE					
Vis @ 60°C, P	5191	7969	9341	4890	5274
Vis @ 135°C, cST	551	704	852	538	539
Pen @ 4°C	17	18	17	13	20
Pen @ 25°C	40	36	43	55	37
Softening Pt., C	57	59	57	55	59
% Loss	13	.02	0.27	0.08	0.03
SHRP					
Grade	PG 64-16	PG 64-22	PG 64-22	PG 64-16	PG 64-16
DSR-Original 64°C, KPa	1.02	1.78	1.40	1.04	1.23
DSR-Original 70°C, KPa	0.49	0.84	0.69	0.52	0.62
DSR-RTFO-64°C, KPa	2.28	3.50	3.13	2.31	2.77
DSR-RTFO-70°C, KPa	1.10	1.67	1.52	1.13	1.29
DSR-PAV-10°C, MPa	-	-	-	-	-
Flexural Creep-18°C	424	302	324	382	437
MPa					
m	0.24	0.27	0.29	0.26	0.25

STATE	GA	GA	GA	GA	GA
GRADE OF AC	AC-20	AC-20	AC-30	AC-20	AC-30
CODE	6	7	8	9	10
Vis @ 60°C, P	2162	2172	3172	2225	3196
Vis @ 135°C, cST	397	497	573	538	460
Pen @ 4°C	96	17	23	32	28
Pen @ 25°C	109	91	67	76	67
Ductility @ 25°C, mm	150+	150+	150+	150+	150+
Softening Pt., C	48	51	51	49	51
TFO RESIDUE					
Vis @ 60°C, P	5761	6643	9555	5961	8386
Vis @ 135°C, cST	534	843	892	664	806
Pen @ 4°C	26	54	19	20	18
Pen @ 25°C	60	23	30	52	42
Softening Pt., C	58	54	57	55	56
% Loss	0.25	0.36	0.34	0.15	0.22
SHRP					
Grade	PG 64-28	PG 64-28	PG 64-16	PG 64-22	PG 64-22
DSR-Original 64°C, KPa	1.06	1.32	1.84	1.39	1.88
DSR-Original 70°C, KPa	0.53	0.67	0.92	0.69	0.96
DSR-RTFO-64°C, KPa	2.76	3.21	4.52	3.56	6.16
DSR-RTFO-70°C, KPa	1.29	1.6	2.21	1.66	3.09
DSR-PAV-10°C, MPa	-	5.44	6.27	4.93	5.62
Flexural Creep-18°C	-	251.5	628.8	538.7	260.5
MPa					
m	-	0.33	0.23	0.25	0.27

- NOT AVAILABLE

(continued on next page)

TABLE 1 (*continued*)

STATE	LA	LA	LA
GRADE OF AC	AC-30	AC-30	AC-30
CODE	1	2	3
Vis @ 60°C, P	3298	3370	3570
Vis @ 135°C, cST	557	481	484
Pen @ 4°C	9	6	18
Pen @ 25°C	66	58	84
Ductility @ 25°C, mm	150+	150+	150+
Softening Pt., C	41	54	51
TFO RESIDUE			
Vis @ 60°C, P	7634	7640	7933
Vis @ 135°C, cST	708	613	707
Pen @ 4°C	8	5	13
Pen @ 25°C	48	37	63
Softening Pt., C	57	57	58
% Loss	0.09	0.17	0.04
SHRP			
Grade	PG 64-22	PG 64-16	PG 64-34
DSR-Original 64°C, KPa	1.78	2.00	1.74
DSR-Original 70°C, KPa	0.85	0.93	0.87
DSR-RTFO-64°C, KPa	4.81	4.71	4.16
DSR-RTFO-70°C, KPa	2.31	2.10	2.00
DSR-PAV-10°C, MPa	6.23	10.23	1.61
Flexural Creep-18°C	347.7	513.6	75.4
MPa			
m	0.277	0.237	0.31

STATE	MI	MI	MI	MI
GRADE OF AC	AC-1	AC-2.5	AC-5	AC-10
CODE	1	2	3	4
Vis @ 60°C, P	-	-	541	1240
Vis @ 135°C, cST	-	-	212	311
Pen @ 4°C	-	-	49	25
Pen @ 25°C	-	-	185	105
Ductility @ 25°C, mm	-	-	-	-
Softening Pt., C	-	-	40	45
TFO RESIDUE				
Vis @ 60°C, P	-	-	1350	3190
Vis @ 135°C, cST	-	-	316	445
Pen @ 4°C	-	-	40	22
Pen @ 25°C	-	-	94	61
Softening Pt., C	-	-	46	52
% Loss	-	-	-	-
SHRP Grade	PG 40-40	PG 46-34	PG 52.50	PG 58-22
DSR-Original 52°C, KPa	0.27	0.83	1.468	0.589
DSR-Original 58°C, KPa	-	0.41	0.806	1.301
DSR-RTFO-52°C, KPa	0.29	2.55	3.905	1.554
DSR-RTFO-58°C, KPa	-	-	1.806	3.621
DSR-PAV-10°C, MPa	-	2.14	2.789	-
Flexural Creep-24°C	106	265	573	248
MPa				
m	0.355	0.300	0.280	0.290

- NOT AVAILABLE

(continued on next page)

TABLE 1 *(continued)*

STATE	MN	MN	MS	MS	MS	MS
GRADE OF AC	AC-5	AC-10	AC-30	AC-30	AC-30	AC-30
CODE	1	2	1	2	3	4
Vis @ 60°C, P	597	1090	3015	3118	2744	3184
Vis @ 135°C, cST	217	300	542	548	482	465
Pen @ 4°C	42	31	-	-	-	-
Pen @ 25°C	173	113	55	61	96	58
Ductility @ 25°C, mm	-	-	150+	150+	150+	150+
Softening Pt., C	40	46	51	49	51	48
TFO RESIDUE						
Vis @ 60°C, P	1440	2850	8195	7065	12726	13528
Vis @ 135°C, cST	316	449	810	634	849	854
Pen @ 4°C	33	21	-	-	-	-
Pen @ 25°C	85	63	38	40	57	36
Softening Pt., C	46	52	57	55	57	58
% Loss	-	-	0.06	0.22	0.4	0.01
SHRP						
Grade	PG 52-28	PG58-22	PG 64-22	PG 64-22	PG 64-28	PG 64-22
DSR-Original 64°C, KPa	1.352	0.536	1.89	1.69	1.62	1.70
DSR-Original 58°C, KPa	0.653	1.192	0.93	0.80	0.83	0.83
DSR-RTFO-64°C, KPa	4.060	1.385	4.47	3.65	5.69	6.73
DSR-RTFO-58°C, KPa	1.930	3.146	2.11	1.67	2.84	3.30
DSR-PAV-10°C, MPa	2.865	4.089	7.10	7.66	1.95	5.77
Flexural Creep-18°C	565	223	375.5	548.9	77.5	284.0
MPa						
m	0.290	0.285	0.26	0.26	0.31	0.26

STATE	SC	SC	SC	TX	TX	TX	TX
GRADE OF AC	AC-20S	AC-30	AC-20S	AC-20	AC-20	AC-20	AC-20
CODE	1	2	3	1	2	3	4
Vis @ 60°C, P	2364	3278	2011	1937	1647	1840	1765
Vis @ 135°C, cST	427	500	391	417	311	369	350
Pen @ 4°C	25	24	21	26	20	16	22
Pen @ 25°C	79	65	74	66	59	57	63
Ductility @ 25°C, mm	100+	100+	100+	150+	150+	150+	150+
Softening Pt., C	---	---	---	48.8	49.4	50	51.1
TFO RESIDUE							
Vis @ 60°C, P	5665	9436	4930	4080	3228	3293	4610
Vis @ 135°C, cST	631	778	561	534	485	495	515
Pen @ 4°C	18	18	15	20	16	14	19
Pen @ 25°C	48	43	41	44	39	46	40
Softening Pt., C	---	---	---	53	54	53	58
% Loss	0.17	0.21	0.02	0.2	0.2	0.01	0.2
SHRP							
Grade	PG 64-28	PG 64-22	PG 64-22	PG 64-22	PG 58-22	PG 58-16	PG 58-16
DSR-Original 64°C, KPa	1.288	1.641	1.142	1.171	0.982	0.934	0.950
DSR-Original 70°C, KPa	0.641	0.792	0.564	0.579	-	-	-
DSR-RTFO-64°C, KPa	2.949	6.382	2.867	2.396	2.201	2.136	1.450
DSR-RTFO-70°C, KPa	1.386	3.033	1.356	1.106	-	-	-
DSR-PAV-10°C, MPa	5.761	5.062	5.273	4.904	8.59	5.065	5.818
Flexural Creep-18°C	300.0	263.5	324.5	321.5	424	-	-
MPa							
m	0.31	0.27	0.25	0.26	0.24	-	-

- NOT AVAILABLE

(continued on next page)

TABLE 1 (*continued*)

STATE	VA	VA	VA	VA	VA
GRADE OF AC	AC-20	AC-20	AC-20	AC-20	AC-20
CODE	1	2	3	4	5
Vis @ 60°C, P	1865	1835	1800	2357	2005
Vis @ 135°C, cST	393	400	393	388	417
Pen @ 4°C	-	-	-	-	-
Pen @ 25°C	62	79	88	66	80
Ductility @ 25°C,mm	150+	150+	150+	150+	150+
Softening Pt.,C	50	48	47	48	49
TFO RESIDUE					
Vis @ 60°C, P	5241	4770	4416	5044	5280
Vis @ 135°C, cST	578	604	583	535	621
Pen @ 4°C	-	-	-	-	-
Pen @ 25°C	48	48	53	44	49
Softening Pt., C	58	54	53	54	55
% Loss	<.03	<.16	<.02	<.30	<.13
SHRP					
Grade	PG 64-22	PG 64-22	PG 58-22	PG 64-22	PG 64-22
DSR-Original 64°C, KPa	1.023	1.143	0.983	1.246	1.128
DSR-Original 70°C, KPa	0.499	0.566	-	0.575	.554
DSR-RTFO-64°C, KPa	2.566	3.268	2.822	2.675	2.914
DSR-RTFO-70°C, KPa	1.228	1.510	1.338	1.202	1.358
DSR-PAV-10°C, MPa	6.273	3.694	3.157	7.033	4.117
Flexural Creep-18°C	340.5	239	185.5	443	242
MPa					
m	0.25	0.29	0.29	0.27	0.27

STATE	VA	VA	VA	VA	VA
GRADE OF AC	AC-30	AC-30	AC-30	AC-30	AC-30
CODE	6	7	8	9	10
Vis @ 60°C, P	3028	2999	3593	2982	2751
Vis @ 135°C, cST	489	489	543	561	493
Pen @ 4°C	-	-	-	-	-
Pen @ 25°C	48	57	61	67	65
Ductility @ 25°C, mm	150+	150+	150+	150	150
Softening Pt., C	53	50	53	50	51
TFO RESIDUE					
Vis @ 60°C, P	8226	7836	10793	7833	7679
Vis @ 135°C, cST	696	738	860	761	731
Pen @ 4°C	-	-	-	-	-
Pen @ 25°C	30	38	57	45	40
Softening Pt.,C	58	57	58	54	57
% Loss	<.006	<.15	<.11	<.30	<.11
SHRP					
Grade	PG 64-16	PG 64-16	PG 64-22	PG 64-22	PG 64-22
DSR-Original 64°C, KPa	1.67	1.56	1.71	1.66	1.72
DSR-Original 70°C, KPa	0.807	0.77	0.88	0.85	.89
DSR-RTFO-64°C, KPa	4.61	4.99	5.40	4.90	4.71
DSR-RTFO-70°C, KPa	2.09	-	-2.55	2.33	2.22
DSR-PAV-10°C, MPa	6.80	4.94	4.97	6.02	5.23
Flexural Creep-18°C	379.5	318	233.5	336	276.4
MPa					
m	0.23	0.25	0.28	0.29	0.28

- NOT AVAILABLE

(continued on next page)

TABLE 1 *(continued)*

STATE	WV	WV	WV	WV	WY	WY	WY
GRADE OF AC	AC-20	AC-20	AC-10	AC-20	85-100	AC-10	AC-10
CODE	1	2	3	4	1	2	3
Vis @ 60°C, P	2035	1875	1163	2143	1710	1000	1100
Vis @ 135°C, cST	525	412	333	424	370	285	276
Pen @ 4°C	44	42	40	37	23	27	30
Pen @ 25°C	91	83	100	75	84	90	101
Ductility @ 25°C, mm	145	142	115	146	-	-	-
Softening Pt., C	-	-	-	-	48	47	47
TFO RESIDUE							
Vis @ 60°C, P	5050	4983	2492	5183	4120	2180	3490
Vis @ 135°C, cST	621	572	416	599	537	380	423
Pen @ 4°C	20	25	28	24	23	15	30
Pen @ 25°C	53	49	67	47	54	57	57
Softening Pt., C	-	-	-	-	54	51	52
% Loss	0.07	0.10	0.04	0.03	-	-	-
SHRP							
Grade	PG 64-28	PG 64-22	PG 64-22	PG 64-22	PG 58-22	PG 58-22	PG 58-22
DSR-Original 64°C, KPa	1.19	1.16	0.72	1.24	0.827	0.548	0.535
DSR-Original 70°C, KPa	0.60	0.65	0.37	0.62	1.876	1.261	1.213
DSR-RTFO-64°C, KPa	3.12	2.88	1.43	2.44	2.186	1.162	1.548
DSR-RTFO-70°C, KPa	1.48	1.39	0.71	1.16	5.245	2.770	3.681
DSR-PAV-10°C, MPa	3.47	4.66	4.3	4.99	5.412	-	-
Flexural Creep-18°C	187.5	237.0	261.5	275.5	249	321	215
MPa							
m	0.30	0.29	0.28	0.28	0.280	0.260	-

- NOT AVAILABLE

TABLE 2 Properties of AC-10, AC-20, and AC-30 Asphalt Cements

PROPERTY	AC-10		AC-20		AC-30	
	$\bar{x}$	σ	$\bar{x}$	σ	$\bar{x}$	σ
Viscosity @ 60C, P	1130	77	2051	207	3107	259
Viscosity @ 135C, cST	298	19	425	69	508	45
Pen @ 4C	30	5	25	20	18	10
Pen. @ 25 C	101	7	75	12	63	10
Pen. Index	-	-	3.83	4.43	3.22	2.13
PVN	-	-	-0.48	0.28	-0.32	0.25
Ductility @ 25C, MM	-	-	137	21	147	10
Soft Pt., C	46	17	49	17	51	15
TFO Viscosity 60C, P	2897	446	5017	836	8294	2117
TFO Viscosity 135C, cST	421	22	588	78	739	105
TFO Pen. 4C	22	5	16	7	13	7
TFO Pen. 25C	60	4	48	5	42	8
TFO Pen. Index	-	-	3.9	3.6	5.1	3.1
TFO PVN	-	-	-0.28	0.27	0.02	0.40
TFO Soft. Pt., C	52	17	54	16	57	11
TFO, % Loss	-	-	0.15	0.10	0.14	0.11
DSR Original 64C, KPa	0.59	0.06	1.14	0.12	1.72	0.17
DSR Original 70C, KPa	-	-	0.58	0.06	0.85	0.09
DSR RTFO 64C, KPa	3.39	0.37	2.87	0.94	4.54	1.19
DSR RTFO 70C, KPa	-	-	1.42	0.043	2.64	1.75
DSR PAV 10C, MPa	-	-	5.27	1.32	6.06	1.89
DSR PAV 13C, MPa	-	-	4.44	1.26	4.71	1.50
Flexural Creep, 18C, MPa	281	37	335	97	345	129
m	0.28	0.01	0.27	0.02	0.26	0.02

- NOT AVAILABLE

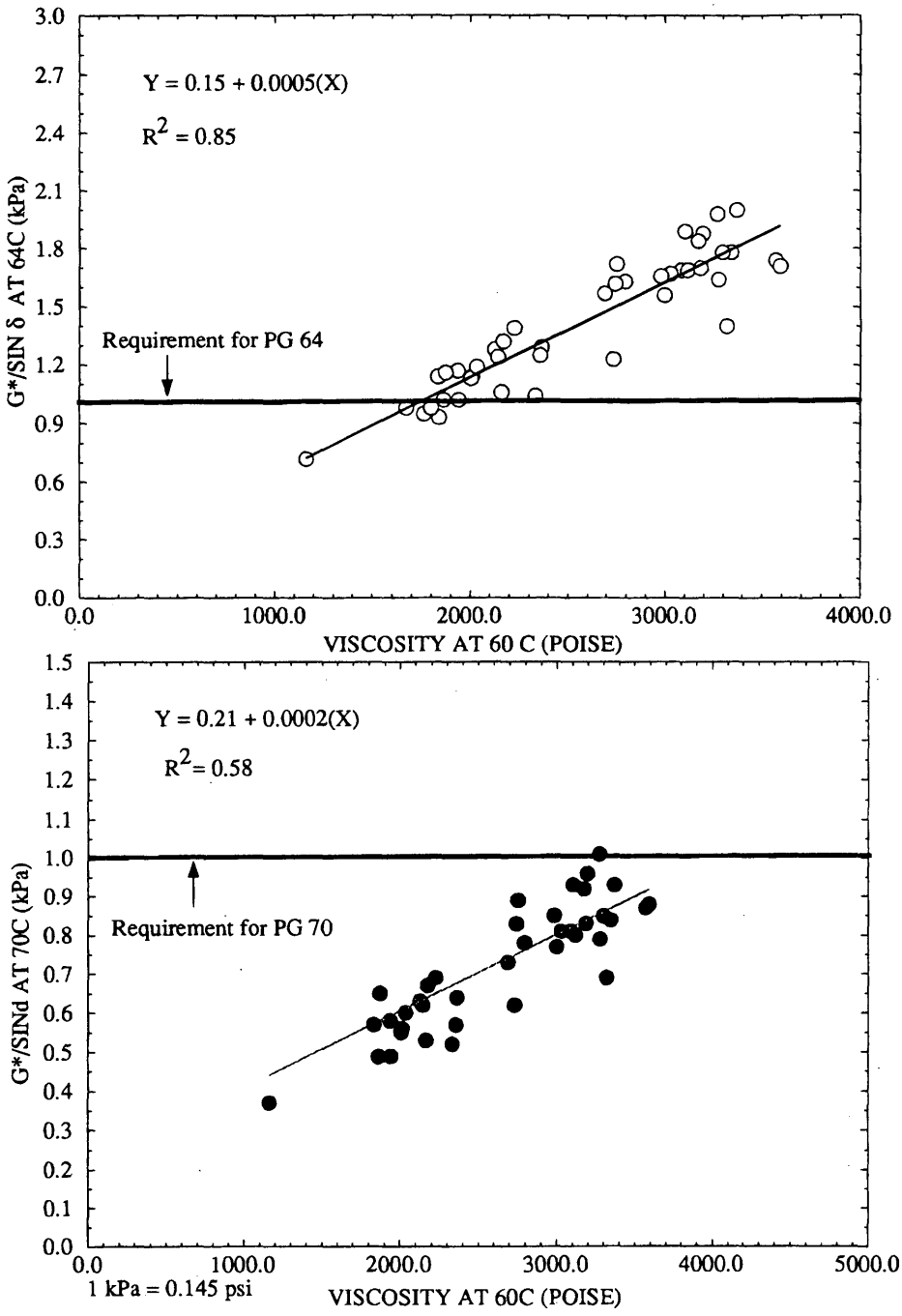

FIGURE 1 Viscosity at 60°C versus $G^*/\sin\delta$ for original asphalt cement.

RTFOT aging. Even though the relationship is strong (R^2 = 0.79) for both 64°C and 70°C, it is weaker than that observed for the neat asphalt cement. This may be explained in part by the different aging characteristics of the two aging procedures, TFOT versus RTFOT. As Zupanick (*5*) pointed out the TFOT and the RTFOT tests are not interchangeable. He also pointed out that the results will vary with the asphalts being tested.

Bending Beam Rheometer Stiffness Versus m.

There has been considerable discussion about the concept of changing the temperature requirements in the AASHTO specification for cold temperatures. The current requirement is that the relaxation modulus (stiffness) determined by the bending beam rheometer (in megapascals) be less than 300 and that the *m*-value be more than

0.30. It has been proposed that the m-value be reduced from 0.30 to something less. Figure 3 provides a plot of m versus the relaxation modulus (stiffness) for all asphalts and all test temperatures evaluated in the study. A best-fit curve was drawn through the points. The relationship is found to be very strong ($R^2 = 0.84$). The data indicate that for a stiffness of 300 MPa the corresponding stiffness is 0.274. The best-fit curve presented here is not meant for actual use but to justify the experimentally obtained correlation. Thus, based on the asphalt tested in the present study, the m-value will control the specification limits. Because of the limited number of asphalts tested, no adjustment in the specification is recommended here. These data do not support a specification change.

Difference Between High and Low

To assess the availability of asphalt cements both the high-temperature and the low-temperature properties of the asphalt cement must be considered. A rule of 90 has been discussed a great deal throughout the industry. This rule states that if an agency wants

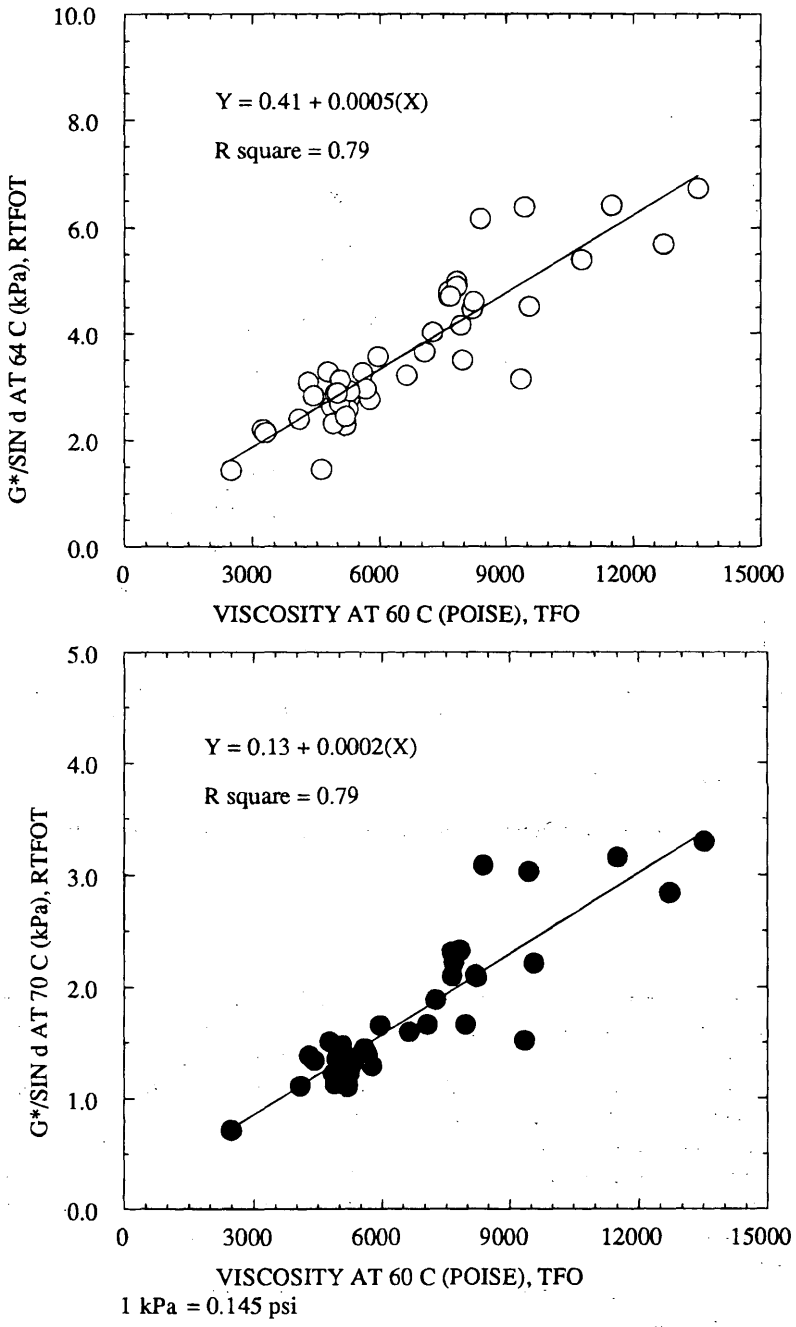

FIGURE 2 Viscosity at 60°C (TFOT) versus $G^*/\sin\delta$ for RTFOT asphalt cement.

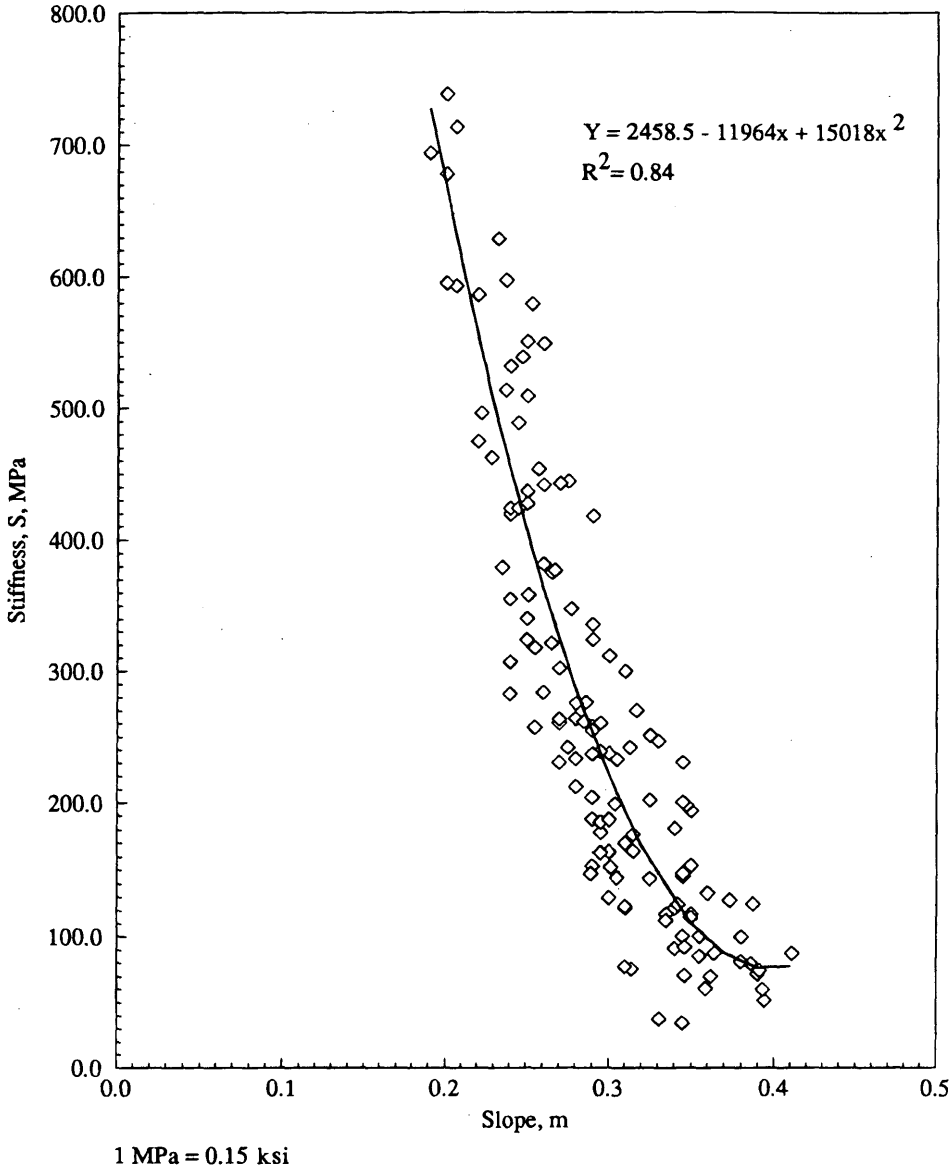

FIGURE 3 Bending beam rheometer stiffness versus bending beam rheometer slope.

to limit its asphalts to unmodified asphalt cements the difference between the top and bottom range for the asphalts must be less than 90°C. For example, a PG 64–22 would have a difference of 86°C, which would mean that an agency could probably obtain an unmodified asphalt cement that would meet that requirement. If the agency specified a PG 76–22 the difference would be 98°C, which would mean that the agency would probably need to purchase a modified asphalt cement to meet this specification.

To test this hypothesis the temperature at which each of the asphalt cements tested where they met the requirement for high temperature [stiffness (S) = 1 kPa] and where they met the temperature at which each of the asphalts tested met the requirement for low temperature (m = 0.30) was determined. Table 3 presents the results of this analysis. To assess the specification 10°C must be added to the difference. This is required because the cold test temperature is 10°C higher than the specification temperature. A review of the data in Table 3 shows that for an AC-20 asphalt cement the average specification difference would be 89.2°C, with a range of 96.2°C to 82.7°C. For an AC-30 asphalt cement the average specification difference would be 92.3°C, with a range of 99.7°C to 84.3°C. Thus, it would appear that the rule of 90, on average, is a good approximation. Depending on the asphalt cements being used, however, it may not apply.

CONCLUSIONS

Based on the research conducted in the present study it is concluded that:

TABLE 3 Difference Between High and Low Temperatures

VISCOSITY GRADE	AVG. TEMP @ DSR STIFF. 1 KPa, C	AVG. TEMP @ m 0.3,C	AVG. DIFF. BETWEEN HIGH & LOW	MAXM. DIFF. BETWEEN HIGH & LOW	MINM. DIFF. BETWEEN HIGH & LOW
AC-5*	55.1	22.4	75.5	75.5	75.5
AC-10*	60.0	15.6	75.7	77.7	72.5
AC-20	65.0	14.2	79.2	86.2	72.7
AC-30	68.6	14.2	82.3	89.7	74.3

*** Based on very limited testing**

1. The asphalt cements tested as part of the study will generally fall into the following categories:

- AC-5 is PG 52–28,
- AC-10 is PG 58–22,
- AC-20 is PG 64–22, and
- AC-40 is PG 70–16.

2. The viscosity of neat asphalt cement (60°C) shows a fairly strong correlation with DSR stiffness ($G^*/\sin\delta$ at 64°C and 70°C).

3. For the asphalt cements tested in the study the *m*-value was found to be about 0.27 for the corresponding *S* value of 300 MPa. Thus, the currently specified *m*-value of 0.3 is generally the controlling value for this specification.

REFERENCES

1. *Standard Practice for Accelerator Aging of Asphalt Binder Using a Pressurized Aging Vessel (PAV).* AASHTO Designation PP1, edition 1A. AASHTO, Sept. 1993.
2. *Standard Practice for Determining the Flexural Creep Stiffness of Asphalt Binder Using the Bending Beam Rheometer (BBR).* AASHTO Designation TP1, edition 1A. AASHTO, Sept. 1993.
3. *Standard Practice for Performance Graded Asphalt Binder.* AASHTO Designation MP1, edition 1A. AASHTO, Sept. 1993.
4. *Standard Practice for Determining the Rheological Properties of Asphalt Binder Using a Dynamic Shear Rheometer (DSR).* AASHTO Designation TP1, edition 1A. AASHTO, Sept. 1993.
5. Zupanick, M. Comparison of the Thin Film Oven Test and the Rolling Thin Film Oven Test. Presented at 1994 Annual Meeting of the Association of Asphalt Paving Technologists, March 1994.

Quantitative Determination of Polymers in Asphalt Cements and Hot-Mix Asphalt Mixes

CHRISTINE W. CURTIS, DOUGLAS I. HANSON, SHOU TA CHEN, GUEI-JEN SHIEH, AND MEI LING

The addition of polymers in asphalt cement has been widespread. Quantitative analysis of these polymers is essential to verify if specifications are being met. The analysis of two styrene butadiene rubber (SBR) latexes and ethylene vinyl acetate (EVA) and styrene butadiene styrene (SBS) polymers in three different asphalts was accomplished by Fourier transform infrared (FTIR) spectroscopy. Although the behavior of each SBR latex in each asphalt yielded somewhat different calibration curves, each latex-modified asphalt cement was successfully quantified. The values for latex determined by FTIR spectroscopy yielded a more linear relationship between the dynamic shear measurements and the latex concentration than the nominal values that accompanied the mixtures. Both EVA and SBS polymers were also quantified by using the analysis that was developed for the SBR latex-modified asphalt. The infrared analysis of SBR latex in asphalt was directly applied to the analysis of SBR latex in asphalt-aggregate mixes. Analysis of 3 weight percent SBR latex in asphalt concrete samples was achieved by removing the SBR latex-modified asphalt from aggregates and analyzing the latex content by FTIR spectroscopy. Three different aggregate types, gravel, granite, and limestone, were used.

In recent years the Alabama Department of Transportation has made extensive use of styrene butadiene rubber (SBR) latex as a modifier for asphalt cement. It has specified the material to provide a binder that would provide enhanced performance in the field in terms of rutting resistance, fatigue resistance, and stripping resistance. The department's specification for latex-modified asphalt cement was a recipe type specification, which called for the addition of 3 percent SBR latex to an asphalt cement (generally an AC-20 asphalt cement). In general, until very recently SBR latex was added to the asphalt cement at the contractor's hot-mix asphalt (HMA) plant. The Alabama Department of Transportation had to rely on the supplier and the contractor to ensure that the specified amount of modifier had been added to the asphalt cement. The department did not have the capability to verify independently that the correct amount of SBR latex had been added to the asphalt cement. Thus, there was a need to develop such a capability.

OBJECTIVE

The objectives of the present study were to evaluate existing procedures and develop a readily usable procedure for determining the percent latex in asphalt cement for use by the Alabama Department of Transportation. Another objective was to apply this method with appropriate modifications to determine the amount of latex in HMA mixes.

C. W. Curtis, Department of Chemical Engineering, Auburn University, Auburn, Ala. 36849. D. I. Hanson, National Center for Asphalt Technology, 211 Ramsay Hall, Auburn University, Auburn, Ala. 36849-5354. S. T. Chen, G.-J. Shieh, and M. Ling, Auburn University, Auburn, Ala, 36849.

SCOPE

The study evaluated the use of Fourier transform infrared (FTIR) spectroscopy as a method for determining the percent latex in asphalt cement and HMA. The study was accomplished with two different SBR latexes from Ultrapave, UP70 and UP2897, and three different asphalt cements that are routinely supplied to roads in the state of Alabama. Three different aggregates were used. These aggregates are produced in Alabama and are routinely used in Alabama's pavements. The scope of the objectives was also expanded to two other polymers, ethylene vinyl acetate (EVA) and styrene butadiene styrene (SBS) copolymer. In this research SBR latex was analyzed both qualitatively and quantitatively in asphalt cement so that both the presence and amount of latex present in the asphalt cement were successfully determined. The procedure that was developed for analyzing the latex in asphalt cement was applied to latex-modified asphalt concrete with four different aggregates. Asphalt modified with 3 percent SBR latex was first added to aggregates, removed with tetrahydrofuran (THF), and then analyzed for SBR latex content by using the calibration curves obtained previously. The procedure for analyzing SBR latex in asphalt cement was then applied to EVA- and SBS-modified asphalt cement.

BACKGROUND

Polymers are added to asphalt cement to improve the performance characteristics of the asphalt cement. Properties that the addition of these materials is seeking to improve are temperature susceptibility, cohesive strength, elastic recovery, and adhesive power or tackiness (*1*). The polymer-modified asphalt cement must be able to maintain its desirable characteristics during storage and service life, be chemically and physically stable and usable through all aspects of processing, and be cost-effective.

A number of different methods have been used to determine the amount of SBR latex in asphalt. Lenoble (*2*) used microscopic techniques with UV fluorescence reflection to determine if natural segregation occurred with two incompatible polymers, a polyolefin and SBS, in several different asphalts. Lenoble (*2*) determined that the

polydispersity of the phases and the fineness of the SBS dispersion were influenced by blending conditions, asphalt composition, and aging susceptibility. Similarly, Paukkau et al. (*3*) used an automated morphological analysis system to analyze polymer-modified asphalt materials. The system was composed of a scanning electron microscope with a television camera. Another method, gel permeation chromatography, was used successfully to determine the low-gel polymer content in polymer-modified asphalt and tar (*4*).

Of all of the methods reviewed, methods that use infrared (IR) spectroscopy for analyzing latex in asphalt appear to be the most practical and widely used. IR spectroscopy is both accurate and relatively simple to perform. When IR radiation is imposed on a sample the amount of light that is either transmitted or absorbed is measured typically over a nominal wavelength range of 4000 to 400 cm^{-1}. Unique spectra are obtained for different compounds since each functional group absorbs at specific wavelengths and produces a unique fingerprint in the region from 1500 to 400 cm^{-1} because of long-range molecular interactions. The IR spectrum of a mixture such as asphalt cement represents the IR absorbances of all of the compounds present, yielding a sum of the individual absorbances. When asphalt cement is considered as a single entity, then the addition of another material such as a polymer is apparent in the IR spectrum if the IR absorbances from the polymer's molecular bonds are distinct from those in asphalt and are IR active.

IR spectroscopy is a powerful technique and has been successfully applied to the analysis of asphalt (*5,6*). Polymers themselves have also been extensively analyzed by IR spectroscopy (*7,8*). An ASTM procedure for the analysis of polymers in asphalt that uses IR spectroscopy was developed by Choquet and Ista (*9*). For the three polymers used, the method was successful for the SBS latex- and EVA polymer-modified asphalt binders tested. The third polymer, atactic polypropylene, had to be subjected to an intensive separation procedure before analysis.

The two IR methods that are discussed here were the two that served as starting points for the study. The test procedures were TEX 533-C, Determination of Polymer Additive Percentages in Polymer Modified Asphalt Cements (*10,11*), from the Texas State Highway Department and AHTD Test Method 432, Test for Polymers in Asphalt, from the Arkansas State Highway Department (*12*). The Arkansas method (*12*) for determining polymers in asphalt was very similar to the Texas method except that 1,1,1-trichloroethane rather than THF was used as the solvent.

The Texas State Department of Highways and Public Transportation's Materials and Tests Division developed a methodology for determining the percentage of polymer additives in polymer-modified asphalt cements (*10,11*). The particular additives that were targeted in their procedure were SBR latex, SBS block copolymer, ethylene acrylic acid, and EVA. These polymers were analyzed in polymer-modified asphalt cements. The procedure involved the use of IR spectroscopy to develop calibration curves from asphalt standards containing 1, 2, 3, 4, and 5 percent polymer (by weight) and then tested the unknown polymer-asphalt samples to determine the amount of polymer present in the asphalt. Standards were prepared from hot asphalt at 160°C at (320°F). The polymer-modified asphalt samples analyzed by IR analysis were prepared by placing a THF solution of the polymerized asphalt on a salt plate, evaporating the THF, and allowing the thin film to solidify. This method only worked when the polymers were soluble in THF. When the polymers were not soluble in THF, a hot melt of dispersed polymer in asphalt was made and the hot melt was spread as a thin film onto the salt plate.

Both types of samples were analyzed identically by setting the baseline transmission to 80 percent at 4000 cm^{-1} and scanning the sample from 4000 to 600 cm^{-1}. The calibration curves were analyzed by obtaining the ratio of the relative peak height of the IR peak of the polymer to that of the IR peak of the asphalt cement. For SBR latex the IR peak of interest is at 965 cm^{-1} (A1), and for asphalt the peak is at 1375 cm^{-1} (A2). Baselines were drawn at the peaks of interest, and the peak heights A1 and A2 were measured. The ratio of peak height A1 to peak height A2 was calculated and was used to plot the polymer concentration versus the A1/A2 ratio. The unknown samples were prepared by the same procedure used to prepare the calibration curve. The calibration curve was used to determine the concentration of the unknown.

TEST PLAN

Materials

The materials used in the present study were three different asphalts from Coastal, Hunt, and Ergon; SBR latexes; and EVA and SBS polymers. The crude source for Coastal asphalt was Venezuelan crude, that for the Hunt asphalt was Mexican crude, and that for Ergon asphalt was sour Venezuelan crude. The SBR latexes used were obtained from Ultrapave and are designated UP70 and UP2897. The characteristics of these latexes are given in Table 1. The latex-modified asphalt cement samples used for calibration were prepared by Ultrapave at nominal concentrations ranging from

TABLE 1 Properties of Polymers

Properties	Polymer	
	UP 2897	UP 70
Solids Content,%	68.0 ± 5.0	70.0
pH	9.5-10.5	10.0
Viscosity, Brookfield, cps	1200-1500	1650
Weight per Gallon, lbs	7.95 ± 0.3	7.9
Density, kg/L	0.9526	0.9466
Styrene Butadiene Ratio	24:76 ± 2.0	24:76

0.5 to 8.0 weight-percent latex in asphalt. Bulk samples were also prepared by Ultrapave at nominal concentrations of 2, 3, and 4 weight-percent latex in asphalt. The characteristics of these latex-modified asphalt cements are given in Table 2.

The EVA polymer, EVA in asphalt cement samples, and SBS in asphalt cement samples were obtained from Exxon; another set of SBS in asphalt cement samples was obtained from Koch. The EVA-modified and the SBS-modified asphalt cement samples were prepared at concentrations of 2, 3, and 4 weight-percent in the three asphalts mentioned previously. The characteristics of these polymers are also given in Table 1.

The aggregates used in the present study in conjunction with the asphalt containing latex were a 1.3-cm (0.5-in.) open-graded and dense-graded Mt. Meigs gravel from Montgomery, Alabama. These materials have very low absorptions. Two other aggregates were also used: a dense-graded limestone from Dravo, Auburn, Alabama, and a dense-graded granite from Columbus or LaGrange, Georgia. The gradation of the aggregate ranged from 0.075 to 19 mm, with 0.075- to 2.36-mm aggregates composing one-half of the material.

IR Analysis of Latex in Asphalt Cement: Experimental Procedure

IR analysis of SBR latex in asphalt cement was performed with an FTIR spectrometer (Nicolet 5SXC). The IR cells used were single

TABLE 2 Properties of Latex-Modified Asphalt Cements

Asphalt Binder	Latex		Penetration		Capillary Viscosity		Softening Point
	Type	%	39°F	77°F	Absolute 140°F (P)	Kinematic 275°F (cSt)	°C
Coastal	None	0	22	78	2357	394	117.0
Coastal	UP2897	2	24	74	3411	704	125.0
Coastal	UP2897	3	23	64	4608	916	126.0
Coastal	UP2897	4	26	57	16518	2790	138.0
Coastal	UP70	2	24	65	5067	779	128.0
Coastal	UP70	3	23	48	8484	1264	132.0
Coastal	UP70	4	25	70	11453	1781	138.0
Ergon	None	0	21	72	2118	370	118.0
Ergon	UP2897	2	23	76	3148	647	122.0
Ergon	UP2897	3	22	60	4482	850	125.0
Ergon	UP2897	4	23	52	8263	1926	132.0
Ergon	UP70	2	24	68	5951	1092	127.0
Ergon	UP70	3	24	57	7035	1069	129.0
Ergon	UP70	4	57	87	8629	1597	133.0
Hunt	None	0	25	71	2273	475	122.0
Hunt	UP2897	2	28	61	3119	793	124.0
Hunt	UP2897	3	23	66	6739	1228	131.0
Hunt	UP2897	4	28	59	8943	2941	140.0
Hunt	UP70	2	28	57	5249	1076	129.0
Hunt	UP70	3	30	66	5867	1183	131.0
Hunt	UP70	4	54	82	11483	2362	136.0

sodium chloride salt plates mounted in a holder. The salt plates and holder were obtained from Harrick Scientific. While in use the spectrometer was purged with dry nitrogen to remove the CO_2 and water in the ambient air. Desiccant was also placed in the spectrometer to absorb any moisture that may seep into the spectrometer. Asphalt samples containing different amounts of SBR latex, 0.0, 0.5, 1.0, 1.5, 2.0, 2.5, 3.0, 3.5, 4.0, 6.0, and 8.0 weight-percent latex in asphalt, were prepared by Ultrapave. THF was used as the solvent and was high-pressure liquid chromatographic grade from Fisher Scientific.

The method used for analysis of SBR latex in asphalt was a modification of test method TEX 533-C from the Texas State Department of Highways and Public Transportation (*11*). The procedure used IR spectroscopic determination of the IR bands corresponding to latex at 965 cm^{-1} and to asphalt at 1375 cm^{-1}. The 965-cm^{-1} latex band (A1) is attributed to =C–H in phase out-of-plane bending of *trans*-1,4-butadiene in SBR latex (*13*). The IR absorption band at 1375 cm^{-1} (A2) corresponds to C–CH_3 deformation of aliphatic compounds in asphalt (*13*). The presence of the 965-cm^{-1} band in the asphalt IR spectrum indicated the presence of SBR latex in the asphalt since that absorption was not present in the virgin asphalts. The ratio of absorbance bands, A1:A2, was used as the quantitative method.

The general procedure for obtaining the analysis is given in the following description. Before analysis a background spectrum of the NaCl salt plate and spectrometer atmosphere was obtained. A sample was prepared from each latex-modified asphalt cement by dissolving 10 weight-percent of the latex-modified asphalt cement in THF. A thin film of latex-modified asphalt was prepared on an NaCl salt plate by placing 0.3 ml of solution on the salt plate and spreading the solution evenly over the surface of the salt plate. Most of the THF evaporated during the process, since the sample was prepared in the fume hood. The thin film was then dried in an oven at 60°C for 20 min to evaporate the THF completely. The salt plate was removed from the oven and was allowed to cool for 5 min. The sample was then analyzed by FTIR spectroscopy. Each sample on a salt plate was analyzed 3 times by rotating the plate 120 degrees for each analysis. Averaging the three ratios allowed the effect of any unevenness in the sample to be minimized. The absorbance of the 1375-cm^{-1} peak normally fell between 0.35 and 0.65 absorbance units, although slightly higher or lower absorbances gave satisfactory results. A tangent-line baseline method was used to calculate the absorbance of the analytical bands.

Calibration Curves

Calibration curves of latex-modified asphalt cement containing 0.0, 0.5, 1.0, 1.5, 2.0, 2.5, 3.0, 3.5, 4.0, 6.0, and 8.0 weight-percent latex were obtained by using the combinations of Hunt, Coastal, and Ergon asphalts with Ultrapave latexes UP70 and UP2897. These calibration standards were prepared in bulk and were sampled after preparation by placing several drops in a sample vial. Each asphalt was combined with each latex yielding six combinations of latex-modified asphalt cement. The calibration curves were developed for each combination and are given in Figure 1. Each analysis was duplicated. Although the calibration curves were similar to each other, the characteristics of the SBR-asphalt combination varied sufficiently in terms of the linear relationship between SBR concentration and area ratio that each latex-modified asphalt required a separate calibration curve.

IR Analysis of EVA and SBS

The same experimental procedure that was used for SBR latex in asphalt was applied to asphalt samples containing EVA and SBS. The IR absorbances used in the analysis of EVA were 1242 cm^{-1} (h_1), which is attributable to C–O–C in acetate, and 1736 cm^{-1} (h_2), which is attributable to C=O in acetate (*13*). These absorbances are unique for EVA and are not present in the asphalt spectrum. The ratio of each of these two peaks against the 1375-cm^{-1} peak from asphalt was determined. Analyses of EVA at three concentrations in each of the three asphalt cements were performed. Since SBS contains the same monomers as SBR latex, a similar IR spectrum is obtained. The SBS peak of interest was at 966 cm^{-1}, which is attributable to the =C–H bend in *trans*-1,4-butadiene. The ratio of each of these peaks against the 1375 cm^{-1} asphalt peak was determined. The SBS polymer from two different suppliers was also analyzed at three concentrations in each of the three asphalt cements.

ANALYSIS OF RESULTS

Applicability of Analysis Method for Latex-Modified Asphalt

Figure 2 presents the FTIR spectra of virgin asphalt and asphalts that contain SBR latex, EVA, and SBS. The characteristic peak for each polymer and for asphalt is marked on the spectrum. The calibration curves prepared from the SBR latexes in asphalt cement provided a means by which to analyze the SBR latex contents in these three asphalts. These calibration curves are presented in Figure 1; the solid circles represent the SBR latex concentration-versus-peak area data. The R^2 values for these calibration curves were 0.99 for SBR latex (UP2897 and UP70)-modified Coastal and Ergon asphalts. The R^2 value for UP2897 in Hunt asphalt was also 0.99, whereas the UP70 latex in Hunt asphalt gave a R^2 value of 0.98. Hence, two different latexes were successfully quantified in three different asphalts, which confirmed the applicability of the method to a variety of materials and to a concentration range of from 0 to 8 weight-percent of SBR in asphalt.

An example of the applicability and usefulness of this technique for analysis of the amount of latex present occurred in a project in which the storage of latex-modified asphalt cement was being investigated by researchers at the National Center for Asphalt Technology (NCAT). Bulk samples of nominal, 2, 3, and 4 weight-percent SBR latex in Coastal, Hunt, and Ergon asphalts were prepared for NCAT by Ultrapave. These samples were prepared in the laboratory by using laboratory quantities; the preparation procedures were, however, similar to those that would be used for introducing SBR latex into asphalt cement for road construction. Researchers at NCAT performed physical tests on the samples of different concentrations and evaluated the effects of storage on these samples. For some of the samples the results from the physical tests did not appear to follow the nominal concentrations stated by Ultrapave. At that point the samples with nominal 2, 3, and 4 weight-percent SBR latex in asphalt were analyzed by FTIR spectroscopy by using the procedure and calibration curves developed for each asphalt and SBR latex combination. The concentrations of the laboratory-produced bulk samples were determined. The actual concentrations of the SBR latex in the asphalt bulk samples as determined by FTIR spectroscopy varied, in some cases considerably, from the nominal values. The results from the physical tests were in better agreement with the SBR latex concentrations determined

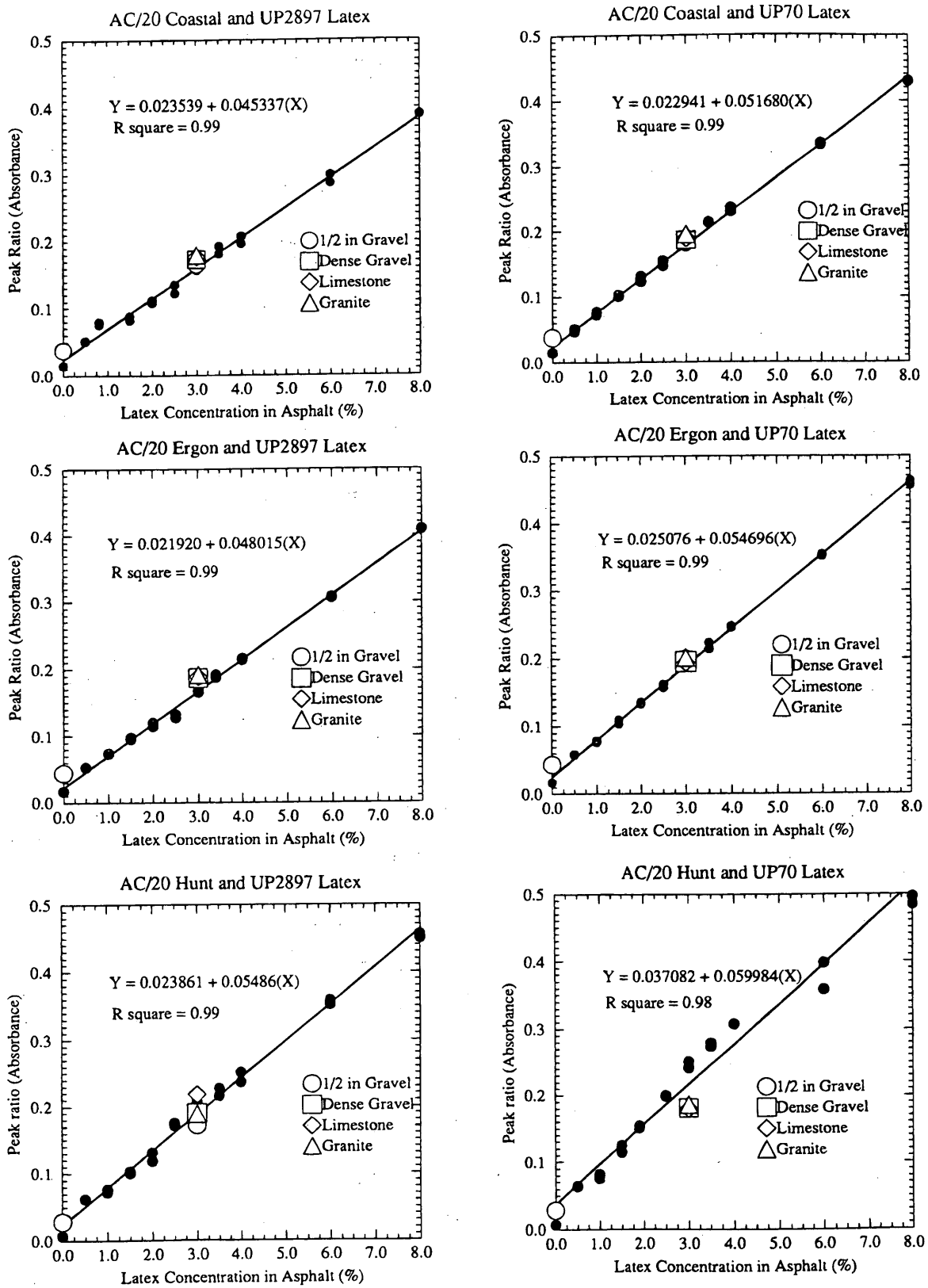

FIGURE 1 Calibration curves of SBR latex in asphalt and results from asphalt–aggregate mixes.

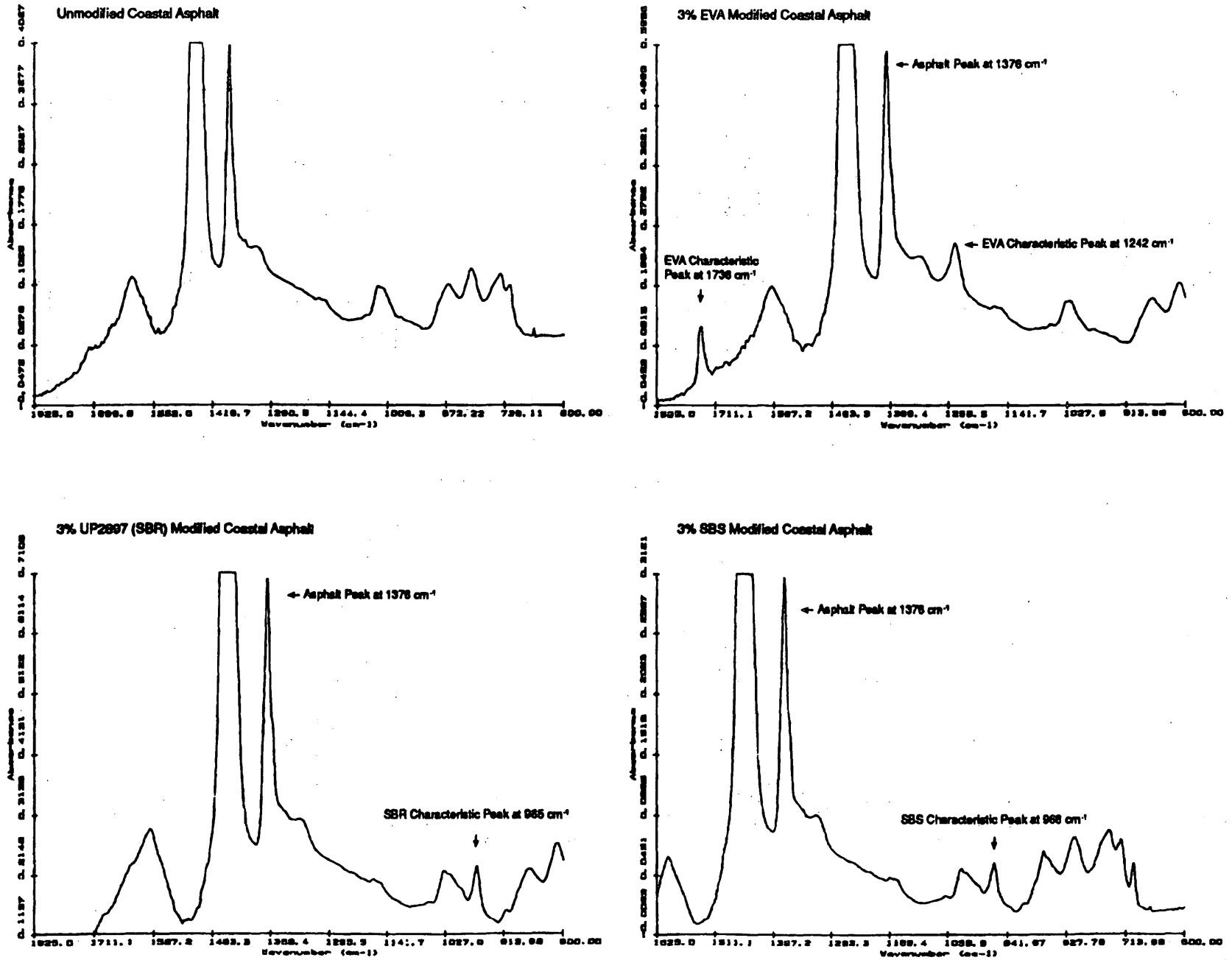

FIGURE 2 IR spectra of polymer-modified and virgin asphalts.

from the calibration curves than the nominal values, as shown in Figure 3 in which the dynamic shear, $G^*/\sin\delta$ (in kilopascals, where G^* is the complex shear modulus and δ is the phase angle) of the SBR latex-modified asphalt cement is compared with the latex concentrations determined by FTIR spectroscopy. The latex concentrations determined by FTIR spectroscopy yielded a more linear relationship between the dynamic shear measurement and the latex concentration for the SBR-modified Coastal and Ergon asphalts than did the nominal values. The Hunt asphalt, which was produced from a Mexican crude, whereas the other two asphalts were produced from Venezuelan crudes, showed nonlinear behavior. SBR latexes are known to be incompatible with some Mexican crudes and tend to separate rapidly, which could explain some of the variability with the Hunt asphalt. The interaction between the SBR latex and the asphalt appeared to be dependent on the asphalt characteristics and the interaction between SBR latex and asphalt.

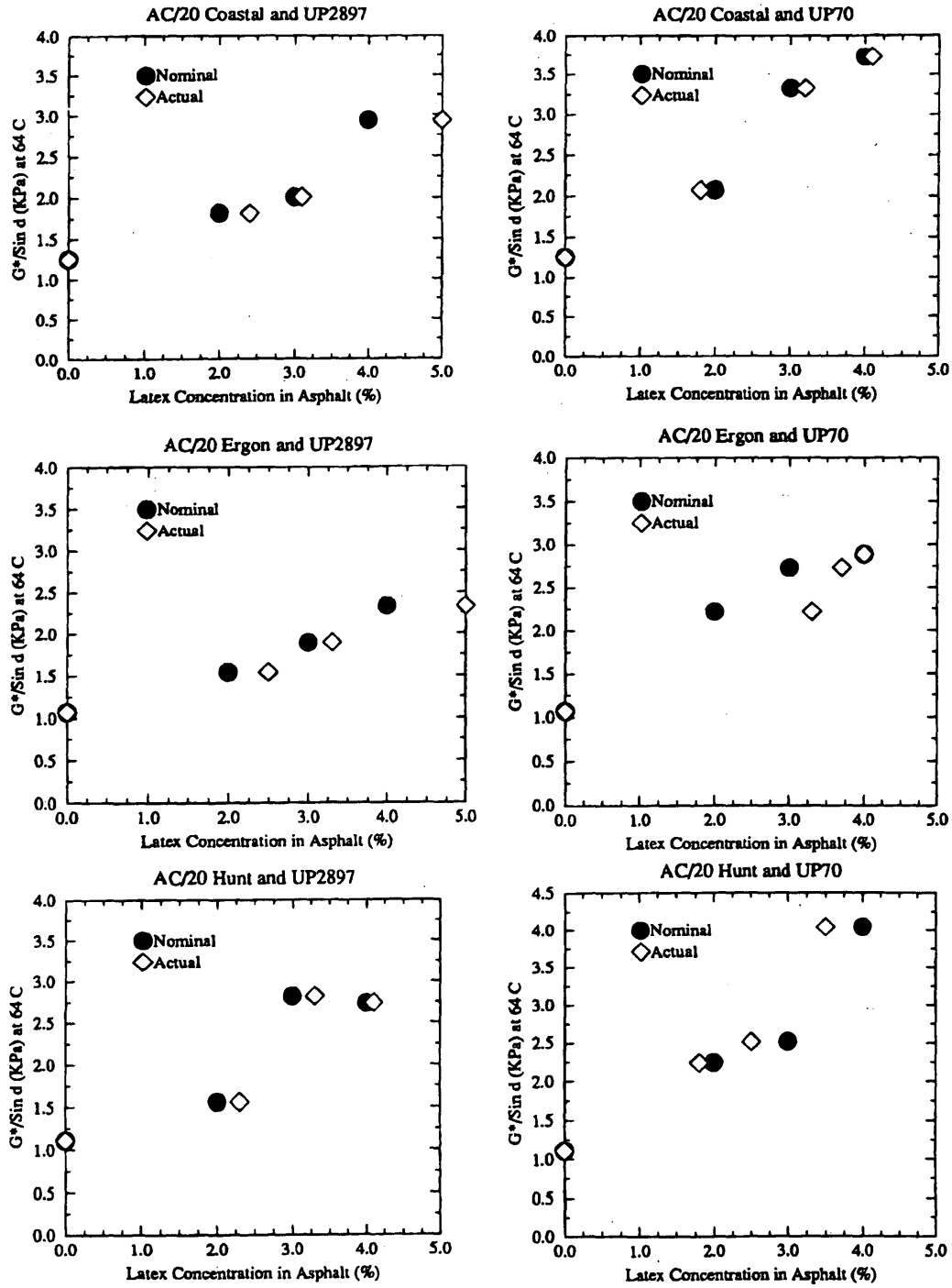

FIGURE 3 Relation between $G^*/\sin\delta$ and latex concentration in asphalt.

IR Analysis of Latex-Modified Asphalt in an Asphalt–Aggregate Mixture

A feasibility study was conducted to determine if the latex content of latex-modified asphalt could be accurately analyzed after the latex–asphalt mixture had been mixed with aggregate. The tests performed involved a gravel and a granite, which are siliceous, non-absorbing aggregates, and a limestone. Two different samples of the gravel were used: (a) 1.3-cm (0.5-in.) aggregates were coated with asphalt cement containing 3 weight-percent latex; a heavy coat of asphalt was applied so that the asphalt content was 8 percent of the mix; (b) a typical gradation of gravel was coated with 6 percent asphalt cement containing 3 percent latex; and (c) typical gradations of both limestone and granite were coated with 6 percent asphalt containing 3 percent latex. The asphalts used were Coastal, Ergon, and Hunt asphalts, and the latexes used were UP70 and UP2897, yielding six combinations. Baseline experiments in which the asphalt cements without latex were coated on the 1.3-cm (0.5-in.) aggregate were also performed.

For each of these asphalt–aggregate mixtures the asphalt cement was removed from the aggregate surface with THF. The sample was shaken with the THF for approximately 4 hr. The THF solution containing asphalt was then removed from the flask, centrifuged to remove any particulates from the aggregate, and analyzed as a thin film cast on an NaCl salt plate by FTIR spectroscopy. The presence of latex was detectable in the asphalt cement. The amount of latex present was quantitatively determined by using the calibration curves developed for the six combinations of asphalt and latex used in the study. Figure 1 presents the analysis of the asphalt–aggregate mixtures containing latex-modified asphalt; the points representing the latex content of asphalt abstracted from aggregate are the open circles. Baseline results from samples that do not contain latex are also presented. The amount of SBR latex (3 percent) present in the asphalt cement was accurately determined for all four aggregates. SBR latex-modified Coastal and Ergon asphalts yielded results that closely agreed with the calibration curves. Calculation of the average difference from the calibration line for these two asphalts ranged from −0.0139 to −0.0876. On the same scale the Hunt asphalt–UP70 sample yielded a larger difference of −0.1398. The Hunt asphalt–UP2897 samples gave more scatter among the four latex-modified asphalts removed from the different aggregates, although the difference from the calibration curve was small (−0.0147). Hence, the SBR latex-modified Hunt asphalt yielded results that deviated from the calibration curve more than results for the other two latex-modified asphalts did.

To evaluate the reproducibility of the method for removing latex-modified asphalt cement from aggregate, these analyses were performed by two different researchers. The analyses for open- and dense-graded gravel were performed by both Researcher 1 and Researcher 2. Researcher 1 had developed the technique, whereas Researcher 2 performed the analysis from the written procedure. Since both researchers obtained 3 weight-percent latex in all of the samples analyzed (Table 3), the procedure developed appears to be insensitive to operator variability. After the reproducibility was established Researcher 2 proceeded to perform the analysis of SBR latex–asphalt mixes of limestone and granite as presented in Figure 1.

TABLE 3 Absorbance Ratios from Latex-Modified Asphalt Concrete Mixes Obtained by Two Researchers

Asphalt-Aggregate Mix	No polymer	UP 2897 Modified Asphalt	UP 70 Modified Asphalt
Coastal + ½" gravel	0.0357±0.0029[a,b] 0.0395±0.0021[b] 0.0277±0.0002[c]	0.1649±0.0100[b] 0.1653±0.0026[b] 0.1690±0.0000[c]	0.1829±0.0010[b] 0.1886±0.0056[b] 0.1924±0.0007[c]
Ergon + ½" gravel	0.0041±0.0041[b] 0.0440±0.0027[b] 0.0341±0.0001[c]	0.1847±0.0017[b] 0.1871±0.0025[b] 0.1857±0.0018[c]	0.1891±0.0004[b] 0.2092±0.0207[b] 0.1959±0.0018[c]
Hunt + ½" gravel	0.0275±0.0029[b] 0.0291±0.0033[b] 0.0339±0.0001[c]	0.1711±0.0024[b] 0.1721±0.0035[b] 0.1829±0.0030[c]	0.1867±0.0007[b] 0.1758±0.0025[b] 0.1821±0.0007[c]
Coastal + dense graded gravel	NA[d]	0.1723±0.0019[b] 0.1733±0.0028[b] 0.1742±0.0006[c]	0.1836±0.0028[b] 0.1891±0.0036[b] 0.1870±0.0009[c]
Ergon + dense graded gravel	NA	0.1841±0.0007[b] 0.1890±0.0039[b] 0.1892±0.0004[c]	0.1966±0.0034[b] 0.1939±0.0023[b] 0.2007±0.0007[c]
Hunt + dense graded gravel	NA	0.1925±0.0051[b] 0.1876±0.0018[b] 0.1913±0.0011[c]	0.1802±0.0052[b] 0.1815±0.0006[b] 0.1870±0.0005[c]

[a] Standard deviation of three FTIR scans on the same salt plate
[b] Performed by researcher 1.
[c] Performed by researcher 2.
[d] NA = not available.

Analysis of EVA- and SBS-Modified Asphalt

The analysis procedure developed for SBR latex in asphalt cement was applied to samples of 2, 3, and 4 weight-percent EVA polymer in asphalt cement. The same three asphalts used in the analysis with SBR latex were used in this analysis. The EVA samples yielded two peaks that were unique, both of which were attributable to acetate: 1242 cm^{-1}, which corresponds to C–O–C, and 1736 cm^{-1}, which corresponds to C=O. The ratio of the height of each of these peaks to the asphalt peak at 1375 cm^{-1} was determined. Ratios from both peaks are presented in Figure 4. The EVA in all three asphalt cements yielded R^2 values of 0.99. These analyses showed that the EVA polymer is readily quantified at these concentrations in three different asphalts.

Analysis of SBS in asphalt cement had one unique peak that was suitable for analysis. This peak appears at 966 cm^{-1} and is characteristic of the bending of the =C–H bond in the environment of the diene. The ratio of the 966-cm^{-1} peak against the 1375-cm^{-1} asphalt peak was determined. The data from the Exxon SBS in the three

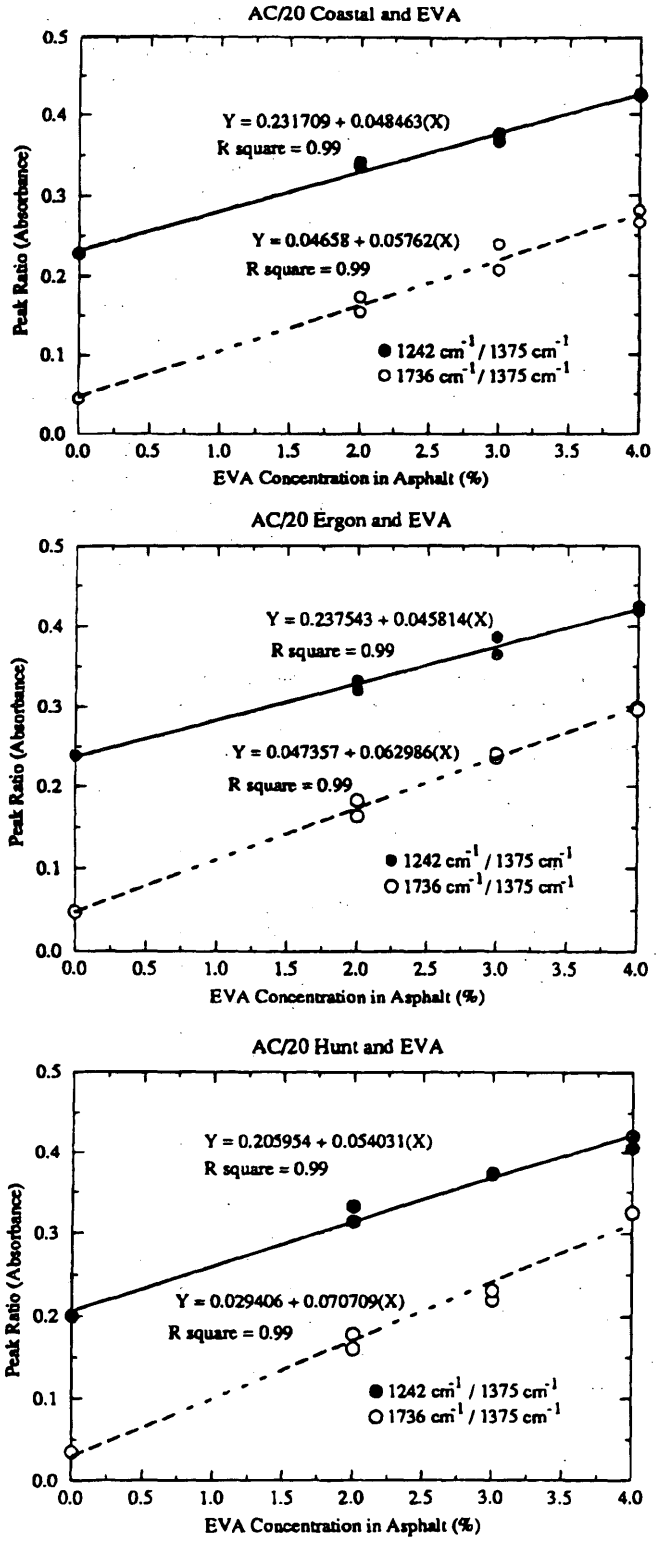

FIGURE 4 Calibration curves of EVA in asphalt.

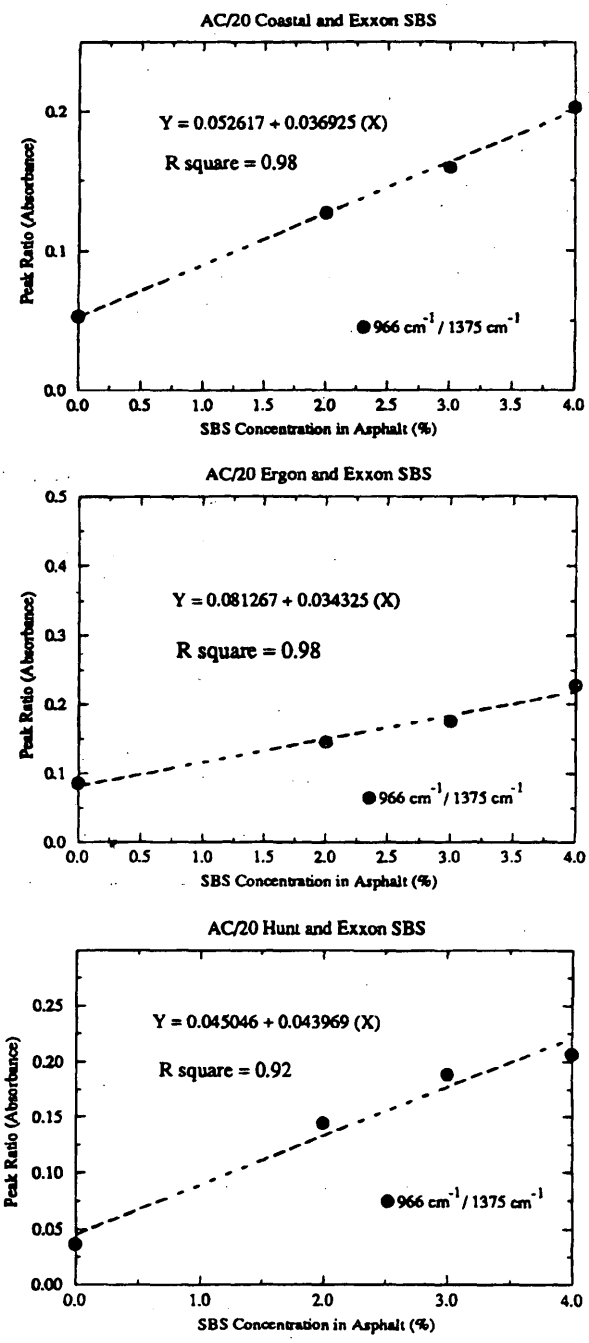

FIGURE 5 Calibration curve of SBS in asphalt.

asphalts are presented in Figure 5. The SBS in Coastal asphalt and Ergon asphalt yielded R^2 values of 0.98, whereas SBS in Hunt asphalt gave an R^2 value of 0.92. Figure 6 presents the data for SBS from Koch. The R^2 values obtained from Koch SBS were 0.98 for Coastal, Ergon, and Hunt asphalts; these values were slightly higher than those from Exxon SBS.

SUMMARY AND CONCLUSION

An analytical method that uses FTIR spectroscopy was developed for the analysis of two SBR latexes and EVA and SBS polymers in asphalt cement. The method is reproducible and readily applicable to different latexes and asphalts. Calibration of EVA and SBS of 2 to 4 weight-percent polymer in asphalt was also achieved. Calibration curves of the SBR latex, EVA, and SBS materials in asphalt yielded R^2 values that ranged from 0.92 to 0.99. Application of the analysis to determine the actual concentration of latex in asphalt cement samples helped to explain the results from dynamic shear measurements. Successful analysis of 3 weight-percent SBR latex in asphalt samples was accomplished by removing the latex-modified asphalt with THF and analyzing the SBR latex content by the analysis procedure that was developed.

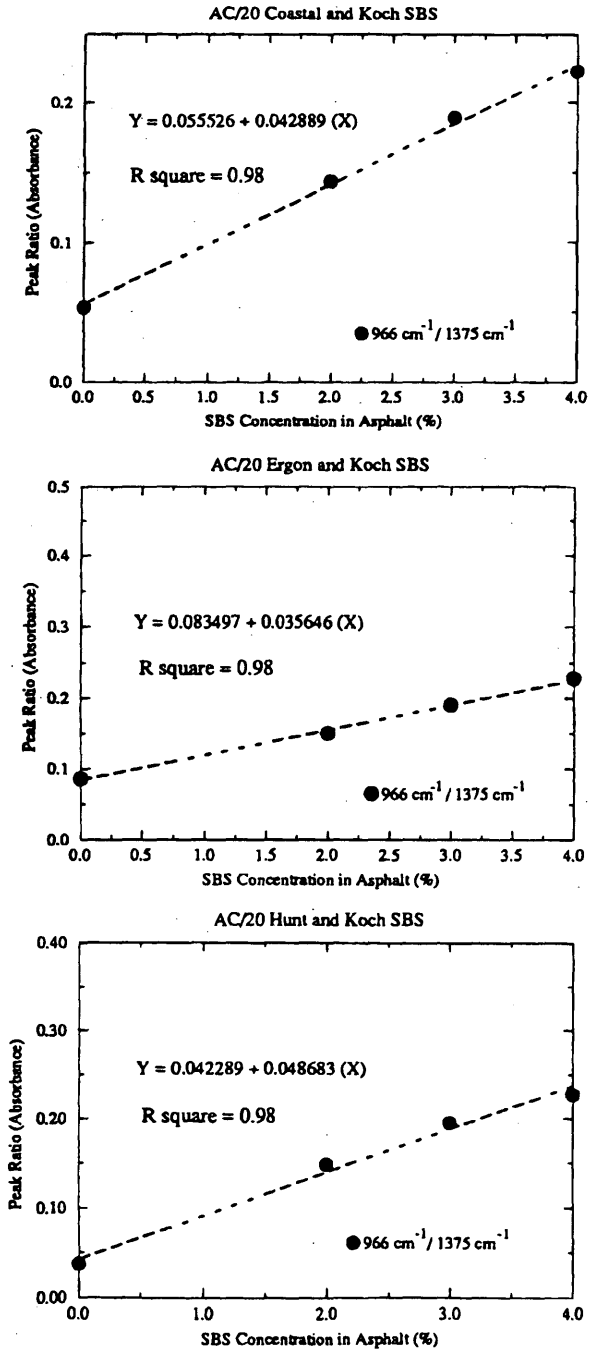

FIGURE 6 Calibration curve of Koch SBS in asphalt.

ACKNOWLEDGMENT

The authors gratefully acknowledge the Alabama Department of Transportation for support of this work. The authors also appreciate the assistance of Rajib Basu Mallick in the computer analysis and graphing of the data. The supply of materials from Ultrapave, Exxon, Koch Coastal, Ergon, and Hunt is also gratefully acknowledged.

REFERENCES

1. Hoban, T. Modified Bitumen Binders for Surface Dressing. In *Chemistry and Industry,* Society of Chemical Industry, London, England, Sept. 3, 1990, pp. 538–542.
2. Lenoble, C. Performance/Microstructure Relationship of Blends of Asphalts with Two Incompatible Polymers. *Fuel Science Technology International,* Vol. 10, No. 4–6, 1992, pp. 549–564.
3. Paukkau, A. V. A. Ovchinnikov, R. K. Zacheslavskaya, E. R. Tsyrkun, and C. Y. Rappoport. Use of a Modified Morphological-Analysis System in Studies of Polymer-Asphalt Materials. *Stroitelńye Materialov,* Ministerstvo Promyshlennosti, Moscow, Russia, 1990, pp. 21–22.
4. Loucks, D. A., and F. P. Sequin. Determination of Low-Gel Polymer Content in Polymer-Modified Asphalt. U.S. Patent 4990456A, Feb. 5, 1991.
5. Petersen, J. C., H. Plancher, and S. M. Dorrence. Identification of Chemical Types in Asphalts Strongly Adsorbed at the Asphalt-Aggregate Interface and Their Relative Displacement by Water. *Proc, Association of Asphalt Pavement Technologists,* Vol. 46, 1977.
6. Petersen, J. C. Quantitative Functional Group Analysis of Asphalts Using Differential Infrared Spectrometry and Selective Chemical Reactions—Theory and Application. In *Transportation Research Record 1096,* TRB, National Research Council, Washington, D.C., 1986.
7. Koenig, J. L. Spectroscopic Characterization of Polymers. *Analytical Chemistry,* Vol. 59, 1987, p. 1142.
8. Painter, P. C., M. M. Coleman, and J. L. Koening. *The Theory of Vibrational Spectroscopy and Its Application to Polymeric Materials,* John Wiley and Sons, Inc., New York, 1982.
9. Choquet, F. S., and E. J. Ista. *Polymer Modified Asphalt Binders.* ASTM STP 1108 (K. R. Wardlaw and S. Shules, eds.), American Society for Testing and Materials, Philadelphia, 1991.
10. Romine, R. A. The Determination of SBR-Latex Concentration in Asphalt Cements. Materials and Test Division, Texas State Department of Highways and Public Transportation, March 1987.
11. Determination of Polymer Additive Percentages in Polymer Modified Asphalt Cements. Test Method TEX 533-C. Materials and Tests Division, Texas State Department of Highways and Public Transportation, March 1991.
12. Test for Polymers in Asphalts. AHTD Test Method 432. Arkansas Highway Department.
13. Lambert, J. B., H. F. Shurrell, L. Verbit, R. S. Cooks, and S. H. Stout. *Organic Structural Analysis,* MacMillan Publishing Co., Inc., New York, 1976, pp. 237–241.

Evaluation of Physical Properties of Fine Crumb Rubber-Modified Asphalt Binders

ROBERT B. MCGENNIS

The results of a laboratory experiment aimed at evaluating the physical properties of asphalt binder containing fine crumb rubber modifier are outlined. Binder characterization procedures developed as part of the Strategic Highway Research Program (SHRP) were used in the analysis. The collective products of SHRP asphalt research are now called Superpave. The crumb rubber modifier used was produced from a wet ambient grind process. The maximum rubber particle size was 180 μm, with an average particle size of 74 μm. Testing showed that when compared with the base asphalts, the fine crumb rubber-modified binders were stiffer at high pavement temperatures, were less stiff at low pavement temperatures, and had approximately the same or slightly less stiffness at intermediate temperatures. The behavior of the asphalt rubber binders during rolling thin film oven (RTFO) aging was unlike that of the base asphalts. The fine rubber-modified binders tended to veil across the RTFO bottle during aging, or in other cases it congregated in a thick film around the perimeter of the RTFO bottle during the aging process. Viscosity tests showed that the asphalt rubber binders are subject to viscosity building when they are stored at high temperatures. No other difficulties were encountered in using the Superpave binder analysis procedures to characterize fine crumb rubber-modified binders.

This report summarizes a laboratory experiment aimed at characterizing the physical properties of paving asphalt cement modified with fine crumb rubber modifier (CRM). The Intermodal Surface Transportation and Efficiency Act of 1991 has mandated that state departments of transportation (DOTs) incorporate increasing amounts of scrap tires in asphalt pavements. Concurrently, state DOTs are in the process of implementing Strategic Highway Research Program (SHRP) asphalt research products. Thus, this experiment was principally aimed at determining whether this new method of testing and specifying asphalt binders was suitable for use with fine crumb rubber-modified (CRM) binders. Of particular interest in this analysis were those physical properties necessary to evaluate the rubber-modified asphalt according to the new Superpave performance graded binder specification, which has now been provisionally adopted by AASHTO as MP1 (*1*).

EXPERIMENTAL PLAN

Materials Tested

The rubber product used was a fine crumb rubber produced by Rouse Rubber Industries of Vicksburg, Mississippi. According to the manufacturer it was produced by wet ambient grinding from whole truck tires and is 100 percent finer than 180 μm, with an average particle size of 75 μm. Figure 1 illustrates the particle size distribution of the fine rubber used throughout this project.

It has been reported (*2,3*) that asphalt source and chemical composition interact significantly with various crumb rubbers with respect to binder properties. To minimize this effect asphalts from a single source were used in the study. However, asphalt cements from this one supplier were selected to encompass a wide variety of grades in use in the United States. For one asphalt cement grade another source was used to demonstrate the effect of asphalt source.

The source of the paving asphalt cement for most of the study was Coastal Refining & Marketing, Inc. Five asphalts were used, all meeting the requirements listed in Table 2 of AASHTO M226-80 (*4*). They were AC-2.5, AC-5, AC-10, AC-20, and AC-30. The fine rubber was blended in various concentrations with the asphalt cement to produce a binder on which physical properties were measured. An additional sample of AC-2.5 from Amoco Oil Company was also included in the experiment to demonstrate the effect of asphalt source on binder properties. Physical properties were also measured on the base asphalts.

Blending was accomplished by using a laboratory mixer operated at 3,000 rpm. The fine crumb rubber was slowly added to the asphalt over a period of approximately 5 min. The temperature of the binder during blending was maintained at 175°C. Mixing of the binder continued for a total of 1 hr while the temperature was maintained at 175°C. A single batch of blended material was held constant at 1 L.

Unaged Binder Properties

The unaged binder was tested to determine its viscosity at 135°C by using a rotational coaxial cylinder viscometer. The procedure outlined in ASTM D4402-87 (*5*) was used.

AASHTO TP5 (*6*) was used to measure the viscoelastic properties of the binders, which are complex shear modulus and phase angle. A constant stress dynamic shear rheometer (DSR) operated with parallel plate geometry was used to measure these properties. The maximum rubber particle size (180 μm) is less than the maximum particle size allowed (250 μm) by AASHTO TP5 for filled systems. The complex shear modulus (G^*) is a measure of the total stiffness of the binder and is the vector sum of the elastic and viscous components of binder stiffness. The phase angle (δ) is a measure of the degree to which the binder is acting like an elastic material. Low values of δ indicate a greater contribution of the elastic stiffness component to total stiffness. The parameter of interest, $G^*/\sin\delta$, was usually captured at a sufficient number of temperatures to bracket the specified minimum value of 1.00 kPa from AASHTO MP1.

Asphalt Institute Research Center, P.O. Box 14052, Lexington, Ky. 40512–4052.

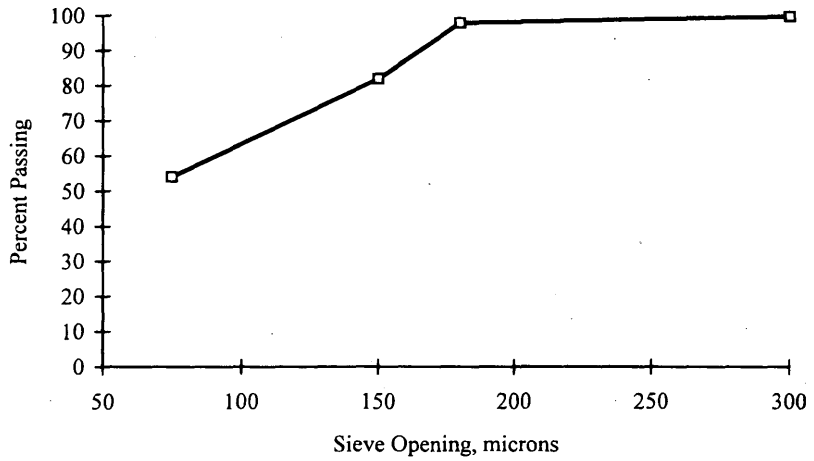

FIGURE 1 Particle size distribution of fine CRM.

Oven-Aged Binder Properties

The rolling thin film oven (RTFO) aging procedure, AASHTO T240 (*7*), was used to age the binders. To estimate the effect of the aging procedure, one binder was oven aged by using the thin film oven (TFO) as described by AASHTO T179-88 (*8*). The oven-aged binder was tested in the DSR to determine $G^*/\sin\delta$. Once again, $G^*/\sin\delta$ was captured at a sufficient number of temperatures to bracket the specified minimum value of 2.20 kPa. The parameter $G^*/\sin\delta$ measured and specified on unaged and oven-aged binder is intended to ensure that the binder is stiff enough to contribute to the overall rutting resistance of an asphalt mixture.

Pressure-Aged Binder Properties

RTFO residue was aged in a pressure aging vessel (PAV) according to AASHTO PP1 (*9*). The PAV residue was tested in the DSR to determine the parameter $G^*\sin\delta$. This parameter was measured at a variety of intermediate temperatures to verify that the PAV-aged residue exhibited a $G^*\sin\delta$ less than 5000 kPa. This specified limit is used in MP1 to ensure that a soft, elastic binder will be present to contribute to overall asphalt mixture resistance to fatigue cracking.

PAV-aged residue was also tested at low temperatures by using the bending beam rheometer (BBR) to measure creep stiffness (S) and logarithmic creep rate (m) as outlined in AASHTO TP1 (*10*). The AASHTO binder specification requires S to be less than 300 MPa and m to be greater than 0.300. These limits are used in MP1 to ensure that the aged binder is suitably soft at low temperatures to ameliorate low-temperature cracking.

Storage Properties

Because pumping and handling of asphalt rubber binders are of concern to many agencies, a limited experiment was performed to assess the viscosity characteristics of various blends. In this portion of the experiment various concentrations of fine mesh rubber were mixed with an AC-5, AC-10, AC-20, and AC-30 asphalt cement. As before, the viscosity of the blends was measured by using a rotational coaxial cylinder viscometer according to the procedures outlined in ASTM D4402–87. Three test temperatures, two shear rates, and two concentrations were tested.

TEST RESULTS

Table 1 illustrates the binder classifications for all binders tested. In Table 1 PG *XX-YY* is binder performance grade. *XX* refers to the high-temperature grade and is the average 7-day maximum pavement design temperature in AASHTO MP1. *YY* refers to the low-temperature grade and is the minimum pavement design temperature. For the materials tested the addition of fine rubber resulted in an increase in high-temperature grade and a decrease in low-temperature grade. A trend observed in these data is that 7.5 percent fine rubber increased the high-temperature grade by about one grade from that of the base asphalt. Fifteen percent fine rubber increased the high-temperature grade by two to three grades and the low-temperature grade by one grade. As expected AC-2.5 binders from two sources resulted in different performance properties.

In Table 1 a borderline grade is indicated when the m-value is within 0.010 of the specified value of 0.300. For example, the AC-20 with 7.5 percent rubber exhibited an m-value at -18°C of 0.296, which resulted in the classification of performance grade PG 70–22. Only a small increase in the m-value of 0.004 would have caused the binder to be classified as PG 70–28; hence, it is shown as a borderline grade.

In every case the low-temperature grade of asphalt rubber blends was controlled by the m-value. Only in the case of the neat AC-2.5 (Amoco) was the low-temperature grade influenced by the 5000-kPa limit placed on $G^*\sin\delta$.

The increase in high-temperature grade with the addition of fine-mesh rubber was a result of the increase in high-temperature stiffness as manifested by measured values for $G^*/\sin\delta$ (Table 2). Table 3 shows individual values for $G^*$and δ at various testing temperatures. The increase in $G^*/\sin\delta$ with increasing rubber concentration was almost entirely caused by an increase in G^*. The effect of δ was marginal, although higher rubber concentrations resulted in lower δ values.

TABLE 1 Classifications of Fine CRM Binders According to AASHTO MP1

Material	Performance Grade	Borderline Performance Grade[1]
AC-2.5 (Coastal)	PG 46-28	-
10% Fine CRM	PG 52-34	-
20% Fine CRM	PG 58-34	PG 58-40
AC-2.5 (Amoco)	PG 46-28	-
7.5% Fine CRM	PG 58-34	-
15% Fine CRM	PG 70-34	PG 70-40
20% Fine CRM	PG 70-34	-
AC-5 (Coastal)	PG 58-28[2]	-
7.5% Fine CRM	PG 58-28	-
15% Fine CRM	PG 70-34	-
AC-10 (Coastal)	PG 58-22	-
7.5% Fine CRM	PG 64-22	PG 64-28
15 % Fine CRM	PG 70-28	-
AC-20 (Coastal)	PG 64-22	-
7.5% Fine CRM	PG 70-22	PG 70-28
7.5% Fine CRM (TFO)	PG 70-22	-
15% Fine CRM	PG 82-28	-
20 % Fine CRM	PG 82-28	-
AC-30 (Coastal)	PG 64-22	-
7.5% Fine CRM	PG 76-22	-
15% Fine CRM	PG 82-28	PG 82-34

[1] Borderline grade indicates that $0.290 \leq m < 0.300$ at grading temp shown.
[2] Base asphalt was borderline PG 52-28 because $G^*/\sin\delta = 1.01$ kPa.

Table 4 shows $G^*$and δ values for RTFO-aged binders. As with unaged binders, the stiffness parameter $G^*/\sin\delta$ increases with increasing rubber concentration. Again, the effect is almost entirely due to G^*, with very little contribution of δ. A higher rubber concentration resulted in a lower δ value.

During this testing fine rubber-modified binders exhibited unusual RTFO aging characteristics. Two scenarios were observed. Harder base asphalt (AC-20 and AC-30) with 15 percent or more fine rubber tended to veil across the RTFO bottle during the aging procedure. In some cases the bottle was not coated along its entire length, even after the 85-min aging period. The softer asphalts containing fine rubber tended to flow around the perimeter of the bottle, but without a level of material continually in the bottom of the bottle, which is the trait exhibited by normal paving asphalts. Figure 2 illustrates these effects.

TABLE 2 $G^*/\sin\delta$ (kPa) Values for Fine CRM Binders (Unaged)

Material	Testing Temperature, °C						
	46	52	58	64	70	76	82
AC-2.5 (Coastal)	1.85	0.76	-	-	-	-	-
10% Fine CRM	-	2.41	1.10	0.53	-	-	-
20% Fine CRM	-	-	2.17	1.14	0.62	-	-
AC-2.5 (Amoco)	2.12	0.95	-	-	-	-	-
7.5% Fine CRM	-	-	1.54	0.75	-	-	-
15% Fine CRM	-	-	-	-	1.11	0.64	-
20% Fine CRM	-	-	-	-	1.55	0.92	-
AC-5 (Coastal)	-	-	1.01	-	-	-	-
7.5% Fine CRM	-	-	1.61	-	-	-	-
15% Fine CRM	-	-	-	2.34	1.21		-
AC-10 (Coastal)	-	-	1.83	0.87	-	-	-
7.5% Fine CRM	-	-	3.93	1.87	-	-	-
15 % Fine CRM				-	1.81	1.23	-
AC-20 (Coastal)	-	-	2.58	1.15	-	-	-
7.5% Fine CRM	-	-	-	-	1.42	-	-
7.5% Fine CRM (TFO)	-	-	-	-	1.42	-	-
15% Fine CRM	-	-	-	-	-	2.93	1.65
20% Fine CRM	-	-	-	-	-	-	2.10
AC-30 (Coastal)	-	-	-	1.70	0.79	-	-
7.5% Fine CRM	-	-	-	-	2.25	1.23	-
15% Fine CRM	-	-	-	-	-	4.01	2.17

TABLE 3 $G^*/\sin\delta$ Values for Fine CRM Binders (Unaged)

Material	Test Temp (°C)	G* (kPa)	δ (degrees)	G*/sin δ (kPa)
AC-2.5 (Coastal)		-	-	-
10% Fine CRM	58	1.11	81.63	1.13
20% Fine CRM		2.01	74.98	2.17
AC-2.5 (Amoco)		-	-	-
7.5% Fine CRM	70	-	-	-
15% Fine CRM		1.08	75.81	1.11
20% Fine CRM		1.50	74.95	1.55
AC-5 (Coastal)		1.00	87.07	1.01
7.5% Fine CRM	58	1.60	84.06	1.61
15% Fine CRM		-	-	-
AC-10 (Coastal)		0.87	87.39	0.87
7.5% Fine CRM	64	1.86	83.54	1.87
15 % Fine CRM		-	-	-
AC-20 (Coastal)		-	-	-
7.5% Fine CRM		-	-	-
7.5% Fine CRM (TFO)	82	-	-	-
15% Fine CRM		1.60	75.66	1.65
20% Fine CRM		2.03	75.08	2.10
AC-30 (Coastal)		-	-	-
7.5% Fine CRM	76	1.17	72.74	1.23
15% Fine CRM		3.78	70.43	4.01

To investigate the effect of the oven aging procedure, one sample (AC-20 with 7.5 percent fine CRM) was aged in the TFO and tested. For this binder the method of oven aging did not affect the final classification, although the RTFO-aged binder was less stiff when it was tested at 70°C. As noted previously only a small change in the *m*-value at −18°C would have caused the RTFO-aged sample to be classified differently. The TFO-aged sample was not borderline with respect to the *m*-value. Table 5 shows a more direct comparison of the various parameters of interest. For this binder the method of oven aging did not have a great effect on binder stiffness. The most significant difference between the two aging methods was the *m*-value at −18°C.

Table 6 shows the values of $G^*/\sin\delta$ before and after RTFO aging. These data compare the increase in $G^*/\sin\delta$ of modified binders with those of the base asphalts after RTFO aging. No consistent trend in these data exists. The base asphalts exhibit an

TABLE 4 $G^*/\sin\delta$ (kPa) Values for Fine CRM Binders (RTFO)

Material	Test Temp (°C)	G* (kPa)	δ (degrees)	G*/sin δ (kPa)
AC-2.5 (Coastal)		-	-	-
10% Fine CRM	58	1.79	78.35	1.83
20% Fine CRM		2.100	74.98	2.17
AC-2.5 (Amoco)		-	-	-
7.5% Fine CRM	70	-	-	-
15% Fine CRM		2.07	68.65	2.23
20% Fine CRM		3.37	66.89	3.66
AC-5 (Coastal)		2.39	84.10	2.40
7.5% Fine CRM	58	4.19	75.07	4.33
15% Fine CRM		-	-	-
AC-10 (Coastal)		3.97	83.40	3.99
7.5% Fine CRM	58	6.35	74.19	6.60
15 % Fine CRM		-	-	-
AC-20 (Coastal)		-	-	-
7.5% Fine CRM		-	-	-
7.5% Fine CRM (TFO)	82	-	-	-
15% Fine CRM		2.50	69.77	2.66
20% Fine CRM		3.66	67.87	3.95
AC-30 (Coastal)		-	-	-
7.5% Fine CRM	-	-	-	-
15% Fine CRM		-	-	-

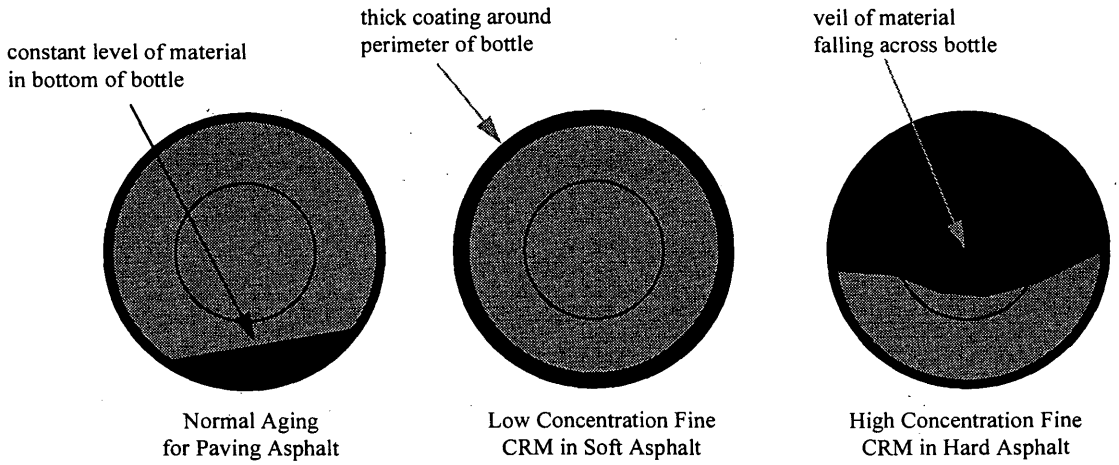

FIGURE 2 RTFO aging characteristics of fine rubber binders (end view of bottle).

TABLE 5 Comparison of Classification Test Parameters as Function of Oven Aging

AC-20, 7.5% Fine CRM (Coastal)		
Parameter	Oven Aging Technique	
	RTFO	TFO
Tests on Unaged Material		
G*/sin δ @ 70° C	1.42 kPa	
Tests on Oven Aged Residue		
G*/sin δ @ 70° C	3.60 kPa	3.91 kPa
Tests on PAV Residue		
G*sin δ @ 16° C	4955 kPa	5293 kPa
G*sin δ @ 19° C	3640 kPa	3950 kPa
S @ -12° C	104 MPa	99 MPa
m @ -12° C	0.355	0.345
S @ -18° C	212 MPa	227 MPa
m @ -18° C	0.296	0.277

TABLE 6 Comparison of Increase in *G/sin δ for Fine CRM Binders**

Material	Test Temp (°C)	G*/sin δ unaged	G*/sin δ RTFO aged	Increase (%)
AC-2.5 (Coastal)	46	1.85	3.73	101.6
10% Fine CRM	52	2.41	3.71	53.9
20% Fine CRM	64	1.14	1.55	36.0
AC-2.5 (Amoco)	46	2.12	5.29	149.5
7.5% Fine CRM	58	1.54	3.31	114.9
15% Fine CRM	70	1.11	2.23	100.9
20% Fine CRM	70	1.55	3.66	136.1
AC-5 (Coastal)	58	1.01	2.41	138.6
7.5% Fine CRM	58	1.61	4.33	168.9
15% Fine CRM	70	1.21	3.17	162.0
AC-10 (Coastal)	58	1.83	3.99	116.9
7.5% Fine CRM	64	1.87	3.03	62.0
15% Fine CRM	70	1.81	4.00	121.0
AC-20 (Coastal)	64	1.15	2.40	108.7
7.5% Fine CRM	70	1.42	3.60	153.5
7.5% Fine CRM (TFO)	70	1.42	3.91	175.4
15% Fine CRM	82	1.65	2.66	61.2
20% Fine CRM	82	2.10	3.95	88.1
AC-30 (Coastal)	64	1.70	4.00	135.3
7.5% Fine CRM	76	1.23	2.86	132.5
15% Fine CRM	82	2.17	3.93	81.1

TABLE 7 $G^*/\sin\delta$ Values for Fine CRM Binders

Material	Test Temp (°C)	G* (kPa)	δ (degrees)	G*sin δ (kPa)
AC-2.5 (Coastal)		7009	45.43	4993
10% Fine CRM	13	3644	48.43	2726
20% Fine CRM		2851	47.91	2116
AC-2.5 (Amoco)		5073	46.64	3688
7.5% Fine CRM	13	5475	39.86	3509
15% Fine CRM		4095	39.79	2621
20% Fine CRM		3219	39.08	2029
AC-5 (Coastal)		5209	44.59	3657
7.5% Fine CRM	16	3635	43.87	2519
15% Fine CRM		-	-	-
AC-10 (Coastal)		7820	37.82	4795
7.5% Fine CRM	16	4455	39.14	2812
15 % Fine CRM		-	-	-
AC-20 (Coastal)		8314	39.79	5321
7.5% Fine CRM		5756	39.23	3640
7.5% Fine CRM (TFO)	19	-	-	3950
15% Fine CRM		5528	35.74	3229
20% Fine CRM		5326	35.30	3078
AC-30 (Coastal)		9725	38.54	6059
7.5% Fine CRM	19	7481	37.50	4554
15% Fine CRM		6091	35.71	3555

increase in $G^*/\sin\delta$ ranging from about 100 to 150 percent. This roughly matches the specification value of 120 percent, which results from the minimum specified values of 1.00 and 2.20 kPa for unaged and RTFO-aged binders, respectively. For the rubber-modified binders this increase is considerably more variable, with values ranging from about 36 to 175 percent.

Table 7 shows values of $G^*\sin\delta$ for PAV residue for the various materials. In every case the addition of rubber facilitated a decrease in $G^*\sin\delta$. At these intermediate temperatures (approximately 10°C to 20°C) the effect of the rubber on $G^*\sin\delta$ was almost entirely due to G^*. In other words the profound reduction in $G^*\sin\delta$ was caused by a large reduction in G^* and not δ. The intermediate testing temperatures shown in Table 7 were chosen in a range for binder classification purposes. At these temperatures binders containing fine-mesh rubber exhibited a lower G^* value than the base asphalt. At high temperatures (see Tables 2, 3, and 4) the unaged rubber blends exhibited higher G^* values than the base asphalts. In other words the effect of fine-mesh rubber on $G^*\sin\delta$ must be less profound at higher intermediate temperatures. To demonstrate this phenomenon a temperature sweep was performed on the PAV-aged residues of four samples: AC-5, AC-20, and these two binders with 10 percent fine rubber. Figure 3 shows the results of that experiment. All four binders have very similar stiffness values in the range from 30°C to 40°C. On the basis of this limited experiment hotter climates would tend to favor neat asphalts or possibly neither with respect to fatigue life since the neat asphalts exhibit less stiffness at higher interme-

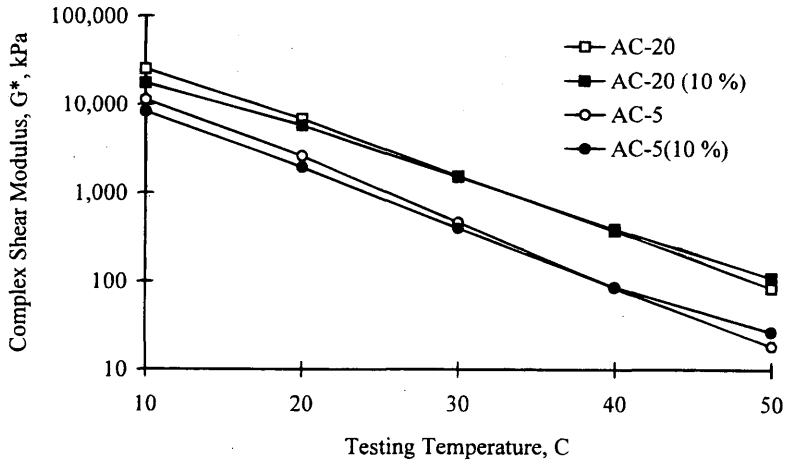

FIGURE 3 Complex shear modulus characteristics of PAV-aged fine rubber binders.

TABLE 8 Creep Stiffness and Logarithmic Creep Rate for Fine CRM Binders

Material	Test Temp (°C)	Creep Stiffness (MPa)	Creep Rate
AC-2.5 (Coastal)		337	0.279
10% Fine CRM	-24	219	0.318
20% Fine CRM		143	0.361
AC-2.5 (Amoco)		-	-
7.5% Fine CRM	-24	199	0.316
15% Fine CRM		138	0.336
20% Fine CRM		114	0.331
AC-5 (Coastal)		350	0.265
7.5% Fine CRM	-24	243	0.288
15% Fine CRM		174	0.304
AC-10 (Coastal)		200	0.289
7.5% Fine CRM	-18	131	0.298
15 % Fine CRM		118	0.321
AC-20 (Coastal)		251	0.276
7.5% Fine CRM		212	0.296
7.5% Fine CRM (TFO)	-18	227	0.277
15% Fine CRM		163	0.309
20% Fine CRM		132	0.306
AC-30 (Coastal)		306	0.286
7.5% Fine CRM	-18	232	0.287
15% Fine CRM		96	0.335

diate temperatures. Cooler climates would tend to favor the fine rubber binders since they exhibit less stiffness at lower intermediate temperatures. However, the technical literature and anecdotal experience with the performance of pavements containing fine crumb rubber binders seem to support neither assertion. This limited experiment coupled with field observations of real pavement performance suggests that intermediate temperature binder rheology alone is not sufficient to predict mixture fatigue behavior when using fine rubber binders. Sweeping comparisons of relative fatigue behavior on the basis of neat versus rubber-modified binders may be very tenuous.

Table 8 compares the creep stiffnesses of binders at various temperatures. These data show that an increase in rubber concentration results in a decrease in S and an increase in the m-value. The increase in the m-value is the reason that the addition of fine rubber resulted in lower low-temperature binder grades. One possible reason for this result is that higher concentrations of fine rubber may result in less aging through the RTFO because of the observed aging behavior illustrated in Figure 2. Less aging may also be the result of the presence of antioxidants in tire compounds. Another possible reason is that at low temperatures the rubber component is softer than the base asphalt, resulting in the same type of softening effect seen at intermediate temperatures for the parameter $G^*\sin\delta$. A third possible reason is that the rubber releases a constituent that has a softening effect on the asphalt at lower temperatures.

The viscosity of each blend was measured at 135°C (Table 9). In all cases the fine rubber caused an increase in binder viscosity at 135°C compared with that of the base asphalt. AASHTO MP1 requires that the viscosity at 135°C be less than 3 Pa·sec. Several of the binders violated this requirement. However, MP1 states that the viscosity criterion may be violated if the supplier warrants that the asphalt can be pumped and mixed at safe temperatures.

To assess the effects of fine-mesh rubber on handling characteristics, the viscosities of various blends of asphalt and fine-mesh rubber were tested. The following factors were evaluated:

- Asphalt grade (AC-5, AC-10, AC-20, and AC-30),
- Test temperature (150°C, 175°C, and 200°C),
- Rubber concentration (0, 10, and 20 percent), and
- Shear rate (20 and 50 rpm).

Figures 4 through 7 show the effects of these factors on blend viscosity. Several trends emerged from this experiment. First, there is a large increase in viscosity by increasing the concentration from 0 to 10 percent and from 10 to 20 percent. All blends shear thinned at all test temperatures. For the neat asphalts the viscosity test results

TABLE 9 Viscosity of Fine CRM Binders

Material	Viscosity at 135° C (Pa·s)
AC-2.5 (Coastal)	0.135
10% Fine CRM	0.485
20% Fine CRM	2.378
AC 2.5 (Amoco)	0.158
7.5% Fine CRM	0.480
15% Fine CRM	2.215
20% Fine CRM	6.550
AC-5 (Coastal)	0.190
7.5% Fine CRM	0.750
15% Fine CRM	1.800
AC-10 (Coastal)	0.240
7.5% Fine CRM	1.217
15 % Fine CRM	3.225
AC-20 (Coastal)	0.400
7.5% Fine CRM	1.175
15% Fine CRM	4.750
20% Fine CRM	12.687
AC-30 (Coastal)	0.490
7.5% Fine CRM	1.275
15% Fine CRM	5.425

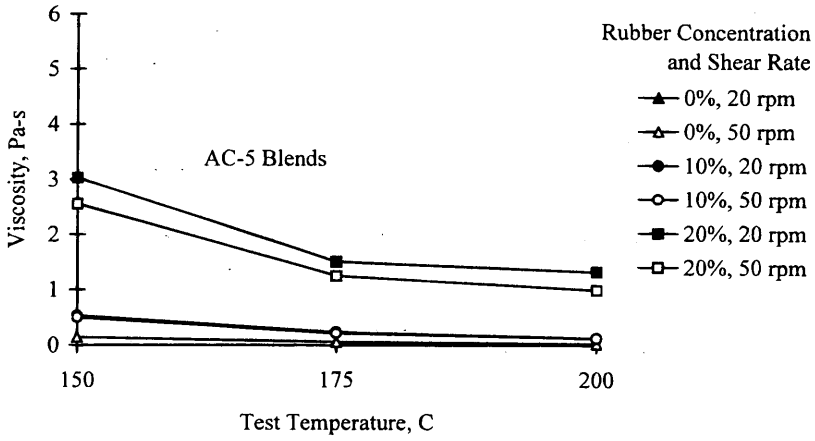

FIGURE 4 Effects of test temperature, rubber concentration, and shear rate on viscosities of AC-5 blends.

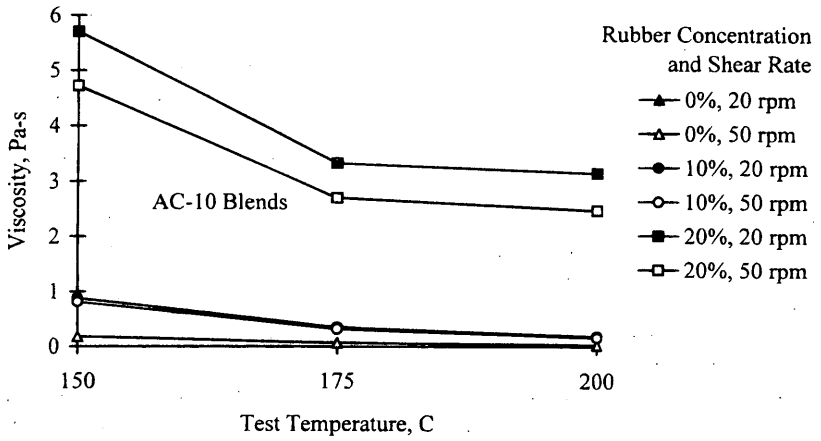

FIGURE 5 Effects of test temperature, rubber concentration, and shear rate on viscosities of AC-10 blends.

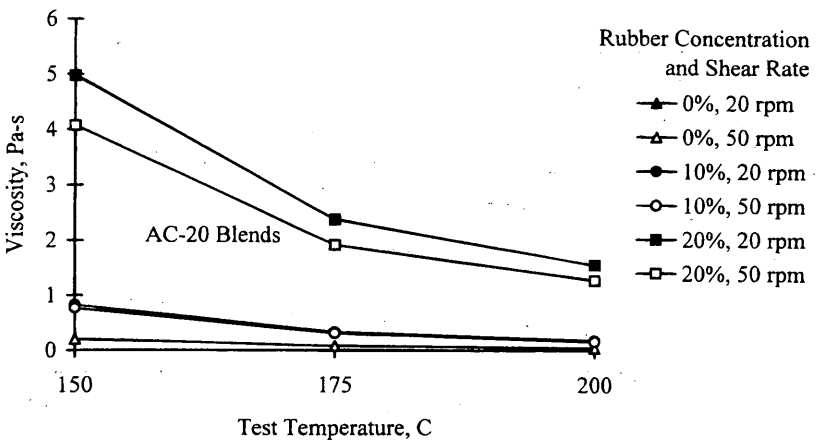

FIGURE 6 Effects of test temperature, rubber concentration, and shear rate on viscosities of AC-20 blends.

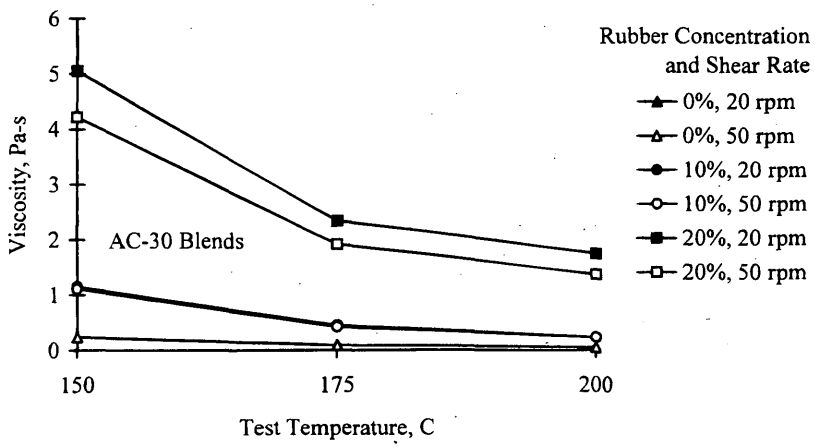

FIGURE 7 Effect of Test Temperature, Rubber Concentration, and Shear Rate on viscosity of AC-30 blends.

were identical for the two shear rates (i.e., the lines of data in Figures 4 through 7 coincide for the neat asphalts).

One unexpected result was the relatively small decrease in viscosity for the 20 percent fine rubber blends when the testing temperature was increased from 175°C to 200°C. This effect was also evident, but to a lesser degree, for the 10 percent blends. The effect is clearly caused by the presence of the fine-mesh rubber since the same phenomenon did not occur with the neat asphalts. During these tests it was observed that when changing test temperature, the viscosity would briefly stabilize when the sample equilibrated at the test temperature and then would begin to rise slowly. This effect was also observed by Bahia and Davies (*2*). Thus, it is possible that an additional asphalt rubber reaction is occurring at these relatively high test temperatures and that this reaction causes a stiffening of the binder. Although this stiffening is not sufficient to completely overcome the effect of test temperature, the net effect is to impede the effect of temperature on viscosity, which flattens the slope of the temperature-viscosity plot between 175° and 200°C.

To estimate the effect of storage time at elevated temperature on viscosity, a simple experiment was performed. One liter each of AC-20 and AC-30 containing 10 percent fine rubber was mixed as normal at 177°C. A sample of neat AC-20 was also tested. The viscosity at 175°C was measured immediately after blending and after 4, 24, 48, and 72 hr. Figure 8 shows the test results. After an initial increase in viscosity between blending and 4 hr, the viscosity begins a gradual increase with time. The rate of increase is approximately the same for the fine rubber binders and neat asphalt.

CONCLUSIONS

The analysis presented here shows that fine mesh rubber affects binder physical properties and classification according to the AASHTO performance graded binder system. For the asphalts tested the addition of a small amount of fine rubber resulted in a binder that was generally classified one high-temperature grade

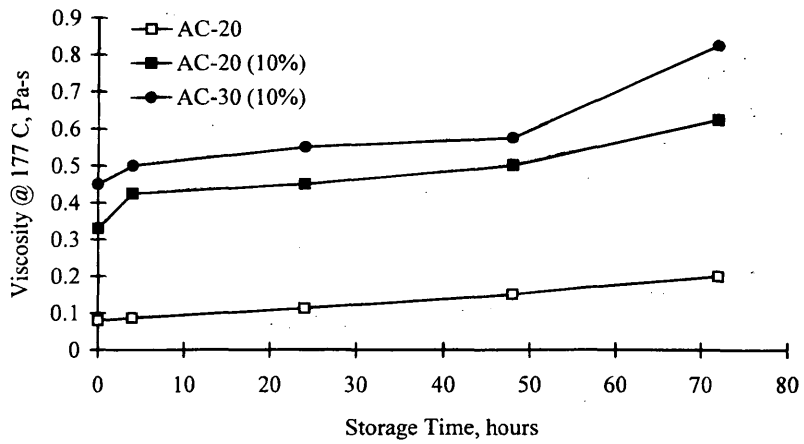

FIGURE 8 Effect of storage time on viscosity.

higher than that of the base asphalt. For the asphalts tested the addition of a moderate amount of rubber resulted in a binder that was generally classified two or three high-temperature grades higher and one low-temperature grade lower than those of the base asphalt. It is well known that the asphalt source and rubber composition have a profound effect on the physical properties of an asphalt–rubber blend. The present study was limited in scope because it generally involved only one asphalt source and one rubber source.

Other than the curious binder behavior during RTFO aging, no problems were encountered by using the Superpave methods of binder characterization required by AASHTO MP1. DSR, BBR, and PAV did not exhibit any difficulties in characterizing fine rubber-modified asphalt. However, the study suggests that the current AASHTO procedure, which uses RTFO, may or may not be producing a properly aged sample when used to analyze asphalt binders containing fine-mesh rubber.

Viscosity test results showed that at typical storage and handling temperatures, asphalt binders containing fine-mesh rubber are very viscous. Furthermore, rotational viscosity testing showed that at normal storage and handling temperatures, viscosity slowly increases with time. This suggests that when testing fine-mesh rubber binders, the thermal history of the samples must be carefully controlled if repeatable test results are to be achieved. It also suggests that field storage time will have a great effect on the handling characteristics of fine-mesh rubber binders.

REFERENCES

1. *Standard Specification for Performance Graded Asphalt Binder.* AASHTO Designation MP.1 AASHTO, Gaithersburg, Md., Sept. 1993.
2. Bahia, H. U., and R. Davies. Effect of Crumb Rubber Modifiers (CRM) on Performance-Related Properties of Asphalt Binders. *Journal of the Association of Asphalt Paving Technologists,* Vol. 63, 1994.
3. Chehoveits, J. G. Crumb Rubber Modifier Workshop Notes, Design Procedures and Construction Practices, Session 9: Binder Design Procedures Office of Technology Applications, FHWA, U.S. Department of Transportation, March 1993.
4. *Standard Specification for Viscosity Graded Asphalt Cement.* AASHTO Designation M226–80. AASHTO, Gaithersburg, Md., 1986.
5. *Standard Test Method for Viscosity Determinations of Unfilled Asphalts Using the Brookfield Thermosel Apparatus.* ASTM Designation D4402–87. ASTM, Philadelphia, 1991.
6. *Standard Test Method for Determining the Rheological Properties of Asphalt Binder Using a Dynamic Shear Rheometer (DSR).* AASHTO Designation TP.5 AASHTO, Gaithersburg, Md., Sept. 1993.
7. *Standard Test Method for Effect of Heat and Air on a Moving Film of Asphalt (Rolling Thin Film Oven Test).* AASHTO Designation T240–87. AASHTO, Gaithersburg, Md., 1987.
8. *Standard Test Method for Effect of Heat and Air on Asphalt Materials (Thin-Film Oven Test).* AASHTO Designation T179–88. AASHTO, Gaithersburg, Md., Sept. 1988.
9. *Standard Practice for Accelerated Aging of Asphalt Binder Using a Pressurized Aging Vessel (PAV).* AASHTO Designation PP.1 AASHTO, Gaithersburg, Md., Sept. 1993.
10. *Standard Test Method for Determining the Flexural Creep Stiffness of Asphalt Binder Using the Bending Beam Rheometer (BBR).* AASHTO Designation TP.1 AASHTO, Gaithersburg, Md., Sept. 1993.

Evaluation of Rheological Measurements for Unmodified and Modified Asphalt Cements

MARY STROUP-GARDINER AND DAVE NEWCOMB

A rigorous evaluation of the dynamic shear rheometer (DSR) with both unmodified and modified asphalts indicated that testing problems such as potential compliance-related problems, plate slip, and equipment limitations could be easily identified during testing. Once these problems were identified changes in either the test configuration or the testing parameters could eliminate the problem. The relationship between the complex modulus (G^*) and the complex viscosity (η^*) showed that G^* (in kilopascals) is equal to η^* (in poise) at 10 rad/sec. It was also shown that η^*, the DSR viscosity, could be estimated by $\eta(\gamma)$, the traditional vacuum viscosity for test temperatures of 46°C and above for unmodified asphalt cements. Typical values for the phase shift (δ) for test temperatures of 46°C and 64°C were 81 and 89 degrees, respectively, for unmodified asphalt cements and 60 and 81 degrees, respectively, for polymer-modified asphalts. For this range of test temperature the temperature had a greater influence on changes in δ than in the change of asphalt source or grade for unmodified asphalts. Changes in the phase shift for modified binders were dependent on the test temperature, type of polymer, and asphalt source or grade. A quick method of estimating the temperature at which $G^*/\sin\delta$ equals 1 kPa for unmodified asphalts is presented. Briefly, if sin δ can be assumed to be 1 for unmodified asphalts, then the traditional viscosity measurements at both 60°C and 135°C can be used to estimate the temperature at which the viscosity would be 1000 P (i.e., $G^* = 1$ kPa). This approach compared well with the DSR-developed temperatures reported by Strategic Highway Research Program researchers.

Rheology is the study of material flow and deformation characteristics. Various methods of obtaining rheological measurements serve as the basis for the final Strategic Highway Research Program (SHRP) asphalt binder specification. A preliminary review of AASHTO test method TP5, Determining the Rheological Properties of Asphalt Binder Using a Dynamic Shear Rheometer (*1*), indicated that the percent strain, plate diameter, and gap height have been standardized for all binders. Since both the test method and the specification limits have been developed primarily from an evaluation of unmodified binders, a method of verifying the applicability of the specified test parameters should be added to the test method. This would ensure that all test results are as reliable as possible for a wide range of binders. Other critical information that has not been included in either TP5 or the supporting SHRP reports is a general frame of reference for reasonable ranges of values for complex modulus (G^*) and sin δ (where δ is the phase shift), independent methods of quickly verifying the dynamic shear rheometer (DSR) results, and an estimate of the within-laboratory testing variability (*2–4*). A research program was developed to address these needs.

Civil Engineering Department, University of Minnesota, 500 Pillsbury Drive, S.E., Minneapolis, Minn. 55455.

BACKGROUND

As stated in the introduction rheology is the study of both material flow and deformation. This is accomplished by measuring shear rate, shear stress, and in the case of oscillatory testing, the phase shift between the applied stress or strain and the corresponding response. Although most materials engineers in the highway industry equate a rheometer for measuring these properties with DSR, few people recognize that the traditional vacuum and kinematic viscometers are also rheometers. The vacuum viscometer is correctly classified as a pressure-driven, steady-state shear flow rheometer because the material moves through the capillary tube under a steady pressure. Information on the shear rate can be obtained from this test when Asphalt Institute tubes are used. The kinematic viscometer is also a pressure-driven, steady-state shear flow rheometer but can provide information at only a single, unknown shear rate. The rotational viscometer (e.g., Brookfield) used to determine the SHRP specification 135°C viscosity is classified as a steady-state drag flow rheometer.

The difference between the traditional and rotational rheometers and DSR (a dynamic drag flow rheometer) is that DSR also provides information on a material's storage and loss components. This information is especially important when binders are modified to increase their elastic properties.

It stands to reason that if the traditional vacuum viscometers and the new DSR are all rheometers, then the information obtained from each should be related. For low strain rates

$$\eta(\dot{\gamma}) = \eta'(\omega) \text{ for } \omega = \dot{\gamma} \rightarrow 0$$

where

$\dot{\gamma}$ = shear rate (sec^{-1}) (typical range for Asphalt Institute tubes is between 0.5 and 3 sec^{-1}),
ω = angular frequency (rad/sec),
$\eta(\dot{\gamma})$ = steady-state viscosity (e.g., vacuum viscosity measurement for unmodified asphalt cement), and
$\eta'(\omega)$ = dynamic loss component of viscosity.

For high frequencies an empirical relationship known as the Cox-Merz rule can be applied (*5*):

$$\eta(\dot{\gamma}) = \eta^*(\omega) \text{ for } \dot{\gamma} = \omega$$

Bouldin et al. (*6*) have shown that this relationship is generally applicable for both unmodified and polymer-modified asphalt cements.

Viscosity measurements are related to modulus by:

$$\eta^* = \frac{G^*}{\omega}$$

where η^* is the complex viscosity (in Pa · sec and, G^* is the complex modulus (in Pa). When ω is equal to 10 rad/sec, as specified in TP5, and viscosity is expressed in terms of poise (1 Pa · sec = 10 P), the equation reduces to

$$\eta^* = G^*$$

For Newtonian materials the viscosity will be independent of the shear rate. This means that for unmodified asphalt cements the traditional vacuum viscosity should be equal to G^* at 10 rad/sec.

For dynamic measurements both the complex viscosity and the complex modulus can be separated into loss and storage components by the following equations:

Storage component: $\eta'' = \frac{G'}{\omega}$; $G' = G^* \cos \delta$

Loss component: $\eta' = \frac{G''}{\omega}$; $G'' = G^* \sin \delta$

For materials with very low values of storage viscosity (η'') the loss component of viscosity (η'') is essentially the complex viscosity (η^*). It should be noted that the superscripts for loss and storage for viscosity and modulus are traditionally reversed (i.e., η' and η'' and G'' and G' are loss and storage components, respectively).

RESEARCH PROGRAM

Objectives

The objectives of this research program were to

1. Develop a laboratory procedure to ensure the collection of reliable DSR data for both unmodified and modified asphalt cements.
2. Assess the applicability of the current version of TP5 for use with modified asphalt cements.

Scope

The hypothesis was that if the unaged, modified asphalt cements required changes in the test parameters, then the higher-viscosity aged materials would definitely need test method adjustments. The higher end of the temperature range in the SHRP specification is used to test either the original or rolling thin film oven (RTFO)-aged asphalt cements. All unaged materials were tested at these temperatures; a limited number of materials were selected for RTFO aging on the basis of the results for the unaged samples. Although the SHRP specification uses the lower test temperatures to evaluate pressure aging vessel-aged binders, this equipment was not available. Therefore, only unaged samples were tested at this temperature. When the TP5 test method was evaluated, single points obtained from frequency sweeps (0.1 to 100 rad/sec) were used.

Unmodified asphalt cements were chosen from the SHRP Materials Reference Library (MRL) and were selected to cover a wide range of viscosities. These binders included AC-10 (AAF-2), AC-20 (AAF-1), and 200/300 pen (AAA-2) asphalt cements.

Polymer modifiers were limited to the SBS (styrene-butadiene-styrene block copolymer) category. These included two different suppliers of SBS (Shell's Kraton, Dexco's Vector), two architectures (linear, radial), and four different molecular weights of saturated SBS [i.e., styrene-ethylene-butadiene-styrene, (SEBS)]. The concentration of polymer used for modifying the asphalt cement was limited to 4 percent; this was based on both a literature review and preliminary laboratory results.

TESTING PROGRAM

A Rheometrics RAA DSR was used to conduct frequency sweep testing at 5°C, 10°C, 15°C, 20°C, 25°C, and 30°C by using 8-mm-diameter plates and various gap heights ranging from 1.5 to 2 mm and at 20°C, 30°C, 40°C, 50°C, and 60°C by using 25-mm-diameter plates and gap heights ranging from 1 to 2 mm. The percent strains for each test temperature were based on the results of strain sweeps; strains in the middle of the linear viscoelastic region were selected. Additional single-point measurements were made for 46°C, 52°C, 58°C, and 64°C at 10 rad/sec and 12 percent strain. These single-point measurements were made in accordance with TP5.

Since G^* can be directly related to η^* and the dynamic and steady-state viscosities should be equivalent, traditional vacuum viscosities were also determined to confirm this relationship. This testing was completed at 60°C according to ASTM D2170.

All materials were tested in their unaged condition. For the polymer-modified asphalt cements this refers to samples molded immediately after the completion of blending as described in the next paragraph. After all unaged samples were tested, selected unmodified and modified binders were subjected to RTFO aging according to ASTM D2872. Materials were selected so that a wide range of both viscosities and polymer structures were represented. A discussion of the polymer structure is beyond the scope of this paper and will be mentioned only as a means of explaining specific differences in viscosity and modulus data.

For blending of the polymer-modified asphalt cements 4 percent polymer by weight of asphalt cement was added to approximately 450 g of preheated (between 175° and 185°C) base asphalt cement in a 1-L can. A high-shear blender set at 3,500 rpm was used to blend the polymer and the asphalt. A heating mantle was used around the can so that the asphalt temperature was maintained at the original temperature throughout mixing; the temperature was monitored throughout mixing. Blending was continued until Brookfield viscosity measurements (disk configuration) taken every 15 min either were consistent or began to decrease. Typical mixing times ranged from 45 min to 1.45 hr depending on the compatibility of the polymer with the asphalt cement.

Once blending was completed molds for the DSR were poured and the vacuum viscosities were determined.

ANALYSIS

Development of Guidelines for Quality Control of Data and Common Testing Problems

Quality can be corrupted by reporting data that have not been checked for evidence of potential compliance-related problems, plate slip, and equipment limitation problems. Potential compliance problems occur at cold temperatures; true compliance problems occur when the angular deflection produced by the motor is trans-

ferred into the deflection of the force transducer instead of the sample. Although true compliance may or may not be accounted for by the equipment software, other related problems such as exceeding a lower limit of angular deflection because of the stiffness of the material can be a part of this problem. Stiffness-related problems occur at different temperatures, plate sizes, and gaps for various materials. Plate slip occurs when the bond between the binder and the plate surface is lost and can also be a function of the sample preparation as well as the material stiffness. Since DSR takes only two measurements, torque and angular rotation, all results (e.g., strain, G^* and η^*) are calculated from these measurements. Therefore, it is essential that the limits for these measurements be carefully monitored.

Figure 1 shows how to identify stiffness-related problems. Figure 1 shows test results for AC-20 (AAF-1) modified with 4 percent of a radial SBS (Kraton D1184), the stiffest modified asphalt cement tested in the program described here. At 40°C the percent strain was very close to the target strain of 0.5 percent by using the 25-mm diameter plates. As the test temperature decreased it became increasingly apparent that the target strain could not be met. This is seen as a marked decrease in the measured percent strain and can be explained by the working equation used by the DSR:

$$\gamma = \frac{\theta R}{h}$$

where

γ = strain,
θ = angular rotation,
R = radius of plate (mm), and
h = gap between plates (mm).

The percent strain, gap height, and radius are entered into the equipment software by the operator at the beginning of the testing. However, there are limits on the minimum angular rotation that can be easily exceeded at a low strain level. Either the angular rotation should be calculated to ensure that this is not a problem or the testing configuration should be changed to prevent the actual percent strain from differing from that for the target.

Plate slip or sample fracture occurring during a test can be identified by a sudden drop in the torque measurements. Plate slip due to improperly bonded samples can result in uniformly lower values. An indication of this problem can be seen when the individual curves forming the master curve do not overlap. When plate slip is suspected it can be easily identified by running a sample at either two different gaps or two different plate diameters (*5,7*). Figure 2 shows test results for unmodified AC-20 (AAF-1) from 25-mm-diameter plates with a gap height of 2 mm and 8-mm-diameter plates with a gap of 1.5 mm for a test temperature of 30°C. Both results overlapped very well between about 1 and 10 rad/sec.

Although plate slip is a potential problem that needs to be considered, no evidence of this problem was seen for any of the materials tested. This was attributed to the sample preparation procedure detailed in TP5 that specifies that the sample should be loaded onto preheated plates. It appeared that the preheating procedure effectively eliminates this problem.

Figure 2 also shows an apparent departure of results for the 25- and 8-mm-diameter plate results at the higher frequencies (above 10 rad/sec). An examination of the torque and percent strain values shows that this can be traced to stiffness-related problems (Figure 3). Because the percent strain decreased for the larger-diameter plates at the higher frequencies, the torque values did not increase as much as they should have. This resulted in the slightly higher viscosity for the 25-mm-diameter plates at the higher frequencies.

The erratic behavior for the 8-mm-diameter plate results at the lower frequencies can be traced to the fact that the limits of the measurement system were exceeded (Figure 3). For the Rheometrics RAA equipment the force transducer limits were a minimum of 2 g·cm and a maximum of 2000 g-cm. The manufacturer reported that although the minimum limit was 2 g·cm, reliable results may be obtained at as low as 0.2 g·cm. This appears to be the case in Fig-

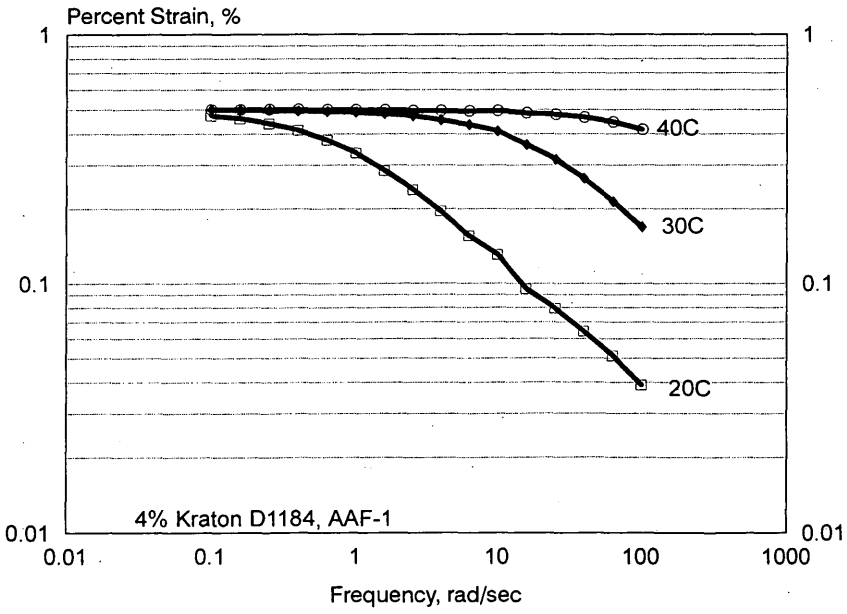

FIGURE 1 Identification of stiffness-related problems.

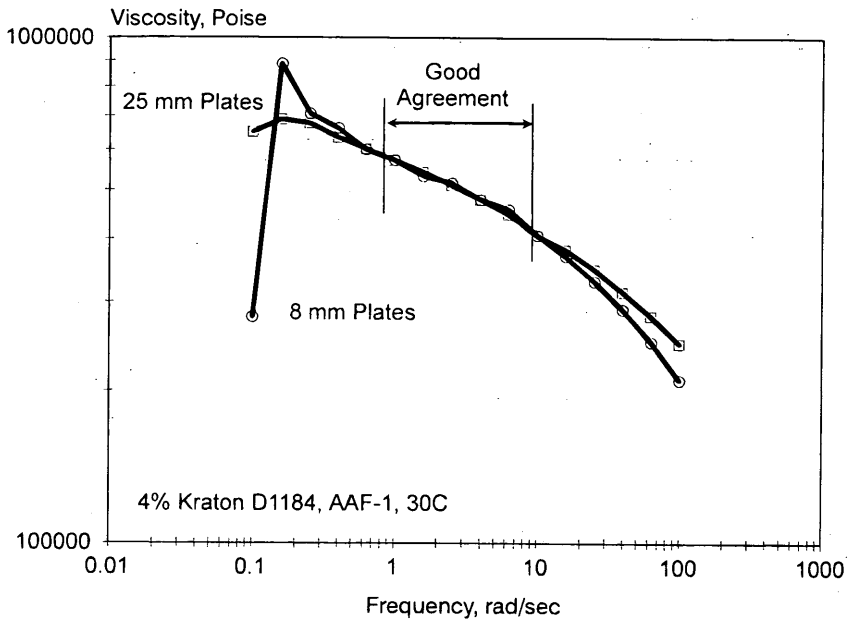

FIGURE 2 Identification of wall slip.

ure 3 because viscosity values above 0.2 g·cm provided a good overlap with the 25-mm-diameter plate data (Figure 2). However, torque values below 0.2 g·cm appear to be responsible for the erratic data seen in Figure 3.

Exceeding the maximum limit did not pose an identification problem with this equipment, because the equipment halts the testing when the maximum limit is reached.

Since DSR measurements rely solely on software to calculate test results, an additional manual check should be conducted to ensure that there are no software problems. This check has the additional advantage of identifying another common problem: errors in geometry entered by the operator. Ordinarily, manual checking of software calculations can be too time-consuming and difficult for general laboratory personnel. However, since the basic working equations for DSR are simple, the manual check is also simple. Start by calculating the shear stress:

$$\tau = \frac{M}{2\pi R^3}\left(3 + \frac{d\ln M}{d\ln \dot{\gamma}_R}\right)$$

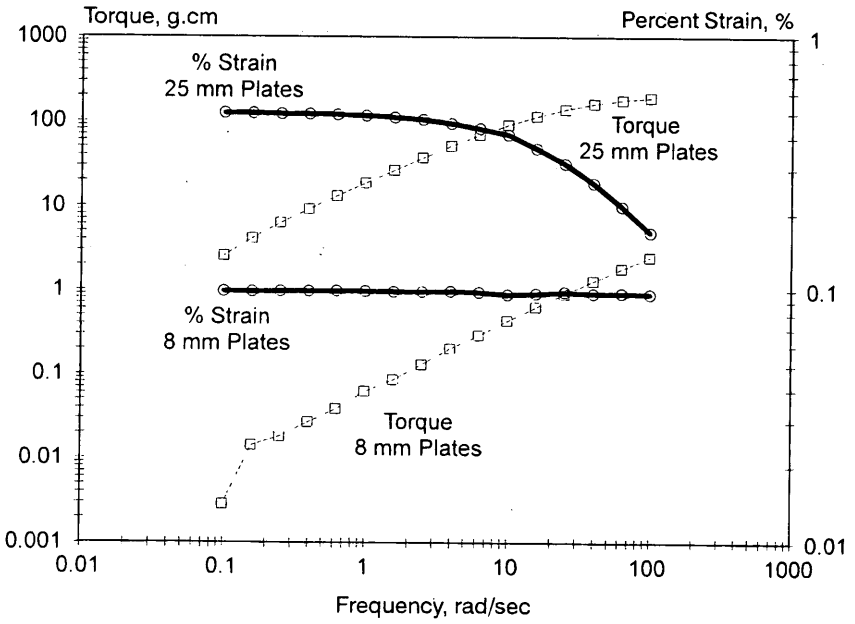

FIGURE 3 Identification of exceeded measurement limits.

TABLE 1 Solutions to Common DSR Problems

Problem	Solution
Stiffness-Related Problems	Reduce Plate Diameter Reduce Percent Strain
Plate Slip	Reduce Plate Diameter Reduce Percent Strain Check Sample Preparation
Max. Torque Limits Exceeded	Reduce Plate Diameter Reduce Percent Strain
Min. Torque Limits Exceeded	Increase Plate Diameter Increase Percent Strain

where

M = torque value measured by equipment,
R = radius of plate (cm), and
$d\ln M/d\ln\dot{\gamma}_R = 1$ for measurements within the linear viscoelastic region.

Then calculate G^*:

$$G^* = \frac{\tau}{\gamma}$$

where γ is the software-reported strain. If the calculated value and the software-reported values do not match, there is most likely an error in the geometry values. The most common mistakes appear to be entering the plate diameter instead of the radius or forgetting to change the gap after loading a new sample.

Once compliance, plate slip, and limit problems have been identified they can easily be eliminated. Table 1 summarizes solutions to these problems. As Table 1 shows all of the problems mentioned earlier can be addressed by changing either the plate diameter or the target percent strain. Compliance and related low angular deflections, slip, and upper-limit torque problems typically occur when the material is too stiff. The working equation for calculating the shear stress (presented earlier) explains why a change in the plate diameter will eliminate the problem. For a given level of shear stress the torque (M) decreases proportionally with the radius of the plates cubed (R^3). This also explains why increasing the plate size will eliminate any problems with low torque values.

Although these are very simple testing changes care must be taken to ensure that the values chosen are still within the linear viscoelastic region. This means that when one changes any of the testing parameters a strain sweep at a median frequency should be conducted. Figure 4 shows typical results from a strain sweep. Figure 4 shows that even the stiffest modified asphalt cement was still within the linear viscoelastic range for strains of up to 30 percent. These results indicate that there should be a wide latitude for changing the percent strain and still be within the linear viscoelastic region.

Evaluation of Test Parameters Specified by TP5

Once methods for identifying potential testing problems were developed, a range of both unmodified and modified asphalt cements was evaluated to check the appropriateness of the TP5 testing parameters. The specified testing parameters for original materials of 12 percent strain, 25-mm-diameter plates, 1-mm gap, and 10 rad/sec were appropriate for all materials tested. This conclusion was based on examining the torque and strain values at the warmest SHRP specification temperature (e.g., 46°C, 52°C, 58°C, or 64°C) at which a value of $G^*/\sin\delta$ was greater than or equal to 1 kPa. There were also no problems with testing RTFO-aged materials at a 10 percent strain level.

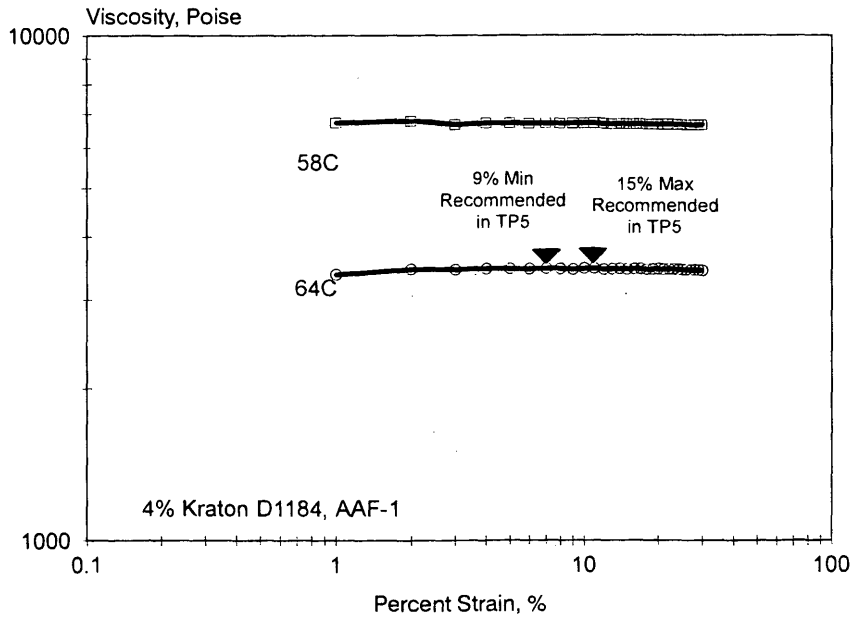

FIGURE 4 Strain sweep conducted to check for extent of linear viscoelastic region.

Changes had to be made for the unaged polymer-modified binders at the lower end of the 4°C to 40°C testing range. Typical strains used for the stiffer polymer-modified binders (AC-10 and AC-20 base asphalts) were between 0.05 and 0.2 percent for temperatures between 4°C and 19°C and between 0.5 and 1 percent for temperatures 22°C and 40°C.

Sample preparation also had to be changed for the modified asphalt cements at the colder temperature. The gap was set at the median of the test temperature range, the plates were heated to about 50°C, and the sample was loaded according to TP5. However, when the temperature was lowered back to the median temperature so that the sample could be trimmed, most of the polymer-modified asphalt cements showed a tensile stress buildup of greater than 1 kg or 50 percent of the capacity of the transducer. This was due to the quick drop in temperature (from 50°C to about 15°C in 3 min). The sample was contracting faster than it could dissipate the stress built up through a deformation response. To prevent the sample from debonding from the plates because of tension the operator manually decreased the gap height as the temperature dropped so that the force on the transducer was approximately zero. Once the sample and temperature stabilized, the edges of the sample were trimmed and the final gap distance was set.

Summary

The information presented on ensuring the quality of the reported data has been summarized into a flow chart for general laboratory use (Figure 5). This flow chart for checking data is relevant either for single-point measurements used in the SHRP specification or in the development of master curves for research purposes.

One problem with evaluating test results was that there was no apparent means of assessing the reasonableness of the reported data. This led to the development of general ranges of material properties for common testing conditions. These ranges are given in Table 2. As expected the value of G^* reflects the range of viscosities of the various materials. The phase shift (δ), which is used to calculate sin δ, varied more with a 6°C change in test temperature than with a change in asphalt cement grade (unmodified) from what would be about an AC-5 to an AC-20. This difference decreased with increasing test temperature.

The RTFO aging of the unmodified asphalts significantly increased the G^* values; this reflects the increase in viscosity due to aging. The phase angle showed a slight, uniform decrease after aging for the lower test temperatures. This difference gradually diminished as the temperature increased.

There was little difference between either the source of the SBS product or the architecture of the polymer (i.e., linear versus radial). There was, however, an approximately 300 percent increase in the G^* values for a given asphalt cement source and grade due to the modification. The phase shift showed a significant increase with increasing test temperature and was also significantly influenced by the asphalt source or grade. In general, adding an SBS polymer resulted in a decrease in the phase angle from the mid to the high 80s to between 60 and the low 80s for unmodified materials. The

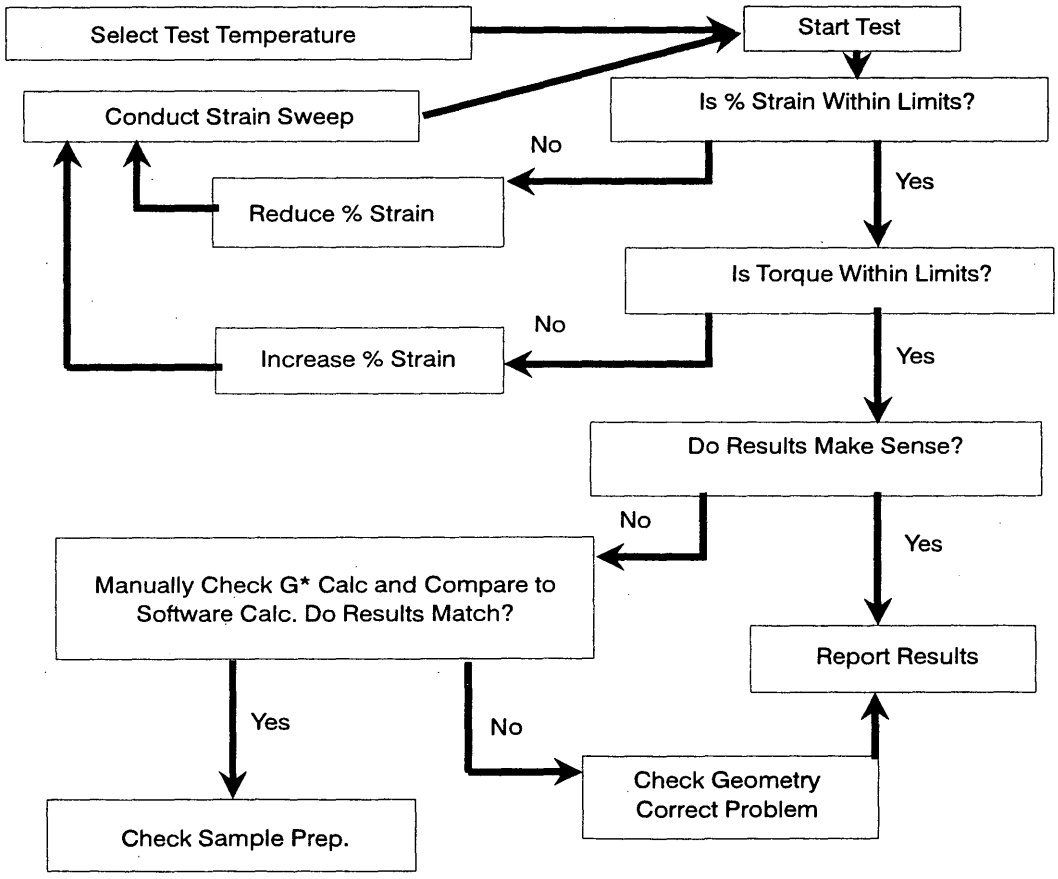

FIGURE 5 Quality control of reported data.

TABLE 2 Ranges of Rheological Parameters for Unmodified and Modified Asphalt Cements

Category of Materials	Test Temp., °C	G*, kPa[1] or η*, Poise at 10 rad/sec.		Phase Shift, δ[1]	
Unaged, Unmodified Asphalt	46	2,600 - (Not Available)		82.5 - 85.0	
	52	1,200 - 7,500		85.4 - 86.6	
	58	594 - 2,755		87.2 - 88.3	
	64	298 - 1,159		88.5 - 88.9	
RTFO Aged Unmodified	46	27,180[3] - 50,857		81.1 - 82.5	
	52	9,003[3] - 17,293		84.1 - 85.5	
	58	3,303[3] - 6,451		86.3 - 87.2	
	64	1,328[3]- 2,571		87.7 - 88.5	
Linear SBS Modified Asphalts 4% Polymer	46	Kraton D1101	Vector 2518	Kraton D1101	Vector 2518
		7,153 - 38,971	8,395 - 45,051	70.7 - 72.7	69.1 - 72.0
	52	3,605 - 15,764	4,106 - 18,251	73.46 - 75.2	71.2- 73.2
	58	1,899 - 6,916	2,228 - 8,085	74.7 - 77.2	72.6 - 74.9
	64	1,026 - 3,211	1,155 - 3,844	75.0 - 77.7	73.5 - 75.7
Radial SBS Modified Asphalts 4% Polymer	46	Kraton D1184	Vector 2411	Kraton D1184[2]	Vector 2411
		7,722 - 39,033	9,451- 33,156	68.6 - 72.7 (72.1)	60.6 - 76.2
	52	4,002 - 15,693	5,182 - 12,843	73.7 - 75.17 (72.9)	66.4 - 78.6
	58	2,071 - 6,887	2,826 - 5,375	76.9 - 77.2 (72.4)	72.0 - 80.5
	64	1,073 - 3,344	1,490 - 2,415	78.8 - 77.7 (69.4)	75.6 - 81.2
SEBS Modified Asphalt 4% Polymer	46	Kraton G1652	Kraton G1651	Kraton G1652	Kraton G1651
		11,106 - 46,894	12,006 - 52,766	64.5 - 74.2	61.2 - 70.8
	52	5,708 - 18,893	6,508 - 21,632	68.6 - 75.9	65.6 - 72.2
	58	2,994 - 8,064	3,345 - 9,589	72.2 - 76.4	68.4 - 73.0
	64	1,553 - 3,826	1,675 - 4,594	76.0 - 73.0	72.2 - 73.0

1: The first value in each column is for the 200/300 Pen (AAA-2) asphalt and the second value is for the AC20 (AAF-1). The value for the AC10 (AAF-2) was always between these two values.
2: The values in parentheses are for the AC20 modified asphalt cement; the last number of this range is for the modified AC10 (AAF-2).
3: Data for AC10 (AAF-2) instead of AAA-2.

magnitude of the change was dependent on the source and structure of the polymer.

The same trends were also seen for the SEBS products of different molecular weights. The higher-molecular-weight Kraton G1651 (SEBS), which is 3.6 times the molecular weight of the G1652 (as reported by the supplier), increased G^* slightly, and there was a corresponding decrease in the phase shift. There did not appear to be any significant difference between the SEBS products, regardless of differences in molecular weight. The range of phase shift values was also lower for these saturated SBS products; these values ranged from 64.5 to 76.4 degrees.

Theoretically, the traditional vacuum viscosity should provide an excellent estimate of the DSR viscosity and hence G^*. Figure 6 shows a wide range of vacuum-versus-DSR viscosity results (Table 3). Very good correlations were obtained for the unmodified asphalt cements and for the lower-viscosity modified binders (i.e., the modified AAA-2 series). This can be explained by verifying the Newtonian behavior of these materials (Figure 7). There was very little change in the viscosity with increasing shear rate for any of the unmodified asphalts, either aged or unaged. This implies that the vacuum tube viscosities with typical shear rates for Asphalt Institute tubes of between 0.5 and 3 sec^{-1} should represent viscosities at 10 sec^{-1}, the steady-state counterpart of the 10 rad/sec used for dynamic shear testing. As the non-Newtonian behavior of the modified asphalts increases, the vacuum viscosities at shear rates of less than 5 sec^{-1} showed a higher estimate of the dynamic viscosity at 10 rad/sec. For this reason the use of vacuum viscosities as a measure of G^* should be limited to unmodified asphalts. Any modified

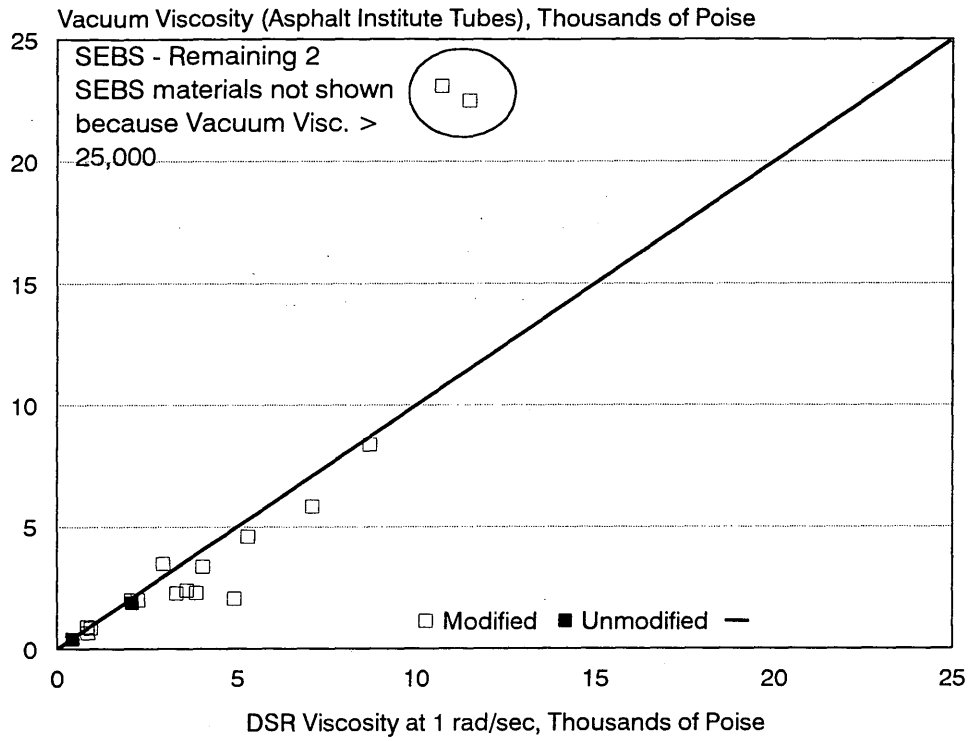

FIGURE 6 Comparison of vacuum and DSR viscosity versus shear rate results.

asphalts with undetermined shear rate-dependent behavior will be subject to an overestimation of G^*.

Table 2 shows that 4 percent Kraton D1184-modified AC-20 (AAF-1) behaved differently from the other modified asphalts. Although the viscosity decreased with increasing test temperature, the phase shift was essentially constant for all temperatures. It is possible that this phenomenon is a result of the highly developed polymer network formed within this asphalt. This network also appears to be responsible for the poor relationship between the vacuum and DSR viscosity (Table 3). This large difference between the viscosities can be explained in part by a closer examination of the vacuum viscosity data.

The DSR data exhibited shear thinning behavior typical of non-Newtonian materials. The vacuum tube results showed just the opposite behavior; the material appeared to be shear thickening. A closer examination of the theory behind capillary viscometers revealed that there is an assumption of fully developed shear flow within the measurement area (*5*). Before the full development of shear flow a region of extensional flow exists in all capillary rheometers. If the shear flow is not fully developed extensional thickening characteristics can show up as apparent shear thickening with highly networked materials. The increased viscosity with increased shear rate is due to the material stiffening response for the faster extensional flow. On the basis of this observation vacuum

TABLE 3 Comparison of Traditional Vacuum and DSR Viscosity Measurements

Asphalt Cement	Modifier	Vacuum Viscosity Measurement[1] (Poise)	DSR Viscosity Measurement (Poise)
200/300 Pen (AAA-2)	0%	410	439
	4% Kraton D1101 (Linear SBS)	2,010	2,271
	4% Kraton D1184 (Radial SBS)	2,160	2,078
	4% Vector 2411 (Radial SBS)	3,495	2,976
AC20 (AAF-1)	0%	1,872	2,089
	4% Kraton D1101 (Linear SBS)	5,834	7,097
	4% Kraton D1184 (Radial SBS)	201,630	9,344
	4% Vector 2518 (Linear SBS)	8,723	8,370
	4% Vector 2411 (Radial SBS)	4,935	2,056

1: Asphalt Institute tubes were used so that the shear rate for a given timing mark could be calculated. The vacuum tube viscosity and the DSR viscosity were compared at a shear rate of 1 sec^{-1}.

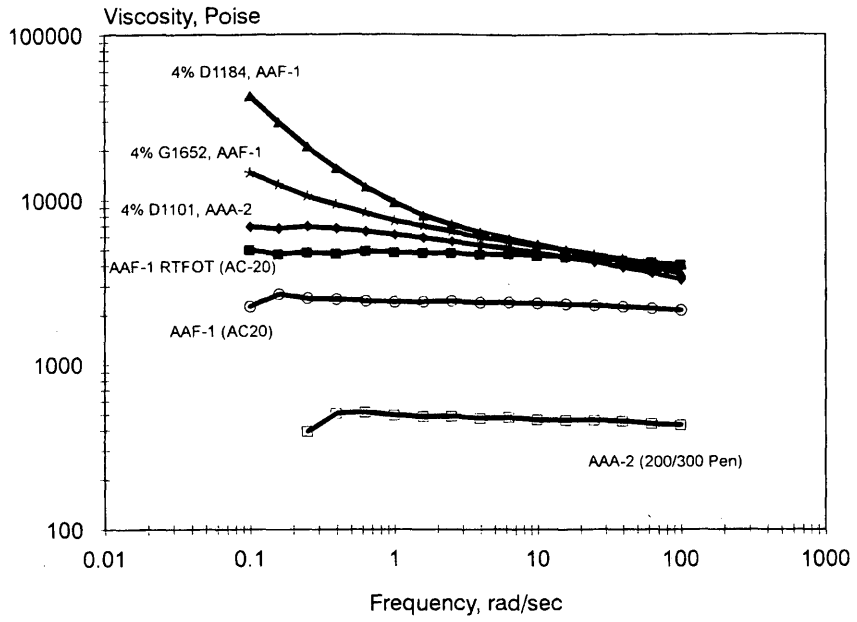

FIGURE 7 Viscosity versus shear rate for various materials.

viscosity results of modified asphalt cements should be used with caution and only as general estimates of the true material viscosity and G^* values.

Traditional viscosity measurements can be used to estimate not only G^* values for checking DSR results for unmodified asphalts but also the SHRP specification grade for an unclassified asphalt cement. Figure 8 compares the results of using the 60°C and 135°C viscosity data reported by the SHRP MRL to estimate the temperature at which $G^*/\sin\delta$ equals 1 kPa and the DSR-determined temperatures reported by SHRP researchers (*2*). $G^*/\sin\delta$ was estimated from the traditional viscosity data plotted on the Shell Bitumen Test Data Chart. The actual equations for the line for these plots were calculated to provide a more accurate estimate than just the graphical approach. Since δ only varied from about 81 to 89 degrees, which translated into sin δ values from 0.987 to 0.999, an assumption of sin δ equal to 1 was considered close enough for a reasonable estimate. Since the specific gravities of the asphalts were not reported in the SHRP MRL information, the kinematic viscosities were converted from centistokes to centipoise by assuming a constant specific gravity of 1.000.

Figure 8 shows that this quick approach to estimating the temperature at which a material has a $G^*/\sin\delta$ of 1 kPa is very good (r^2 = 0.87). This approach, however, tends to increasingly underestimate the temperature for increasing higher-viscosity asphalt cements. This is most likely due to the assumption of a constant 1.000 for specific gravities converting the kinematic results to poise. Generally, as the viscosity increases the specific gravity also increases; this would result in an increasing underestimation of the kinematic viscosity.

CONCLUSIONS

The following conclusions can be drawn from the results presented here:

1. Testing problems such as stiffness-related problems, plate slip, and exceeding the equipment limits can influence the quality of the reported test results. However, these problems are easily identified and corrected with changes in either the plate diameter or the specified percent strain.
2. The linear viscoelastic region of even the stiffest polymer-modified asphalt cement extended to at least 30 percent strain for temperatures as low as 58°C.
3. It appears that for test temperatures of between 4°C and about 30°C the AASHTO TP5 test parameters will have to be adjusted for polymer-modified asphalt cements. Some changes that are indicated include a reduction in the target percent strain and changes in sample preparation procedures.
4. G^* at 10 rad/sec is exactly equal to η^*. Since most asphalt cements at warmer temperatures (i.e., > 48°C) are Newtonian, their viscosities are not shear rate dependent. Hence, typical values for G^* can be approximated by measuring the viscosity of the asphalt cement with conventional vacuum tube viscometers.
5. It is not recommended that vacuum viscosities be used to estimate G^* for modified asphalts because of their distinct non-Newtonian behavior.
6. Typical δ values for unmodified and RTFO-aged asphalts ranged from about 81 to 89 degrees for test temperatures between 46°C and 64°C. These values were more dependent on the test temperature than the grade of asphalt cement.
7. Typical phase shift values for modified asphalts ranged from 60 to 81 degrees for test temperatures of between 46°C and 64°C and were dependent on the type of polymer, the source or grade of the asphalt cement, as well as the test temperature.
8. A range of sin δ from 0.987 to 0.999 appears to be reasonable for unmodified asphalt cement for test temperatures of between 46°C and 64°C. Therefore, an assumption was made that the viscosity (in poise) was equal to G^* (in kilopascals). Traditional viscosity data for 60°C and 135°C test temperatures were used along with the Shell viscosity-temperature graph to estimate the temperature at which the viscosity (i.e., $G^*/\sin\delta$) would be equal to 1 kPa (the SHRP mini-

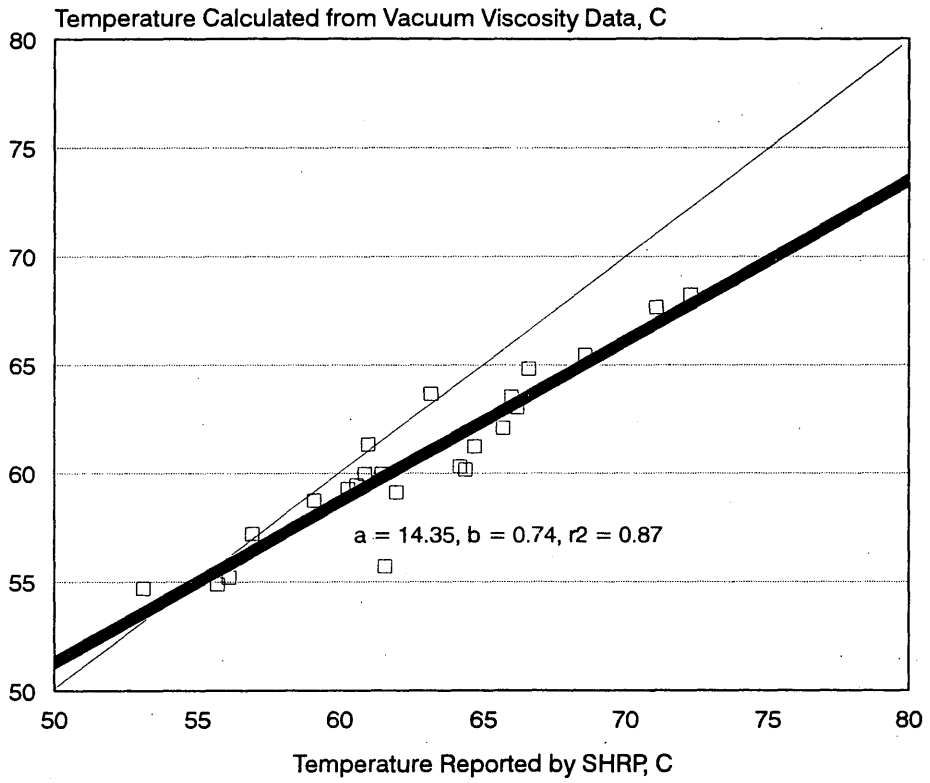

FIGURE 8 Estimating temperature at which $G^*/\sin\delta$ is equal to or greater than 1 kPa.

mum requirement for original binders). This method of estimating proved very good, with only a slight tendency to underestimate the SHRP-reported values reported for DSR results. The tendency to underestimate DSR results increased with increasing viscosity; however, the worst comparison was only 4°C too low.

ACKNOWLEDGMENTS

The authors thank FHWA for funding this research and both Roger Olson and Dave Janisch of the Minnesota Department of Transportation for technical guidance and support.

REFERENCES

1. Determining the Rheological Properties of Asphalt Binder Using a Dynamic Shear Rheometer. AASHTO Test Method TP5. AASHTO, 1993.
2. Petersen, J. C., R. E. Robertson, J. F. Branthaer, P. M. Harnsberger, J. J. Duvall, S. S. Kim, D. A. Anderson, D. W. Christiansen, and H. U. Bahia. *Binder Characterization and Evaluation,* Vol. 1. SHRP Report SHRP-A-367. SHRP, National Research Council, Washington, D.C., 1994.
3. Anderson, D. A., D. W. Christiansen, H. U. Bahia, C. E. Antle, and J. Button. *Binder Characterization and Evaluation,* Vol. 3. *Physical Characterization.* SHRP Report SHRP-A-369. SHRP, National Research Council, Washington, D.C. 1994.
4. Petersen, J. C., R. E. Robertson, J. F. Branthaer, P. M. Harnsberger, J. J. Duvall, S. S. Kim, D. A. Anderson, D. W. Christiansen, H. U. Bahia, R. Dongre, C. E. Antle, M. G. Sharma, and J. Button. *Binder Characterization and Evaluation,* Vol. 4. *Test Methods.* SHRP Report SHRP-A-370. SHRP, National Research Council, Washington, D.C., 1994.
5. Macosko, C. W., R. G. Larson, T. P. Lodge, J. Mewis, and M. Tirrell. *Rheology: Principles, Measurements and Applications.* 1994.
6. Bouldin, M. G., J. H. Collins, and A. Berker. Rheological and Microstructure of Polymer-Asphalt Blends. *Rubber Chemistry and Technology,* Vol. 64, 1991.
7. Collins, J. H., M. G. Bouldin, R. Gelles, and A. Berker. Improved Performance of Paving Asphalts by Polymer Modifications. *Journal of the Association of Asphalt Paving Technologists,* Vol. 61, 1991.

Critical Evaluation of Asphalt Modification Using Strategic Highway Research Program Concepts

HUSSAIN U. BAHIA

With the introduction of the Strategic Highway Research Program (SHRP) binder tests an evaluation of how different additives affect the critical properties of binders was conducted. Testing done as a part of several projects involved asphalt binders modified with three different types of additives: crumb rubber, polymeric additives, and mineral fillers. The testing included rheological and failure characterization at a number of different temperatures. The temperatures were selected to cover those in the climatic regions encountered in the United States and Canada. The measurements included high- and intermediate-temperature measurements with the dynamic shear rheometer at several temperatures, low-temperature creep with the bending beam rheometer, and low-temperature failure strains by the direct tension test. The need for asphalt modification is discussed, a summary of the results of that testing program is presented. The present work includes information on how these modifiers affect the rheological and failure properties at ranges of temperatures and loading frequencies that simulate application conditions. The changes in the performance-related parameters used in the SHRP specifications as a result of these modifications are also discussed. The results indicate that the proposed specification parameters are sensitive to the effects of the modifiers and that different additives can be used to alter the performance-related properties of asphalts. The results also indicate that major improvements in properties can be achieved with certain modifiers and that these improvements in properties are generally achieved at relatively high temperatures.

During the last two decades the paving industry has seen a continuous increase in the use of asphalt modifiers. Many of these modifiers have resulted in the enhanced contribution of asphalt binders to the superior performance of pavements (*1–4*). The selection of modifiers has mainly been done by conventional testing methods to meet the requirements focused around viscosity or penetration grading systems. As a result of the Strategic Highway Research Program (SHRP) a new set of testing techniques and a new grading system have been introduced (*5*). The testing and grading systems are based on measuring fundamental properties that are related in a more rational way to pavement performance.

The purpose of this paper is to discuss the need for asphalt modification, to discuss the main modification targets for paving asphalts, and to show how selected modifiers that are currently used alter the critical properties of asphalt binders. The paper includes results collected during several testing programs conducted to evaluate the roles of different modifiers in changing the rheological and failure properties of asphalt binders.

Department of Civil and Environmental Engineering, The University of Wisconsin-Madison, Wis. 53706.

ASPHALT PRODUCTION AND NEED FOR MODIFICATION

The main source of asphalt for paving applications is crude petroleum of the type with a high specific gravity. Depending on the type of refining process and the source of crude petroleum, the asphalt yield from crude petroleums can vary between 10 and 60 percent (*6*). The chemical composition of an asphalt and, as a consequence, its properties is largely dependent on the crude petroleum's nature and source.

Asphalt production, however, is not one of the main profit-generating processes in the refining industry. Most refineries in the United States deal with asphalt as a by-product of crude fractionation. The production of better-performing asphalts is not considered one of the common strategies in planning refining practices. These facts have left pavement engineers throughout the years with the challenge of selecting the suitable asphalt for their specific application conditions including climate, traffic, and pavement structure. When the asphalt that is produced does not meet the requirements, modification of the asphalt with additives has served as one of the cost-effective engineering solutions. Modification of asphalts has increased steadily within the last decade because modification provides the versatile properties needed to build better-performing roads. Asphalt modification is expected to increase in the future because of the economic barriers involved with improving asphalts through refining processes and because of the logistical difficulties of using crudes that naturally produce better-performing asphalts.

NATURE OF ASPHALT VISCOELASTIC PROPERTIES

At any combination of time and temperature viscoelastic behavior within the linear range is best characterized by two properties: (a) the total resistance to deformation and (b) the relative distribution of that resistance between an elastic part and a viscous part. By using the dynamic (oscillatory) shear loading mode, these properties can be represented by the complex modulus (G^*) and the phase angle (δ). G^* represents the total resistance to deformation under a load, whereas δ represents the relative distribution of this total response between an in-phase component and an out-of-phase component.

The rheological properties of asphalt are very sensitive to temperature and time of loading. Within the range of pavement application (temperature range of -40°C to 80°C and loading rate of static to 100 rad/sec), a typical asphalt changes its modulus by more than 7 orders of magnitude. It changes its phase angle by approximately 90 degrees.

In addition to the prefailure properties of asphalts as measured by rheology, asphalt failure properties need to be characterized. The failure behavior of asphalts is also highly dependent on temperature and time of loading. They are brittle at low temperatures, with a plateau zone showing a strain at failure that is relatively small (limiting value of approximately 1.0 percent strain). As the temperature increases a transition from brittle to ductile failure can be observed; at high temperatures this converts into a flow zone. The most critical part of this behavior for pavement applications is the temperature and loading rate at which the transition from the brittle to the ductile behavior occurs. For many unmodified asphalts there is some correlation between the stiffness measured at small strains (rheological prefailure properties) and this transition. The correlation, however, may not hold for modified asphalts or specially produced asphalts. (*7*).

ASPHALT MODIFICATION STRATEGIES AND TARGETS

For the successful modification of asphalt binders the binders should be engineered to improve one or more of the basic properties of asphalt related to one or more pavement distress modes. These properties can be classified into four main types. For each type SHRP has introduced certain response parameters that can be measured.

- Rigidity: total resistance to deformation that can be measured by complex moduli such as G^* under dynamic loading or by creep stiffness, $S(t)$, under quasistatic loading. Higher rigidity is favorable at high temperatures or low loading rates to resist rutting, whereas lower rigidity is favorable at intermediate and low temperatures to resist fatigue and thermal cracking, respectively.
- Elasticity: recovery of deformation by using the stored energy applied. It can be determined by measuring either the phase angle (δ) or the logarithmic creep rate (m). To resist rutting and fatigue damage more elasticity is favorable. To resist thermal cracking less elasticity and a greater ability to relax stress by flow are favorable.
- Brittleness: failure at low strains, which is the best definition of brittleness. To improve resistance to fatigue and thermal cracking, brittleness should be reduced by enhancing strain tolerance or ductility.
- Durability: oxidative aging, physical hardening, and volatilization, which are key durability properties. Resistance to all of these changes is favorable.

A modifier can be selected to improve one or more of these main properties. Also, different modifiers that affect different properties can be combined to improve several properties. The new test methods introduced by SHRP offer the capability of measuring each of these properties under conditions that simulate the loading and climatic conditions encountered in the field.

MATERIALS AND EXPERIMENTAL DESIGN

For the present study three types of modifiers were used: polymer, crumb rubber, and mineral fillers. Polymer modifiers included styrene-butadiene (SB)-based modifiers and polyethylene-based modifiers (PE1 to PE5). Crumb rubber modifiers (CRM) included ambient shredded crumb rubber (RB3), cryogenic grinded crumb rubber (RB2), and a crumb rubber–plastic composite (RB1). All crumb rubbers were produced from whole tire stock with a maximum particle size of 1.0 mm. Mineral fillers included manufactured quartz and natural calcite with a maximum particle size of 75 μm. The polymer modifiers were preblended by manufacturers at concentrations varying between 3 and 6 percent. The crumb rubber modifiers were mixed at 15 percent by weight of binder in the laboratory by using a blender at 160°C for 1 hr. The mineral fillers were mixed by using the same technique used for the crumb rubber. The mix proportions were kept at a ratio of 0.50 filler to asphalt by volume.

Testing of the base and modified binders included full characterization by the dynamic shear rheometer at different temperatures and frequencies. The binders were characterized by running frequency sweeps of 1 to 100 rad/sec at temperatures ranging between −30°C and 60°C. The testing geometry deviated from the standard geometry later selected for testing neat asphalts. For parallel plate geometry a 2.0−mm gap was used for all binders at high and intermediate temperatures. At temperatures below 5°C torsion bar geometry was used to cover the range of high moduli measured for the different binders.

In addition to the dynamic shear rheometer, the bending beam rheometer was used to measure creep properties at several low temperatures. Also, the direct tension test device was used to measure failure properties at low temperatures. Oxidative aging was done by using the thin film oven test (AASHTO T179) and the pressure aging vessel. No changes were made in the standard procedures for the creep, failure, and aging tests except for taking extra care to prepare specimens and to ensure the uniform dispersion of the additives. Selected data were used in this paper to present the important points observed during the study.

EFFECT OF MODIFICATION ON RHEOLOGY OF ASPHALT

Data collected by using the dynamic shear rheometer were used to develop and compare the master rheological curves of the modified binders with their base asphalts. The following discussion is divided into sections according to the type of modifier or additive used.

Polymer Modification

Figure 1 depicts the master rheological curves measured by using a dynamic shear rheometer for an asphalt before and after modification with the SB polymer at two different concentrations (c = 3 percent and $2c$ = 6 percent). Changes in both G^* and δ as a function of temperature are shown. The effects of this modifier show favorable trends of change. At high temperatures G^* is higher, whereas δ is lower. This indicates increases in rigidity and elasticity, which results in better resistance to permanent deformation. At intermediate temperatures (0°C to 30°C) lower values of G^* can be observed, whereas δ values remain indifferent. The reduction in G^* values is favorable for fatigue cracking under strain-controlled conditions, which are typical of conditions for thin pavements. At low temperatures (−20°C to 0.0°C) a more pronounced reduction is observed for G^* and a minor increase in δ is seen. Both of these effects are favorable since they make the binder less rigid and less elastic or more prone to stress relaxation under a load. The changes shown appear to improve the properties with respect to pavement performance at all temperatures. Considering the relative changes in G^*

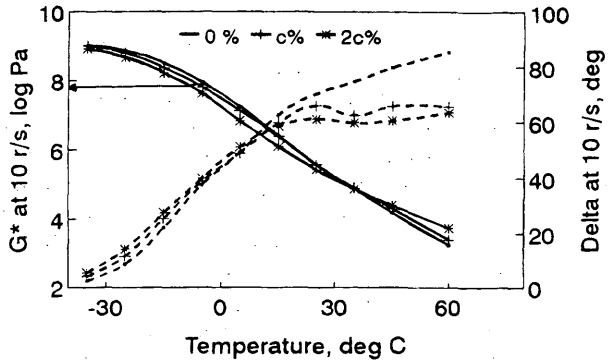

FIGURE 1 Isochronal rheological curves for an asphalt before and after SB modification.

and δ, it is evident that the main effect is the change in the rigidity of the binder as determined by measuring G^*. The data presented in Figure 1 indicate that although the G^* value is increased by 100 to 200 percent at 60°C, the δ value is reduced by approximately 16 to 30 percent. At low temperatures the same trend can be observed; the G^* value is reduced by 40 to 50 percent, whereas the δ value is increased by only few degrees. Similar trends of change were observed for the other types of polymers that were used in the study. Considering the fact that energy dissipation and the rate of relaxation of binders are functions of sin δ or tan δ, it appears that the effects of these commonly used polymeric additives on binders at small strains or stresses are mainly caused by changes in rigidity, whereas only secondary effects are caused by changes in elasticity.

CRM Modification

Figure 2 depicts master rheological curves for an asphalt before and after modification with a CRM at a 15 percent weight concentration. The data in Figure 2 are presented in terms of loading frequency rather than temperature. As discussed earlier frequency and temperature are interchangeable; the effect of high temperature corresponds to that of low frequencies and vice versa. Changes in master curves are similar to the changes observed for polymer modification shown in Figure 1. G^* values increase at low frequencies (high temperatures), whereas they decrease at intermediate and high frequencies (intermediate and low temperatures). The δ values are lower at low frequencies but higher at high frequencies. The relative changes in either parameter are of the same order of magnitude as those for the polymer modification. The effects of CRM can therefore also be described mainly as changes in the rigidity of the asphalt.

The mechanism by which CRM changes properties is, however, different. Although the polymer is dispersed in the asphalt and causes changes in the molecular structure of the asphalt, CRM is observed to keep its physical identity and to behave as a flexible particulate filler in the asphalt. The overall effect of CRM on the master rheological curve is a reduction of the dependencies of G^* and δ on frequency. This effect is similar in nature to the effect of polymer modification, despite the difference in the nature of the material. Polymer modification usually results in a more homogeneous binder that is more favorable than the nonhomogeneous CRM modification. The trade-off, however, is the relatively higher cost of the polymer modifiers compared with the cost of CRM.

Mineral Fillers

Figure 3 depicts master rheological curves for an asphalt before and after the addition of two mineral fillers. Unlike the previous modifiers the effect of mineral fillers results in increasing the G^* value and decreasing the δ value at all frequencies (temperatures). This distinct change is expected because of the rigid nature of the mineral fillers. Although some polymers and CRMs have moduli that are lower than those of typical asphalts at low or intermediate temperatures, mineral fillers have moduli that are much higher than those of asphalts. This is true even at very low temperatures where asphalts reach their glassy modulus. Furthermore, since mineral fillers lack the viscoelastic nature, they do not impart any significant changes in δ. The upward shift in the G^* curves seen in Figure 3 is simply the effect of the addition of these rigid particles that increases the moduli at all temperatures. The increase is larger at high temperatures (low frequencies), at which the asphalt moduli are lower. The effect at low temperatures (high frequencies) is not favorable since it indicates an increase in modulus and a decrease in the ability of relaxing stresses. At high temperatures the effect is favorable and, for the fillers shown, much more pronounced than the effect for the modifiers considered earlier.

One of the similarities between the effects of fillers and the other modifiers is the reduction in the dependency of G^* and δ on

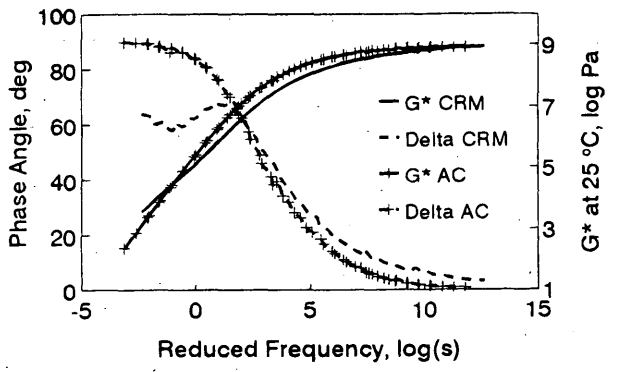

FIGURE 2 Master rheological curve for an asphalt before and after CRM modification (15 percent CRM).

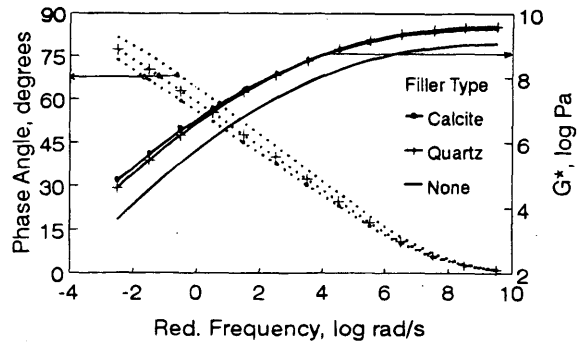

FIGURE 3 Master rheological curves for an asphalt before and after addition of mineral.

temperature or loading frequency. Also, it is evident that the rheological behaviors of binders with fillers as well as the two other modifiers remain relatively simple in nature. At low temperatures a glassy modulus asymptote is reached, at which the response is mainly elastic, and at high temperatures a viscous asymptote is reached, at which behavior is mainly if not completely viscous.

EFFECTS OF MODIFICATION ON FAILURE PROPERTIES

By using the direct tension test developed by SHRP the binders modified with the different additives were tested at temperatures ranging between −30°C and 0.0°C. The tests were conducted at a deformation rate of 1.0 mm/min in three replicates, and the stress and strain at failure were calculated. To evaluate the effects of the modifiers the failure stress and failure strain values of the base and the modified binders are compared.

Polymer Modification

Figure 4 shows strain-at-failure and stress-at-failure plots as a function of temperature for an asphalt before and after modification with 3 and 6 percent SB-based polymer. The strain curves show that the polymer increases the strain at failure within the brittle and the brittle–ductile zone but converge to the same values as the flow zone is approached. The effect can be considered to be shifting the strain-at-failure curve horizontally to lower temperatures without significantly changing the shape of the curve. The effect of polymer addition is favorable because it tends to increase the strain at failure within the critical region. The results also indicate that the effect is more favorable with higher concentrations of the polymer. The stress-at-failure curves are similar for all binders, which indicates that use of the polymer does not result in significant changes in the strengths of the binders.

The results shown in Figure 4 may not apply to all types of polymer modifiers. The effects of different polymers on failure properties are expected to depend largely on the type of interaction between the asphalt and the polymer, on the molecular nature of the polymer additives, and on the way the polymer is dispersed in the asphalt. The effects of polymers on failure properties can be hypothesized in different ways. One hypothesis is that polymers form some kind of molecular network inside the asphalts, resulting in more strain-tolerant material. Another hypothesis is that the dispersed polymer particulates may serve as reinforcements, arresting microcrack propagation and increasing the toughness of the binders. The typical trend observed from a review of polymer modification work, however, is that not many of the currently used polymers improve low-temperature failure properties. This may be attributed to the fact that there has been no simple technique that can be used to measure the brittle failure of asphalt. It can also be attributed to the fact that none of the binder specifications that are now used addresses the brittleness of asphalt in a rational and fundamental form. These issues did not encourage many polymer modifier producers to concentrate on designing a modifier to mainly enhance low-temperature failure properties.

CRM Modification

Figure 5 depicts failure plots for an asphalt before and after modification with crumb rubber at concentrations of 10 percent (CRM1) and 20 percent (CRM2) by weight of total binder. The effect of the CRM modification is similar to that of the polymer modification with respect to the strain-at-failure values; higher strains are observed at low temperatures, but similar strains are observed as the flow region is reached by the binders. The effect also represents a shift of the failure curve along the temperature scale toward lower temperatures. The shift is larger for the higher CRM content. The stress-at-failure curves for the CRM modification, however, show a trend different from that for the polymer modification. The CRM

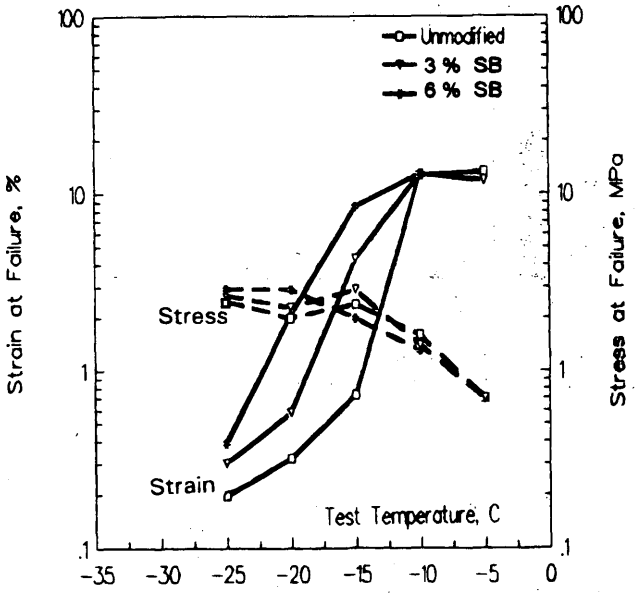

FIGURE 4 Failure strain isochronal curves for an asphalt before and after SB modification.

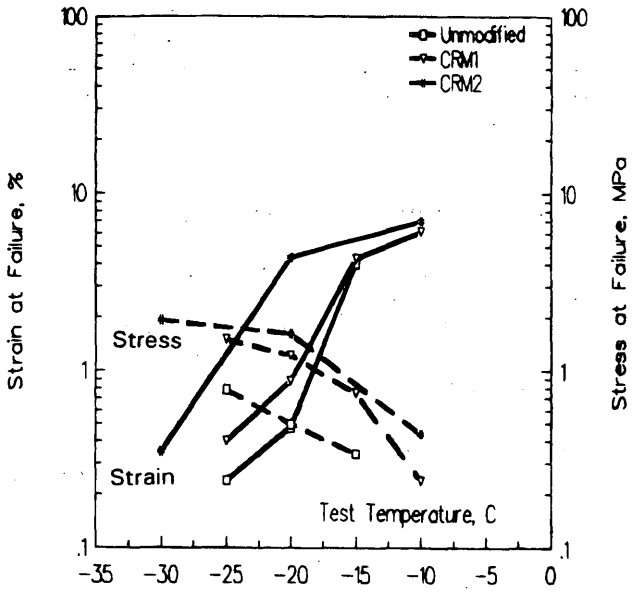

FIGURE 5 Failure strain isochronal curves for an asphalt before and after CRM modification.

modification results in stress values that are significantly higher than those for unmodified asphalt at all temperatures. This behavior can be attributed to the reinforcing effect of the rubber particles. The crumb rubber particles do not dissolve in asphalt; the particles maintain their integrity and tend to swell in asphalts, resulting in effective volumes that are larger than their initial volume (*8–10*). It is speculated that the swelling results in the selective absorption or adsorption of certain components of the asphalt. Such interactions are expected to reinforce the matrix of the binder and result in higher strength, as observed in Figure 5. The increases in strain and stress at failure are favorable for paving-grade asphalts, particularly when they are accompanied by a reduction in stiffness, as shown in Figure 2.

Mineral Fillers

Limited data were collected for the failure properties of asphalts modified with mineral fillers. The data, discussed in a later section, show significant increases in strain at failure at all temperatures. The data also show equal or higher stress-at-failure values. Although the fillers may be considered less reactive with asphalt than the other additives, their presence appears to result in an important reinforcing effect. From a fracture mechanics consideration the fillers may serve to arrest cracks or result in longer crack paths. From the limited data that have been collected, however, it appears that the improvements are highly dependent on asphalt type and test temperature. Because of the different natures of mineral fillers, their effects continue to be important even within the ductile flow region. The rigid filler particles are expected to enhance resistance to flow within the ductile region and to increase the peak stress and strain under these conditions.

EFFECT OF MODIFICATION ON SHRP GRADING PARAMETERS

The research efforts of the SHRP binder program have resulted in the introduction of several response parameters that are indicators of the contribution of binders to pavement performance. Three failure modes were identified as critical pavement distress modes in which the binder plays an important role: rutting, fatigue cracking, and thermal cracking (*11*).

Effect of Polymers on SHRP Parameters

Figure 6 depicts the ratios of the SHRP parameters. The ratios represent the relative changes in parameters for an asphalt after modification with the SB-based polymer at three concentrations. The data in Figure 6 indicate that there is a favorable trend in the changes of all performance parameters: $G^*/\sin\delta$ ratios range between 1.2 and 3.4, indicating a favorable increase in the value of the parameter. $G^*/\sin\delta$ ratios range between 0.1 and 0.5, and $S(60)$ ratios range between 0.25 and 0.5, indicating favorable decreases in both of these parameters. The ratios for $m(60)$ range between 1.1 and 1.2, which is a limited but favorable increase. For this class of polymers the modification is also extended to the strain at failure, which has ratios of between 3.4 and 6.0.

Figure 7 depicts the ratios of SHRP parameters for five types of polyethylene-based polymers (PE1 to PE5). At the high temperatures the $G^*/\sin\delta$ ratios show favorable values ranging between 2.2 and 6.3. At intermediate and low temperatures, however, the ratios of $G^*\sin\delta$, $S(60)$, and $m(60)$ do not show significant changes, and for some of these polymers an unfavorable change can even be seen. The strain at failure also shows only minor changes.

The data shown in Figures 7 and 8 indicate that polymer modification can have major effects on the rutting parameter at high tem-

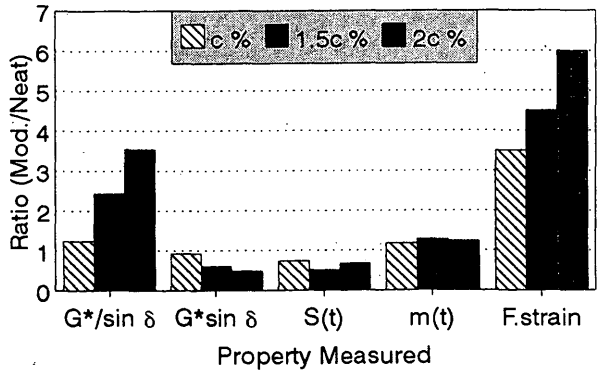

FIGURE 6 Relative change in SHRP performance-related parameters after modification with SB-based modifiers (c = 3 percent).

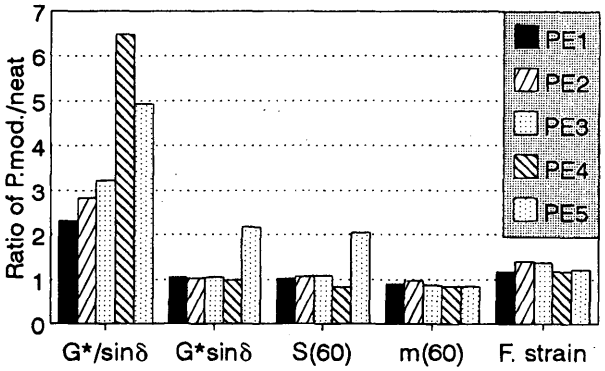

FIGURE 7 Relative change in SHRP performance-related parameters after modification with polyethylene-based modifiers.

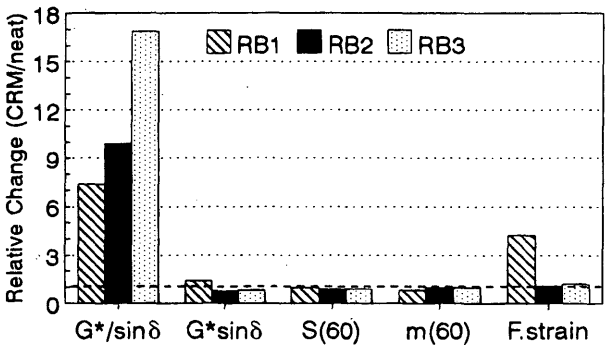

FIGURE 8 Relative change in SHRP performance-related parameters after modification with CRM.

peratures. The changes in the parameters related to fatigue cracking and thermal cracking are, however, relatively small except for the strain at failure for the SB-based modifier. The effects on strain at failure should not be exaggerated; Figures 4 and 5 indicate that strain at failure is very sensitive to temperature, and the transition from brittle to ductile failure occurs over a narrow temperature range. Thus, a minor shift in the strain curve as a result of modification may show very high strain ratios. The conclusion that can be drawn here is that the polymer modification appears to be very effective at high temperatures but may have limited effects at intermediate and low temperatures. The trend observed in the present study agrees with previous experience reported for polymers (*12,13*).

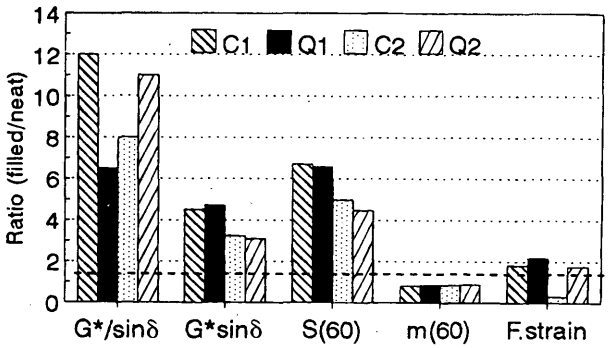

FIGURE 9 Relative change in SHRP performance-related parameters after addition of mineral fillers.

Effect of Crumb Rubber on SHRP Parameters

Figure 8 depicts bar charts for the CRMs used in the study similar to those in Figure 7 for polyethylene based polymers. The difference between the CRMs used is the process by which they are manufactured. The parameters' ratios show the same trend as the polymer modification (Figures 6 and 7), but they differ in magnitude. The ratios for the rutting parameter ($G^*/\sin\delta$) are higher than those for the polymer modification, whereas the ratios for the fatigue parameter ($G^* \sin\delta$) are lower. $S(60)$ ratios are also lower, whereas the ratios of $m(60)$ and strain at failure are very close to 1.0 (no change). The data in Figure 8 indicate that, similar to polymer modification, crumb rubber modification shows its main effects at high temperatures. This is expected because of the nature of the CRMs. Crumb rubber acts mainly as a flexible filler. At high temperatures it is stiffer than the asphalt and thus contributes significantly to the increased moduli. With decreasing temperatures the asphalt becomes stiffer, whereas the properties of the crumb rubber do not change significantly. At a certain temperature the asphalt may become stiffer than the crumb rubber, and thus, a reduction in stiffness can be observed for the modified binder. Crumb rubber at moderate concentrations that are used in practice (10 to 20 percent), however, cannot reduce the stiffness by large margins because of its own relatively high stiffness at low temperatures. It is therefore expected that the main effects of crumb rubber remain to be seen at higher temperatures and to affect mainly the rutting parameter.

Effect of Mineral Fillers on SHRP Parameters

Figure 9 depicts ratios for two asphalts after modification with two types of fillers. Ratios of $G^*/\sin\delta$ range between 6.5 and 12 for a filler volume concentration of 50 percent. The increases in $G^*/\sin\delta$ are favorable and indicate that the addition of mineral fillers can increase the contribution of binder to resistance to pavement rutting. The ratios of $G^* \sin\delta$, however, do not show a favorable trend; ratios of 3.1 to 4.7 are shown, which indicate that fillers can be detrimental with respect to fatigue damage under strain-controlled loading conditions. The effects are even more detrimental with respect to low-temperature properties; $S(60)$ ratios range between 4.5 and 6.7, and $m(60)$ ratios are all less than 1.0. Strain ratios show some improvements for certain combinations, but a value of 0.3 is shown for one of the modified binders. As mentioned earlier fillers are not expected to modify intermediate- and low-temperature properties, for which a softer binder is more favorable. Mineral fillers are rigid particles with stiffness values that far exceed those of conventional asphalt cements, even at very low temperatures. They are therefore expected to always result in stiffer binders that may not meet the needs for paving applications.

SUMMARY OF FINDINGS

In the present study the effects of polymeric additives, crumb rubber additives, and mineral fillers on the performance-related properties of asphalt cements have been analyzed by using data collected for a number of binders. The analysis included rheological and failure properties measured by using new characterization techniques developed by SHRP. The findings were as follows.

1. Polymer modification of paving-grade asphalts can result in improved rheological and failure properties. The effects are highly dependent on asphalt properties and polymer type. The polymer modifiers reduce the sensitivity of rheological properties (G^* and δ) to temperature and loading frequency. The main effects are observed at high temperatures (low frequencies), at which the polymers result in a higher stiffness and a lower phase angle. At intermediate and low temperatures the effects are less pronounced and can be unfavorable.
2. Crumb rubber modification has effects similar to those of polymer modification. The improvement at high temperatures can be higher than the levels normally achieved by polymers. CRMs also result in a reduction in the dependency on temperature and loading frequency. Effects at intermediate and low temperatures are small but favorable, depending on the properties of the asphalt. CRMs remain as particulates after mixing with asphalts. They mainly function as interactive fillers.
3. Mineral fillers also reduce the dependency of asphalt rheology on temperature and loading frequency. However, they result in increased stiffness at all temperatures and frequencies. This indicates that although their effects at high temperatures are favorable, their effects at intermediate and low temperatures are not favorable and can be detrimental with respect to fatigue and thermal cracking.
4. By using the performance parameters introduced by SHRP, the effects of the different additives on the contribution of binders to resistance to distress mechanisms can be summarized as follows:

- Rutting resistance. Polymers, crumb rubbers, and mineral fillers result in significant increases in G^* and decreases in $\sin\delta$.

These effects are favorable for rutting resistance because they indicate higher levels of resistance to total deformation under a load and a higher elasticity of response.

- Resistance to fatigue damage. Polymers and crumb rubbers can result in marginal improvements by reducing G^* and sin δ. These effects are considered favorable because they indicate a softer and more elastic response. Such a response results in less energy dissipated under strain-controlled fatigue. Mineral fillers, however, result in significantly higher G^* values, which is not favorable for strain-controlled fatigue.
- Thermal cracking resistance. Certain polymers result in lower $S(t)$ values, higher $m(t)$ values, and higher strains at failure. Such favorable effects were not observed for all polymers evaluated in the present study. Crumb rubbers generally have $S(t)$ values that are less than the $S(t)$ values of most conventional asphalts at critical low temperatures. They can therefore result in a reduction in $S(t)$ values. The effects of crumb rubber on $m(t)$ are not significant. Crumb rubbers are observed to cause significant increases in strain at failure and stress at failure. Mineral fillers are not expected to have favorable effects on thermal cracking resistance; higher $S(t)$ and low $m(t)$ values were observed for all systems tested in the present study. Mineral fillers can, however, increase the strain at failure and stress at failure, depending on the properties of asphalt and filler characteristics.

ACKNOWLEDGMENTS

This work was supported by SHRP and by a grant from the Ben Franklin Technology Center of Pennsylvania. The author expresses gratitude for that support. The assistance of the staff of the Pennsylvania Transportation Institute in performing the SHRP binder characterization and the assistance of David Anderson are acknowledged. The assistance of Koch Materials Company and TYREPLEX Corporation in providing the modified binders or the modifiers is appreciated.

REFERENCES

1. Terrel, R. L., and J. A. Epps. *Using Additives and Modifiers in Hot Mix Asphalt.* QI Series 114. National Asphalt Pavement Association Riverdale, Md., 1989.
2. Button. J. W., D. N. Little, Y. Kim, and J. Ahmed. Mechanistic Evaluation of Selected Asphalt Additives. *Journal of the Association of Asphalt Paving Technologists,* Vol. 56, 1987, p. 62.
3. Goodrich, J. L. Asphalt and Polymer Modified Asphalt Properties Related to Performance of Asphalt Concrete Mixtures. *Journal of the Association of Asphalt Paving Technology,* Vol. 57, 1988.
4. King, G. N., et al. Influence of Asphalt Grade and Polymer Concentration on the Low Temperature Performance of Polymer Modified Asphalt. *Journal of the Association of Asphalt Paving Technologists,* Vol. 62, 1993.
5. Anderson, D. A, D. W. Christensien, and H. U. Bahia. Physical Properties of Asphalt Cements and the Development of Performance-Related Specifications. *Journal of the Association of Asphalt Paving Technologists,* Vol. 60, 1991, p. 437.
6. Roberts, F. L., et al. *Hot Mix Asphalt Materials, Mixture Design, and Construction* NAPA Education Foundation, Lanham, Md., 1991.
7. Anderson, A. A., D. W. Christensen, H. U. Bahia, R. Dongre, M. G. Sharma, and J. Button. *Binder Characterization and Evaluation,* Vol. 3. *Physical Characterization.* Report SHRP-A-369. Strategic Highway Research Program, National Research Council, Washington, D.C. 1994.
8. Bahia, H. U., and R. Davies. Effect of Crumb Rubber Modifiers (CRM) on Performance Related Properties of Asphalt Binders. *Journal of the Association of Asphalt Paving Technologists,* Vol. 63, 1994.
9. Oliver, J. W. H. Optimizing the Improvements Obtained by the Digestion of Comminuted Scrap Rubbers in Paving Asphalt. *Proc., Association of Asphalt Paving Technologists,* Vol. 51, 1982, p. 169.
10. Chehoveits, J. G., R. L. Dunning, and G. R. Morris. Characteristics of Asphalt-Rubber by the Sliding Plate Microviscometer. *Proc., Association of Asphalt Paving Technologist,* Vol. 51, 1982, p. 240.
11. Anderson, D. A., and T. W. Kennedy. Development of SHRP Binder Specification. *Journal of the Association of Asphalt Paving Technologists,* Vol. 62, 1993, p. 481.
12. Collins, J., M. G. Bouldin, R. Gelles, and A. Berker. Improved Performance of Paving Asphalts by Polymer Modification. *Journal of the Association of Asphalt Paving Technologists,* Vol. 59, 1990.
13. King, G. N., et al. Influence of Asphalt Grade and Polymer Concentration on the High Temperature Performance of Polymer Modified Asphalt. *Journal of the Association of Asphalt Paving Technologists,* Vol. 61, 1992.

Rheological Properties of Chemically Modified Asphalts

N. SHASHIDHAR, S. P. NEEDHAM, AND BRIAN H. CHOLLAR

Asphalt chemically modified with furfural and furyl acrolein was performance graded (PG), and its performance was predicted according to the criteria developed by the Strategic Highway Research Program (SHRP). These asphalts were aged in a thin film oven, a rolling thin film oven, and a pressure aging vessel to investigate the aging behaviors of the chemically modified asphalts. The rheological properties were determined from 10°C through 70°C by the dynamic shear rheometer and from −25°C through −5°C by the bending beam rheometer. By using the SHRP criteria chemical modification was shown to increase the temperature range over which the asphalt can be used by primarily increasing the high-temperature stiffness of the asphalt. Differences in properties and PG grading were observed when the asphalts were aged in a rolling thin film oven compared with that when they were aged in the thin film oven, especially for the modified asphalts. The resistance to rutting was predicted to increase with chemical modification. The resistance to fatigue was predicted to change insignificantly at the range of temperatures considered in the PG specifications. The low-temperature properties were not significantly affected because of modification.

Conventionally refined asphalts have been modified by various means to extend the temperature range at which they can be used. These modifications have been made through the addition of rubber-related products and polymers and through chemical modification. Researchers at FHWA have been investigating the modification of asphalts by chemicals such as maleic anhydride, chromium trioxide, and furfural (*1*). Among these modifiers furfural-modified binders showed better adhesion to aggregate and less temperature susceptibility (of viscosity), especially at low temperatures. Consequently, further research was performed on furfural modification to study the effects of certain reaction variables on the physical properties of the products of the chemical reaction between asphalt and furfural (*2,3*). From that study the conditions for the method of preparation of an AC-20-modified asphalt from an AC-5 asphalt and furfural were obtained. Subsequent research at FHWA (*2–4;* this study) used this method to prepare AC-20 or higher asphalt cement (AC)-grade modified asphalts with furfural and AC-5 or AC-10 asphalts. Since Strategic Highway Research Program (SHRP) binder testing was not fully developed when those studies (*2–4*) were performed, there has been little effort to optimize the furfural reaction according to the performance criteria used in the performance-graded (PG) grading.

The nature of the reaction of furfural with asphalt was studied by using partial furfural analogs such as furyl acrolein, furan, allyl alcohol, and furanone (*3*). The results indicated that the furan ring was the principal component in producing modified asphalts with increasing stiffness at high temperatures, and furan with or without a conjugated aldehyde group was important in improving the low-temperature properties. Memon and Chollar (*4*) showed that the furfural reacts with the phenolic groups in the asphalt by a condensation reaction in the presence of an acid catalyst. Initially, the rheological properties of the chemically modified asphalts were evaluated primarily by traditional methods such as penetration at 10°C and 25°C and viscosity at 60°C and 135°C. In addition, a dynamic shear rheometer equipped with a cup and stepped plate geometry was also used to characterize the rheology of unaged reaction products (*1,2*).

Anderson and Kennedy (*5*) presented new criteria for evaluating the distress modes that were developed by SHRP for the new binder specifications. These performance criteria were based on the fundamental properties of properly aged asphalt binders measured at the appropriate distress temperatures. At the beginning of the study SHRP had recommended that either the thin film oven test (TFOT) or the rolling thin film oven test (RTFOT) be used for specification purposes. The AASHTO provisional specifications later adopted the RTFOT aging procedure for the performance grading of asphalt binders (*6*).

The objectives of the present study were threefold: to evaluate the benefits of chemical modification on the predicted performance based on the SHRP criteria, to understand the effect of chemical modification on the rheological properties of asphalts, and to study the aging characteristics of chemically modified asphalts.

BACKGROUND

The PG grading system evaluates the resistance of an asphalt to the primary distress modes in the pavements: rutting, fatigue cracking, and low-temperature cracking. This information is then used to define a climate range based on the temperature at which the asphalt can be used for a designed period of time without causing the pavement to fail. Certain rheological parameters were chosen to evaluate the resistance of the asphalt to these distress modes (*5*). In this section the basis for the selection of these rheological parameters, as available in the literature, are summarized.

Rutting

Rutting of flexible pavements is effectively the total permanent deformation accumulated in the pavements due to the repeated application of loads (*5,7*). Since the pavements rut because of plastic deformation, one approach to quantifying the rutting behavior would be to look at the energy dissipated (as plastic deformation, among other mechanisms) during each loading cycle under stress-controlled conditions. This work dissipated in a loading cycle is given by (*7*)

FHWA, HNR-20, 6300 Georgetown Pike, McLean, Va. 22101.

$$W_c = \pi \sigma_0 \epsilon_0 \sin(\delta) \quad (1)$$

where

σ_0 = maximum stress amplitude,

ϵ_0 = maximum strain amplitude, and

δ = loss angle.

For a stress-controlled loading ϵ_0 can be substituted with σ_0/G^*, where σ_0 is the applied stress and G^* is the complex shear modulus, to obtain

$$W_c = \pi \sigma_0^2 \left[\frac{1}{G^*/\sin(\delta)} \right] \quad (2)$$

Equation 2 relates the work dissipated per loading cycle, a measure of rutting, to $G^*/\sin(\delta)$, the parameter used in the specification. In another variation Bouldin (*8*) related the loss compliance J'' to the total accumulated deformation as follows:

$$\frac{1}{J''} = \frac{\sigma_0}{y_{acc}} = \frac{G^*}{\sin(\delta)} \quad (3)$$

where y_{acc} is the accumulated strain. In either case the greater the $G^*/\sin(\delta)$, the lower the tendency of the pavement to rut. Since a pavement is most susceptible to rutting soon after it is laid down, the specifications call for a minimum $G^*/\sin(\delta)$ for short-term-aged asphalt at the maximum temperature for which the pavement is designed.

Fatigue

Fatigue cracking of pavements occurs under repeated application of loads of magnitudes far less than the fracture strength. The current criterion for fatigue cracking specification is based on a measure of the total dissipated energy, which includes the energy expended in propagating cracks in the pavement (*9*). Under a strain-controlled loading, typical for a thin pavement layer, the dissipated work per cycle W_c is given by (*5*)

$$W_c = \pi \sigma_0 \epsilon_0 \sin(\delta) \quad (4)$$

where ϵ_0 is the strain amplitude applied, or

$$W_c = \pi \epsilon_0^2 [G^* \sin(\delta)] \quad (5)$$

since σ_0 is equal to $G^*\epsilon_0$ (*5*). Thus, the tendency of the asphalt pavement to crack because of fatigue is related to the loss shear modulus G'', which is equivalent to $G^* \sin(\delta)$. At higher values of G'' there is an increased tendency for the pavement to crack because of fatigue. The SHRP specification limits the G'' for pressure aging vessel (PAV)-aged asphalts to 5 MPa at a temperature 4°C above the midpoint between the highest and the lowest design temperatures of the pavement.

Low-Temperature Cracking

The low-temperature cracking tendency in pavements is evaluated by two independent tests: the direct tension test and the bending beam rheometer test. The strain at failure at a 1-mm/min loading rate (as determined by the direct tension procedure) is a direct measure of the failure properties of asphalt. However, for asphalt the strain to failure is related to the stiffness (*5*), leading to the concept of a limiting stiffness (when pavement will crack) and a limiting stiffness temperature (when the pavement will attain the limiting stiffness). As the stiffness of asphalt increases at low temperatures the tendency of asphalt pavements to crack increases. The stiffness of asphalt at a 60-sec loading time was measured on a bending beam rheometer.

EXPERIMENTAL

An Alaskan North Slope asphalt with the SHRP designation AAV was used as the base asphalt. This asphalt was reacted with furfural and furyl acrolein in the presence of a catalyst to yield an AC-20 asphalt with furfural modification and an AC-30 asphalt with furyl acrolein modification (*2*). These products were coded FUM for the furfural-modified asphalt and FAM for the furyl acrolein-modified asphalt. The various asphalts tested and the characterization techniques used are summarized in Table 1.

The asphalts were aged by standard TFOT and RTFOT procedures and in a PAV according to the AASHTO provisional standard procedure (*10*). The complex modulus and the loss tangent for all of the asphalts were measured with a dynamic shear rheometer (DSR) (Model RDA-II; Rheometrics, Inc. Piscataway, New Jersey) at temperatures of 10°C, 20°C, 30°C, and 40°C with an 8-mm parallel plate geometry and at 40°C, 50°C, 60°C, and 70°C with a 25-mm parallel plate geometry by the procedure in the AASHTO pro-

TABLE 1 Asphalts, Aging Treatments, and Tests Conducted

	AAV	FUM	FAM
Unaged	DSR	DSR	DSR
TFO aged	DSR	DSR	DSR
RTFO aged	DSR	DSR	DSR
TFO-PAV aged	DSR, BBR	DSR, BBR	DSR, BBR
RTFO-PAV aged	DSR, BBR	DSR, BBR	DSR, BBR

All dynamic shear rheometer (DSR) measurements were made at 10, 20, 30 and 40°C with 8 mm parallel plate and at 40, 50, 60 and 70°C with 25 mm parallel plate geometry.
All bending beam rheometer (BBR) measurements were made at -5, -15 and -25°C

TABLE 2 PG of Chemically Modified Asphalts

		TFOT BASED			RTFOT BASED		
	Specification limits	AAV	FUM	FAM	AAV	FUM	FAM
Tank							
G*/sin(δ)	Min: 1000 Pa	56.5	67.0	67.0	56.5	67	67
TFOT/RTFOT Residue							
G*/sin(δ)	Min: 2200 Pa	55.0	67.0	64.0	58	62.5	61
PAV Residue							
G*.sin(δ)	Max: 5000 kPa	17.5	17.5	16.0	16	19	19
S(60)	Max: 300 MPa	-19.0	-20.0	-20.0	-18	-18	-18
m(60)	Min: 0.3	-18.0	-18.0	-19.0	-19	-18	-17
PG GRADE		**52-28**	**64-28**	**64-28**	**52-28**	**58-28**	**58-22**
Continuous grade		55-28	67-28	64-29	57-28	63-28	61-27
Useful temperature range		83	95	93	85	90	88

Useful temperature range is the temperature range in which the asphalts can be used and is the difference between the upper and lower limit temperatures. For example, for PG 55-28 (in the continuous grade) the useful temperature range is 55-(-28)=83

visional specifications (*11*). For each measurement three repetitions (three separate samples from a single reaction) were made and averaged. All DSR measurements reported in this paper were measured at 10 rad/sec unless stated otherwise. The flexural creep stiffnesses of the PAV-aged asphalts were measured at temperatures of −5°C, −15°C, and −25°C with a bending beam rheometer (Cannon Instruments, State College, Pennsylvania). A constant load of 100 g was applied, and the deflection was recorded as a function of time. The creep stiffnesses and the slope of the logarithm of creep stiffness–logarithm of time curve (*m*-value) at 60 sec were measured according to the procedures described in the AASHTO provisional specification (*12*).

RESULTS AND DISCUSSION OF RESULTS

Table 2 gives the SHRP PG grading (*6*) of these asphalts as determined by both the TFOT and RTFOT procedures for short-term aging. The differences between PG for these asphalts were determined by the TFO and RTFO aging techniques. For AAV the PG was 52–28 when both TFOT and RTFOT procedures were used. In the case of furfural- and furyl acrolein-modified asphalts, the TFO route graded PG 64−, whereas the RTFO route graded PG 58− because of factors discussed later. The low-temperature limit for all asphalts was unchanged after RTFO aging except for the furyl acrolein-modified asphalt. This change was primarily due to the lower *m*-value for this asphalt.

Effect on Rutting Characteristics

Figure 1 shows the isochronal curve for $G^*/\sin(\delta)$ at 10 rad/sec illustrating the effect of modifications for the unaged and TFO- and RTFO-aged asphalts. Each datum point in the curve is an average of three independent measurements, with the error bars denoting ± 1 standard deviation. The modification caused a substantial increase in $G^*/\sin(\delta)$ over the entire temperature range for the unaged asphalts. The difference in $G^*/\sin(\delta)$ between the furfural- and furyl acrolein-modified asphalts was not significant. In the case of TFOT residues, the increase in $G^*/\sin(\delta)$ due to modification was significant, but it was not as dramatic as that for the unaged asphalts. Also, the increase in $G^*/\sin(\delta)$ was greater at higher temperatures. For RTFOT residues the increase in $G^*/\sin(\delta)$ due to chemical modification was reduced even further. Also, the furfural-modified

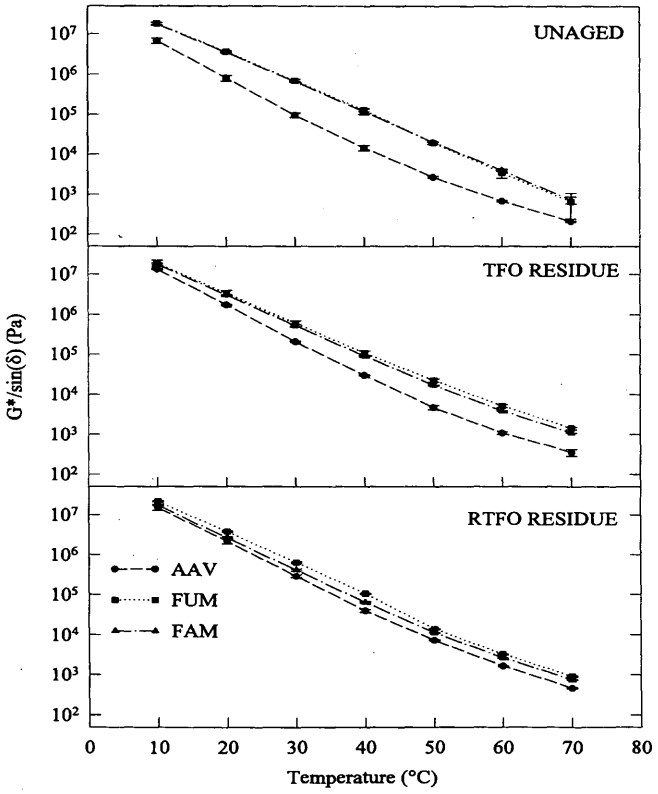

FIGURE 1 Effect of modification on $G^*/\sin(\delta)$ for unaged and short-term-aged asphalts.

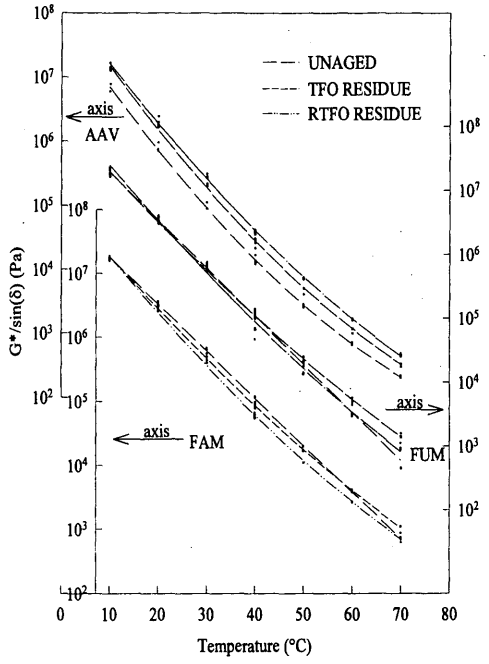

FIGURE 2 Effect of short-term aging on $G^*/\sin(\delta)$ of unmodified and modified asphalts.

product had a significantly higher $G^*/\sin(\delta)$ value than the furyl acrolein-modified product.

From the same data the effect of aging the asphalts by the TFO and RTFO methods can also be studied. Such a study will yield information on the rheological nature of the modified asphalts. In Figure 2 the isochronal curves from Figure 1 are grouped by asphalts to enable an analysis of the effects of aging. In Figure 2 the three measurements that made up the average $G^*/\sin(\delta)$ at a given temperature (Figure 1) were plotted as separate datum points and were fitted with a second-order polynomial (shown in Figure 2). Such a fit will also take the measurement error into consideration to better estimate the significance of the observed changes. Each of the curves in Figure 2 had a regression coefficient greater than 0.997, indicating a good fit. For the unmodified asphalt aging shifts the curve toward a higher $G^*/\sin(\delta)$ value without changing its shape significantly. In the case of furyl acrolein-modified asphalts the shape of the isochronal curve for the unaged asphalt is markedly different from that of the aged asphalt. The curvature of the curve for the unaged asphalt was much less than that of the curves for aged asphalts. Consequently, at temperatures of about 30°C and 40°C, the TFO- and RTFO-aged samples had $G^*/\sin(\delta)$ values significantly lower than those for the unaged asphalt. Such a difference in the shapes of the curves suggests that the unaged furyl acrolein-modified asphalt has properties rheologically different from those of the unmodified asphalts. However, the aged furfural- and furyl acrolein-modified asphalts behave similarly to the unmodified asphalt. Furfural-modified asphalt also shows a similar behavior, but it is not as definitive as that of the furyl acrolein-modified asphalt.

Since the asphalts are in the PG 52- through PG 64- grade range, it is useful to compare the $G^*/\sin(\delta)$ values at 60°C for these asphalts, as illustrated in Figure 3. For the unmodified asphalt,

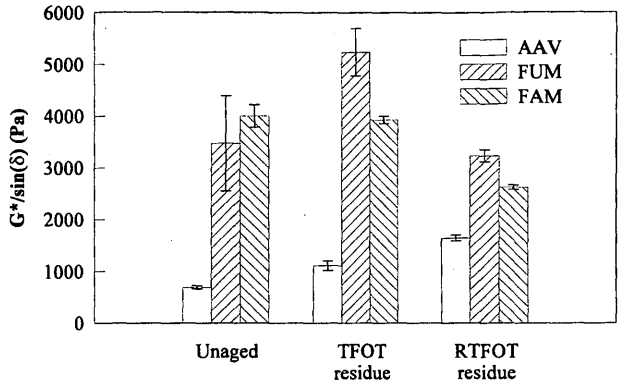

FIGURE 3 Effect of short-term aging on $G^*/\sin(\delta)$ at 60°C for unmodified and modified asphalts.

$G^*/\sin(\delta)$ increases from unaged to TFO-aged to RTFO-aged, in that order. This observation is consistent with the conclusions of Zupanick (*13*), who has shown the RTFOT to have a more severe aging effect than TFOT on asphalts. However, in the case of the furfural-modified asphalt, the $G^*/\sin(\delta)$ values for the RTFO residues were comparable to those for the unaged samples, whereas the TFO residues had $G^*/\sin(\delta)$ values higher than those for the unaged samples. In the case of furyl acrolein-modified samples, $G^*/\sin(\delta)$ values for TFO-aged samples remained essentially unchanged compared with the value for unaged samples, whereas they decreased for RTFO-aged samples aging.

One can interpret these observations as being two mechanisms that are operating during aging and that are trying to affect $G^*/\sin(\delta)$ in an opposite manner. One mechanism is the normal aging characteristics, which tend to increase $G^*/\sin(\delta)$ as the severity of aging increases. The other mechanism decreases $G^*/\sin(\delta)$ as the severity of aging increases. The combined actions of these two mechanisms could lead to the behavior observed in Figure 3. Similar observations can be made by examining the data in Table 2 for the temperatures at which the asphalt meets the specification. These temperatures for AAV are 56.5°C, 55.0°C, and 58.0°C for unaged, TFOT-aged, and RTFOT-aged asphalts, respectively. For the furfural-modified asphalt the corresponding temperatures are 67.0°C, 67.0°C, and 62.5°C, and for the furyl acrolein-modified asphalts they are 67.0°C, 64.0°C, and 961.0°C.

It is unknown what mechanism could be operating to decrease the $G^*/\sin(\delta)$ values for asphalts during short-term aging. Perhaps one of two things could be happening. The modification reaction products may be unstable when they are heated and partially break down to smaller molecules that volatilize upon heating. On the other hand the reaction could be reversible at high temperatures, causing the chemical modification to partially reverse into asphalt and furfural, and the latter then volatilizes, causing a decrease in $G^*/\sin(\delta)$. The loss of $G^*/\sin(\delta)$ for the furyl acrolein-modified asphalt is more than that for the furfural-modified asphalts.

Effect on Fatigue

Figure 4 shows the isochronal curves of $G^*/\sin(\delta)$ (or G'') at 10 rad/sec, which were used to study the effects of modifications under various aging conditions. G'' increased on modification except at the lower temperatures. At temperatures below 25°C,

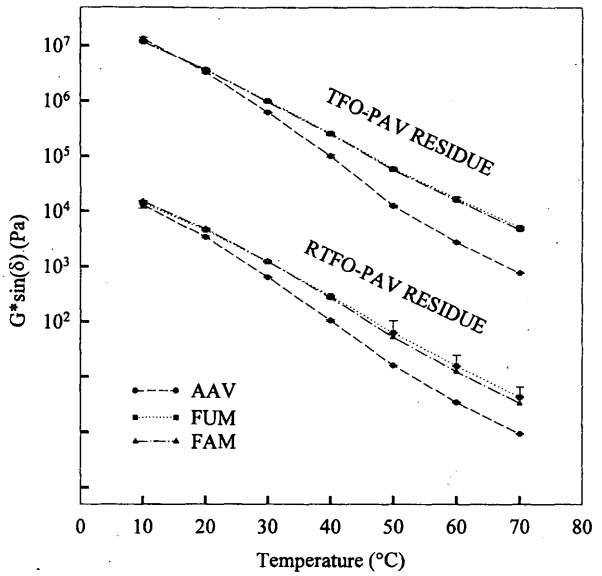

FIGURE 4 Effect of modification on $G^*/\sin(\delta)$ for TFO-PAV- and RTFO-PAV-aged samples.

which is the temperature range at which fatigue cracking would be a problem, G'' values for the modified asphalts are only slightly higher than, if not equal to, those for the unmodified asphalts. This indicates that for these temperatures modification had little effect on fatigue resistance.

Figure 5 shows $G^*/\sin(\delta)$ (or G'') at 10°C and 30°C for these asphalts comparing the TFO-PAV and RTFO-PAV aging procedures. Several observations can be made from Figure 5, as follows:

1. No significant differences were found between samples of AAV aged by TFO-PAV and RTFO-PAV at both 10°C and 30°C, whereas significant differences were apparent in chemically modified asphalts.
2. At 30°C modification increased G'' by about 60 percent for the TFOT-PAV-aged residues and 100 percent for the RTFOT-PAV-aged residues. At 10°C modification decreased G'' for the TFO-PAV-aged residues, whereas it showed an insignificant increase for the RTFO-PAV-aged residues.
3. For the modified asphalts at both 10°C and 30°C the RTFO-PAV-aged residues had higher G'' values than the TFO-PAV-aged residues. This is in contrast to the short-term-aged (modified) asphalts, for which the $G^*/\sin(\delta)$ values for the TFO-aged residues were higher than those for the RTFO-aged residues. It was verified that this observation was also true when G^* alone was considered.

These data point to an interesting case when the SHRP ranking of asphalts for fatigue is different at various temperatures. Table 2 shows the temperatures at which G'' is 5 MPa for asphalts subjected to both TFO-PAV and RTFO-PAV aging. This temperature increased for RTFO-PAV-aged residues compared with that for unaged asphalt. For TFO-PAV-aged residues it remained the same for furfural-modified asphalts and decreased for furyl acrolein-modified asphalts. This indicates that the fatigue resistance may be predicted to remain the same or increase (based on TFO-PAV aging) for chemically modified asphalts. When the aging is more severe during mixing with aggregates, as simulated by RTFO aging, the chemically modified asphalts show higher G'' values, probably predicting slightly decreased fatigue resistance. Such an interpretation can also be made from the data in Figure 5 at 10°C. At 30°C, however, modification increases G''on TFO-PAV aging, and it increases further for RTFO-PAV aging. Thus, at 30°C the ranking of these asphalts is different from that at 10°C and the SHRP ranking.

Effect on Low-Temperature Cracking

Figure 6 shows the creep stiffness of asphalts at a 60-sec loading time, $S(60)$, at various temperatures. Because repetitions were not made, a measurement error of 6 percent was used (based on prior determinations) to help interpret the differences between the curves. From the plot in Figure 6 it can be seen that except for RTFO-PAV-aged AAV at −25°C, all points overlap, indicating that the modification has little effect on the low-temperature creep stiffness. This behavior confirms the data in Table 2, which simply show that for RTFOT-PAV-aged asphalts the temperature at which $S(60)$ is equal to 300 MPa remains the same after chemical modification. For TFO-PAV-aged residues, however, chemical modification decreases the temperature at which $S(60)$ is 300 MPa. On the basis

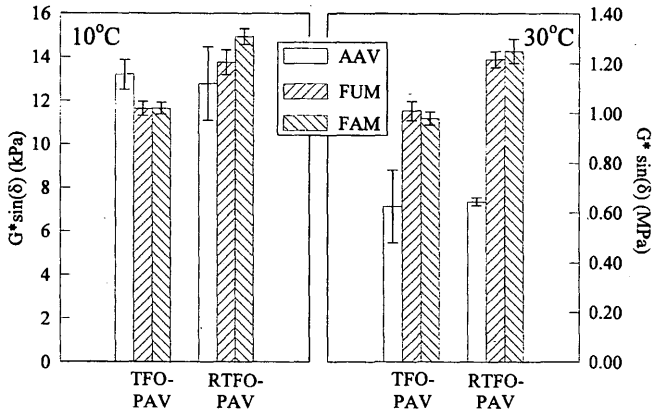

FIGURE 5 Effect of aging on $G^*/\sin(\delta)$ at 30°C and 10°C at 10 rad/sec.

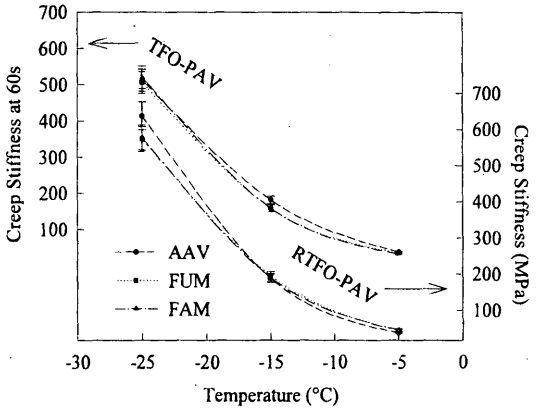

FIGURE 6 Effect of modification on the flexural creep stiffness of unmodified and modified asphalts.

of $S(60)$ alone it is concluded that chemical modification has no significant effect or a slightly beneficial effect on the tendency for low-temperature cracking. What is not obvious from Figure 6 is that the creep stiffness of RTFO-PAV-aged residues of the modified asphalts is higher than that of the TFO-PAV-aged residues, whereas there is no such difference in that of the unmodified asphalts.

Another factor considered in the specification is the m-value. This is related to the rate at which thermal stresses are relieved. The faster the rate of release of the thermal stresses the more durable the pavement. An asphalt with a high m-value would release stresses faster than an asphalt with a lower m-value. Figure 7 shows the m-value as a function of temperature. For TFO-PAV-aged residues at temperatures greater than approximately −19°C the modification decreases the m-value compared with that of the unmodified asphalt, decreasing the rate of release of built-up stresses. At temperatures below approximately −19°C modification has a beneficial effect. For RTFO-PAV-aged residues at temperatures higher than approximately −24°C, chemical modification reduces the m-value. If the PG specification limits the use of the asphalt binders to above an m-value of 0.300, the m-values of the unmodified asphalts are always higher than those of the chemically modified asphalts. In other words, the modification decreases the m-value and therefore has a slight deleterious effect on the thermal stress release rate.

The PG may be too coarse a scale when the effects of modifications (such as polymer and rubber additions or chemical modifications) on the performance of binders are to be studied. In such cases it is useful to consider a continuous grading scale in which the upper and lower temperatures (rounded to the nearest integer) are specified. To determine the continuous grade the actual temperature at which the specification criterion is met is determined for each parameter, as illustrated in Table 2. The upper temperature limit is the lower of the two temperatures that satisfy the high-temperature criteria [$G^*/\sin(\delta)$ for tank- and RTFOT-aged asphalts], and the low-temperature limit is 10°C lower than the higher of the two temperatures that satisfy the low-temperature criteria [$S(60)$ and $m(60)$]. The intermediate temperature is not limiting as long as the temperature for which the intermediate temperature criterion [$G^*\sin(\delta)$ for PAV-aged residue] is met is less than or equal to fatigue specification temperature (4°C higher than the midpoint between the high- and low-temperature limits). This is true for most asphalts and is certainly true for the modified asphalts considered in the present experiments.

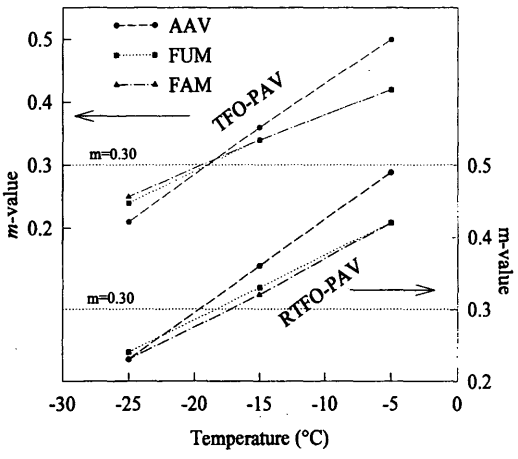

FIGURE 7 Effect of modification on m-value.

The continuous grading is also presented in Table 2. It can be noted that the furfural modification increased the high-temperature limit by 12°C (for TFOT-based aging) or 5°C (for RTFOT-based aging), whereas the low-temperature limit remained the same. The furyl acrolein modification increased the high-temperature limit by 9°C (TFOT-based aging) or 4°C (RTFOT-based aging), whereas the low-temperature limit essentially remained the same. Such an analysis gives more insight into the degree of the effect that modification has on the rheological properties than simply stating that the modification caused an increase of two high-temperature grades. An increase in two such grades could be due to an increase of 7°C or 12°C at the high-temperature end.

CONCLUSIONS

The following conclusions are based on the rheological properties measured for the asphalts chemically modified by furfural and furyl acrolein.

1. Chemical modification increased the $G^*/\sin(\delta)$ values, which is predicted to increase the resistance of the pavements to rutting.
2. The increase in $G^*/\sin(\delta)$ became less pronounced upon short-term aging, but the increase was still significant.
3. On short-term aging it was apparent that another mechanism (other than aging) that tended to decrease the stiffness was active in chemically modified asphalts. However, this mechanism was not identified.
4. $G^*\sin(\delta)$ increased slightly because of modification, indicating that the fatigue resistance was slightly reduced. Even with the slight increase $G^*\sin(\delta)$ was not the limiting parameter in the specification, suggesting that this decrease in fatigue resistance would not lead to pavements that fail because of fatigue cracking.
5. The creep stiffness did not change significantly on modification, but the m-value decreased slightly, indicating that the pavement in which these modified asphalts are used may not be able to relieve thermal stresses at the same rate as that in which the unmodified asphalt is used.
6. The PG of asphalts based on RTFOT as the short-term aging test changed from 52–28 to 58–28 for the furfural modification and 58–22 for the furyl acrolein modification. When TFOT instead of RTFOT was used for short-term aging, the PG changed from 52–28 to 64–28 for both furfural- and furyl acrolein-modified asphalts.
7. Continuous grading provided a more practical way of assessing the degree of effect that modification had on the rheological properties of asphalt.

ACKNOWLEDGMENTS

The authors thank G. M. Memon for preparing the modified asphalts for the present study.

REFERENCES

1. Kumari, D., B. H. Chollar, J. A. Zenewitz, and J. G. Boone. *Chemical Modification of Asphalts.* FHWA Report FHWA-RD-91-123. FHWA, U.S. Department of Transportation, 1992.

2. Chollar, B. H., et al. Characteristics of Furfural Modified Asphalts. Presented at 72nd Annual Meeting of the Transportation Research Board, Washington, D.C., 1993.
3. Memon, G. M., J. G. Boone, and B. H. Chollar. Furfural Substitutes for Chemical Modification of Asphalts. In *Physical Properties of Asphalt Cement Binders,* ASTM STP 1241 (John Hardin, ed.), ASTM, Philadelphia, in press.
4. Memon, G. M., and B. H. Chollar. Nature of the Chemical Reaction for Furfural Modified Asphalt. Preprint. Division of Fuel Chemistry, American Chemical Society, Vol. 39, No. 3, 1994.
5. Anderson, D. A., and T. W. Kennedy. Development of SHRP Binder Specification. *Proc., Association of Asphalt Paving Technologists,* Vol. 62, 1993, pp. 481–507.
6. *Standard Specification for Performance Graded Asphalt Binder.* AASHTO Provisional Standard MP1, Edition 1A. AASHTO, Washington, D.C., 1993.
7. Bahia, H. U., and D. A. Anderson. The New Rheological Properties of Asphalt Binders: Why They Are Required and How Do They Compare to Conventional Properties. Presented at ASTM Conference, Dallas, Tex., 1993.
8. Bouldin, M. Discussion to "California Desert Test Road—A Step Closer to Performance Based Specifications," by R. E. Reese and J. L. Goodrich. *Proc., Association of Asphalt Paving Technologists,* Vol. 62, 1993, pp. 294–297.
9. Rowe, G. M. Performance of Asphalt Mixtures in the Trapezoidal Fatigue Test. *Proc., Association of Asphalt Paving Technologists,* Vol. 62, 1993, pp. 344–384.
10. *Standard Practice for Accelerated Aging of Asphalt Binder Using a Pressurized Aging Vessel (PAV).* AASHTO Provisional Standard PP1, Edition 1A. AASHTO, Washington, D.C., 1993.
11. *Standard Test Method for Determining the Rheological Properties of Asphalt Binder Using a Dynamic Shear Rheometer (DSR).* AASHTO Provisional Standard TP5, Edition 1A. AASHTO, Washington, D.C., 1993.
12. *Standard Test Method for Determining the Flexural Creep Stiffness of Asphalt Binder Using the Bending Beam Rheometer (BBR).* AASHTO Provisional Standard TP1, Edition 1A. AASHTO, Washington, D.C., 1993.
13. Zupanick, M. Comparison of the Thin Film Oven Test and the Rolling Thin Film Oven Test. *Proc., Association of Asphalt Paving Technologists,* Vol. 63, 1994.

Results of Road Trials of Two Asphalt Antioxidants

JOHN W. H. OLIVER

Laboratory testing indicated that two antioxidants, lead diamyldithiocarbamate (LDADC) and hydrated lime (HL), were effective in reducing the rate of oxidative hardening of asphalt binders. Road trial sections with sprayed seals of of both materials were placed at a number of sites in Australia and were monitored for up to 10 years. Each trial consisted of a number of sections that were identical to each other except for the concentration of antioxidant incorporated into the asphalt. The trials were regularly inspected and sampled. Samples were taken back to the laboratory, the asphalt binder was recovered, and its viscosity was measured. By comparing the viscosities of sections onto which asphalt binders containing antioxidant were laid with control sections (asphalt only, no additive) it was possible to determine how effective the antioxidant was in reducing asphalt hardening. The results suggest that LDADC gives the greatest benefit in pavement situations in which binder hardening is rapid. The addition of more than 2.5 percent LDADC appears to produce substantial reductions in the hardening rate. When binder hardening occurs slowly (a durable asphalt in a temperate climate) the addition of LDADC does not appear to reduce binder hardening rate. Although HL was found to retard the rate of hardening of a range of asphalts under laboratory test conditions, it was shown to have no significant effect under long-term exposure (up to 10 years in a sprayed seal).

Sprayed seals are very important to Australia. Use of this low-cost technology has allowed the establishment of an all-weather road network by a population of 18 million people in a country with a land mass of almost 8 million km^2 (80 percent the size of the United States). When proper design and construction techniques are used, sprayed seals can give satisfactory service on roads carrying in excess of 5,000 vehicles per lane per day.

Of the total Australian road network comprising 800 000 km, approximately 200 000 km is sealed, generally with a single-application sprayed seal. Hot-mixed asphalt is normally used as a thin surfacing only on roads in or close to the major metropolitan centers, but its use is growing. Portland cement concrete roads are very much in the minority, enjoying limited popularity in only one of the six Australian states.

The average seal life before extensive maintenance or a reseal is required is about 10 years in the eastern Australian states and about 16 years in Western Australia, where better road building materials are available. Although Australia is free of the problems associated with freeze-thaw cycles, high ambient temperatures are common and road surface temperatures can exceed 70°C (*1*). Under these conditions the asphalt binder in a surfacing can oxidize rapidly, and binder hardening is thought to be the critical factor in determining the service life of about half of all seals.

The resistance of asphalt binders to hardening is controlled in most Australian states through specification of a minimum durability result in which the binder is tested according to an Australian standard procedure (*2*). The durability test result has been correlated with binder hardening in the field through a number of full-scale road trials (*3*).

A second means of controlling the binder hardening rate in thin surfacings may be through incorporation of an antioxidant in the binder. Two additives that have shown promise in laboratory testing are lead diamyldithiocarbamate (LDADC) and hydrated lime (HL). These antioxidants were evaluated in a series of sprayed seal road trial sections laid in different climatic areas of Australia. The trial sections were regularly inspected and sampled, and binder viscosity was measured in the laboratory. The oldest trial sections are now more than 10 years old, and the monitoring program has been terminated. This paper summarizes the road trial results.

EXPERIMENTAL PROCEDURES

Durability Testing

The Australian Road Research Board Ltd (ARRB) Durability Test (*2*) is a laboratory procedure that measures the intrinsic resistance of an asphalt to thermal oxidation hardening. The test consists of a rolling thin film oven (RTFO) pretreatment (*4*) and then exposure of a 20-μm-thick film of asphalt in an oven at 100°C. This is achieved by depositing a specimen of RTFO-treated asphalt onto the walls of glass bottles that are placed in a rotating rack in a special oven. The bottles are withdrawn periodically, and the asphalt is removed and its viscosity is measured at 45°C. The durability of the asphalt is the time (in days) for it to reach an apparent viscosity of 5.7 log Pa·sec. A high number indicates a durable bitumen that should give a long life.

Sampling and Treatment of Field Samples

Samples from road trial sections were normally taken in the outer (curbside) wheelpath. A motor-powered Carborundum-cutting disk was used to cut a section of seal approximately 200-mm square. The seal sample, with any adhering material, was carefully removed from the surface and was transported to the laboratory for testing.

The seal sample was warmed in an oven, and individual stones were plucked from the surface. The asphalt adhering to the undersides of these stones was recovered by solution in toluene, centrifuging and decanting the solution, and then removing the solvent by evaporation.

The degree of hardening of the recovered asphalt was determined by measuring the apparent viscosity at 45°C and a shear rate of 5×10^{-3} sec^{-1} by using a Shell sliding plate microviscometer.

Australian Road Research Board, P.O. Box 156, Nunawading, 3131, Victoria, Australia.

LDADC ROAD TRIALS

Previous Studies

The addition of antioxidants to asphalt has been shown to be effective in reducing the rate of asphalt hardening. Martin (*5*) studied 33 antioxidants belonging to four major classifications and identified the chemical class known as "peroxide decomposers" as the most promising of those tested. This class includes zinc and lead dialkylcarbamates.

Work by Håxo and White (*6*) on the effect of a series of lead and zinc antioxidants on asphalt hardening identified LDADC as being particularly effective in reducing the rate of hardening. The good solubility of LDADC in asphalt was considered an important factor.

Laboratory Testing

The ARRB Durability Test (*2*) was used to evaluate the effect of adding LDADC to the eight core asphalts used in the Strategic Highway Research Program (SHRP). Figure 1 shows the results of this experiment, whereas Figure 2 gives the results for the three asphalts used in the Australian road trials. The effect of LDADC on the rate at which an asphalt oxidizes appears to depend on the durability of the original asphalt. For low-durability asphalts the addition of LDADC always produces an increase in durability. For more durable asphalts, however, LDADC concentrations of less than 2 percent can result in a reduction in durability, and this is discussed in a later section.

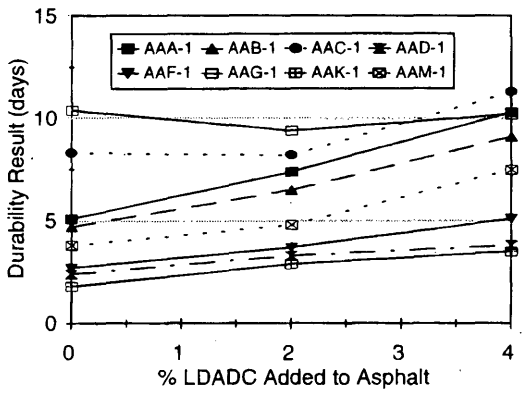

FIGURE 1 Effect of LDADC addition on durability of SHRP asphalts.

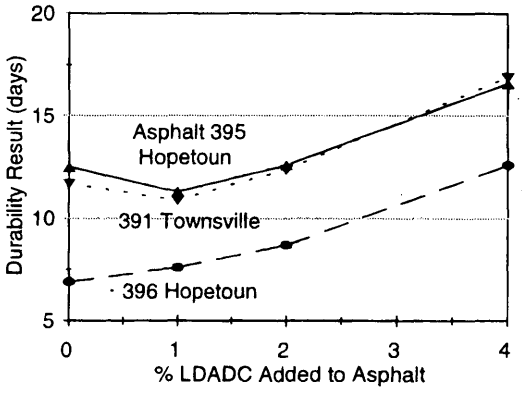

FIGURE 2 Effect of LDADC addition on durability of LDADC trial section asphalts.

Construction of Trial Sections

Two full-scale LDADC road trial sections were laid in Australia. They both comprised sprayed seal surfacings laid over an unbound granular base and used a Class 170 (*7*) (85/100 pen) asphalt. Each trial consisted of a number of sections that were identical to each other except for the concentration of LDADC incorporated into the asphalt. A description of the binders used is given in Table 1. Further information on the construction of Australian sprayed seals is given elsewhere (*8*).

The first trial was laid in a tropical environment 100 km inland from the city of Townsville (yearly average maximum daily air temperature, 28.6°C) in northern Queensland during November 1985. Eleven experimental sections with 16-mm seals were placed by using a single asphalt. The sections had nominal LDADC contents of 0, 1, 2, 3, 4, and 5 percent (by mass), and each concentration, except the highest, was duplicated.

The second trial section, laid in April 1986 at Hopetoun in the more temperate south of Australia, had a 10-mm seal. In this experiment two asphalts were used, and the LDADC concentrations were not duplicated. In both trial sections the sections were between 400 and 500 m in length, and the trial section layouts are shown in Figure 3.

So that LDADC, which is a thick viscous liquid, could be easily pumped or poured for addition to asphalt, the material was dedrummed and diluted with mineral turpentine in the mass ratio of 90 parts of LDADC to 10 parts of mineral turpentine. The material was then pumped into the asphalt distributor on site by using the port normally used for kerosene addition (under cool conditions Australian asphalts are cut back with kerosene on site). Further information on the construction of the trial sections and on early performance is given elsewhere (*9*).

Results

Degradation of Antioxidant

Binder samples were collected by placing trays on the pavement and removing them after the distributor had passed but before application of the cover aggregate. The contents of the collection trays were assayed for LDADC content by using an infrared spectrometric procedure (*10*) and for lead content by atomic absorption spectroscopy. The latter determination was carried out by an analytical laboratory. The lead, determined by atomic absorption, was used to calculate the concentration of LDADC added to the binder in each section (Figure 3). If degradation of the antioxidant were to occur during the construction process, the lead concentration would be unchanged. However, the infrared procedure, which is based on measurement of the diamyldithiocarbamate entity, would record a drop in concentration. The difference between the two measurements would thus give an indication of the degree of degradation of the antioxidant.

LDADC is believed to act sacrificially as an antioxidant. That is to say that the LDADC decomposes as it provides protection for the bitumen against oxidation. Infrared spectrometry testing (*10*) indi-

TABLE 1 Asphalt Used in LDADC Trials

Asphalt No	Trial	Production Method	Durability (days)*
391	Townsville	Kuwait crude, blend of PPA and vacuum tower residue	10.4
395	Hopetoun	Light Arabian crude, straight run blended with 25% PPA	12.6
396	Hopetoun	Air blown Heavy Arabian	7.0

* Binder sampled after spraying - no RFOT pre-treatment applied before durability testing.

Townsville (Asphalt 391)	Hopetoun (Two Asphalts)
4.8% LDADC	396 + 0%
2.5% LDADC	396 + 2.0%
1.6% LDADC	396 + 5.8%
0.8% LDADC	395 + 3.9%
0% LDADC	396 + 1.0%
4.1% LDADC	395 + 2.0%
2.5% LDADC	396 + 2.1%
2.1% LDADC	395 + 1.0%
0.8% LDADC	396 + 3.8%
0% LDADC	395 + 0%
0% LDADC	396 + 0%

FIGURE 3 Layout of trial sections in two LDADC trials.

cated that for both trial sections only those sections that originally contained about 4 percent or more LDADC had any dithiocarbamate structure remaining after 2 years of pavement service. The concentration of dithiocarbamate in these sections was observed to reduce further, and no material was detected after 6 years.

Viscosity Testing of Samples

The trial sections were inspected and sampled at regular intervals, and the viscosity of the recovered binder was determined.

Figure 4 shows the results for the Townsville LDADC trial. These results indicate that all sections containing LDADC either hardened less than the control section or hardened approximately the same as the control section. For samples initially containing 2.5 percent or more LDADC a substantial reduction in the hardening rate due to LDADC addition was obtained.

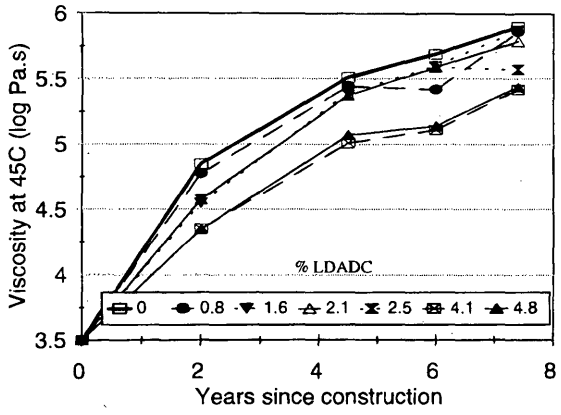

FIGURE 4 Hardening at Townsville site (tropical climate).

Binder hardening at the Hopetoun trial section (Figures 5 and 6) has proceeded more slowly than that at the Townsville trial section because of the lower ambient temperatures at the Hopetoun site. The yearly average maximum daily air temperature at Hopetoun was 23.5°C, compared with 30.1°C at the site near Townsville.

In the case of asphalt 395, sections containing LDADC hardened more slowly than the control section (no LDADC) for the first 2

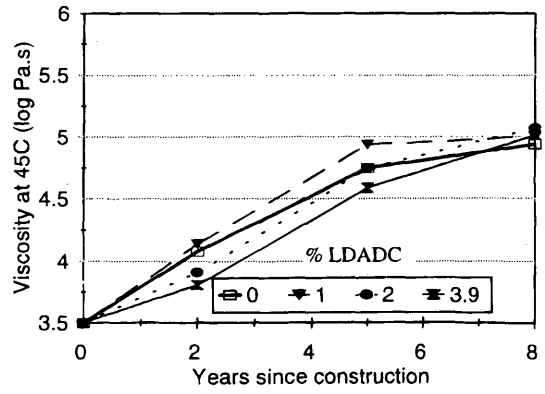

FIGURE 5 Hardening of Asphalt 395 at Hopetoun (temperate climate).

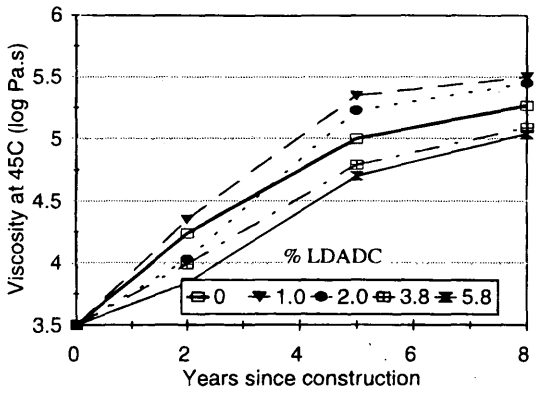

FIGURE 6 Hardening of Asphalt 396 at Hopetoun (temperate climate).

years. After 4 years only the section containing 3.9 percent LDADC had hardened less than the control section. After 8 years none of the LDADC sections had a lower viscosity than the control section.

Asphalt 396 is less durable than Asphalt 395 and has hardened through oxidation more rapidly. After 2 years those sections with more than 2.0 percent LDADC had hardened less than the control section. After 5 years only sections with 3.8 percent or more LDADC had hardened less than the control section, and the situation was unchanged for samples taken 8 years after construction.

Discussion of Results

Results from long-term road exposure of LDADC-modified binders have indicated that when binder hardening occurred slowly (a high-durability asphalt in a temperate climate) LDADC did not provide a significant benefit in the long term. When binder hardening was more rapid a significant reduction in the hardening rate was obtained for LDADC concentrations of 2.5 percent or more.

It is possible that in some asphalts natural antioxidants, perhaps of a phenolic nature, may be present, and these may be antagonistic to the peroxide decomposing carbamates. Part of the carbamate antioxidant reacts with the natural antioxidants and is destroyed, so that small concentrations of LDADC are ineffective.

The road trial results suggest that the most beneficial use of LDADC would be to improve the oxidation resistance of (a) binders used in hot environments, where hardening is likely to occur rapidly, and (b) low-durability binders, that is, those binders most likely to give short service lives. Most North American asphalts appear to fall into this latter category.

Whether the process would be cost-effective depends on the price charged for LDADC. The material used in the trials was manufactured in comparatively small batches, and a considerable reduction in cost might be expected if large-scale manufacture were to be undertaken to supply the road construction industry. No information was available on the future cost of LDADC under these circumstances.

HL ROAD TRIALS

Previous Studies

Plancher et al. (*11*) observed that the rate of hardening of some asphalts by oxidation was reduced when they were first treated with 0.5 to 1.0 percent (by mass) HL. HL is often a constituent of fillers used in hot-mixed asphalt manufacture and is believed to improve the resistance of the mixes to stripping by water action.

Petersen et al. (*12*) later studied the effect of adding between 10 and 30 percent (by mass) HL to asphalt that was then oxidized by a thin film accelerated aging test (113°C, 0.16-mm film for 3 days). The lime was left in the specimens during oven exposure, and a reduction in oxidative hardening was observed for concentrations of up to 20 percent (by mass). This was believed to be due to (a) a reduction in the formation of oxidation products by removal of oxidation catalysts and promoters and (b) reduced sensitivity to the oxidation products through removal of reactive polar molecules that would otherwise interact with the oxidation products to cause an increase in binder viscosity (*11*).

Laboratory Testing

Dickinson (*13*) subjected asphalts with suspensions of HL-containing fillers to the ARRB Durability Test procedure. The asphalts were recovered by solvent extraction after the oven exposure phase. Control tests run in the absence of filler indicated that the solvent recovery procedure did not affect the viscosity of the hardened asphalt. Table 2 gives the results for a number of Class 170 (*7*) (85/100 pen) asphalts manufactured from Middle East crudes. The industrial HL used contained 81 percent calcium hydroxide and 10 percent cement kiln dust (CKD).

Construction of Trial Sections

In all of the chip seal lime trials HL was added to the asphalt by using a transfer box in the line connecting the bulk supply tanker to the distributor. The hot asphalt was sucked by the sprayer pump from the tanker, and the HL was tipped into the transfer box from the bag by hand. Dispersion of the HL in the asphalt was achieved by passing the crude mixture through the distributor pump (either piston or gear type) and subsequent circulation in the sprayer.

Information on the Class 170 (*7*) (85/100 pen) asphalts used in the lime trials is given in Table 3, together with data on the percentage of HL in each section and the period for which each trial section was observed.

Results

Samples from the collection trays (placed in the path of the distributor during placement of the trial) were assayed for lime content. They were also subjected to a shortened form of the Durability Test by measuring the viscosity after 10 days of exposure in the durability oven (rather than determining the days to reach a viscosity of 5.7 log Pa·sec as in the full test). The exception was Manangatang, where a full viscosity test was carried out on two samples. The results are given in Tables 4 and 5.

The results indicate that, in general, the degree of dispersion of the lime in asphalt was satisfactory. For samples from all trials the laboratory Durability Test treatment indicated that increased resistance to oxidative hardening was obtained with the addition of HL.

TABLE 2 Effect of HL-Containing Fillers on Asphalt Durability Test Result

Asphalt Crude Source and Processing	Durability (days)		
	Without Additive	With CKD	With Industrial HL
Additive Concentration 26.6% by mass PPA from Light Arabian distillation residue fluxed with furfural extract of lub. oil stock	4.5	-	7.0
Kuwait blown residue at 300°C to 30/40 pen then fluxed with unblown residue	5.0	7.0	7.0
Kuwait residue blown to grade at 245°C	8.0	11.0	-
Basrah residue blown to grade at 250°C	13.0	18.0	-
PPA from Basrah residue fluxed with that residue	17.0	>23.0	-
Additive Concentration 6.4% by mass Safaniyah (Heavy Arabian) residue blended with PPA from Light Arabian residue	10	-	13

PPA is Propane Precipitated Asphalt - indicates sample not tested

TABLE 3 Details of HL Road Trial Sections

Location	Asphalt	Durability (days)	HL in Sections (% by mass of binder)	Period Observed (years)
Hopetoun (YMMT 23.5°C)	Source uncertain (two asphalts used in the region)	13.2	0, 0, 0, 0, 5.7, 10.7, 15.3	7.7
Lake Boga (YMMT 22.8°C)	Blend of PPA from a Light Arabian crude and a distillation residue from a Heavy Arabian (Safaniyah) crude	8.3	0, 5.7, 10.7, 15.3	9.3
Anna Plains (YMMT 32.4°C)	Imported from Singapore. A blend of a vacuum distillation residue from a Light Arabian crude and a PPA derived from this distillation residue	14.5	0, 3, 6, 9, 12	9.0
Manangatang (YMMT 23.5°C)	Blend of distillation residue from Heavy Arabian (Safaniyah) and a PPA from the vacuum residue of a Light Arabian crude	9.5	0, 1.5, 2.9, 6.1	10.6

PPA = Propane Precipitated Asphalt
YMMT = Yearly average of the maximum daily air temperature

TABLE 4 Testing of Collection Tray Samples: Hopetown and Lake Boga Trial Sections

	Hopetoun Trial		Lake Boga Trial	
HL added (% by mass)	HL in binder sample (% by mass)	Durability Result (10 days exposure) (Log Pa.s)	HL in binder sample (% by mass)	Durability Result (10 days exposure) (Log Pa.s)
0	-	5.27	-	5.78
5.7	4.2	5.11	6.2	5.60
10.3	9.3	5.12	8.2	5.52
15.3	17.3	5.05	15.2	5.45

- indicates sample not tested

TABLE 5 Testing of Collection Tray Samples: Broome and Manangatang Sections

Broome Trial			Manangatang Trial		
HL added (% by mass)	HL in binder sample (% by mass)	Durability Result (10 day exposure) (Log Pa.s)	HL added (% by mass)	HL in binder sample (% by mass)	Durability Test Result (Full Test) (days)
0	-	4.94	0	-	10
3	2.4	-	1.5	1.0	-
6	6.1	4.90	2.9	2.3	-
9	6.4	4.78	6.1	5.5	15
12	10.8	4.79			

- indicates sample not tested

The test sections were sampled and tested by the same procedures used for the LDADC trials. The viscosity of the recovered binder (treated to remove the lime particles) is shown as a function of the added lime content in Figure 7.

The results for Hopetoun trial sections suggest that the addition of lime has caused an increase in the binder hardening rate, whereas the opposite seems to be the case for Lake Boga trial sections. At both the Anna Plains and Manangatang trial sections, sections to which HL was added show little difference in viscosity from the control sections (0 percent HL). Taking all four trials together, it appears that a clear reduction in binder hardening rate with the addition of lime has not been demonstrated.

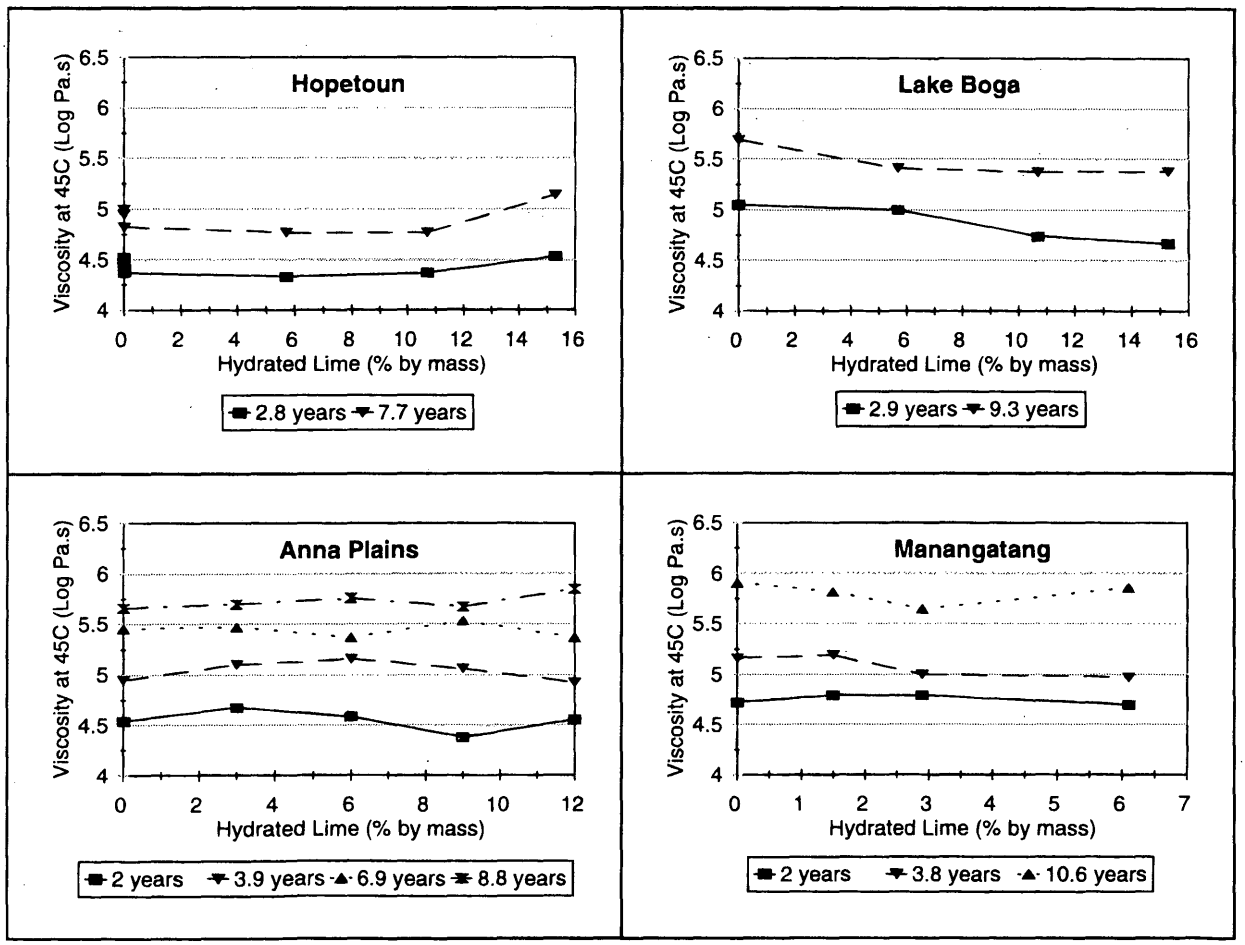

FIGURE 7 Asphalt hardening at HL road trial sections.

Discussion of Results

Although HL was found to retard the rate of hardening of asphalts due to atmospheric oxygen attack under laboratory test conditions (20-μm film at 100°C for 10 days or more), it has now been shown to have no significant effect under long-term exposure (up to 10 years in a sprayed seal).

Finely divided calcium carbonate was found to be ineffective in retarding hardening under the Durability Test conditions (*13*), and carbonation of the surface of the HL particles by atmospheric carbon dioxide early in the life of the seal (converting the HL to calcium carbonate) may have nullified its retarding effect in the pavement.

GENERAL CONCLUSIONS

1. LDADC appears to give the greatest benefit in pavement situations in which binder hardening is rapid. The addition of more than 2.5 percent LDADC appears to produce substantial reductions in binder hardening rate.
2. When binder hardening occurs slowly (a durable asphalt in a temperate climate) the addition of LDADC does not appear to reduce the binder hardening rate.
3. The most beneficial use of LDADC would be to improve the oxidation resistance of binders used in hot environments and low-durability binders. Most North American asphalts appear to fall into this latter category.
4. Although HL was found to retard the rate of hardening of asphalts due to atmospheric oxygen attack under laboratory test conditions, it was shown to have no significant effect under long-term exposure (up to 10 years in a sprayed seal).
5. A possible explanation for the anomalous behavior of HL is that attack by atmospheric carbon dioxide causes carbonation of the surface of the HL particle early in the life of the surfacing.

REFERENCES

1. Dickinson, E. J. *Pavement Temperature Regimes in Australia: Their Effect on the Performance of Bituminous Constructions and Their Relationship with Average Climate Indicators.* Special Report SR 23. Australian Road Research Board, 1981.
2. *Methods of Testing Bitumen and Related Products. Durability of Bitumen.* AS 2341.13. Standards Association of Australia, 1986.
3. Oliver, J . W. H. *Models to Predict Bitumen Hardening Rate and Distress Viscosity Level in Sprayed Seals.* Research Report ARR 182. Australian Road Research Board, 1990.
4. Effect of Heat and Air on a Moving Film of Asphalt. *Annual Book of ASTM Standards D 2872–88,* Vol. 043.03. ASTM, Philadelphia, 1988.
5. Martin, K. G. Laboratory Evaluation of Antioxidants for Bitumen. *Proc., 4th ARRB Conference,* Vol. 4. No. 2, 1968, pp. 1477–1494.
6. Haxo, H. E., and R. M. White. Reducing the Hardening of Paving Asphalts Through the Use of Lead Antioxidants. *Proc., Association of Asphalt Paving Technology,* Vol. 48, 1979, pp. 611–645.
7. *Residual Bitumen for Pavements.* AS 2008. Standards Association of Australia, 1980.
8. Leach, R. D., and J. W. H. Oliver. Long-Life Western Australian Seal Coat. In *Transportation Research Record 1337,* TRB, National Research Council, Washington, D.C., 1992, pp. 37–41.
9. Oliver, J. W. H. Field Trials of a Lead Based Asphalt Antioxidant. In *Transportation Research Record 1228,* TRB, National Research Council, Washington, D.C., 1989, pp. 138–144.
10. Huxtable, A. E., and J. W. H. Oliver. *Determination of the LDADC Content of Oxidised Bitumens.* Internal Report AIR 410–4. Australian Road Research Board, 1989.
11. Plancher, H., E. L. Green, and J. C. Petersen. Reduction of Oxidative Hardening of Asphalts by Treatment with Hydrated Lime. *Proc., Association of Asphalt Paving Technology,* Vol. 45, 1976, pp. 1–24.
12. Petersen, J. C., H. Plancher, and P. M. Harnsberger. Lime Treatment of Asphalt to Reduce Age Hardening and Improve Flow Properties. *Proc., Association of Asphalt Paving Technology,* Vol. 56, 1987, pp. 632–653.
13. Dickinson, E. J. *Bituminous Roads in Australia.* Australian Road Research Board, 1984, pp. 253–259.